Program

LPI

USRA

Comparative Climatology of Terrestrial Planets III
from Stars to Surface

August 27–30, 2018 • Houston, Texas

Institutional Support

NASA Science Mission Directorate
Lunar and Planetary Institute
Universities Space Research Association
National Aeronautics and Space Administration

Conveners

Adriana Ocampo, *NASA Planetary Science Division*
Giada Arney, Co-Convener, *NASA Goddard Space Flight Center*
Shawn Domagal-Goldman, Co-Convener, *NASA Goddard Space Flight Center*
Victoria Hartwick, Co-Convener, *Laboratory of Atmospheric and Space Physics*
Alejandro Soto, Co-Convener, *Southwest Research Institute*

Science Organizing Committee

Giada Arney, *NASA Goddard Space Flight Center*
Simona Bordoni, *California Institute of Technology*
David Brain, *University of Colorado, Boulder*
Amanda Brecht, *NASA Ames Research Center*
Ofer Cohen, *University of Massachusetts, Lowell*
Shawn Domagal-Goldman, *NASA Goddard Space Flight Center*
Richard Eckman, *NASA Earth Science Division*
Colin Goldblatt, *University of Victoria*
Victoria Hartwick, *University of Colorado, Boulder*
Sarah Hörst, *Johns Hopkins University*
Doug Hudgins, *NASA Astrophysics Division*
Jared Leisner, *NASA Heliophysics Science Division*
Janet Luhmann, *University of California, Berkeley*
Adriana Ocampo, *NASA Planetary Science Division*
Jonathan Rall, *NASA Planetary Science Division*
Chris Reinhard, *Georgia Institute of Technology*
Antigona Segura, *Universidad Nacional Autónoma de México*
Alejandro Soto, *Southwest Research Institute*
Elsayed Talaat, *NASA Heliophysics Science Division*
Allan Treiman, *Lunar and Planetary Institute*
Thomas Woods, *University of Colorado, CU*
Mary Voytek, *NASA Science Mission Directorate*

Lunar and Planetary Institute 3600 Bay Area Boulevard Houston TX 77058-1113

Abstracts for this conference are available via the conference website at

https://www.hou.usra.edu/meetings/climatology2018/

Abstracts can be cited as

Author A. B. and Author C. D. (2018) Title of abstract. In *Comparative Climatology of Terrestrial Planets III: From Stars to Surfaces,* Abstract #XXXX. LPI Contribution No. 2065, Lunar and Planetary Institute, Houston.

Guide to Sessions

Comparative Climatology of Terrestrial Planets III

Lunar and Planetary Institute

3600 Bay Area Boulevard • Houston TX 77058-1113

Monday, August 27, 2018

11:30 p.m.	Great Room	Registration
12:15 p.m.	Lecture Hall	Climate Evolution
3:30 p.m.	Lecture Hall	Star-Planet Connection
6:00 p.m.	Great Room	Poster Session

Tuesday, August 28, 2018

8:15 a.m.	Great Room	Networking and Continental Breakfast
8:50 a.m.	Lecture Hall	Biogeochemistry, Photochemistry, and Climate I
11:00 a.m.	Lecture Hall	Biogeochemistry, Photochemistry, and Climate II
2:00 p.m.	Hess and Berkner Rooms	Unconference I
4:00 p.m.	Lecture Hall	CCTP Town Hall
7:00 p.m.	NASA JSC Gilruth Conference Center	Public Event: Storms of the Solar System and Beyond

Wednesday, August 29, 2018

8:15 a.m.	Great Room	Networking and Continental Breakfast
8:50 a.m.	Lecture Hall	Climate Diversity I
10:45 a.m.	Lecture Hall	Climate Diversity II
1:45 p.m.	Lecture Hall	Climate Models, Tools, and Observations I
3:30 p.m.	Hess and Berkner Rooms	Unconference II
7:00 p.m.	NASA JSC Gilruth Conference Center	Public Event: Storms of the Solar System and Beyond *(Presented in Spanish)*

Thursday, August 30, 2018

8:15 a.m.	Great Room	Networking and Continental Breakfast
8:50 a.m.	Lecture Hall	Climate Models, Tools, and Observations II
11:30 a.m.	Lecture Hall	Lessons To and From Earth
1:30 p.m.	Berkner Rooms	Working Lunch: CCTP Goals, Future Plans, and CCTP-3 Wrap-Up

Program

Monday, August 27, 2018
CLIMATE EVOLUTION
12:15 p.m. Lecture Hall

12:15 p.m. *Welcome and Introduction*

12:30 p.m. Wordsworth R. D. * [INVITED]
Abiotic Oxidation of Planetary Atmospheres: Physical Mechanisms and Consequences for Climate, Habitability, and Biosignatures **[#2020]**
This review highlights the central importance of planetary oxidation inside the solar system and beyond. Processes and implications for climate, life, and the observable characteristics of atmospheres are discussed.

1:00 p.m. Arney G. N. * Venus Exploration Analysis Group
Venus: The Exoplanet Laboratory Next Door **[#2019]**
Here, we will review what present and past Venus teaches us context of comparative planetology and processes that shape habitability and biosignature "false positives" in exoplanet atmospheres.

1:15 p.m. Harman C. E. * Sohl L. E. Wolf E. T. Way M. J. Tsigaridis K. Del Genio A. D.
What Does It Take to Glaciate? Exploring the Climatic Link Between Atmospheric Methane and the Rise of Oxygen **[#2060]**
The change in climate across the GOE is thought to be driven by the loss of the CH_4 greenhouse effect. Here, we show ROCKE-3D simulations of climate with and without CH_4, using known constraints on other surface and atmospheric parameters.

1:30 p.m. Way M. J. * Del Genio A. D.
How Studies of Ancient Earth Inform Studies of Ancient Venus: Venus' Evolutionary History and Its Implications for Venus-Like Exoplanetary Worlds **[#2038]**
We try to leverage what scientists have learned about Earth's 4Gyr climatic history to learn more about Venus' climatic history using a 3-D General Circulation Model.

1:45 p.m. Goldblatt C. McDonald V. * McCusker K.
Physical Feedbacks on Stratus Cloud Amount Resolve the Faint Young Sun Paradox **[#2013]**
We perform a series of model runs with the Community Atmosphere Model to test the hypothesis that an Archean atmosphere warmed less by sunlight and more by CO_2 results in less stratus cloud due to a weaker inversion at the planetary boundary layer.

2:00 p.m. Zahnle K. J. * [INVITED]
Climatic Effect of Impacts on the Ocean **[#2056]**
Documented geological evidence of very large cosmic impacts on Earth during the Archean provides some guidance to models of impact-induced catastrophic climate change on land and sea.

2:30 p.m. *Break*

Monday, August 27, 2018
STAR-PLANET CONNECTION
3:30 p.m. Lecture Hall

3:30 p.m. Lean J. L. * [INVITED]
Solar-Driven Climatology of Earth's Extended Environment **[#2016]**
Solar radiation is the energy source for the Earth and other terrestrial planets in the solar system. The climatology of Earth's environment is a combination of orbitally-driven and solar-activity-driven fluctuations in received solar radiation.

4:00 p.m. Howard W. S. * Tilley M. A. Corbett H. T. Youngblood A. A. Loyd R. O. P. Ratzloff J. K. Law N. M. Fors O. del Ser D. Shkolnik E. L. Ziegler C. A. Goeke E. E. Pietraallo A. D. Haislip J.
Evryscope Detection of the First Proxima Superflare: Impacts on the Atmosphere and Habitability of Proxima b **[#2039]**
We detect the first superflare from the nearest star, Proxima Centauri, with the Evryscope array of small telescopes. We explore the impact of this extreme stellar activity on the atmosphere and surface of Proxima's terrestrial planet, Proxima b.

4:15 p.m. Hughes G. B. * Adams J. Cockburn J. M. H.
Spectral Content Variations Through a Solar Cycle and Abetting Decrease in Spectral Albedo of Glacial Ice **[#2004]**
Solar activity directly influences melting of glacial ice via increased ultraviolet emission at solar maximum coupled with decreased spectral albedo of glacial ice; the effect is independent of any effects that solar activity might have on climate.

4:30 p.m. Egan H. * Jarvinen R. Brain D.
Understanding Stellar Influence on Ion Escape from Exoplanets **[#2029]**
By performing a systematic study of how ion loss processes vary with stellar input for typical M-dwarf conditions, we build a generalized framework to understand how ion loss processes vary from the current solar system paradigms.

4:45 p.m. Dong C. F. *
Atmospheric Escape from M-Dwarf Exoplanets and Implications for Long-Term Climate Evolution and Habitability **[#2053]**
We study the atmospheric escape from M-dwarf exoplanets (including Proxima b and seven Earth-sized planets in the TRAPPIST-1 system) and its implications for long-term climate evolution and habitability by using the state-of-the-art numerical tools.

5:00 p.m. Jakosky B. M. * [INVITED]
Mars Climate and Volatile Evolution **[#2072]**
Examination of the behavior of Mars climate and volatiles, starting from the annual behavior and building up to long-term evolution.

5:30 p.m. Poster Lightning Talks
Each poster presenter will have an opportunity to present a one-minute introduction.

Monday, August 27, 2018
POSTER SESSION
6:00–8:00 p.m. Great Room

Nikolaidou T. N.
Employing Ray-Tracing to Probe Mars Atmosphere **[#2048]**
The study presents a novel experiment where the ray-tracing technique is utilized to retrieve information on Mars neutral atmosphere. Spatial and temporal properties of the martian atmosphere will be presented and compared to Earth's.

Rushby A. J. Domagal-Goldman S. D. Som S. M. Woffard A. Arney G. Hoehler T.
Revisiting the Early Earth's Methanogen Biosphere **[#2040]**
We investigate the effect of a putative sediment-dwelling methenogen biosphere on the climate and atmospheric chemistry of the Archean using a coupled ecosystem-climate-photochemistry model, and discuss implications for paleoclimatology and biosignatures.

Chandler C. O. Robinson T. D.
Efficient Atmospheric Model Equilibrium Searching and Assessment **[#2026]**
We present novel atmospheric model computational techniques, newly formulated metrics for analyzing model output quality, and we demonstrate our new approach through applications to both Super-Earth and Mini-Neptune exoplanets.

Kochemasov G. G.
Cyclonic Activities on Jupiter and Earth; Catastrophic Atmospheric Phenomena of the Wave Nature: El-Nino, Cyclones, Tornado **[#2009]**
Cyclonic lay-outs on Earth and Jupiter are observed and compared, though they occupy different latitudinal zones of the planets. Catastrophic terrestrial cyclones are tied to the equatorial belt requiring diminishing mass and thus enhanced rotation.

Guzewich S. D. Lustig-Yaeger J. Kopparapu R. Way M. J.
The Impact of Planetary Rotation Rate on the Reflectance Spectrum of Terrestrial Exoplanets **[#2022]**
We conduct general circulation model simulations with ROCKE3D to model terrestrial planet climate with varying rotation rates. We then evaluate how the reflectance spectrum of the planet changes using two radiative transfer codes.

Hartwick V. L. Toon O. B.
Implementing a New Earth Based Dust Lifting Scheme in Mars Global Circulation Models **[#2055]**
We implement a new dust lifting scheme based on parameterizations for Earth in MarsCAM-CARMA. We investigate the impact on the distribution and timing of dust activity and its role in generating observed interannual variability.

Tao T. T.
Did Outburst of Supermassive Black Hole Sagittarius A Cause an Extreme Glaciation on Earth? **[#2002]**
A theory suggests our planet Earth had an extreme cooling from 5.9 to 5.33 million years ago, a most extensive glaciation "Miocene Glacier" since the dinosaur's era. The cosmic ray outburst from Sagittarius A, ca 6 MYA, emerges as the leading cause.

Britt A. V. Domagal-Goldman S.
Simulations of Methane on Mars Utilizing Curiosity Data **[#2035]**
The presence of methane in the martian atmosphere has been a photochemical mystery. But, NASA's Curiosity mission measures local surface abundances of methane and we investigate the temporal and transient signals measured using 1D model techniques.

Felton R. Arney G. Domagal-Goldman S. Neveu M. Desch S.
Developing Tighter Constraints on Exoplanet Biosignatures by Modeling Atmospheric Haze **[#2064]**
Atmospheric haze may be the next piece of an atmosphere that we can use to better understand, identify, and distinguish life-bearing planets from lifeless ones. We use models to compare hazes to identify potentially life-bearing exoplanets.

Tilipman D. Linsky J. L. Vieytes M. France K. **CANCELED**
Computing Models of M-Type Host Stars and Their Panchromatic Spectral Output **[#2034]**
We compute semi-empirical models of low-mass stars that are known to host exoplanets in order to obtain high-resolution panchromatic spectra. Here we present the first model of an active M5 V dwarf GJ 876 and compare it with our model of GJ 832.

Farrish A. O. Maruo M. Barnes W. T. Alexander D. Bradshaw S. DeRosa M.
Simulation of Exoplanet Host Star Magnetic Activity on Stellar Cycle Timescales **[#2043]**
We apply solar physics modeling tools to the study of star-exoplanet interaction, with a focus on how variations in stellar magnetic field and energetic emission on cycle timescales may impact planetary habitability.

Ceja A. Y. Kane S. R.
Using Exoplanet Climate Simulations as a Tool for Constraining Astroecology Models **[#2044]**
A modeling approach is outlined for which simulated climatic temperatures of Earth analogs on variable eccentric and oblique orbits serve as inputs for a previously developed astroecology model. The climate simulations are run with the GCM ROCKE-3D.

Asemani D. Roberts D. R. **CANCELED**
Hazardous Risks of Long-Term Non-Ionizing Electromagnetic Radiation on the Astronauts' Brain in Deep Space **[#2069]**
We hypothesize that the long-term exposure to these kinds of radiation, potentially possible on the spaceflight expeditions, may result in serious health concerns, particularly on the brain due to the synergistic interaction of microgravity environment.

Ogunbiyi A. O.
Online STEM Education and Aerospace Micro-Lesson in Nigeria (A Panacea to African Development) **[#2003]**
The project is designed to mould the next generation of scientists by providing resources to teachers, students, and professionals and actively involving students in the support of researches being conducted on the ISS or NASA ground-based laboratory.

Kurt C. Dessler A. E.
Comparison of Climate Sensitivity and Feedbacks Calculated by a Traditional and a New Equation **[#2066]**
Using two sets of GCM ensembles (pre-industrial control runs and abrupt $4\times CO_2$ runs) from CMIP5 models and satellite observations (CERES), we calculated climate sensitivity and feedbacks splitting into components with two different approaches.

Mischna M. A. Piqueux S.
The Role of Atmospheric Pressure on Mars Surface Properties and Early Mars Climate Modeling **[#2070]**
Thermal conductivity of planetary regolith is controlled by atmospheric pressure, via interstitial pore space gas conductivity within the soil. We propose an obliquity-driven cycle of surface evolution that accounts for this behavior.

McKinney M. M.
Applying Science to Fiction: A Look at the Fictional Planet Mesklin **[#2063]**
In 1953, Hal Clement created the fictional planet "Mesklin." This planet was based on a 1943 finding of a 16-Jupiter-mass exoplanet in the 61 Cygni system. What kind of climate might this fictional planet have, based on the parameters from Clement?

Jiang J. J.
Using Deep Space Climate Observatory Measurements to Study the Earth as an Exoplanet **[#2058]**
More than two years of DSCOVR Earth images were employed to produce time series of multi-wavelength, single-point light sources, in order to extract information on planetary rotation, cloud patterns, surface type, and orbit of an Earth-like exoplanet.

Dong C. F. Lee Y. Ma Y. J. Lingam M. Bougher S. W. Luhmann J. G. Curry S. M. Toth G. Nagy A. F. Tenishev V. Fang X. Mitchell D. L. Brain D. A. Jakosky B. M.
Modeling Martian Atmospheric Losses Over Time: Implications for (Exo)Planetary Climate Evolution and Habitability **[#2052]**
We make use of the one-way coupled framework (linking our GCM, DSMC, and MHD models), known to accurately reproduce MAVEN observations, for studying the atmospheric ion and photochemical escape rates and climate evolution over the history of Mars.

Miura Y. **CANCELED**
Comparative Climatology of Planets With and Without Global Ocean System **[#2065]**
Planets are formed air-solid system at collisions of planetary formation. Ocean liquid system can be formed only Earth planet. Climates of air-solid planets are wind-induced circulation climate in Mars-Venus, which is the same in exosolar planets.

Colose C. C. Del Genio A. D. Way M.
Climate Hysteresis at High Obliquity **[#2054]**
We employ the newly developed NASA GISS ROCKE-3d GCM (with a dynamic ocean) to investigate the climate dynamics of various planets at high obliquity, and discuss the susceptibility of such planets to undergo global glaciation.

Yang J. Ji W.
Increased Ice Coverages on TRAPPIST-1e, LHS 1140b, and Proxima b by Sea Ice Dynamics **[#2005]**
For the three nearby potentially habitable exoplanets — TRAPPIST-1e, LHS1140b, and Proxima b — our 3D climate simulations show that sea ice flows are able to expand their sea ice coverages or even push them into globally ice-covered snowball states.

Shirley J. H.
Advancing the State of the Art of Martian Weather and Climate Modeling with Orbit-Spin Coupling **[#2025]**
The historic record of global dust storm occurrence on Mars has been reproduced within a general circulation model that incorporates atmospheric accelerations due to a weak coupling of planetary orbital and rotational motions.

Guendelman I. Kaspi Y.
Planetary Climate Dynamics Over a Wide Range of Orbital and Atmospheric Characteristics **[#2008]**
Using an idealized aquaplaned general circulation model, we study the climate dependence on obliquity, orbital period, atmospheric mass, and rotation rate. We explain physically our results and suggest a future observable based on them.

Fortney J. J. Robinson T. D. Domagal-Goldman S. D. Del Genio A.
Laboratory Needs for Exoplanet Climate Modeling **[#2068]**
This is a summary of the Nexus for Exoplanet Systems Science (NExSS) white paper on laboratory needs for understanding exoplanet atmospheres.

Costa de Ammeida E.
Atmospheric Parameters and Ages of M Dwarfs in the Solar Neighborhood **[#2073]**
M dwarfs are the most numerous stars in the galaxy, accounting for about 70% of its baryonoc mass. They are prime candidates to shelter habitable earthlike planets.

Wang L. Dong C. Hakim A. Bhattacharjee A. Germaschewski K.
Effects of Dipolar Magnetic Fields in Space Weather at Outer Magnetospheres **[#2074]**
Some terrestrial bodies within our solar system have strong, intrinsic magnetic fields, in a few cases, Earth-like, dipolar fields. These magnetic files play critical roles in space weather within the bodies' magnetospheres.

Tuesday, August 28, 2018
BIOGEOCHEMISTRY, PHOTOCHEMISTRY, AND CLIMATE I
8:50 a.m. Lecture Hall

8:50 a.m. *Welcome*

9:00 a.m. Schaefer L. * [INVITED]
Atmosphere-Mantle Volatile Exchange Throughout Planetary Evolution **[#2047]**
Fluxes of volatiles into and out of the mantle play a key role in the stability of habitable conditions at the surface on geological timescales. In this talk, I will review atmosphere-mantle volatile exchange on Earth, Venus, and Mars and applications to exoplanets.

9:30 a.m. Komacek T. D. * Abbot D. S.
The Atmospheric Circulation and Cloud Behavior in a Large Suite of Terrestrial Planet GCMs **[#2007]**
We simulate the atmospheres of planets around G and M-dwarf stars with varying incident stellar flux, rotation period, radius, gravity, surface pressure, and cloud particle size to study the resulting atmospheric circulation and cloud distribution.

9:45 a.m. Weller M. B. * Lenardic A. Jellinek M. Seales J. Way M.
Venus' Early Potential for Habitability: Connecting Climate and Geologic Histories **[#2014]**
Surface breaks, melting / Gases emit and sun closer / Waters potential.

10:00 a.m. Gao P. *
Photochemistry of Terrestrial Worlds Orbiting M Dwarfs **[#2050]**
Photochemistry / Of Mars, Titan, and Venus / Orbiting M dwarfs.

10:15 a.m. Ramirez R. M. * Craddock R. A. Kaltenegger L.
The Role of Methane on an Icy Early Mars and in Exoplanetary Atmospheres **[#2001]**
The early martian climate is presently thought to have either been icy and cold or warm and semi-arid. We show that transiently warming an icy climate is challenged by the high albedo of surface ice. Exoplanet implications are also discussed.

10:30 a.m. *Break*

Tuesday, August 28, 2018
BIOGEOCHEMISTRY, PHOTOCHEMISTRY, AND CLIMATE II
11:00 a.m. Lecture Hall

11:00 a.m. Olson S. L. * [INVITED]
Coevolution of Oceanic and Atmospheric Chemistry **[#2021]**
This talk will examine the relationship between oceanic and atmospheric chemistry through Earth's history and will emphasize the potential for chemical disequilibrium despite efficient sea-air gas exchange.

11:30 a.m. Planavsky N. J. * Isson T. T. Kalderon-Asael B.
Reverse Weathering and Climate **[#2045]**
Elevated rates of reverse weathering — the consumption of alkalinity and the generation of acidity accompanying clay authigenesis — led to the sustenance of a significantly elevated atmospheric carbon dioxide concentrations in Earth's early history.

11:45 a.m. Reinhard C. T. * Ozaki K.
The Importance of Anoxygenic Photosynthesis for Climate and Atmospheric Biosignatures on Reducing Worlds **[#2067]**
Model exploring the impact of anoxygenic photosynthesis on climate and atmospheric biosignatures on primitive Earth-like planets.

12:00 p.m. Kiang N. Y. * [INVITED]
The Land Biosphere and Planetary Climate: Feedbacks to Habitability **[#2042]**
Does life on land lead to homeostatisis or unstable feedbacks to climate? This talk reviews how land-based ecosystems influence climate through the water, energy, and carbon cycles, and the implications for climatology of habitable exoplanets.

12:30 p.m. *Lunch*

Tuesday, August 28, 2018
UNCONFERENCE I
2:00–3:30 p.m. Hess and Berkner Rooms

The unconference session is a participant-led session to discuss topics of importance to the comparative climatology community.

For this third CCTP conference, we want to promote interdisciplinary discussion, particularly between scientists who traditionally do not work together and/or attend the same meetings. We also want to foster "organic" discussions that are not directed by the conveners of the meeting, but instead initiated by the participants. Basically, we want to foster discussions that already occur in the hallways and at the meals of a traditional conference, but in a way that is more inclusive and that does not rely on pre-existing social and professional networks among conference participants.

To do this, we are implementing two "unconference" discussion sessions at CCTP-3. An unconference is a meeting driven by the participants, where top-down planning and elaborate presentations are avoided. Participants will suggest discussion topics, vote on the discussions to have, and then run/participate in the discussions.

We will set up a board where participants will write their suggested discussion topic along with their name. Monday afternoon and evening we will collect discussion ideas on the board. On Tuesday, participants should put their votes next to the sessions they would like to attend. At the end of the lunch break, the organizers will tally up the votes and assign the sessions to rooms. We will have three concurrent discussions during each unconference session. After the Tuesday unconference session, people can add more discussion topics for the Wednesday session and start voting for those Wednesday sessions.

We encourage everyone to attend one of the voted-for discussions during the unconference session. These discussions have no presentations, no agenda, and are open to all. The person who suggested the selected topic will lead the session. They should consider themselves a moderator, not a presenter or a leader. We encourage people to leave a session if they're not getting anything out of it, and try another one. The goal is for everyone to be involved in discussing comparative climatology science and future directions.

CCTP TOWN HALL
4:00 p.m. Lecture Hall

The Comparative Climatology of Terrestrial Planets III Town Hall will be an opportunity to discuss with NASA representatives the current state and future direction of comparative climatology research.

Wednesday, August 29, 2018
CLIMATE DIVERSITY I
8:50 a.m. Lecture Hall

8:50 a.m. *Welcome*

9:00 a.m. Abbot D. S. * [INVITED]
The Diversity of Climate States of Terrestrial Planets **[#2006]**
This is a review talk about the diversity of climate states of terrestrial planets. It will focus on planets that are habitable (have surface liquid water), could have been in the past, or could be in the future.

9:30 a.m. Li L. * Jiang X.
Exploration of Planetary Atmospheres and Climates from an Energy Perspective **[#2011]**
We present some recent progresses in exploring the radiant energy budgets and mechanical energy cycles in the atmospheric systems of the gas giant planets (Jupiter and Saturn) and terrestrial bodies (e.g., Earth and Titan) in our solar system.

9:45 a.m. Lincowski A. P. * Meadows V. S. Crisp D. Robinson T. D. Luger R. Lustig-Yaeger J.
Evolved Climates of the TRAPPIST-1 Planetary System **[#2024]**
The seven-planet TRAPPIST-1 system provides the opportunity to study terrestrial planet evolution with JWST around an alien star, in and around the HZ. We compare climate-photochemistry results of these planets with those in the solar system.

10:00 a.m. Fauchez T. * Turbet M. Mandell A. Kopparapu R. Arney G. Domagal-Goldman S. D.
Impact of Clouds and Hazes in the JWST Simulated Transmission Spectra of TRAPPIST-1 Planets in the Habitable Zone **[#2033]**
We present the impact that clouds and/or hazes may have on the detection on biosignatures through transmission spectroscopy with JWST for the TRAPPIST-1 system.

10:15 a.m. *Break*

Wednesday, August 29, 2018
CLIMATE DIVERSITY II
10:45 a.m. Lecture Hall

10:45 a.m. Lora J. M. * [INVITED]
The Circulation and Volatile Cycles of Solar System Atmospheres **[#2030]**
I will describe and compare the climate systems of terrestrial worlds in our solar system, particularly focusing on their atmospheric circulations and the role of volatile cycles.

11:15 a.m. Ishiwatari M. * Noda S. Nakajima K. Takahashi Y. O. Takehiro S. Hayashi Y.-Y.
GCM Experiments on Occurrence Condition of the Runaway Greenhouse State: Aquaplanets and Landplanets **[#2059]**
In order to examine the occurrence condition of the runaway greenhouse state for aquaplanet, landplanet, synchronously rotating planet, Earth-like non-synchronously rotating planet, GCM experiments are performed for various conditions.

11:30 a.m. Lobo A. H. * Bordoni S.
Climates of High Obliquity Terrestrial Planets in Idealized Simulations with a Seasonal Cycle **[#2037]**
We show the seasonal behavior of large scale atmospheric circulations on high obliquity Earth-like planets, where the seasonal cycle is critical to a proper understanding of the average planetary climate conditions.

11:45 a.m. Barth E. L. *
Hydrocarbon Condensation on Titan and Pluto: Comparisons Using PlanetCARMA **[#2051]**
The Community Aerosol and Radiation Model for Atmospheres (CARMA) has been adapted to model cloud microphysics for many solar system atmospheres. The model changes will be described along with applications to Titan and Pluto.

12:00 p.m. Paradise A. Y. * Menou K. Valencia D. Lee C.
Generalizing the Habitable Zone: Temperate Continental Regions on Some Snowball Planets **[#2036]**
Habitable planets are commonly imagined to be temperate, like Earth. This carries an implicit assumption that the surfaces of Snowball planets are not habitable. We use a GCM to show that Snowball planets can have temperate land regions.

12:15 p.m. *Lunch*

Wednesday, August 29, 2018
CLIMATE MODELS, TOOLS, AND OBSERVATIONS I
1:45 p.m. Lecture Hall

1:45 p.m. Cowan N. B. * [INVITED]
Characterizing Terrestrial Exoplanets: Diversity Flexes Its Muscles **[#2057]**
Extrasolar planets are more varied than solar system worlds, but their great distance makes them hard to observe in detail. I will discuss three archetypal terrestrial exoplanets and how we hope to characterize them in the foreseeable future.

2:15 p.m. Stark C. C. * Bolcar M. Fogarty K. Pueyo L. Eldorado Riggs A. J. Ruane G. Soummer R. St. Laurent K. Zimmerman N. T.
The Exoplanet Yield Landscape for Future Space Telescope Missions **[#2061]**
The expected yield of potentially Earth-like planets is a crucial metric for future missions aiming to characterize exoplanets. I will review technologies for exoplanet detection, their scientific return, and exoplanet yields for a range of missions.

2:30 p.m. Feng Y. K. * Robinson T. D. Fortney J. J.
Characterizing Earth Analogs in Reflected Light: Information Content from the Ultraviolet Through the Near-Infrared **[#2010]**
We explore the information content in simulated data spanning the near-ultraviolet to the near-infrared (0.2–1.8 μm) from terrestrial planets around Sun-like stars as observed in reflected light with future direct imaging space missions.

2:45 p.m. Checlair J. * Abbot D. S. Bean J. L. Kempton E. M.-R. Robinson T. D. Webber R.
A Statistical Comparative Planetology Approach to Test the Habitable Zone Concept **[#2041]**
We develop a statistical approach to test the silicate-weathering feedback directly by taking low-precision CO_2 measurements on many planets with future observing facilities such as JWST, LUVOIR, or HabEx.

3:00 p.m. *Break*

UNCONFERENCE II
3:30–5:00 p.m. Hess and Berkner Rooms

The unconference session is a participant-led session to discuss topics of importance to the comparative climatology community.

Thursday, August 30, 2018
CLIMATE MODELS, TOOLS, AND OBSERVATIONS II
8:50 a.m. Lecture Hall

8:50 a.m. *Welcome*

9:00 a.m. Marsh D. R. * [INVITED]
Current Status and Future Directions of Climate Modeling **[#2071]**
This talk will summarize current model capability in simulating the past, present and future climates of Earth and their adaptation to modeling planetary atmospheres.

9:30 a.m. Villanueva G. L. * Smith M. D. Protopapa S. Faggi S. Mandell A. M.
The Planetary Spectrum Generator (PSG): An Online Simulator of Exoplanets **[#2017]**
We have developed an online radiative-transfer suite (https://psg.gsfc.nasa.gov) applicable to a broad range of exoplanets (e.g., terrestrial, super-Earths, Neptune-like, and gas-giants).

9:45 a.m. McGouldrick K. *
Lessons from Akatsuki: Comparative Meteorology **[#2062]**
To understand exoplanets and their habitability we must understand their atmospheres. To understand planetary atmospheres, we must study planetary atmospheres the way we study Earth's atmosphere. Akatsuki has shown how this is possible.

10:00 a.m. Ding F. * Wordsworth R.
A New Line-by-Line General Circulation Model for Simulation of Diverse Planetary Atmospheres **[#2027]**
We describe the development of a new flexible and accurate three-dimensional general circulation model (GCM) that for the first time uses a line-by-line model to describe radiative transfer.

10:15 a.m. Goldblatt C. *
Simple Models of Terrestrial Planet Energy Balance: Understanding Moist and Runaway Greenhouse States **[#2012]**
I introduce tutorial models of the energy balance of moist worlds. These address the transition between damp, moist, and runaway climate states on Earth and Earth-like planets.

10:30 a.m. Tyrrell T. *
A Minimum Complexity Model for Investigating Long-Term Planetary Habitability **[#2031]**
It is hard to investigate how Earth managed to remain continuously habitable over geological timescales because the phenomenon is inaccessible to observations and experiments. A new low-complexity modelling approach may yield insights.

10:45 a.m. Lorenz R. D. *
Titan's Tropical Hydrological Cycle: Constraints from Huygens, Cassini, and Future Missions **[#2046]**
Titan's methane rain / What we know from Cassini / And what's to be learned.

11:00 a.m. *Break*

Thursday, August 30, 2018
LESSONS TO AND FROM EARTH
11:30 a.m. Lecture Hall

11:30 a.m. Cable M. L. * [INVITED]
Laboratory Investigations Connecting Terrestrial Climates to Icy Worlds **[#2023]**
Terrestrial climate models can be applied to icy bodies in the solar system with atmospheres — Titan, Pluto, and Triton — when modified appropriately. Laboratory measurements play an important role in this process.

12:00 p.m. Soto A. * Rafkin S. C. R.
Atmospheric Circulations of Lakes and Seas on Earth and Titan **[#2028]**
We compare the atmospheric circulations over lakes and seas on Earth and Titan.

12:15 p.m. Rafkin S. C. R. *
Dynamics, Structure, and Importance of Deep Atmospheric Convection on Earth, Mars, and Titan **[#2032]**
Earth, Mars, and Titan exhibit deep convection. The similarities and differences of these convective phenomena are considered, as is the influence of the environment on the convection and the impact of the convection on global climate cycles.

12:30 p.m. He F. * Clark P. U. Carlson A. E.
Solar Forcing of the Abrupt Last Glacial Inception **[#2049]**
We will show the results from the first Transient synchronously coupled global ClimatE simulation of Last InterGlaciation (TraCE-LIG), which is able to produce a rapid last glacial inception due to the gradual changes of orbital forcing.

12:45 p.m. Koll D. D. B. * Cronin T. W.
The Emergent Linearity of Outgoing Longwave Radiation in a Moist Atmosphere: Implications for the Climates of Earth and Extrasolar Planets **[#2015]**
The physics that sets Earth's outgoing longwave radiation (OLR) is complex and non-linear, yet observations show that OLR is an essentially linear function of surface temperature. Here we explain why, with implications for both Earth and exoplanets.

1:00 p.m. Dewey M. * Goldblatt C.
Empirical Evidence for Radiative-Convective Bi-Stability in Earth's Tropics **[#2018]**
We use satellite observations and models to show the existence of the super-greenhouse gives rise to a radiative-convective bi-stability relevant to Earth's tropics. Implications include understanding the planetary energy balance in a warming world.

1:15 p.m. *Break*

Thursday, August 30, 2018
WORKING LUNCH: CCTP GOALS, FUTURE PLANS, AND CCTP-3 WRAP-UP
1:30–3:30 p.m. Berkner Rooms

During the final session of the Comparative Climatology of Terrestrial Planets III, we will work as a community to identify goals and future plans. Ideally, we will generate a set of research goals for comparative climatology that will guide both the research community and NASA's support of this community. This session should lead to a number of products, including plans for white papers for the upcoming Astrophysics and Planetary Decadal Reports.

We encourage all conference attendees to participate in this important final session of CCTP-3.

Notes

CONTENTS

The Diversity of Climate States of Terrestrial Planets
D. S. Abbot 2006

Venus: The Exoplanet Laboratory Next Door
G. N. Arney and Venus Exploration Analysis Group 2019

Hazardous Risks of Long-Term Non-Ionizing Electromagnetic Radiation on the Astronauts' Brain in Deep Space
D. Asemani and D. R. Roberts 2069

Hydrocarbon Condensation on Titan and Pluto: Comparisons Using PlanetCARMA
E. L. Barth 2051

Simulations of Methane on Mars Utilizing Curiosity Data
A. V. Britt and S. Domagal-Goldman 2035

Laboratory Investigations Connecting Terrestrial Climates to Icy Worlds
M. L. Cable 2023

Using Exoplanet Climate Simulations as a Tool for Constraining Astroecology Models
A. Y. Ceja and S. R. Kane 2044

Efficient Atmospheric Model Equilibrium Searching and Assessment
C. O. Chandler and T. D. Robinson 2026

A Statistical Comparative Planetology Approach to Test the Habitable Zone Concept
J. Checlair, D. S. Abbot, J. L. Bean, E. M.-R. Kempton, T. D. Robinson, and R. Webber 2041

Climate Hysteresis at High Obliquity
C. C. Colose, A. D. Del Genio, and M. Way 2054

Atmospheric Parameters and Ages of M Dwarfs in the Solar Neighborhood
E. Costa de Ammeida 2073

Characterizing Terrestrial Exoplanets: Diversity Flexes Its Muscles
N. B. Cowan 2057

Empirical Evidence for Radiative-Convective Bi-Stability in Earth's Tropics
M. Dewey and C. Goldblatt 2018

A New Line-by-Line General Circulation Model for Simulation of Diverse Planetary Atmospheres
F. Ding and R. Wordsworth 2027

Atmospheric Escape from M-Dwarf Exoplanets and Implications for Long-Term Climate Evolution and Habitability
C. F. Dong 2053

Modeling Martian Atmospheric Losses Over Time: Implications for (Exo)Planetary Climate Evolution and Habitability
C. F. Dong, Y. Lee, Y. J. Ma, M. Lingam, S. W. Bougher, J. G. Luhmann, S. M. Curry, G. Toth, A. F. Nagy, V. Tenishev, X. Fang, D. L. Mitchell, D. A. Brain, and B. M. Jakosky 2052

Understanding Stellar Influence on Ion Escape from Exoplanets
H. Egan, R. Jarvinen, and D. Brain 2029

Simulation of Exoplanet Host Star Magnetic Activity on Stellar Cycle Timescales
A. O. Farrish, M. Maruo, W. T. Barnes, D. Alexander, S. Bradshaw, and M. DeRosa 2043

Impact of Clouds and Hazes in the JWST Simulated Transmission Spectra of TRAPPIST-1 Planets in the Habitable Zone
T. Fauchez, M. Turbet, A. Mandell, R. Kopparapu, G. Arney, and S. D. Domagal-Goldman 2033

Developing Tighter Constraints on Exoplanet Biosignatures by Modeling Atmospheric Haze
R. Felton, G. Arney, S. Domagal-Goldman, M. Neveu, and S. Desch 2064

Characterizing Earth Analogs in Reflected Light: Information Content from the Ultraviolet Through the Near-Infrared
Y. K. Feng, T. D. Robinson, and J. J. Fortney 2010

Laboratory Needs for Exoplanet Climate Modeling
J. J. Fortney, T. D. Robinson, S. D. Domagal-Goldman, and A. Del Genio 2068

Photochemistry of Terrestrial Worlds Orbiting M Dwarfs
P. Gao 2050

Simple Models of Terrestrial Planet Energy Balance: Understanding Moist and Runaway Greenhouse States
C. Goldblatt 2012

Physical Feedbacks on Stratus Cloud Amount Resolve the Faint Young Sun Paradox
C. Goldblatt, V. McDonald, and K. McCusker 2013

Planetary Climate Dynamics Over a Wide Range of Orbital and Atmospheric Characteristics
I. Guendelman and Y. Kaspi 2008

The Impact of Planetary Rotation Rate on the Reflectance Spectrum of Terrestrial Exoplanets
S. D. Guzewich, J. Lustig-Yaeger, R. Kopparapu, and M. J. Way 2022

What Does It Take to Glaciate? Exploring the Climatic Link Between Atmospheric Methane and the Rise of Oxygen
C. E. Harman, L. E. Sohl, E. T. Wolf, M. J. Way, K. Tsigaridis, and A. D. Del Genio 2060

Implementing a New Earth Based Dust Lifting Scheme in Mars Global Circulation Models
V. L. Hartwick and O. B. Toon 2055

Solar Forcing of the Abrupt Last Glacial Inception
F. He, P. U. Clark, and A. E. Carlson 2049

Evryscope Detection of the First Proxima Superflare: Impacts on the Atmosphere and Habitability of Proxima b
W. S. Howard, M. A. Tilley, H. T. Corbett, A. A. Youngblood, R. O. P. Loyd, J. K. Ratzloff, N. M. Law, O. Fors, D. del Ser, E. L. Shkolnik, C. A. Ziegler, E. E. Goeke, A. D. Pietraallo, and J. Haislip 2039

Spectral Content Variations Through a Solar Cycle and Abetting Decrease in Spectral Albedo of Glacial Ice
G. B. Hughes, J. Adams, and J. M. H. Cockburn 2004

GCM Experiments on Occurrence Condition of the Runaway Greenhouse State: Aquaplanets and Landplanets
M. Ishiwatari, S. Noda, K. Nakajima, Y. O. Takahashi, S. Takehiro, and Y.-Y. Hayashi 2059

Mars Climate and Volatile Evolution
B. M. Jakosky 2072

Using Deep Space Climate Observatory Measurements to Study the Earth as an Exoplanet
J. J. Jiang 2058

The Land Biosphere and Planetary Climate: Feedbacks to Habitability
N. Y. Kiang 2042

Cyclonic Activities on Jupiter and Earth; Catastrophic Atmospheric Phenomena of the Wave Nature: El-Nino, Cyclones, Tornado
G. G. Kochemasov 2009

The Emergent Linearity of Outgoing Longwave Radiation in a Moist Atmosphere: Implications for the Climates of Earth and Extrasolar Planets
D. D. B. Koll and T. W. Cronin 2015

The Atmospheric Circulation and Cloud Behavior in a Large Suite of Terrestrial Planet GCMs
T. D. Komacek and D. S. Abbot 2007

Comparison of Climate Sensitivity and Feedbacks Calculated by a Traditional and a New Equation
C. Kurt and A. E. Dessler 2066

Solar-Driven Climatology of Earth's Extended Environment
J. L. Lean 2016

Exploration of Planetary Atmospheres and Climates from an Energy Perspective
L. Li and X. Jiang 2011

Evolved Climates of the TRAPPIST-1 Planetary System
A. P. Lincowski, V. S. Meadows, D. Crisp, T. D. Robinson, R. Luger, and J. Lustig-Yaeger 2024

Climates of High Obliquity Terrestrial Planets in Idealized Simulations with a Seasonal Cycle
A. H. Lobo and S. Bordoni 2037

The Circulation and Volatile Cycles of Solar System Atmospheres
J. M. Lora 2030

Titan's Tropical Hydrological Cycle: Constraints from Huygens, Cassini, and Future Missions
R. D. Lorenz 2046

Current Status and Future Directions of Climate Modeling
D. R. Marsh 2071

Lessons from Akatsuki: Comparative Meteorology
K. McGouldrick 2062

Applying Science to Fiction: A Look at the Fictional Planet Mesklin
M. M. McKinney 2063

The Role of Atmospheric Pressure on Mars Surface Properties and Early Mars Climate Modeling
M. A. Mischna and S. Piqueux 2070

Comparative Climatology of Planets With and Without Global Ocean System
Y. Miura 2065

Employing Ray-Tracing to Probe Mars Atmosphere
T. N. Nikolaidou 2048

Online STEM Education and Aerospace Micro-Lesson in Nigeria (A Panacea to African Development)
A. O. Ogunbiyi 2003

Coevolution of Oceanic and Atmospheric Chemistry
S. L. Olson 2021

Generalizing the Habitable Zone: Temperate Continental Regions on Some Snowball Planets
A. Y. Paradise, K. Menou, D. Valencia, and C. Lee 2036

Reverse Weathering and Climate
N. J. Planavsky, T. T. Isson, and B. Kalderon-Asael 2045

Dynamics, Structure, and Importance of Deep Atmospheric Convection on Earth, Mars, and Titan
S. C. R. Rafkin 2032

The Role of Methane on an Icy Early Mars and in Exoplanetary Atmospheres
R. M. Ramirez, R. A. Craddock, and L. Kaltenegger 2001

The Importance of Anoxygenic Photosynthesis for Climate and Atmospheric Biosignatures on Reducing Worlds
C. T. Reinhard and K. Ozaki 2067

Revisiting the Early Earth's Methanogen Biosphere
A. J. Rushby, S. D. Domagal-Goldman, S. M. Som, A. Woffard, G. Arney, and T. Hoehler 2040

Atmosphere-Mantle Volatile Exchange Throughout Planetary Evolution
L. Schaefer 2047

Advancing the State of the Art of Martian Weather and Climate Modeling with Orbit-Spin Coupling
J. H. Shirley 2025

Atmospheric Circulations of Lakes and Seas on Earth and Titan
A. Soto and S. C. R. Rafkin 2028

The Exoplanet Yield Landscape for Future Space Telescope Missions
C. C. Stark, M. Bolcar, K. Fogarty, L. Pueyo, A. J. Eldorado Riggs, G. Ruane, R. Soummer, K. St. Laurent, and N. T. Zimmerman 2061

Did Outburst of Supermassive Black Hole Sagittarius A Cause an Extreme Glaciation on Earth?
T. T. Tao 2002

Computing Models of M-Type Host Stars and Their Panchromatic Spectral Output
D. Tilipman, J. L. Linsky, M. Vieytes, and K. France 2034

A Minimum Complexity Model for Investigating Long-Term Planetary Habitability
T. Tyrrell 2031

The Planetary Spectrum Generator (PSG): An Online Simulator of Exoplanets
G. L. Villanueva, M. D. Smith, S. Protopapa, S. Faggi, and A. M. Mandell 2017

Effects of Dipolar Magnetic Fields in Space Weather at Outer Magnetospheres
L. Wang, C. Dong, A. Hakim, A. Bhattacharjee, and K. Germaschewski 2074

How Studies of Ancient Earth Inform Studies of Ancient Venus: Venus' Evolutionary History and Its Implications for Venus-Like Exoplanetary Worlds
M. J. Way and A. D. Del Genio 2038

Venus' Early Potential for Habitability: Connecting Climate and Geologic Histories
M. B. Weller, A. Lenardic, M. Jellinek, J. Seales, and M. Way 2014

Abiotic Oxidation of Planetary Atmospheres: Physical Mechanisms and Consequences for Climate, Habitability, and Biosignatures
R. D. Wordsworth 2020

Increased Ice Coverages on TRAPPIST-1e, LHS 1140b, and Proxima b by Sea Ice Dynamics
J. Yang and W. Ji 2005

Climatic Effect of Impacts on the Ocean
K. J. Zahnle 2056

The diversity of climate states of terrestrial planets. D. S. Abbot[1], [1]The Department of the Geophysical Sciences, The University of Chicago, abbot@uchicago.edu.

This is a review talk about the diversity of climate states of terrestrial planets. It will focus on planets that are habitable (have surface liquid water), could have been in the past, or could be in the future. I will give an introduction to the Habitable Zone, the extended H2 Habitable Zone, the dry planet Habitable Zone, the snowball (including climate cycling), the moist greenhouse state, and the runaway greenhouse state.

VENUS: THE EXOPLANET LABORATORY NEXT DOOR. G. N. Arney[1,2,3] and the Venus Exploration Analysis Group (VEXAG), [1]NASA Goddard Space Flight Center (giada.n.arney@nasa.gov), [2]The Virtual Planetary Laboratory, [3]The Sellers Exoplanets Environments Collaboration

Introduction: Venus is the most Earth-like planet in the solar system in terms of its size, mass, and bulk composition, yet the surface conditions of these two worlds could not be more different. Venus has the hottest terrestrial surface in the solar system. Despite this, Venus may once have hosted clement conditions in its deep past, possibly even with an ocean. Here, we will review what present and past Venus teaches us context of comparative planetology and processes that shape habitability and biosignature "false positives" in exoplanet atmospheres.

Ground-truth information from "our" Venus can inform and constrain our interpretations of data from exo-Venus analogs. Important for future observations of exoplanets, Venus-analogs represent one of the most readily observable types of terrestrial planets for the transit transmission observations [1] that will become possible in the near future with the James Webb Space Telescope. This is because Venus-analog worlds orbit closely to their stars and therefore enjoy a higher transit probability and frequency of transit events compared to planets in the habitable zone. Indeed, many terrestrial exoplanets already discovered, and undoubtedly many that will be uncovered by TESS, are likely to be more Venus-like than Earth-like.

However, understanding the processes that affect Venus-like exoplanets will be particularly challenging in the context of characterizing these distant and data-limited worlds. The Venusian environment is a natural laboratory next door to study the complex processes that operate on this type of planet and that can cause the loss of habitability on hot terrestrial worlds.

The atmosphere of Venus hosts an elevated D/H ratio, ~150 x Earth's, that suggests massive water loss in the past [2]: early Venus may have had oceans. However, even at its formation, Venus would have been interior to the inner edge of the solar system's "conservative" habitable zone [3]. Its early putative habitability is therefore a provocative question. Recent 3-D modeling efforts have suggested that a slowly-rotating planet like Venus can generate a thick subsolar cloud deck that would substantially cool the planet, producing surface temperatures that could allow for liquid water for potentially billions of years [4]. These same processes have also been applied to tidally-locked, slowly-rotating planets orbiting M dwarfs, including planets interior to the inner edge of their stars' traditional habitable zones [5]. If hot, slowly-rotating exoplanets are observed to be habitable, this may shed light on processes that operated on Venus in the past to permit the existence of liquid water.

Photochemical and atmospheric loss processes that occur on Venus may also help us to understand the plausibility of mechanisms that could generate abiotic oxygen in exoplanet atmospheres [6], which has important implications for our understanding of oxygen as a robust biosignature for exoplanets.

Massive water loss has been invoked as a possible "false positive" mechanism to generate large quantities of abiotic O_2 in exoplanet atmospheres, including on M dwarf planets within their stars' habitable zones that experience the super-luminous pre-main sequence phase of their stars [7]. Venus may have undergone massive water loss in its past, and photolysis of its H_2O would lead to loss of the lightweight H_2 to space. The fate of the liberated O is less well constrained, but Venus does not exhibit an O_2-rich atmosphere today. The strong "electric wind" recently observed at Venus [8] can strip O+ to space. The unexpected strength of the Venusian electric wind has been suggested to be due to Venus' closer proximity to the sun than Earth, causing it to receive more ionizing radiation. Planets orbiting closely to M dwarfs may experience even stronger electric winds, with important implications for the retention of oxygen and other heavy atmospheric species.

Today on Venus, atmospheric CO_2 is photolytically dissociated to produce oxygen-bearing photochemical products. Recombination of excited O_2 produced by this process generates airglow observable at 1.27 μm on the nightside of Venus, but ground-state O_2 has not been detected on Venus, suggesting rapid removal from the atmosphere, possibly due to catalytic chlorine chemistry [9]. The mechanisms that remove O_2 from the Venus atmosphere have not been included in studies examining the possibility of abiotic O_2 production and accumulation on exoplanets, in large part because these processes are still not well understood. Therefore, better understanding the processes involving O_2 in the Venusian atmosphere are vitally important for understanding the viability of multipe proposed oxygen false positive mechanisms for exoplanets.

Venus is a key player in shaping our understanding of planetary habitability as a dynamic process that

evolves over time. As a world of extremes in temperature and pressure, Venus is particularly useful for model validation across a range of conditions. And because exoVenus planets may be cosmically ubiquitous, it is particularly important to better understand the world next door so that we may be able to better interpret future observations of analog worlds.

References:

[1] Kane, S. R., Kopparapu, R. K., & Domagal-Goldman, S. D. (2014). On the frequency of potential Venus analogs from Kepler data. *The Astrophysical Journal Letters*, *794*(1), L5 [2] Donahue, T. M., & Russell, C. T. (1997). The Venus atmosphere and ionosphere and their interaction with the solar wind: An overview. In *Venus II: Geology, Geophysics, Atmosphere, and Solar Wind Environment* (p. 3). [3] Kopparapu, R. K., Ramirez, R., Kasting, J. F., Eymet, V., Robinson, T. D., Mahadevan, S., et al. (2013). Habitable zones around main-sequence stars: new estimates. *The Astrophysical Journal*, *765*(2), 131. [4] Way, M. J., Del Genio, A. D., Kiang, N. Y., Sohl, L. E., Grinspoon, D. H., Aleinov, I., et al. (2016). Was Venus the first habitable world of our solar system?. *Geophysical research letters*, *43*(16), 8376-8383. [5] Kopparapu, R., Wolf, E. T., Haqq-Misra, J., Yang, J., Kasting, J. F., Meadows, V. et al. (2016). The inner edge of the habitable zone for synchronously rotating planets around low-mass stars using general circulation models. *The Astrophysical Journal*, *819*(1), 84. [6] Meadows, V. S. (2017). Reflections on O2 as a Biosignature in Exoplanetary Atmospheres. *Astrobiology*, *17*(10), 1022-1052. [7] Luger, R., & Barnes, R. (2015). Extreme water loss and abiotic O2 buildup on planets throughout the habitable zones of M dwarfs. *Astrobiology*, *15*(2), 119-143. [8] Collinson, G. A., Frahm, R. A., Glocer, A., Coates, A. J., Grebowsky, J. M., Barabash, S., et al. (2016). The electric wind of Venus: A global and persistent "polar wind"-like ambipolar electric field sufficient for the direct escape of heavy ionospheric ions. *Geophysical Research Letters*, *43*(12), 5926-5934. [9] Yung, Y. L., & DeMore, W. B. (1982). Photochemistry of the stratosphere of Venus: Implications for atmospheric evolution. *Icarus*, *51*(2), 199-247.

Hazardous Risks of Long-Term Non-Ionizing Electromagnetic Radiation on the Astronauts' Brain In Deep Space

Davud Asemani, Ph.D. and Donna R. Roberts Author, M.D.
Neuroradiology Group, Department of Radiology, Medical University of South Carolina, Charleston, SC29407
asemani@musc.edu

Introduction:

The space environment beyond the earth's atmosphere contains different types of ionizing radiation. For the missions in deep space, galactic cosmic radiation (GCR) ions, originated from outside the solar system, contain highly energetic protons and alpha particles, with a small component of high charge and energy (HZE) nuclei moving at relativistic speeds and energies (Simpson 1983). In addition to GCR, unpredictable and intermittent solar particle events (SPEs) can produce large plasma clouds containing highly energetic protons and some heavy ions that may cause a rapid surge of radiation both outside and within a spacecraft (Chancellor, Scott et al. 2014). Exposure to these space radiation affects multiple organs and physiological systems in complex ways (see Figure 1) (Chancellor, Scott et al. 2014). Space radiation is the number one risk to astronaut health on extended space exploration missions beyond the Earth's magnetosphere. Exposure to space radiation increases the risks of astronauts developing cancer, experiencing central nervous system (CNS) decrements, exhibiting degenerative tissue effects or developing acute radiation syndrome. The NASA reports exhibit evidences for radiation-induced health risks and makes recommendations on areas requiring further experimentation to enable future space missions beyond LEO (Schauer and Linton 2009). These four space radiation risks are carcinogenesis, degenerative tissue effects, CNS decrements and acute radiation syndrome (Cucinotta, Manuel et al. 2001, Huff and Cucinotta 2009).

Objective: Only 24 human beings have ventured beyond the Earth atmosphere protective envelope, and then, only for a maximum of approximately 12 days (Apollo 17) (Chancellor, Scott et al. 2014). However, the effects of non-ionizing radiation such as infra-red (IR) and microwave electromagnetic waves have rarely been taken under serious consideration for space climate studies. We hypothesize that the long-term exposure to these kind of radiation, potentially possible on the spaceflight expeditions, may result in serious helath concerns particularly on brain. A small elevation of intracranial temperature can potentially lead to an increase in the intracranial pressure. This is caused by both higer metabolism rate across brain, and a larger cerebrospinal fluid (CSF) production rate at the choroid plexus.

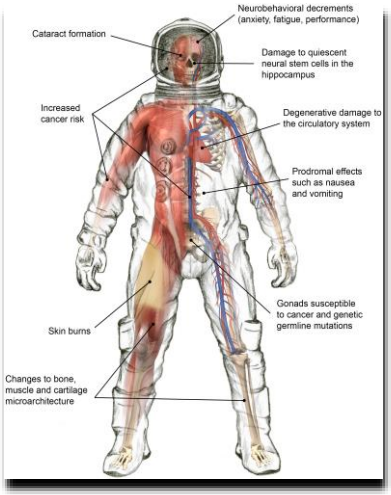

Figure 1. Effects of exposure to space radiation on physiological systems (Chancellor, Scott et al. 2014).

Potential risk of space climate on brain: The evidence for above-mentioned hypothesis comes from brain hypthermia studies and treatment. Brain hypothermia, first reported scientifically by Fay in 1943, has been widely

applied in today's ICU to patients with severe brain injury, cerebral ischemia, cardiac arrest and so on (Gaohua and Kimura 2006). Brain hypothermia treatment is used as a neuro-protectant to decompress the elevated intracranial pressure (ICP) in acute neuro-patients. Gaohua and Kimura developed a general mathematical model integrating hemodynamics and biothermal dynamics to enable a quantitative prediction of transient responses of elevated ICP to ambient cooling temperature (Gaohua and Kimura 2006). The temperature dependence of metabolism in tissue, known as the van't Hoff's effect (Q-effect), and the temperature dependence of capillary filtration, described by the Arrhenius' law (A-effect), were incorporated into the mathematical model to describe the hypothermic effect on physiological functions. They found a model of hypothermic decompression for ICP as a function of cooling temperature that implies: gain of about 4.9mmHg/°C, dead time of about 1.0 h and a time constant of about 9.8 h (Gaohua and Kimura 2006). In contrast, a sub-degree elevation of intracranial temperature is capable of increasing the ICP as much as twice the normal pressure. This is exacerbated by synergistic effects of microgravity exposure.

Space flight puts both the crew and the mission instruments above the filtering effects of the atmosphere on Earth, making the entire electromagnetic spectrum available (Administration 1997). So, the IR and microwave radiation can be prevalent throughout the mission outside the earth's atmosphere. A long-term mission will end up in a high risk of continuous exposure of body to these heating waves and possibly elevating intracranial temperature.

Microgravity Effects on Brain: Our research group has already studied the microgravity effects on the cerebral systems (Roberts, Albrecht et al. 2017). In that study on the effects of spaceflight, the volumes of ventricles and the brain were computed for both pre- and post-flight scans of astronauts. The volume of brain included the entire parenchyma and both sulci and ventricular CSF. There was a significant enlargement of the ventricles post-flight compared to the pre-flight values (14% increase post-flight, p=0.001). In addition, our analysis showed that a global linear change is found in the brain of the astronauts returning to the earth following to a long-duration stay in the international space station. This linear change includes superior shift (+0.6mm) and stretching (+0.66%) along with a lateral compression (-0.3%) as shown in the Figure 2.

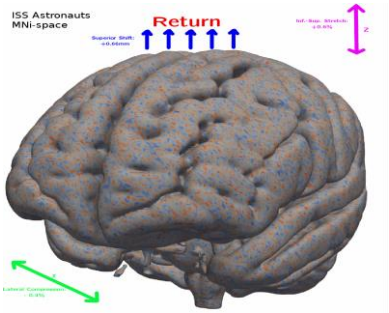

Figure 2. The global linear changes occurring on the brain parenchyma of the astronauts returning to the earth after a long-duration stay in the international space station.

Administration, N. A. a. S. (1997). "Microgravity: A Teacher's Guide With Activitiesin Science, Mathematics, and Technology."

Chancellor, J. C., G. B. Scott and J. P. Sutton (2014). "Space radiation: the number one risk to astronaut health beyond low earth orbit." Life **4**(3): 491-510.

Cucinotta, F., F. Manuel, J. Jones, G. Iszard, J. Murrey, B. Djojonegro and M. Wear (2001). "Space radiation and cataracts in astronauts." Radiation research **156**(5): 460-466.

Gaohua, L. and H. Kimura (2006). "A mathematical model of intracranial pressure dynamics for brain hypothermia treatment." Journal of Theoretical Biology **238**: 882–900.

Huff, J. and F. A. Cucinotta (2009). "Risk of degenerative tissue or other health effects from radiation exposure." Human Health and performance risks of space exploration missions National Aeronautics and Space Administration, NASA SP-2009-3405, Houston, TX: 213-235.

Roberts, D. R., M. H. Albrecht, H. R. Collins, D. Asemani, A. R. Chatterjee, M. V. Spampinato, X. Zhu, M. I. Chimowitz and M. U. Antonucci (2017). "Effects of Spaceflight on Astronaut Brain Structure as Indicated on MRI." Th e new england journal o f medicine **377**(18): 1746-1753.

Schauer, D. A. and O. W. Linton (2009). National Council on Radiation Protection and Measurements report shows substantial medical exposure increase, Radiological Society of North America, Inc.

Simpson, J. (1983). "Elemental and isotopic composition of the galactic cosmic rays." Annual Review of Nuclear and Particle Science **33**(1): 323-382.

HYDROCARBON CONDENSATION ON TITAN AND PLUTO: COMARISONS USING PLANETCARMA. E. L. Barth, Southwest Research Institute, 1050 Walnut Street, Suite 300, Boulder, CO 80301

Introduction: Despite differences in composition and temperature regime, there are common physical processes operating within the atmospheres of the terrestrial-type planetary bodies in our Solar System. The Community Aerosol and Radiation Model for Atmospheres (CARMA) [1] has been updated to include atmospheres of the Solar System outside of Earth. CARMA, as its name suggests, is a coupled aerosol microphysics and radiative transfer model and includes the processes of nucleation, condensation, evaporation, coagulation, and vertical transport. Previous model versions have been applied (by this and other groups) to the atmospheres of Solar System bodies and extrasolar planets. The primary advantage to our version, which we now call PlanetCARMA, is that the core physics routines each reside in their own self-contained modules and can be turned on/off as desired while a separate planet module supplies all the necessary parameters to apply the model run to a particular planet (or planetary body). So a single codebase is used for all planetary studies. Our CARMA model is also now written in Fortran 90 modular format.

Titan: Many of the trace gases created from photochemical reactions involving N_2 and CH_4 in Titan's atmosphere become supersaturated in the lower stratosphere and are likely to form ices on the organic haze particles present. The simulations [2] show ices formed from more than a dozen trace species which include hydrocarbons, nitriles, and CO_2. Ices form and settle into layers between 50 and 80 km (Figure 1). Condensation timescales can be slow, with half the species only growing to a radius $\lesssim$1 μm. Ethane particles grow the largest with radii up to 20 μm. A number of factors, including the vapor pressure equation, nucleation rate, gas abundance, and temperature profile, can have a significant effect on the appearance of the ice particles.

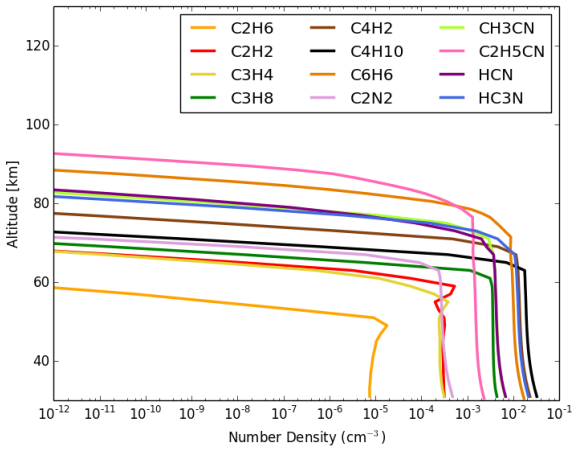

Figure 1. Stratospheric ice layers on Titan.

Pluto: The New Horizons missions has brought us many new insights into conditions in Pluto's atmosphere. Trace species such as C_2H_6, C_2H_2, C_2H_4 and HCN have been confirmed. Given the entry and exit temperature profiles measured by the spacecraft as well as the abundances of these species, each (along with CH_4) will be highly supersaturated near Pluto's surface. Simulations [3] show that each of the above listed species will nucleate onto pre-existing haze particles for the entry temperature profile (Figure 2), whereas only C_2H_6, C_2H_2, and HCN nucleate using the higher surface temperature exit profile. HCN ices form at the highest altitudes ~15 km above the surface. C_2H_6 and C_2H_2 ices form at similar altitudes, 8-10 km at the entry site and below 5 km at the exit site. CH_4 and C_2H_4 ices only form near the surface at the entry site. The cold temperatures near Pluto's surface play an important role in the efficiency of the nucleation and subsequent condensation processes, controlling the number and size of the ice particles.

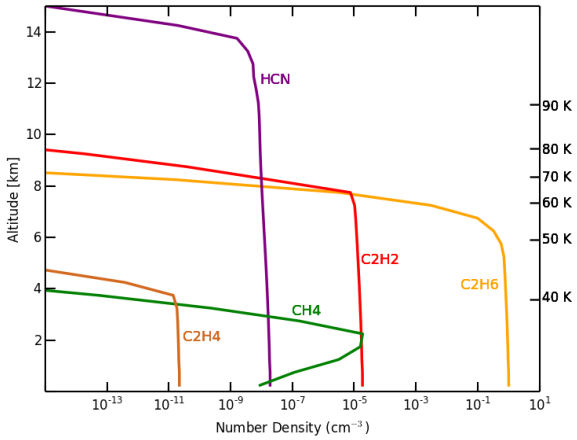

Figure 2. Condensation of methane and Pluto's trace species at the New Horizons entry site.

Summary: The new CARMA framework allowing multiple planetary atmospheres to be modeled will be presented along with a comparison of the hydrocarbon and nitrile microphysics in the atmospheres of Titan and Pluto.

References:

[1] Turco et al. (1979) *J. Atmos. Sci., 36,* 699-717.
[2] Barth (2017) *Planet. Space Sci., 137,* 20-31.
[3] Stern et al. (2017) *AJ, 154,* 43.

SIMULATIONS OF METHANE ON MARS UTILIZING CURIOSITY DATA. A.V.Britt[1,2,3] and S.Domagal-Goldman[2], [1]Fisk University 1000 17th Ave N Nashville, TN 37208, [2]NASA Goddard Space Flight Center 8800 Greenbelt Rd Greenbelt, MD 20771,[3]Vanderbilt University 2201 West End Ave Nashville, TN 37235.

Introduction: The presence of methane in the Martian atmosphere has been a photochemical mystery, in particular following the claims of high concentrations (24±10 ppb) and significant temporal and spatial variability based on Earth-based observations of Mars[1]. These variations on the timescale of Martian seasons were inconsistent with photochemical models[2] that suggest the lifetime of methane on Mars should be ~300 years. Missions like Mars Science Laboratory (MSL) have since then, shed some light on this methane mystery, with various measurements taken with the Sample Analysis at Mars instrument (SAM). SAM has detected lower CH_4 concentrations, but also has observed variations in the CH_4 concentrations. This variance in signal suggests a very localized source at the surface with a seasonal dependence that we have investigated using modeling techniques.

Methods: We utilized a 1D photochemical model to produce steady-state atmospheric simulations; we calculated the surface flux needed to sustain methane at the highest and lowest MSL measured methane concentrations. For these simulations, used time dependent calculations corresponding with solar angle calculations to evaluate the time dependence and seasonal dependence of methane in simulated atmospheres. We also calculated the fluxes needed to sustain the background measurements taken by SAM while incorporating REMS (Rover Environmental Monitoring Station) UV measurements.

Results: Our findings suggest that it is theoretically possible to build up methane on time scales consistent with MSL measurements using the required methane fluxes calculated from steady-state simulations. However, we find that the breakdown at that magnitude takes longer than the observational timescale (Figure1).

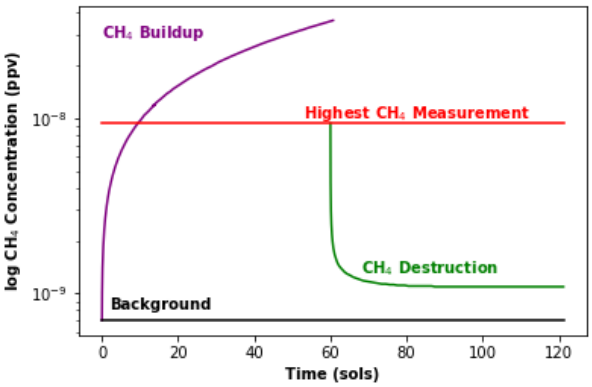

Figure1: Illustrated above is the temporal buildup and breakdown of methane at the site of highest measured methane, using timescales consistent with Curiosity observations.

In Addition, by finding a range of fluxes needed to sustain the background methane measurements taken by SAM, we are able to reproduce seasonal variation of methane using solar angle and REMS UV measurements (Figure2). Taken together, these simulations and the MSL-SAM data are all consistent with a low background flux of methane modulated by seasonal UV fluxes, and a one-time local/regional release of methane that afterwards dissipated in the Martian atmosphere.

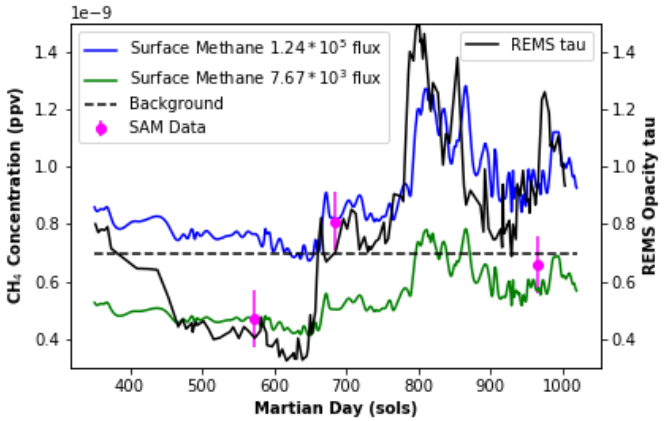

Figure2: Shown above are the steady state calculations for surface methane concentration for a whole Martian year utilizing REMS UV measurements. Notice that variations in the background concentration are reproduced and we are able to predict individual MSL-SAM measurements with a range of fluxes.

Conclusion: This work helps constrain the different sources of methane near the surface, and reconcile the measurements with photochemical modeling. We suggest that by starting at the measured background concentrations it is possible to create MSL methane concentrations on short time scales consistent with observations. Additionally, we can explain much of the seasonal variation assuming different sources of methane throughout the Martian year.

References:

[1] M. J. Mumma et al. (2009) Science, 323, 1041-1045.[2] K. Zahnle, R. Freedman, D. Catling (2011) *Icarus, 212*, 493-503.

LABORATORY INVESTIGATIONS CONNECTING TERRESTRIAL CLIMATES TO ICY WORLDS.

M. L. Cable, NASA Jet Propulsion Laboratory, California Institute of Technology, 4800 Oak Drove Dr., Pasadena, CA 91109 (Morgan.L.Cable@jpl.nasa.gov).

Introduction: Other than Earth, there are five bodies in the solar system that possess atmospheres thick enough to apply terrestrial climate models: Venus, Mars, Titan, Triton and Pluto. Of these, the latter three are considered icy worlds, where water-ice and other condensed volatiles (CH_4, N_2, CO_2, CO, NH_3) dominate on the surface. Application of terrestrial climate models to these icy worlds can provide insights into formation mechanisms and ongoing processes. The accuracy of such models improves significantly with constraints provided either by in situ data or laboratory experiments.

Titan: The largest moon of Saturn, Titan hosts a large chemical inventory of organic compounds. Photochemistry in the atmosphere induced by solar radiation and energy from Saturn's magnetosphere causes a chemical cascade, as N_2 and CH_4 dissociate and generate organic molecules ranging from simple (ethane, acetylene, HCN) to complex (>10,000 Da). These molecules continue to react as they move through Titan's atmosphere, forming aerosol haze layers and eventually depositing on the surface [1]. Climate models of Titan are useful to understand and interpret the complex chemical and physical processes driving atmospheric circulation, seasonal variations, haze formation and dynamics, the distribution of surface liquid methane and ethane, and the formation and distribution of condensate clouds [2].

Titan climate models are often based initially on Earth models – for example a global circulation model (GCM) of Titan's atmosphere and surface reported in 2009 was a modified version of the National Center for Atmospheric Research (NCAR) Community Atmosphere Model (CAM3) [2]. Another 3-D climate model was developed using the LMDZ4 General Circulation Model dynamical core developed by Laboratoire de Météorologie Dynamique (LMD) for Earth, adapted for Titan's atmosphere [3]. More recently, a GCM was developed which uses a physics package based on the Geophysical Fluid Dynamics Laboratory (GFDL) atmospheric component models coupled to the fully three-dimensional Flexible Modeling System (FMS) spectral dynamical core [4]. These Earth climate models must be used judiciously. The radiative timescale of the Titan atmosphere is much longer (~150 Earth years [5]); tidally driven surface winds are also important on Titan but not Earth [6].

Laboratory experiments have supported Titan climate model development in two key ways: (1) providing chemical and physical constants for the molecular constituents of the Titan atmosphere, and (2) bounding optical and physical properties for the particles that make up the Titan haze. The first is relatively straightforward – chemical and physical constants such as photoionization energies, kinetic rates and reactions, and phase diagrams have been experimentally determined and serve as inputs to climate models.

Modeling results for Titan's haze layers depend on the haze particle physical properties (fractal dimension, monomer radius, number of monomers) which influence sedimentation velocity coupling with the meridional circulation [7]. Haze particle size distribution is also critical for Titan, as this informs haze transport – models require active haze transport in order to correctly model heating rates and thus the circulation [8]. Experimental characterization of the Titan haze is challenging, as it is difficult to generate in a laboratory setting; tholins, the complex organics generated experimentally, vary widely in their physical and chemical properties [1]. However, experiments have still been useful to inform models. GCMs for Titan assume particle formation growth via fractal aggregates [3], which has been verified experimentally [9].

Up until fairly recently (2012), modelers used the optical constants of Titan tholins measured by Khare et al. in 1984, who determined refractive indices spanning wavelengths from the far infrared to the X-ray domain [10]. While tholins are similar to Titan aerosols in the shorter wavelength region (<900 nm), they are more absorbent in the thermal infrared, so more recent models utilize a correction to the tholin optical constants in this region.

Pluto: This dwarf planet represents a special case in the application of terrestrial meteorology to an icy world. Its atmosphere is significantly warmer than the surface, increasing from surface values of 38–55 K to approximately 110 K at 20 km and 70–80 K at around 200 km [11, 12]. The atmosphere also has a long radiative timescale (several Earth years), and circulation dominated by condensation/sublimation processes of N_2. Recently a 3D GCM was generated for Pluto to simulate the 2015 New Horizons observations [13]. Key processes were parameterized based on equations including atmospheric dynamics and transport, turbu-

lence, radiative transfer, molecular conduction, as well as phases changes for N_2, CH_4 and CO. Laboratory measurements of these properties informed these processes.

The evolution of pressure on Pluto is highly sensitive to N_2 and CH_4 ice radiative properties, such as albedo and emissivity [14]. These properties are significantly modified by the presence of photochemically-produced complex organics (i.e., tholin). Atmospheric models rely on laboratory measurements to constrain these values (often the same values as are used for Titan).

Solid molecular nitrogen exhibits a phase transition at low temperature. Below 35.6 K, N_2 is present as the cubic α phase; above 35.6 K, it is present in the lower-density hexagonal β phase [15]. Laboratory measurements in the near-infrared of α and β nitrogen ice have shown a complex, temperature-dependent pattern involving several weak features in addition to the strong, narrow band attributed to a double phonon transition [16]. Due to this temperature dependence, the NIR spectrum of N_2 ice (specifically the 2.16-micron overtone band) can be used as a spectral thermometer [17]. These laboratory measurements have been used to constrain the surface temperature of N_2-rich bodies such as Triton and Pluto.

New Horizons revealed the presence of extensive hazes believed to be composed primarily of organic particles produced indirectly by methane photolysis [12]. Models of the formation and transport of these particles [18] are based on laboratory measurements (e.g. [19-21]).

Triton: The largest moon of Neptune, Triton's atmosphere is similar in composition and surface pressure to Pluto. Also like Pluto, Triton has a steep, low-altitude temperature inversion [22] which makes analogies between other solar system bodies such as Mars and Titan difficult. Due to the similarities between Triton and Pluto, often the same or similar climate models can be applied to both [23].

Unlike Pluto, Triton has plumes – likely produced by sublimation of multiple nonpolar gases – that rise from the surface and are sheared off at an altitude of approximately 8 km [24]. Recent modeling efforts reveal that the behavior of the plumes once they have been released into the atmosphere is due to dynamical properties (i.e., strong wind shear) in the lower atmosphere, as opposed to thermal effects [23].

Triton climate modeling efforts face difficulties in that the surface and subsurface parameters (e.g., albedo, surface thermal inertia, and emissivity) still are not well constrained [25]. Laboratory measurements may help to better bound these parameters.

Conclusions: Laboratory measurements are tied to climate models of icy worlds in a variety of ways. As the complexity of these models continues to advance, more detailed measurements of chemical and physical properties of volatiles, simple and complex organics and haze particles under the appropriate conditions will improve the accuracy and fidelity of those models to better understand these alien worlds.

Acknowledgements: This work was conducted at the Jet Propulsion Laboratory, California Institute of Technology, under contract with NASA.

References: [1] Cable, M.L. et al. (2012) *Chem. Rev., 112,* 1882-1909. [2] Friedson A.J., West R.A., Wilson E.H., Oyafuso F. and Orton G.S. (2009) *Planet. Space Sci.*, 57 (14-15) 1931-1949. [3] Lebonnois S., Burgalat J., Rannou P. and Charnay B. (2012) *Icarus*, 218 (1), 707-722. [4] Lora J.M., Lunine J.I. and Russell J.L. (2015) *Icarus*, 250, 516-528. [5] Flasar, F.M., Samuelson R. E. and Conrath B.J. (1981) *Nature*, 292, 693-698. [6] Tokano T. and Neubauer F.M. (2002), *Icarus*, 158, 499-515. [7] West R.A., Seignovert B., Rannou P., Dumont P. et al. (2018) *Nature Astron.*, 2, 495-500. [8] Newman C.E., Lee C., Lian Y., Richardson M.I. and Toigo A.D. (2011) *Icarus*, 213 (2), 636-654. [9] Imanaka H., Khare B.N., Elsila J.E., Bakes E.L.O. et al. (2004) *Icarus*, 168 (2), 344-366. [10] Vinatier S., Rannou P., Anderson C.M., Bezard B. et al. (2012) *Icarus*, 219, 5-12. [11] Hinson D.P., Linscott I., Tyler L., Bird M., Paetzold M., Strobel D., et al. (2015) *AAS/Division Planetary Sci. Meeting*, Vol. 47, 105.01. [12] Gladstone G.R., Stern S.A., Ennico K., Olkin C.B., et al. (2016) *Science*, 351 (6279), aad8866. [13] Forget F., Bertrand T., Vangvichith M., Leconte J., Millour E. and Lellouch E. (2017) *Icarus*, 287, 54-71. [14] Young L.A. (2013) *Astrophys. J.*, 766, L22. [15] Scott T.A. (1976) *Phys. Rep.*, 89-157. [16] Grundy W.M., Schmitt B. and Quirico E. (1993) *Icarus*, 105 (1), 254-258. [17] Tryka K.A., Brown R.H., Cruikshank D.P. et al. (1994) *Icarus*, 112, 513-527. [18] Bertrand T. and F. Forget (2017) *Icarus*, 287, 72-86. [19] Coll, P., Coscia D., Smith N., Gazeau M.-C. et al. (1999), *Planet. Space Sci.*, 47, 1331-1340. [20] Tran B.N., Force M., Briggs R.G., Ferris J.P. et al. (2008) *Icarus*, 193, 224-232. [21] Nna-Mvondo D., de la Fuente J.L., Ruiz-Bermejo M., Khare B. and McKay C.P. (2013) *Planet. Space Sci.*, 85, 279-288. [22] Strobel D.F. and Summers M.E. (1995) in: Cruikshank D.P., Matthews M.S., and Schumann A.M. (Eds.), Neptune and Triton, 1107–1148. [23] Zalucha A.M. and Michaels, T.I. (2013) *Icarus*, 223 (2), 819-831. [24] Smith B.A., Soderblom L.A., Banfield D., et al. (1989) *Science*, 246, 1422-1449. [25] Young L.A. (2012) *Icarus*, 221 (1), 80-88.

USING EXOPLANET CLIMATE SIMULATIONS AS A TOOL FOR CONSTRAINING ASTROECOLOGY MODELS. A.Y. Ceja[1*] and S. R. Kane[1†], [1]University of California, Riverside, Department of Earth Sciences, 900 University Ave., Riverside, CA, 92521, [*]aceja005@ucr.edu, [†]skane@ucr.edu.

Introduction: The field of astrobiology aims to identify other habitable worlds. To date, thousands of exoplanets with a diversity of properties have been discovered, some of which are potentially habitable [1]. Exoplanet habitability is primarily determined by surface climate conditions. The habitability of Earth, for example, is chiefly a consequence of continually (relatively) mild ambient temperatures [2,3,4]. Thus, on first order, exoplanet habitability must be constrained by surface temperature conditions.

Exoplanet temperature profiles are often explored with the use with the use of General Circulation Models (GCMs) [5]. GCMs take as inputs key orbital parameters to simulate the probable climate generated by a planet with such properties. Orbital eccentricity and obliquity regulate the received stellar radiative flux on a planet, thus these parameters drive surface temperature conditions [6] and habitability. For an Earth-like planet in the circumstellar habitable zone (CHZ) with variable eccentricity and obliquity, time-dependent surface temperatures may be significantly perturbed.

In this research, a modeling approach is outlined for which simulated temperature profiles of Earth analogs on variable eccentric and oblique orbits serve as environmental inputs for a previously developed astroecology model. The simulations are run with the program Resolving Orbital and Climate Keys of Earth and Extraterrestrial Environments (ROCKE-3D) [7], a fully-coupled 3-dimensional GCM developed at the NASA Goddard Institute for Space Studies.

Methods: ROCKE-3D is used to produce temperature profiles of Earth analogs on variable eccentric and oblique orbits. These thermal profiles serve as environmental inputs for a previously developed agent rule-based astroecology model. The astroecology model is used to determine thresholds in eccentricity and obliquity of eta-Earths based upon thermophysiological limits of terrestrial organisms. This model will be applied for confirmed CHZ exoplanets.

Conclusions: The applied methodology will place eccentricity and obliquity limits for the habitability of Earth-like planets. CHZ exoplanets with these parameters will be recommended as high-priority targets for future missions (e.g. *James Webb Space Telescope*). Confirmed CHZ exoplanets found to be suitable for terrestrial organisms are termed habitable (concerning only temperature and liquid water). Further, these analyses will identify types of organisms viable to survive on a given exoplanet climate. Thus, we can exploit the known metabolic byproducts to identify potential sources of observable biosignatures of the recommended exoplanet targets.

References: [1] Petigura E. et al. (2013) *PNAS*, *110*, 19273-19278. [2] Huey R.B. and Kingsolver J.G. (1989) *Trends Ecol. Evol.*, *4*, 131-135. [3] Stillman J.H. and Somero G. (1996) *JEB*, 199, 1845-1855. [4] Miller L. et al. (2009) *Fun. Eco.*, 23, 756-767. [5] Woodsworth R. et al. (2015) *JGR*, 120, 1201-1219. [6] Kaspi Y. and Showman A.P. (2015) *ApJ*, 804, 1-18. [7] Way M.J. et al. (2017) *ApJ*, 231, 12-34.

EFFICIENT ATMOSPHERIC MODEL EQUILIBRIUM SEARCHING AND ASSESSMENT

Colin Orion Chandler[1] and Tyler D. Robinson[1]

[1] *Department of Physics & Astronomy, Northern Arizona University, PO Box 6010, Flagstaff, AZ 86011, USA; orion@nau.edu*

1. INTRODUCTION

Climate models are increasingly important to the hunt for life outside our solar system. Upcoming space telescopes (e.g., James Webb Space Telescope) will require weeks or months of integration time in order to probe an exoplanetary atmosphere (Cowan et al. 2015). Any target selected must be thoroughly vetted to ensure the best chance for recovering spectral features of a potentially habitable world.

One-dimensional radiative-convective models provide an efficient method for exploring and understanding the potential climate states of an exoplanet. Such one-dimensional models typically search for an equilibrium atmospheric state given a set of boundary conditions (e.g., the host stellar flux incident on the world) and assumptions about the atmospheric composition (e.g., a composition that is fixed or defined by thermochemical equilibrium). Commonly, an equilibrium climate solution is one that adjoins a convective adiabat in the deep atmosphere to a radiative zone in the upper atmosphere. The task of the one-dimensional climate model is, then, to seek out the radiative-convective boundary that yields an equilibrium climate solution.

Many of the most widely-adopted one-dimensional radiative-convective climate models (McKay et al. 1989; Kasting et al. 1993; Marley et al. 1996) are written in programming language standards that are now out-of-date. Thus, modern packages designed to enable parallelization of computational models cannot be straightforwardly applied to these legacy tools. Here, we explore techniques for increasing the computational efficiency of one-dimensional radiative-convective models. Critically, these techniques do not require implementation of sophisticated parallel-computing algorithms, and are designed to be adopted into legacy models.

2. MODEL DESCRIPTION

For our investigations, we adopt the Marley-Saumon-Fortney one-dimensional brown dwarf and exoplanet climate model (Marley et al. 1996; Fortney et al. 2008). This tool produces a temperature-pressure profile for an atmosphere in radiative-convective equilibrium, and also provides visible and infrared spectra at coarse resolution. The model incorporates numerous parameters potentially affecting climate and habitability, such as host stellar effective temperature and size, planet orbital distance, fraction of cloud coverage, and the condensable species (e.g., water) contained in those clouds.

Myriad input parameters provide flexibility when producing model atmospheres, but one challenging effect is that, in some circumstances, a range of potential near-equilibrium solutions are possible. Ensuring the resulting models are nearest to equilibrium, and thus physically realistic, is critical in evaluating the success of any atmospheric model. Moreover, each model run and corresponding evaluation requires significant computation.

A simple case to model is a free-floating (i.e., not orbiting a star) cloud-free brown dwarf. Typical compute time, given an uninformed guess for the initial atmospheric thermal structure, is 10 minutes. If we vary any one boundary condition (e.g., internal heat flux) N times, then we require N times as much compute time. If, for example, we use 6 different initial internal heat fluxes for a brown dwarf thermal structure grid, then we require one compute hour to execute.

More complicated models (e.g., a Jupiter-type planet with partial surface coverage by clouds formed from several condensing species) can take roughly an hour for a single model run (again, given an uninformed initial guess for the atmospheric state).

To provide a sense for what takes place during a model run, let us consider the initial steps. Our model begins with an initial user-provided "guess" as to where a radiative-convective boundary exists. This boundary describes the place in an atmosphere (usually in the upper troposphere) where the atmosphere thins enough to become less opaque to infrared energy, and radiation becomes the dominant method of heat transfer (Catling & Kasting 2017). If the initial guess does not lead to a solution, the model tries again using a nearby level.

Once a solution is found that is valid, the model is said to have converged. Success is mediated by a predefined error tolerance that comes into play during convergence checking. Unsurprisingly, the degree of error tolerance has a direct impact on compute time: a more forgiving error tolerance ensures arriving at a converged model in less time.

3. APPROACH

We explored several novel approaches to both searching for equilibrium solutions within a one-dimensional radiative-convective modeling framework and for testing the quality of these solutions. Instead of searching for the radiative-convective boundary level by level, we initially explored a parallelized approach that tested every potential radiative-convective boundary simultaneously. In other words, for a model with N_{lvl} levels, we launched N_{lvl} separate model runs with the initial radiative-convective boundary guess moved sequentially up through the atmosphere. This, and subsequent, tests were performed on the Northern Arizona University "Monsoon" computing cluster.

Our new multi-level simultaneous exploration approach makes use of the Message Passing Interface standard which enables communication between "ranks" (tasks) executing in parallel. Rather than each rank acting entirely independently, we designed them to check in with a master process which would assign work and receive model results. Thus, for example, a rank that rapidly finds an acceptably-converged solution can then indicate that other ranks need not continue their search, thereby reducing model runtime.

We describe two newly formulated metrics for quantifying model output quality. These metrics are based on model "physicality", where the best-converged solutions will obey energy conservation and will have lapse rates that do not exceed the adiabatic lapse rate. We record all input parameters and their resulting outputs (be they converged solutions or failed runs) in order to identify patterns. These data help to locate new and unexpected trends, and can also be used to inform machine-learning algorithms aimed at more intelligently selecting initial guesses.

Finally, we demonstrate our new approach through applications to both Super-Earth and Mini-Neptune exoplanets (i.e., planets between the size of Earth and Neptune which orbit stars outside our solar system). Such worlds are the most commonly found class of exoplanet to date, and represent exciting categories of exoplanets not found in our Solar System.

4. CONCLUSIONS

Climate models are critical to our search for life outside our solar system, but many well established models rely on out-of-date programming standards and techniques. Adopting streamlined approaches to modernizing legacy code will, in turn, enable new insight into climate model performance and results. Here, metrics for quantifying model quality will prove essential. Application of these ideas, for example, enables efficient and accurate explorations of Super-Earth and Mini-Neptune climate states.

5. ACKNOWLEDGEMENTS

This work was supported by a grant through NASA's Exoplanets Research Program. Computational analyses were run on Northern Arizona University's Monsoon computing cluster, funded by Arizona's Technology and Research Initiative Fund.

REFERENCES

Catling, D. C., & Kasting, J. F. 2017, Atmospheric Evolution on Inhabited and Lifeless Worlds

Cowan, N. B., Greene, T., Angerhausen, D., et al. 2015, Publications of the Astronomical Society of the Pacific, 127, 311

Fortney, J. J., Lodders, K., Marley, M. S., & Freedman, R. S. 2008, Astrophysical Journal, 678, 1419

Kasting, J. F., Whitmire, D. P., & Reynolds, R. T. 1993, Icarus, 101, 108

Marley, M. S., Saumon, D., Guillot, T., et al. 1996, Science, 272, 1919

McKay, C. P., Pollack, J. B., & Courtin, R. 1989, Icarus (ISSN 0019-1035), 80, 23

A STATISTICAL COMPARATIVE PLANETOLOGY APPROACH TO TEST THE HABITABLE ZONE CONCEPT.

J. Checlair[1], D. S. Abbot[1], J. L. Bean[2], E. M.-R. Kempton[3], T. D. Robinson[4], R. Webber[5];
[1]University of Chicago, Department of the Geophysical Sciences; [2]University of Chicago, Department of Astronomy and Astrophysics; [3]Grinnell College, Department of Physics; [4]Northern Arizona University, Department of Physics and Astronomy; [5]University of Chicago, Department of Statistics; (correspondence: jadecheclair@uchicago.edu)

Abstract: Traditional habitable zone theory assumes that the silicate-weathering feedback regulates the atmospheric CO_2 of planets within the habitable zone to maintain surface temperatures that allow for liquid water. There is some non-definitive evidence that this feedback has worked in Earth history, but it is untested in an exoplanet context. A critical prediction of the silicate-weathering feedback is that, on average, within the habitable zone planets that receive a higher stellar flux should have a lower CO_2 in order to maintain liquid water at their surface (figure 1). We can test this prediction directly by using a statistical approach involving low-precision CO_2 measurements on many planets with future observing facilities such as JWST, LUVOIR, or HabEx. The purpose of this work is to carefully outline the requirements for such a test. The results of this work may influence the usage of JWST and will enhance mission planning for LUVOIR and HabEx.

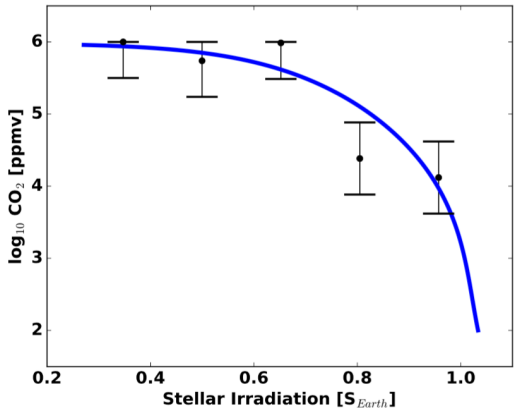

Figure 1. A decrease in atmospheric CO_2 as stellar irradiation increases is expected within the habitable zone, assuming a functioning silicate-weathering feedback. The blue curve shows the predicted CO_2 needed to maintain a surface temperature of 290 K. The error bars represent expected observational and physical uncertainty. Taken from [1].

Methods: First, we use a radiative-transfer model to compute the amount of CO_2 necessary to maintain surface liquid water on planets for different values of insolation and planetary parameters. We run a large ensemble of Earth-like planets with different masses, atmospheric masses, inert atmospheric composition, cloud composition and level, and other greenhouse gases. Second, we post-process this data to determine the precision with which future observing facilities such as JWST, LUVOIR, and HabEx could measure the CO_2. We then combine the variation due to planetary parameters and observational error to determine the number of planet measurements that we would need in order to effectively marginalize over uncertainties and resolve the predicted trend in CO_2 vs. stellar flux.

Preliminary results: My preliminary work has focused on computing the amount of atmospheric CO_2 necessary to maintain surface liquid water on planets for three different sets of parameters. I used the radiative-convective climate model CLIMA [2] to compute vertical profiles of temperature and water vapor mixing ratio at fixed surface temperature for given amounts of CO_2, N_2, and CH_4. I then used the Spectral Mapping

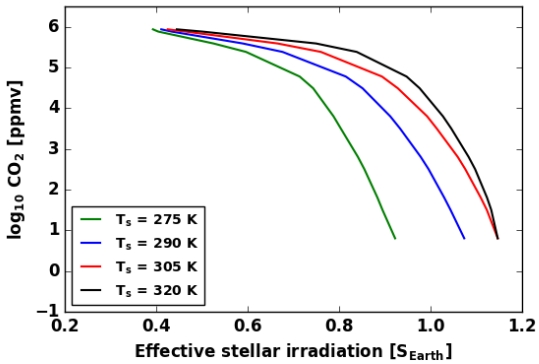

Figure 2. Amount of CO_2 necessary to maintain surface liquid water for different values of surface temperature (T_S) at PN_2 = 1 bar, CH_4 = 0.

Atmospheric Radiative Transfer (SMART) model [3] with a fixed surface albedo of 0.3, to compute the corresponding outgoing longwave radiation and planetary albedo at fixed surface temperature for given profiles from CLIMA. I obtained the effective stellar irradiation from those values. An example of this for surface temperature is shown in figure 2.

I have then performed a preliminary proof-of-concept statistical test to quantify how likely the silicate-weathering feedback hypothesis would be against a null hypothesis when only surface temperature is varied. Ideally, for a large number of exoplanet measurements the CO_2-irradiation curve will have a strongly negative slope, allowing a convincing test for the feedback. The null hypothesis would be a zero slope, implying that the amount of CO_2 does not depend on the irradiation if the feedback does not function. Using the

CO_2-irradiation-T_S values from figure 2 as my data points, I performed an interpolation on the CO_2 mixing ratio for a grid of irradiation and surface temperature values. I then chose a number of model exoplanets to be observed. For each of those model exoplanets, I drew a set of irradiation and surface temperature values. I randomly drew the irradiation values from a uniform distribution, and the surface temperature values based on a fit to a normal distribution of a model reconstruction of Earth history. Each set of irradiation-surface temperature values represents one model exoplanet observation and corresponds to a value of CO_2 mixing ratio obtained from the interpolation function. I repeated this procedure for a large number of simulations, each time with a fixed number of model exoplanets. I computed the fraction of p-values below 0.05 (the power) for this number of simulations. The powers obtained for each number of model exoplanets for a noise of 0.5 log units are shown in figure 3. A power of 0.8 represents an 80% chance that we would detect the silicate-weathering hypothesis if it exists, against the null hypothesis. At least 8 planets would be necessary to provide a convincing test of the feedback for the preliminary case where the only uncertainty accounted for is surface temperature.

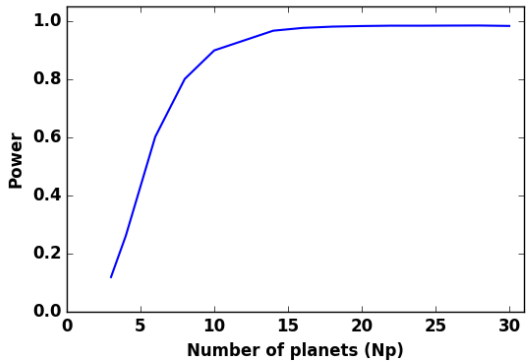

Figure 3. Power as a function of number of model exoplanets. The noise assumed here is 0.5 log units. For a power of 0.8, approximately 8 exoplanets observations would be necessary.

Future work: Ultimately, I will have to account for additional uncertainty parameters in my statistical analysis. Some of those are the surface pressure, planetary mass and radius, atmospheric mass, inert atmospheric compositions, greenhouse gases, cloud level and composition. Those parameters will affect the spread of the slopes with varying degrees. For example, adding different amounts of CH_4 should have a relatively small effect on the slope uncertainty given its small mixing ratio in even an Archean Earth-type of planet.

References:

[1] Bean J. L. et al. (2017), *ApJ Letters*, 841, 2.
[2] Kopparapu R. et al. (2013), *ApJ*, 765, 2.
[3] Meadows and Crisp (1996), *JGR*, 101, E2.

CLIMATE HYSTERESIS AT HIGH OBLIQUITY. C. M. Colose,[1] A. D. Del Genio[1], and M. Way[1] NASA Goddard Institute for Space Studies, New York, NY 10025 (c.m.colose@nasa.gov).

Introduction: Obliquity is a key climate boundary condition that determines the distribution of seasonal and annual-mean flux of instellation on a planet.

Here, we use the NASA GISS ROCKE-3d fully coupled atmosphere-ocean GCM to investigate the susceptibility of low vs. high obliquity planets to undergo planet-wide glaciation and to retain refugia near the outer edge of the habitable zone. We report results for aquaplanets (with a dynamic ocean) as well as a suite of idealized topography simulations.

We show that high obliquity planets remain substantially warmer than low obliquity counterparts at a given orbital distance, retain mild seasonality with moderate amounts of ocean at high latitudes, and are far less prone to enter into a Snowball state. Furthermore, even very cold planets with equatorial ice belts retain favorable conditions for life at high latitudes throughout the entire year.

Universidade Federal do Rio de Janeiro
CCMN – Observatório do Valongo

Rio de Janeiro, June 13th, 2018

Atmospheric Parameters and Ages of M Dwarfs in the Solar Neighborhood

M dwarfs are the most numerous stars in the Galaxy, accounting for about $\sim$70\% of its baryonic mass. They are prime candidates to shelter habitable earthlike planets, as stressed by the recent discoveries of terrestrial exoplanets inside the habitable zones of the nearby M dwarfs Proxima Centauri and Ross 128. Both the transit and radial velocity techniques for detecting exoplanets are much more sensitive to the presence of earth-size planets around M dwarfs than in solar-type dwarfs. Thus the first habitable exoplanet will probably be detected and characterized in a M dwarf environment, making these stars extremely relevant to both astrobiology and planetary science. Even though they are hotspots for the detection of habitable earthlike planets, our knowledge of their properties and even their accurate census stills lags behind with respect to more massive stars. We aim to improve our knowledge of the T_{eff}/[Fe/H] of nearby, still poorly studied M dwarfs, by means of moderate resolution, high S/N NIR spectra, obtained at the coudé spectrograph of the Brazilian 1.6m telescope. We derived a competitive PCA spectral line index calibration able to derive T_{eff}/[Fe/H] with internal errors <100K and <0.1 dex respectively, calibrated against stars with interferometric Teff and [Fe/H] from solar-type binary companions. We present preliminary results for 180 stars, about half of which has no previous T_{eff}/[Fe/H] determination.
We also plan to estimate stellar ages by measuring chromospheric fluxes of the Ca II triplet lines, plus an activity-age calibration specifically tailored to M dwarfs derived by our own group.

Ellen Costa de Almeida

CHARACTERIZING TERRESTRIAL EXOPLANETS: DIVERSITY FLEXES ITS MUSCLES

N. B. Cowan[1], [1]Department of Earth & Planetary Sciences, Department of Physics, McGill University (nicolas.-cowan@mcgill.ca).

Extrasolar planets are more varied than Solar System worlds, but their great distance makes them hard to observe in detail. Low-resolution observations for many exoplanets is therefore an excellent complement to the detailed observations and in situ studies of planets and moons orbiting the Sun. Given that planet formation leads to much more diverse outcomes than ever expected, we can never pretend to understand planets if we only understand the local examples. On the other hand, we have little hope of ever learning the histories of individual exoplanets.

Terrestrial exoplanets are particularly hard to characterize because they are relatively small. Nonetheless, this feat can be achieved by collecting vast numbers of photons from the planetary system and relying on temporal and spectral signatures to separate the light of the planet from that of its host star, or by spatially resolving the planet from its star; in principle, the above techniques can be combined to great effect. Current exoplanet characterization efforts have focused almost entirely on jovian planets because they are easier targets. But all of these techniques can be applied to rocky worlds, given a sufficiently big telescope. I will discuss three archetypal terrestrial exoplanets and how we hope to characterize them in the foreseeable future.

The easiest terrestrial planets to characterize are those orbiting extremely close to their host star producing equilibrium temperatures above the melting point of rock, so-called Lava Planets. Current space-base observatories —Kepler, Hubble, and Spitzer—have given us tantalizing clues about these worlds, and the James Webb Space Telescope (JWST) promises to answer many fundamental questions: Are they synchronously rotating? How reflective, and therefore how hot, are they? Have they entirely lost their volatiles?

Rocky planets orbiting close to small and dim red dwarfs may be habitable because they receive similar amounts of starlight as we receive from the Sun. In recent years, the Kepler mission revealed that such M-Earths are common and indeed many have been discovered in the Solar neighborhood, raising hopes that the Galaxy could be teaming with habitable—if not inhabited—worlds. But major questions remain that JWST will be able to tackle: Do M-Earths have atmospheres? Are they synchronously rotating? Can they maintain water oceans?

The hardest terrestrial planets that we can hope to characterize in the foreseeable future are Earth Twins, those orbiting in the habitable zone of Sun-like stars. By extrapolating from Kepler discoveries, we suspect that Earth Twins are out there, but the uncertainty on their abundance is easily a factor of two, if not an order of magnitude. Detecting Earth Twins around even the nearest stars will require improved, if not completely novel, technology. Nonetheless, missions are in the works—notably WFIRST+Starshade, HabEx, and LUVOIR—which could not only detect these planets, but address fundamental questions: How similar are Earth Twins to Earth? Do they have continents and oceans? Do they exhibit signs of life?

At the end of the day, we stand to learn from these archetypal terrestrial exoplanets because they are subtly—and sometimes radically—different from the Earth.

Empirical evidence for radiative-convective bi-stability in Earth's tropics. M. Dewey[1] and C. Goldblatt[2], [1](mdewey@uvic.ca) School of Earth and Ocean Sciences, University of Victoria, Victoria, British Columbia, Canada, [2](czg@uvic.ca) School of Earth and Ocean Sciences, University of Victoria, Victoria, British Columbia, Canada

Failure of the Planck feedback is described by three, generally independent, branches of prior work: the super-greenhouse effect (SGE, known from tropical meteorology observations), the runaway greenhouse (known from planetary sciences theory), and the multiple unstable equilibria of radiative convective atmospheres. Our work herein links all three of these.

The SGE is an observationally characterized feedback between water vapour, surface temperature, and the greenhouse effect ([1], [2], [3]) which is present over large areas of the tropical oceans. Above a certain SST [2] or greenhouse gas concentration (ie. water vapour) [4] threshold, the rapid increase in absorption of thermal radiation from the surface due to increasing evapouration with increasing SST overpowers the concurrent increase in OLR, and OLR decreases with increasing SST ($dOLR/dSST < 0$). This process is a major contributor to the build up of heat in the tropics, which drives circulation and meridional transport [4]. Whereas there is good agreement on how the SGE operates in clear-sky conditions, disagreement remains regarding the effects of clouds [4].

The runaway greenhouse is defined in theoretical work on planetary atmospheres. When the atmosphere is saturated with water vapour, an asymptotic limit on OLR then emerges, as thermal emission from the surface and lower troposphere is fully absorbed, and all emission to space is from a constant temperature level aloft [5]. There have been many modeling studies focused on calculating OLR limits in the contexts of planetary evolution and habitability ([6], [7], [8], [9], [10], [11]). In general a runaway on Earth is thought to be unattainable through anthropogenic forcing alone ([5], [12], [13], [14]). However it has been noted that some tropical areas are near surface temperatures which cause runaways in models and absorb more sunlight than the limit on thermal emission, and thus suggested that these would experience a local runaway greenhouse if thermally isolated [15].

The existence of multiple equilibria in radiative-convective equilibrium regimes was proposed by [16]. Traditional radiative-convective models use climatological relative humidity (RH) profiles and exhibit a single equilibrium state and OLR limit [17]. Allowing RH to vary with surface temperature can lead to multiple equilibria. [16] found two stable solutions when using an interactive hydrological cycle with RH profiles similar to those found in the tropics. Subsequent work, with simplified step-function-like parameterizations for RH has additionally found multiple equilibria ([18], [19]).

We use satellite observations of Earth's tropics in conjunction with runs of a bespoke 1D radiative transfer model to merge these three branches of work. We show that the radiative-convective bi-stability indeed occurs in Earth's tropics, with the unstable steady state which separates the two stable solutions (one with a dry, and one with a moist troposphere) corresponding to the SGE. We investigate the strength of the SGE for both clear and cloudy-sky conditions, concluding that in general clouds have an amplifying effect on the SGE. Further, we show that the deep convection and column moistening which causes the SGE is driven by the boundary layer becoming optically thick, physics which is related to (but distinct from) the runaway greenhouse. A runaway greenhouse is initiated at higher temperatures.

[1] Raval, A. and Ramanathan, V. (1989). *Nature.* 342, 758-761. [2] Valero, F. P. et al. (1997). *Science.* 275, 1773-1776. [3] Dessler, A. E. et al. (2008). *J. Geophys. R.* 113. [4] Stephens, G. et al. (2016). *J. Climate.* 29, 5469-5482. [5] Goldblatt, C. et al. (2013). *Nat. GeoSci.* 6, 661-667. [6] Simpson, G. C. (1927). *Mem. R. Meterol. Soc.* 11, 69-95. [7] Watson, A. J. et al. (1984). *Earth Planet. Sci. Lett.* 68, 1-6. [8] Kasting, J. F. (1988). *Icarus* 74, 472-494. [9] Abe, Y. and Matusi, T. (1988). *J. of Atmos. Sci.* 45, 3081-3101. [10] Nakajima, S. and Hayashi, Y. (1992). *J. Atmos. Sci.* 49, 2256-2266. [11] Goldblatt, C. and Watson, A. J. (2012). *Phil. Trans. R. Soc. A.* 370, 4197-4216. [12] Leconte, J. et al. (2013). *Nature.* 504, 268-271. [13] Ramirez, R. M. et al. (2014). *Astrobiology.* 14, 714-731. [14] Wolf, E. T. and Toon, O. B. (2014). *Geophy. Res. Lett.* 41, 167-172. [15] Pierrehumbert, R. T. (1995). *J. Atmos. Sci.* 52, 1784-1806. [16] Renno, N. O. (1997). *Tellus.* 49A, 423-438. [17] Manabe, S. and Wetherald, R. T. (1967). *J. Atmos. Sci.* 24, 9121-9132. [18] Pujol, T. and North, G. R. (2002). *J. Meteor. Soc. Japan.* 45, 137-139. [19] Sugiyama, M. et al. (2005). *J. Atmos. Sci.* 62, 2001-2011.

A NEW LINE-BY-LINE GENERAL CIRCULATION MODEL FOR SIMULATION OF DIVERSE PLANETARY ATMOSPHERES.
Feng Ding[1] and Robin Wordsworth[1,2], [1]School of Engineering and Applied Sciences, Harvard University, Cambridge, MA 02138, USA (fengding@g.harvard.edu), [2]School of Engineering and Applied Sciences, Harvard University, Cambridge, MA 02138, USA (rwordsworth@seas.harvard.edu)

Introduction: Investigating exoplanet and solar system planet climates requires a diverse range of tools, including flexible and accurate three-dimensional general circulation models (GCMs). Here we describe the development of a new GCM that for the first time uses a line-by-line model to describe radiative transfer. Compared to other widely used radiative parameterization schemes in GCMs such as the correlated-k method, our direct algorithm allows high computational accuracy and avoids calculating high-dimensional coefficient tables, of which only a small fraction may be used for GCM long-term integration. The model also includes a cubed-sphere gridding technique for atmospheric dynamics, which improves both computational performance and accuracy vs. conventional latitudinal-longitudinal gridding, subgrid closures such as a robust scheme for representing moist convection in both dilute and non-dilute regimes, and an explicit planetary boundary layer model.

This new type of model opens new territory to study a wide variety of important planetary climate problems, including topics on planetary habitability such as characterization of both the inner and outer edges of the habitable zone, water loss, and abiotic oxygen build-up in water-rich atmospheres. The model is designed to be both more accurate and flexible than conventional parameterized GCMs. In addition, the disk-averaged synthetic spectrum of atmospheres can be easily computed in this GCM by the nature of the model framework.

GCM simulations: First we describe the model framework and validation. This GCM is developed based on the "vertically Lagrangian" finite-volume dynamical core [1] of the Geophysical Fluid Dynamics Laboratory (GFDL) Flexible Modeling System (FMS, https://www.gfdl.noaa.gov/fms/) which solves the atmospheric primitive equations in the spherical coordinate. The line-by-line radiative calculation we implemented in the GCM has been validated against a number of analytic results and previous radiative-convective calculations. It agrees closely with published results on the runaway greenhouse calculations for Earth [2], and has been used to compute the thermal evolution of exoplanet GJ 1132b [3] and the transient reducing greenhouse warming on Mars [4].

We show one test run here about a synchronously-rotating terrestrial planet with the spin rate the same as the Earth. **Figure 1** shows the outgoing longwave radiation. The global-mean net radiative flux at the top of the atmosphere is ~10^{-4} W m^{-2}. Then the GCM is energetically closed, which is essential for climate simulations. The zonal-mean zonal wind component is shown in **Figure 2**. Similar to simulations on hot-Jupiter's atmospheres, strong equatorial super-rotation emerges in the upper troposphere due to the momentum convergence by excited planetary waves. Next we present new results on the possible climates on the transiting terrestrial exoplanet GJ 1132b and the problem of atmospheric collapse on tidally locked terrestrial planets.

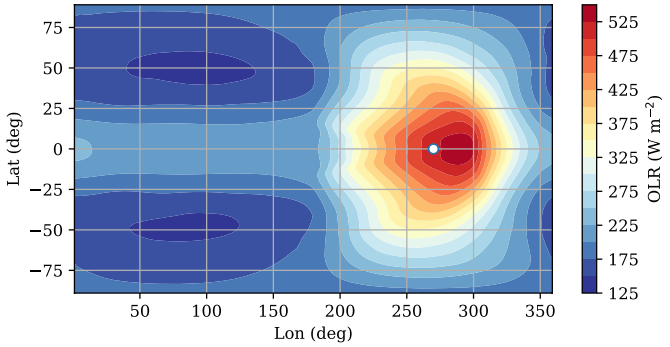

Figure 1: Outgoing longwave radiation (W m^{-2}). The substellar point is marked by the white spot.

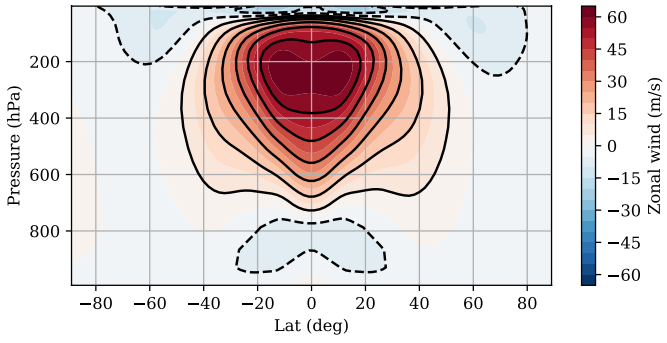

Figure 2: Zonal-mean cross section of the zonal wind component (m s^{-1}).

References: [1] Lin, S. J. (2004) *Mon. Wea. Rev.*, 132(10), 2293-2307. [2] Goldblatt, C., et al. (2013) *Nat. Geosci*., 6, 661. [3] Schaefer, L., et al. (2016) *ApJ*,

829(2), 63. [4] Wordsworth, R., et al. (2017) *GRL*, 44(2), 665-671

Atmospheric Escape from M-dwarf Exoplanets and Implications for Long-term Climate Evolution and Habitability.
C. F. Dong[1], [1]Princeton University (dcfy@princeton.edu)

Introduction: In the last two decades, the field of exoplanets has witnessed a tremendous creative surge. Research in exoplanets now encompasses a wide range of fields ranging from astrophysics to heliophysics and climate science. One of the primary objectives of studying exoplanets is to determine the criteria for habitability, and whether certain exoplanets meet these requirements. Meanwhile, the investigation of the long-term climate evolution of exoplanets has become increasingly important, given its tight relation to planetary habitability. The classical definition of the Habitable Zone (HZ) is the region around a star where liquid water can exist on the planetary surface given sufficient atmospheric pressure, but this definition largely ignores the impact of the stellar wind and stellar magnetic activity on the erosion of an exoplanet's atmosphere. Amongst the many factors that determine long-term climate evolution and habitability, understanding the atmospheric loss is of paramount importance [1,2,10]. Most of the recent attention has been centered around the study of exoplanets orbiting M-dwarfs since the latter are highly numerous in our Galaxy (and in the Universe). The study of these exoplanets has also received a major boost from the discovery of Proxima Centauri b (PCb) [3] and seven Earth-sized planets in the TRAPPIST-1 system [4].

Method: In our Solar system, the most sophisticated codes tend to use magnetohydrodynamic (MHD) models for modeling the interactions of the solar wind with magnetized (such as Earth) and unmagnetized (such as Mars and Venus) planets, and the interactions of planetary magnetospheric flow with its moons (such as Titan). We use the BATS-R-US MHD model [5] that has been well validated and applied to different solar system objects to study the atmosperhic loss from exoplanets [7-10]. For the stellar wind parameters (such as the stellar wind velocity, density and interplanetary magnetic field), we adopt the AWSoM model [6] to simulate those parameters based on the observed magnetograms of M-dwarf stars. The BATS-R-US MHD model is then adapted to exoplanet research by modifying the stellar wind inputs and exoplanetary atmospheric profiles, compositions, and photochemistry.

Results: Fig. 1 presents the contour plots of the O^+ ion density, the magnetic field strength **B** and the magnetic field lines for unmagnetized and magnetized PCb. The total ion escape rate varies from ~ 10^{26} s^{-1} (magnetized) to ~10^{27} s^{-1} (unmagnetized) over one PCb's orbital period, about 1-2 orders of magnitude higher than those of terrestrial planets in our Solar system. As the escape losses for PCb in the unmagnetized case are about two orders of magnitude higher than our Earth (~ 10^{25} s^{-1}), all of the atmosphere could be depleted much faster -- possibly in a span of O(10^8) years. In turn, this has very important ramifications for surface-based life as we know it, given the importance of elements like oxygen. Also, given the loss of the equivalent water [7,8,10], it may lead to the exoplanetary climate changing from a warm and wet environment in the past to the desiccated and frigid state like current Mars in our solar system.

If gases such as oxygen are depleted on these short timescales, sufficient time may not exist for complex life to evolve. Our simulations indicate that the escape rates for PCb in the magnetized case are higher than that of the Earth, implying that some of the above conclusions for the unmagnetized case are also valid here. However, it is equally important to recognize that the magnetized case is quite sensitive to the values of the stellar wind parameters [7]. The atmosphere depletion could occur over O(10^8) and O(10^9) years for the magnetized case with minimum and maximum stellar wind dynamic pressure P_{dyn} over one PCb, respectively.

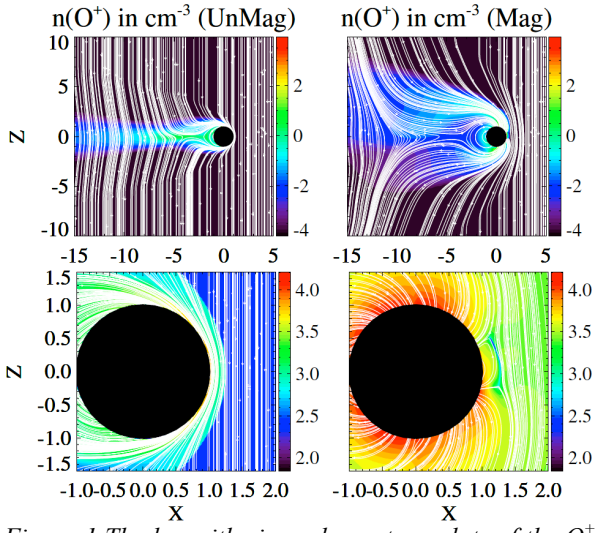

Figure 1 The logarithmic scale contour plots of the O^+ ion (outflow) density (first row) and magnetic field strength (second row) with magnetic field lines (in white) in the meridional plane for the unmagnetized (UnMag) and magnetized (Mag) PCb [7].

Fig. 2 shows the total ion escape rate as a function of the semi-major axis for cases with both maximum (solid curve) and minimal (dashed curve) total pressure over each TRAPPIST-1 planet's orbit [9]. An inspec-

tion of Fig. 2 reveals that the overall escape rate declines monotonically as one moves outwards, from TRAPPIST-1b to TRAPPIST-1h. Hence, taken collectively, this may suggest that TRAPPIST-1h ought to be most "habitable" planet amongst seven planets, when viewed purely from the perspective of atmospheric ion loss. However, it must be recalled that the presence of liquid water on the surface is a prerequisite for habitability, and TRAPPIST-1h is not expected to be conventionally habitable given its cold climate and a snowball state [4,11]. Hence, it seems likely that TRAPPIST-1g will, instead, represent the best chance for a habitable planet in this planetary system to support a stable atmosphere, and thus a hospitable climate over long periods. It is worth mentioning that 3D climate simulations appear to suggest that TRAPPIST-1f and TRAPPIST-1g may not be amenable to surficial life as they enter a snowball state [11], but the effects of tidal heating [12] and induction heating [13], which are expected to be considerable, were not included in the model.

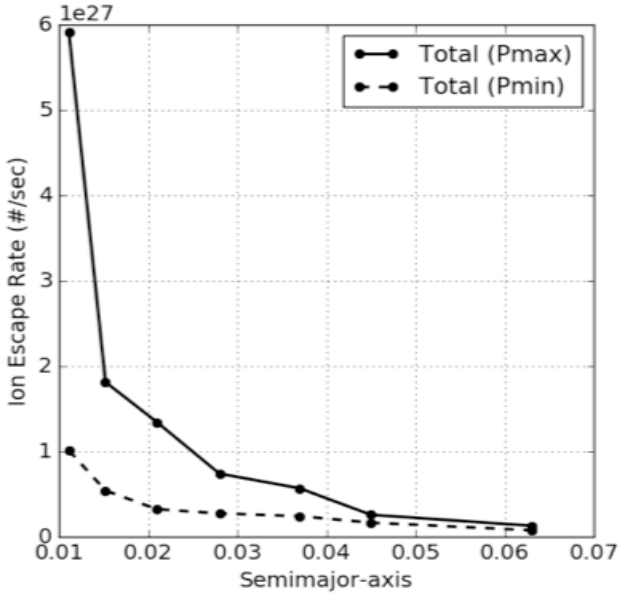

Figure 2: Total atmospheric ion escape rate as a function of the semi-major axis for cases with both maximum (solid curve) and minimal (dashed curve) total pressure over each planet's orbit. The seven distinct points on each curve represent the seven planets of the TRAPPIST-1 system [9].

References: [1] Lammer H. et al. (2009) *Astron. Astrophys. Rev., 17,* 181–249. [2] Ehlmann B. L. et al. (2016) *JGR, 121,* 1927--1961. [3] Anglada-Escude G., et al. (2016) *Nature 536,* 437--440. [4] Gillon M. et al. (2017) *Nature 542,* 456–460. [5] Tóth G. et al. (2012) *JCP 231* 870–903. [6] van der Holst B. et al. (2014) *ApJ 782* 81. [7] Dong C et al. (2017) *ApJL 837* L26. [8] Dong C et al. (2017) *ApJL 847* L4. [9] Dong C et al. (2018) *PNAS 115*, 260-265. [10] Dong et al. (2018) *ApJL 859*, L14. [11] Wolf, E. T. (2017) *ApJL, 839*, L1. [12] Luger, R. et al. (2017) *Nat. Astron., 1* 129. [13] Kislyakova, K. G. et al. (2017) *Nat. Astron., 1* 878.

Modeling Martian Atmospheric Losses over Time: Implications for (Exo)Planetary Climate Evolution and Habitability. C. F. Dong[1], Y. Lee[2], Y. J. Ma[3], M. Lingam[4], S. W. Bougher[5], J. G. Luhmann[6], S. M. Curry[6], G. Toth[5], A. F. Nagy[5], V. Tenishev[5], X. Fang[7], D. L. Mitchell[6], D. A. Brain[7], and B. M. Jakosky[7], [1]Princeton University (dcfy@princeton.edu), [2]NASA GSFC, [3]IGPP, UCLA, [4]Harvard-Cfa, [5]CLaSP, University of Michigan, [6]SSL, UCBerkeley, [7]LASP, CU-Boulder

Introduction: Mars has always represented an important target from the standpoint of planetary science, especially on account of its long-term climate evolution [1-4]. One of the most striking differences between ancient and current Mars is that the former had a thicker atmosphere compared to the present-day value [1], thereby making Noachian Mars potentially more conducive to hosting life. This discrepancy immediately raises the question of how and when the majority of the Martian atmosphere was lost, as well as the channels through which it occurred [5]. There are compelling observational and theoretical reasons to believe that the majority of atmospheric escape must have occurred early in the planet's geological history [6-7], when the extreme ultraviolet (EUV) flux and the solar wind from the Sun were much stronger than today [8]. Moreover, the Martian dynamo shut down ~4.1 Ga and Mars currently has only weak crustal magnetic fields [9]. Our understanding of present-day Martian atmospheric escape has improved greatly thanks to observations undertaken by, e.g., the Mars Atmosphere and Volatile EvolutioN mission (MAVEN [10]) in conjunction with detailed theoretical modeling [11-14].

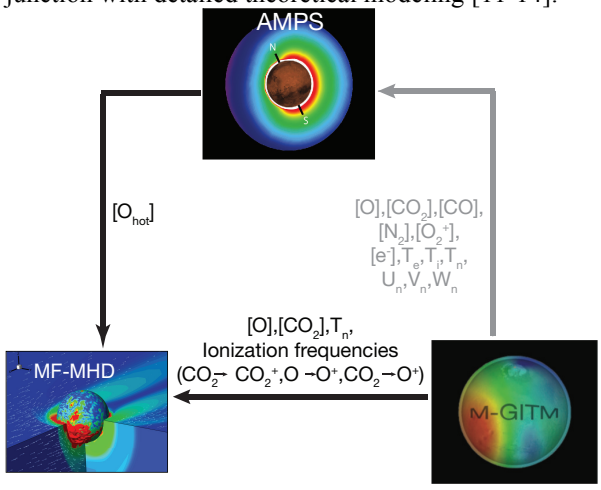

Figure 1: A sketch of a one-way coupling approach between M-GITM, AMPS, and MHD [12]. The notation T_n denotes neutral atmosphere temperatures, and [O], [CO_2], and [O_{hot}] are the neutral O, CO_2, and hot atomic oxygen number densities, respectively.

Method: In this study, we adopted the one-way coupled framework (Fig. 1) which has been employed to study the ion and photochemical losses at the current epoch [11,12]. We adopted the 3-D Mars thermosphere (i.e., neutral temperatures T_n, neutral densities [O], [CO_2], and photoionization frequencies I_O, I_{CO2}) from the Mars Global Ionosphere Thermosphere Model (M-GITM) [13] and the hot atomic oxygen density, [O_{hot}], from the Mars exosphere Monte Carlo model Adaptive Mesh Particle Simulator (AMPS) [11]. These neutral profiles are one-way coupled with the 3-D BATS-R-US Mars multi-fluid MHD (MF-MHD) model [12]. The Mars AMPS hot oxygen corona and the associated photochemical loss rate were calculated based on the thermospheric/ionospheric background from M-GITM. The historical solar radiation and solar wind parameters were adopted from Ref.[8]. We started the simulation at the current epoch based on the autumnal equinox solar cycle moderate conditions.

Results: Fig. 2 depicts the temperature and winds of the Martian thermosphere at ~200 km for equinox conditions. An inspection of Fig. 2 reveals that a high EUV flux is correlated with a hotter thermosphere. Therefore, the EUV heating of the thermosphere is self-consistently computed, which is very important for deriving the atmospheric ion and photochemical losses.

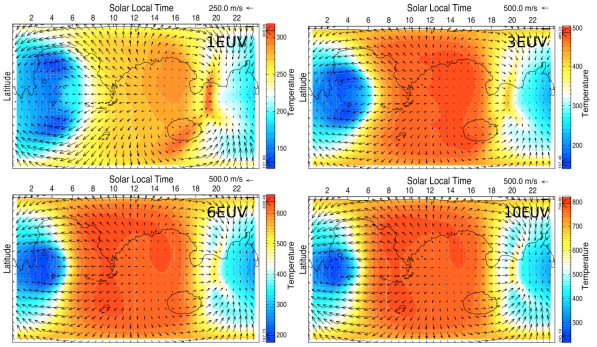

Figure 2: Color contours of temperature (in K) at ~200 km for 1, 3, 6, and 10 EUV under equinox conditions. The arrows in each panel indicate the relative magnitude (reference is given in top-right corner) and the direction of the horizontal winds [4].

Fig. 3 shows the atomic hot oxygen density distribution in the meridian plane from AMPS based on the M-GITM input. The presented asymmetry in the hot oxygen density distribution is a result of higher dayside O_2^+ abundance. Compared to the current epoch with relatively low EUV flux, ancient Mars had a more intensive and extensive oxygen corona resulting from the enhanced O_2^+ density at higher EUV flux.

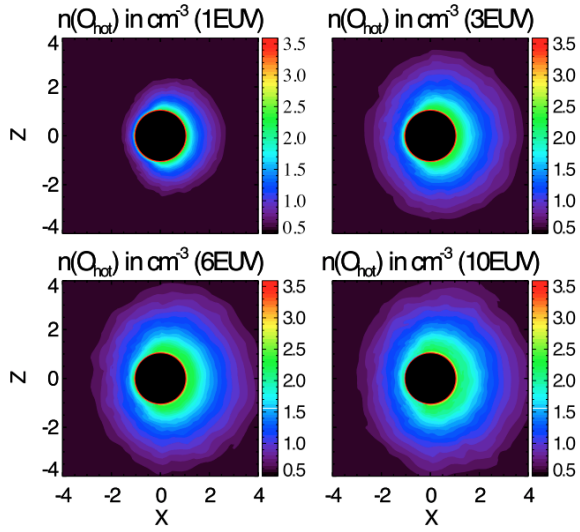

Figure 3: Comparison of the hot oxygen density (in cm^{-3}) distribution in the x–z meridian plane for different EUV cases using a logarithmic scale [4].

In Fig. 4, we present the MF-MHD calculation of O^+ ion escaping from the planet. More O^+ ions escape from the planet at higher EUV and stronger solar wind.

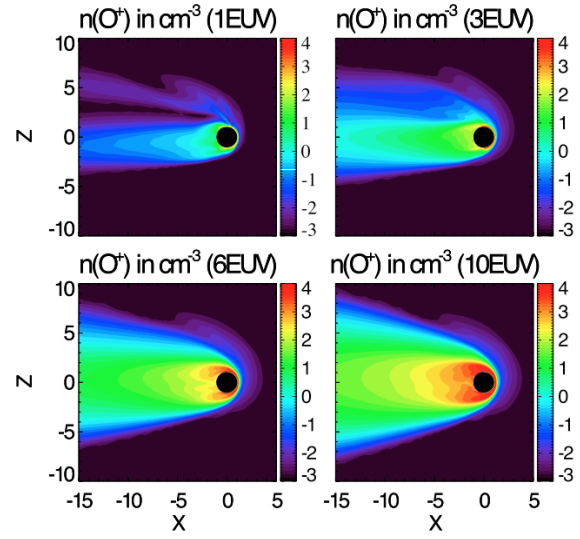

Figure 4: Logarithmic scale contour plots of the O^+ ion density (in cm^{-3}) in the x–z meridian plane for different EUV and solar wind cases [4].

Fig. 5 shows that the total ion escape rate was >100 times higher than today at ~4 Ga. Hence, our results are consistent with Mars having lost much of its atmosphere early in its history, leading to the Martian climate changing from a warm and wet environment in the past to the desiccated, frigid, and thus inhospitable one documented today. Our simulations indicate that the total photochemical and ion atmospheric losses over the span ~0–4 Ga are approximately equal to each other, and their sum amounts to ~0.1 bar being lost over this duration. If we assume that the oxygen lost through a combination of ion and photochemical escape mechanisms was originally derived from surface water, we find ~3.8 × 10^{17} kg of water has been lost from Mars between 0 and ~4 Ga; this mass corresponds to a global surface depth of ~2.6 m (the depth will be greater if the water bodies were more localized) [4]. The calculations do not include other potentially important loss processes such as sputtering; therefore, it provides a lower limit on the escape rates.

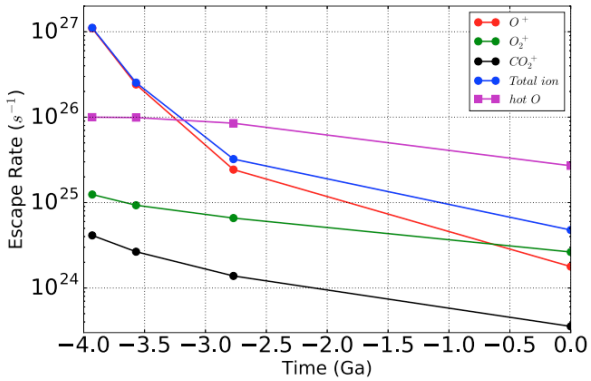

Figure 5: Calculated ion and photochemical escape rates over the Martian history [4].

Conclusion: In our solar system, Mars represents a classic example of a planet where planetary habitability and climate evolution have been unambiguously affected by atmospheric losses. We have studied the atmospheric ion and photochemical escape rates from Mars over time. Our simulations are consistent with the idea that Mars could have transitioned from having a thick atmosphere and global water bodies to its current state with a tenuous atmosphere and arid conditions quite early in its history. This study offers fresh insights concerning the long-term climate evolution and habitability of the increasing number of exoplanets discovered yearly due to atmospheric losses [4,15].

References: [1] Jakosky B. M. and Phillips R. J. (2001) *Nature, 412,* 237. [2] Lillis R. J. et al. (2015) *SSRev, 195,* 357-422. [3] Jakosky B. M. et al. (2018) *Icarus*. [4] Dong C. F. et al. (2018) *ApJL*, *859*, L14. [5] Brain D. A. et al. (2016) *JGR, 121*, 2364. [6] Brain D. A. et al. (2015) *GRL, 42*, 9142-9148. [7] Jakosky B. M. et al (2017) *Science 355*, 1408. [8] Boesswetter A. et al. (2010) *PSS 58,* 2031-2043. [9] Lillis R. J. et al. (2013) *JGR, 118,* 1488. [10] Jakosky B. et al. (2015) *SSRev, 195,* 3-48. [11] Lee Y. et al. (2015) *JGR, 120*, 1880-1892. [12] Dong C. F. et al. (2015) *JGR, 120*, 7857-7872. [13] Bougher S. W. et al. (2015) *JGR, 120,* 311-342. [14] Najib D. et al. (2014) *JGR, 116*, A05204. [15] Dong C et al. (2018) *PNAS 115*, 260.

UNDERSTANDING STELLAR INFLUENCE ON ION ESCAPE FROM EXOPLANETS H. Egan[1], R. Jarvinen[2], and D. Brain[1] [1]University of Colorado Boulder (hilary.egan@colorado.edu), [2]Finnish Meteorological Institute, Helsinki, Finland.

Introduction: All planets undergo atmospheric evolution over the course of their lifetime; in particular non-thermal processes including those that act on ions are thought to be important for the evolution of secondary atmospheres. Observations show ion loss is currently taking place at Earth [11], Mars [8], Venus [10], and Titan [4].

Recent developments in exoplanet observation techniques have allowed the discovery of thousands of planets, including dozens of small, rocky planets that are potentially habitable. Many current studies of exoplanet habitability use estimates of thermal loss [7] or turbulent entrained mass models [12] to estimate scaling of atmospheric evolution, although ion loss from terrestrial exoplanets has been studied for Proxima-b analogs [1,3], the Trappist-1 planets [2], and generic unmagnetized planets [13].

The aforementioned models all directly apply solar system models of ion loss to exoplanetary conditions, but it is also useful to understand how each stellar wind characteristic that differs from typical solar conditions influences ion escape individually. Here we present a systematic study of how ion loss processes vary with stellar input, under conditions appropriate for planets orbiting in the habitable zone of a typical M-dwarf. By scaling toward M-dwarf-like conditions incrementally, we build a generalized framework to understand how ion loss processes vary from the current solar system paradigms.

Simulation Methods: For this project we use the hybrid plasma code RHybrid. Hybrid simulation codes treat ions as macroparticles representative of a population of ions that evolve kinetically according to the Lorentz force, while electrons are treated as a charge-neutralizing fluid. This code has been adapted from the HYB model [6], but is now fully parallelized. By using a hybrid model both Hall and finite armor radius (FLR) effects are automatically included and the ion phase space distribution is fully three-dimensional. This makes it an ideal choice to use for global magnetospheric models where ion kinetic effects are likely to be important, i.e., when ion gyroradii become comparable to the scale size of the planet, although it is also applicable for small gyroradius regimes. Kinetic effects are also important for quasi-parallel shocks, where the magnetic field is nearly parallel to the solar wind flow direction.

Stellar Wind: Here we break down the different parameters considered in scaling existing solar system models of ion escape towards conditions appropriate for M-dwarfs. Table 1 shows a summary of the different model runs.

Run	Θ IMF	P_{dyn} (nPa)	|B| (nT)	Q (s^{-1})
1	82	1	6	10^{25}
2	16	1	6	10^{25}
3	16	3500	150	10^{25}
4	16	3500	150	10^{27}

Table 1: Summary of simulation parameters for each model run, including IMF angle from subsolar line, dynamical pressure, IMF strength, and ion production rate.

Quasi-Parallel IMF: As M-dwarfs are relatively dimmer than the Sun, the habitable zone must be correspondingly closer in. This will lead to more radially oriented IMF as expected from a Parker Spiral model, and often shown in MHD simulations of M-dwarf stellar winds [14].

Stellar Wind Strength: Although it is not yet possible to directly probe the stellar wind of stars outside our own Sun, mass loss rates can constrain upper limits of the total outflow mass [15]. Together with Zeeman-Doppler imaging of magnetic field configuration [16], it is possible to reconstruct stellar winds using MHD models [14]. Such studies show it is possible for planets in the habitable zone of M-dwarfs to encounter ~10^4 times typical solar wind pressures.

EUV Input: Observations show that M-dwarfs have EUV fluxes of 10-1000 times that of the Sun [17]. This will have a critical effect on ion loss and the atmosphere by increasing photo-ionization, and heating the upper atmosphere.

Results: Because ions are constrained to gyrate around magnetic fields, much of the ion outflow morphology is dictated by the magnetic field configuration. Figure 1 shows O_2+ number density and magnetic field magnitude slices for the quasi-perpendicular and quasi-parallel simulations.

A quasi-parallel IMF allows open field lines to connect directly to the dayside of the planet and drives strong asymmetry due to the quasi-parallel shock [18]. The quasi-parallel shock allows the solar wind to approach the planet at a much higher velocity in the un-

stable hemisphere, creating a strong ion pickup region due to the *v* x *B* force.

Behind the planet, the existence and placement of the current sheet influences ion escape. In the quasi-perpendicular simulation the current sheet is in the classical configuration directly behind the planet. The influence of the quasi-parallel IMF changes the current sheet into an S-type configuration and offsets it towards the unstable shock. The S-type current sheet still acts to collimate the outflowing ions by the *J* x *B* force, but changes the location of the open field lines and offsets the outflow.

Plasma beta, or the ratio of thermal to magnetic pressure, determines if the S-type current sheet will persist behind the planet. If a higher thermal pressure erodes the current sheet, the ions become unconfined to the specific outflow channel created by a current sheet.

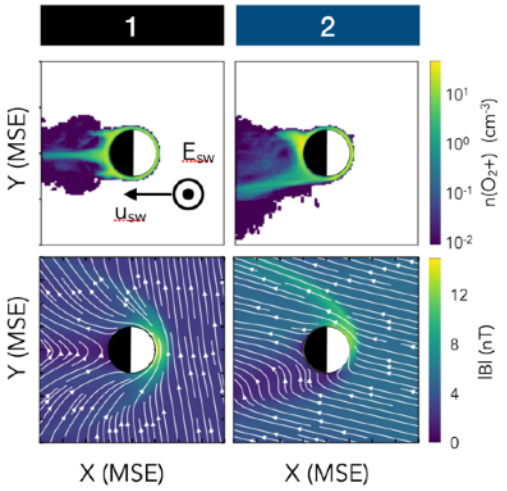

Figure 1: Slices through models 1 (*left*) and 2 (*right*) showing O_2+ number density (*top*) and magnetic field magnitude and field lines (*bottom*). The motional electric field is pointed out of the plane and the stellar wind flows from right to left.

Ion loss rates are also influenced by the stellar wind input parameters. Figure 2 shows the fraction of total injected ions that are escaping as a function of altitude for each simulation. As one might expect, more ions escape in the quasi-parallel configuration compared to the nominal solar wind due to the influence of additional open field lines. At higher stellar wind densities even more ions escape because of the greater energy input into the system. At more intense EUV, although a larger number of ions escape, a smaller fraction of ions input into the simulation escape because the method of increasing EUV effectively increases the ionospheric pressure. This weakens the coupling between the impacting solar wind and the ionosphere.

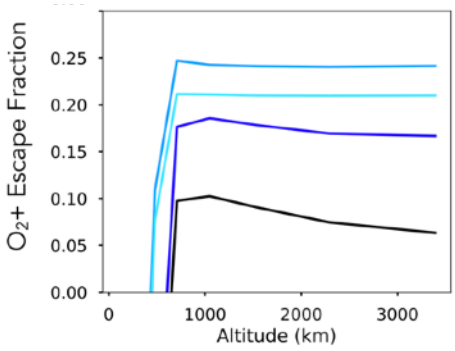

Figure 2: Fraction of O_2+ ions that escape as a function of altitude for each simulation.

Conclusions: We find that as stellar wind inputs to global plasma models scale towards exoplanet-like conditions, both the configuration of the system and overall ion escape fractions change. When applying models and scaling relations from the solar system to exoplanets, it is important to consider how the processes themselves change, in addition to increasing or decreasing in magnitude. The relationship the stellar wind has with the ionosphere varies across stellar input conditions, and to properly understand the ion escape self consistent models that properly treat open field lines are needed.

[1] C. Dong, et. al. (2017) ApJ, 847:L4 [2] C. Dong, M. Lingam, Y. Ma, and O. Cohen (2017) ApJ, 837:L26 [3] K. Garcia-Sage, et. al (2017) ApJ, 844:L13 [4] D. A. Gurnett, F. L. Scarf, and W. S. Kurth. (1982) JGR., 87:1395–1403 [5] R. Jarvinen, et. al. (2009) Annales Geophysicae, 27:4333–4348 [6] E. Kallio and P. Janhunen (2003) Annales Geophysicae, 21:2133–2145 [7] H. Lammer, et. al (2003) ApJ, 598:L121–L124 [8] R. Lundin, et. al. (1989) Nature, 341:609–612 [9] Y. Ma, A. et. al . (2002) JGR-SP 107: 1282 [10] T. Nordstrom, et. al, (2013) JGR-SP 118:3592–3601 [11] R. J. Strangeway, et. al. (2005) JGR-SP 110:A03221 [12] J. Zendejas, et. al. (2010) Icarus, 210:539–544 [13] Cohen et. al. (2015) ApJ 806:41 [14] Vidotto et. al. (2014) MNRAS 1162-1175 [15] Cranmer, S.R. and Saar S.H. (2011) ApJ, 741:54 [16] Donati J.-F., Brown S. F. (1997) A&A, 326, 1135 [17] France, K. et. al. (2016) ApJ 820:89 [18] Treumann, R. A. & Jaroschek, C. H. (2009) A&A 409-435

Simulation of Exoplanet Host Star Magnetic Activity on Stellar Cycle Timescales A. O. Farrish[1], M. Maruo[2], W. T. Barnes[1], D. Alexander[1], S. Bradshaw[1], and M. DeRosa[3], [1]Rice University Department of Physics and Astronomy, [2]Kyoto University, [3]Lockheed Martin Advanced Technology Center

Introduction: We apply an empirical photospheric magnetic flux transport model, derived from solar behavior [1], and a magnetically-driven stellar atmosphere model [2] to explore the range of stellar effects on habitability of Earth-size exoplanets around M dwarf stars. We create detailed, dynamic simulations of stellar activity and its variability over stellar cycle timescales. In particular, we examine how the asterospheric magnetic field and related extreme ultraviolet (EUV) and X-ray emission vary in time and consider the potential impact on exoplanet atmospheres. Of specific interest is the influence on atmospheric properties that may ultimately influence potential habitability, e.g. ionospheric current enhancement, magnetospheric-ionospheric coupling, and atmospheric loss.

References:

[1] Schrijver, C. J., and Title, A. M. (2001), ApJ, 551, 1099

[2] Bradshaw, S., and Klimchuk, J. (2011) ApJ Supplement Series, 194 – 220.

Impact of clouds and hazes in the JWST simulated transmission spectra of TRAPPIST-1 planets in the habitable zone

T. Fauchez[1,2], M. Turbet[3], A. Mandell[1], R. Kopparapu[1], G. Arney[1]

and S. D. Domagal-Goldman[1]

[1] *Sellers Exoplanet Environments Collaboration, NASA Goddard Space Flight Center.*

[2] *Goddard Earth Sciences Technology and Research (GESTAR), Universities Space Research Association, Columbia, MD 21046, USA*

[3] *Laboratoire de Météorologie Dynamique/IPSL, CNRS, Sorbonne Université, Ecole normale supérieure, PSL Research University, Ecole Polytechnique, 75005 Paris, France.*

Introduction: M-dwarfs are the most common type of stars in our galaxy. Ultra-cool dwarfs (T < 2700 K) are a sub-stellar class of late M-dwarfs and represent nearly 20% of astronomical objects in the stellar neighborhood of the Sun. Their smaller size than regular M-dwarfs allows easier detection of rocky exoplanets in close orbits, and this potential was recently realized by the discovery of the TRAPPIST-1 system. Located about 12 pc away, TRAPPIST-1 has seven known planets, and it is one of the most promising rocky-planet systems for follow-up observations due to the depths of the transit signals. Transit-timing variation (TTVs) measurements of the TRAPPIST-1 planets suggest terrestrial or volatile-rich composition. Also, it has been found that three planets (TRAPPIST-1 e, f and g) are in the Habitable Zone (HZ) where surface temperatures would allow surface water to exist. These planets will be prime targets for atmospheric characterization with JWST owing to their relative proximity to Earth and frequent planetary transits.

Atmospheric properties are major components of planet habitability. However, the detectability of gaseous features on rocky planets in the HZ may be severely impacted by the presence of clouds and/or hazes in their atmosphere. We have already seen this phenomenon in the "flat" transit transmission spectra of larger exoplanets such as GJ 1214b, WASP-31b, WASP-12b and HATP-12b.

In this work, we use the LMDG global climate model to simulate several possible atmospheres for TRAPPIST-1 e, f and g: 1) Archean Earth, 2) modern Earth and 3) CO2-dominated atmospheres. We coupled the GCM outputs with a 1D photochemical model (atmos) at the terminator to model photochemical hazes (especially for the Archean Earth-like atmospheres). We also calculate synthetic transit spectra using the GSFC Planetary Spectrum Generator (PSG), and we determine the number of transits needed to observe key spectral features for both JWST NIRspec and MIRI instruments.

We have explored differences in transit depth (and altitude) between cloudy/hazy and clear sky spectra and between equilibrium chemistry and photochemistry assumptions, and calculated the number of transits needed to detect individual spectral features. Preliminary simulations have found that the planets with the most habitable conditions (TRAPPIST-1e with large ice-free oceans) also produce the highest fraction of cloud coverage, which then totally (or partly) hide biosignature gases (CH4, O2, O3) and water vapor detection through transmission spectroscopy with JWST. Further results on the impact of photochemistry and prospects for observational constraints on atmospheric composition and ocean coverage will also be presented.

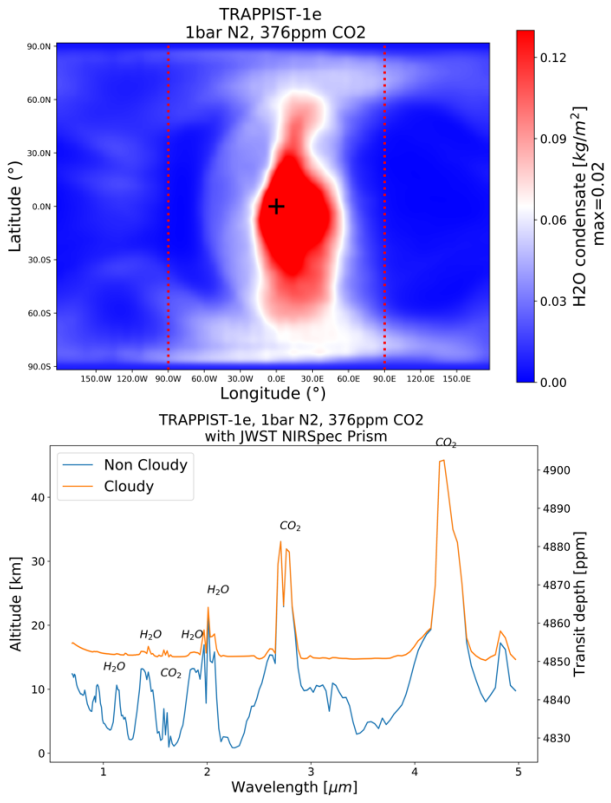

Cloud coverage for TRAPPIST-1e with modern-Earth atmosphere (top) and JWST NIRspec Prism transmission spectra (bottom).

Developing Tighter Constraints On Exoplanet Biosignatures by Modeling Atmospheric Haze. R. Felton[1], G. Arney[2], S. Domagal-Goldman[3], M. Neveu[4], S. Desch[5], [1]Catholic University of America (ryan.c.felton@nasa.gov), [2]NASA Goddard (giada.n.arney@nasa.gov), [3]NASA Goddard (shawn.goldman@nasa.gov), [4]NASA Headquarters D.C. (marc.f.neveu@nasa.gov), [5]Arizona State University (steve.desch@asu.edu)

Introduction: As we increase our capacity to resolve the atmospheric composition of exoplanets, we must continue to refine our ability to distinguish true biosignatures from false positives in order to ultimately distinguish a life-bearing from a lifeless planet. Of the possible true and false biosignatures, methane (CH_4) and carbon dioxide (CO_2) are of interest because, on Earth, geological and biological processes can produce them on large scales. To identify a biotic, Earth-like exoplanet, we must understand how these biosignatures shape their atmospheres.

High fluxes of CH_4 are more likely to be produced by biology [1]. In particular, high atmospheric abundances of CH_4 can produce photochemical organic haze, which dramatically alters the photochemistry, climate, and spectrum of a planet. Arney et al. (2017) [2] have suggested that haze-bearing atmospheres rich in CO_2 may be a type of biosignature, as the CH_4 flux required to produce the haze is similar to the amount of biogenic CH_4 on modern Earth. Atmospheric CH_4 and CO_2 both affect haze-formation photochemistry, and the potential for hazes to form in Earth-like atmospheres at abiotic concentrations of these gases has not been well-studied. We will explore a wide range of parameter space of abiotic concentration levels of these gases to determine what spectral signatures can be found in abiotic environments and look for measurable differences between abiotic and biotic atmospheres.

We use a 1D photochemical model (Atmos) to compare Archean Earth-like atmospheres to abiotic versions while varying atmospheric CH_4 and CO_2 levels and considering global redox balance. We find that detectable hazes form for only the largest CH_4/CO_2 levels, but these results have large global redox imbalances, suggesting they are unphysical and so were unable to create detectable haze abiotically in an Archean Earth-like atmosphere.

To expand on this work in the future, we are implementing upgrades to our Atmos 1-D model. We will show the results of improvements to Atmos that incorporate more complete haze formation pathways that includes nitriles, oxygen-bearing molecules, and higher order hydrocarbons. Other updates include changes to the overall haze production mechanism, updated reaction rate coefficients, and photolysis upgrades using the Kinetic Database for Astrochemistry (KIDA) combined with work done by Hébrard et al., (2012) [3]. These upgrades will be used to improve our Archean Earth template and to develop a Titan-like chemical scheme to examine reducing environments without biology. Overall these upgrades will improve our predictions of haze formation chemistry in organic-rich atmospheres.

References:

[1] Krissansen-Totton et al., (2018) *Science Advances, Vol. 4 no. 1,* eaao5747.

[2] Arney et al. (2017) *The Astrophysical Journal, Vol. 836, no. 1*.

[3] Hebrard et al. (2012) *Astronomy & Astrophysics 541*, A21.

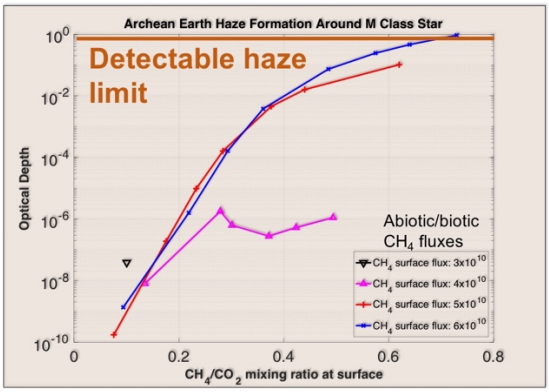

CHARACTERIZING EARTH ANALOGS IN REFLECTED LIGHT: INFORMATION CONTENT FROM THE ULTRAVIOLET THROUGH THE NEAR-INFRARED. Y. K. Feng[1], T. D. Robinson[2], and J. J. Fortney[1], [1]Department of Astronomy and Astrophysics, University of California, Santa Cruz, 1156 High St., Santa Cruz, CA, 95064, USA, kat.feng@ucsc.edu, [2]Department of Physics & Astronomy, Northern Arizona University, Flagstaff, AZ 86011, USA.

Introduction: Characterizing exoplanets is key to unlocking questions surrounding planet formation and evolution, and understanding whether processes taking place on Solar System worlds are common. Current methods rely on transits and moderate contrast direct imaging, well-suited for short-period planets and young, self-luminous giant planets, respectively. In spite of technological challenges, the characterization of habitable Earth-like planets may soon be within reach. Results from NASA's *Kepler* mission suggest that one in ten Sun-like stars hosts a terrestrial planet in a one-year orbit [1]. For such worlds, however, direct imaging is likely to be the preferred method for study and characterization.

The coming decades hold enormous potential for the direct imaging of exoplanets, fueled by NASA's upcoming *Wide-Field InfraRed Survey Telescope* (*WFIRST*) mission and the Habitable Exoplanet Imaging (HabEx) and the Large UltraViolet-Optical-InfraRed (LUVOIR) mission concepts. Critically, the latter two concepts aim to achieve the high contrasts (~10^{-10}) needed to observe Earth-like planets.

Here, we use the Bayesian retrieval framework [2,3] developed in [4] to investigate the information content in data spanning the near-ultraviolet to the near-infrared (0.2 – 1.8μm) from terrestrial planets around Sun-like stars. We examine the feasibility of detecting key atmospheric species when observing an Earth-like planet with a future high-contrast instrument (e.g., HabEx, LUVOIR).

Methods: A retrieval, or inverse technique, is a powerful data driven way to fully characterize uncertainty distributions for quantities used in a parameterized forward model. In our forward model, we utilize a well-tested albedo code [5–8] to simulate the reflected light spectrum of an Earth-sized planet around a Sun-like star. The species of interest in our model atmosphere include water vapor, ozone, and oxygen. We incorporate Rayleigh scattering due to molecular nitrogen, a wavelength-independent surface albedo, and pressure-dependent molecular opacities. We include one parameterized water cloud layer and fractional cloudiness. We also retrieve for planet radius and surface gravity. With wavelength coverage extended into the near-infrared, we are including the possible detection of trace molecules such as carbon dioxide and methane (Figure 1).

We simulate data for wavelength resolutions (R) of 7 in the near-ultraviolet, R = 140 in the visible, and R = 70 in the near-infrared. We examine the retrieval performance at signal-to-noise ratios (SNR) of 5, 10, 15, and 20, using a published high contrast noise model [9]. We discuss future work and improvements, including extensions to super-Earths.

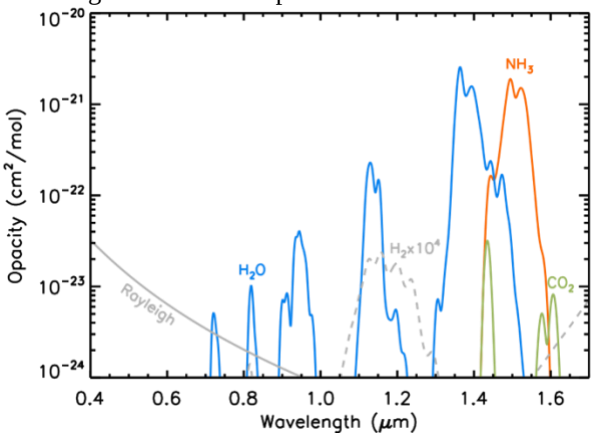

Figure 1: Accessible molecular features spanning the visible and near-infrared wavelength ranges.

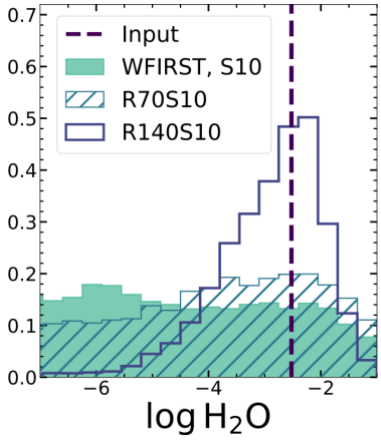

Figure 2: The posterior distributions of water as retrieved from simulated data sets all with characteristic signal-to-noise ratios of 10 but with different instrument resolutions, demonstrating the interplay between data quality and instrument design.

Results: Having multiple sets of data allows us to consider the trade-offs between R and SNR

combinations. In [4], we considered three types of data sets spanning 0.4 – 1.0μm: *WFIRST*, which uses photometric points at shorter wavelengths followed by R = 50 spectrum; a continuous R = 70 spectrum; and a continuous R = 140 spectrum. Figure 2 demonstrates the improvement in constraint of the water vapor abundance for a given SNR as R increases. Our updated study provides valuable insight to our ability to constrain quantities when one data set has a mixture of resolutions.

In [4], we determined that at R = 70, a SNR of 15 is necessary for water vapor, ozone, and oxygen to be measured simultaneously, while at R = 140, a SNR of 10 is needed. With the extended wavelength range, we show several notable findings. First, we easily detect ozone for Earth twins at relatively low SNR using its strong ultraviolet features. We also see a decrease in the required SNRs for species detection with the addition of the near-infrared especially for water vapor. Finally, it is a challenge to detect both carbon dioxide and methane due to overall weak features.

Conclusions: We utilize a Bayesian retrieval framework to interpret data from Earth-like planets to prepare for the era of space-based high contrast imaging. This tool demonstrates the capability to constrain molecular abundances for water and ozone in a terrestrial atmosphere and could be utilized to understand the science return of a mission concept given a proposed architecture, thus aiding the planning of upcoming missions in a concrete statistical manner.

References: [1] Burke C. J. et al. (2015) *Astrophys J, 809*, 1. [2] Line M. R. et al. (2013) *Astrophys J, 775*, 2. [3] Buchner J. et al. (2014) *Astron Astrophys, 564*, A125. [4] Feng Y. K. et al. (2018) *Astron J, 155*, 200. [5] McKay C. P. et al. (1989) *Icarus, 80*, 23. [6] Marley M. S. et al. (1999) *Astrophy J, 513*, 879. [7] Cahoy K. L. et al. (2010) *Astrophy J, 724*, 189. [8] Lupu R. E. et al. (2016) *Astrophys J, 152*, 217. [9] Robinson T. D. et al. (2016) *PASP, 128*, 960.

Laboratory Needs for Exoplanet Climate Modeling. Jonathan J. Fortney[1], Tyler D. Robinson[2], Shawn Domagal-Goldman[3], Tony Del Genio[4], and the Nexus for Exoplanet Systems Science (NExSS), [1]University of California, Santa Cruz, [2]Northern Arizona University, [3]NASA Goddard Space Flight Center

Introduction: Our understanding of exoplanet atmospheres comes from a combination of observations, models to interpret those observations, the laboratory data that feed into those models. Here, we outline the urgent near-term needs in improvements in laboratory data prior to the launch of JWST, as well as the long-term needs to improve our investments in laboratory measurements as we develop the next generation of exoplanet missions. Specifically highlighted are needs for: (1) molecular opacity linelists, with parameters for a diversity of broadening gases, (2) extended databases for collision-induced absorption and dimer opacities, (3) high spectral resolution opacity data for a variety of relevant molecular species, (4) laboratory studies of haze and condensate formation and optical properties, (5) significantly expanded databases of chemical reaction rates, and (6) measurements of gas photoabsorption cross sections at high temperatures. By meeting these needs, we can maximize our community's ability to use future (and past) observations to understand how climate operates on exoplanets.

Photochemistry of Terrestrial Worlds orbiting M Dwarfs. P. Gao[1], [1]Astronomy Department, University of California, Berkeley, 501 Campbell Hall, MC 3411, Berkeley, CA 94720-3411, gaopeter@berkeley.edu.

Introduction: The atmospheric composition of terrestrial planets is one of the deciding factors in their climate and habitability, and it is controlled by a multitude of factors. One major control is photochemistry – destruction of atmospheric molecules by incoming stellar photons and generation of photolysis products. In the Solar System, photochemistry is vital in producing protective ozone shields (e.g. Earth) and aerosols (Venus and Titan), and quickens atmospheric escape (Mars).

Terrestrial worlds orbiting M dwarfs have recently become the focus of astrobiological interest due to their potential abundance [1] and relative ease of detection [2]. However, differences in the spectral energy distribution and evolution of M dwarfs mean that terrestrial Solar System analogues may behave very differently if placed in orbit around such stars. For example, the low luminosity of M dwarfs places their habitable zones close enough to the host stars such that habitable zone planets may be tidally locked [3] or stripped of their water due to the prolonged pre-main sequences of these stars [4]. More subtle are the effects of M dwarf spectra on photochemical cycles that define atmospheric composition, which often respond differently to different regions of the spectrum.

In this presentation, I compare the photochemical responses of two endmember terrestrial planet atmospheres – the oxidized Martian atmosphere and the reducing and hazy Titan atmosphere – to exposure to an M dwarf's spectral energy distribution. I also discuss their implications for a Venus-analogue orbiting an M dwarf, large numbers of which will likely be discovered by TESS to serve as prime targets for JWST [5]. I conduct this comparison by modeling the photochemistry of Mars and Titan analogues using the well-validated Mars [6] and Titan [7] versions of the Caltech/JPL 1D photochemical and transport model KINETICS. The M dwarf spectrum is taken from the MUSCLES survey [8].

Mars: The atmospheric composition of Mars is relatively simple, being composed of mostly carbon, oxygen, hydrogen, and nitrogen that are locked in CO_2, water, and N_2. The key chemical cycle in Mars's atmosphere is the HOx cycle that prevents the CO_2 atmosphere from breaking down into its photolysis products CO and O_2. Participants in the HO_x cycle, such as HO_2, H_2O_2, and O_3, are photolyzed primarily by NUV radiation, where M dwarf emits very little compared to Sun-like stars. Meanwhile, species like CO_2, H_2O, and O_2 are photolyzed by FUV radiation, which M dwarfs emit in abundance. This difference in photolysis rates, coupled with possible water depletion, results in atmospheric compositions very different from that of Mars itself. [9] showed that high abundances of CO, O_2, and O_3 could persist to an extent that the latter two species' mixing ratios rival that of modern Earth. This results in a false biosignature, as the rise of O_2 and O_3 on Earth stems from biology. However, this false signature can be unmasked by noting the lack of water features in the spectrum of the planet, as shown in Figure 1.

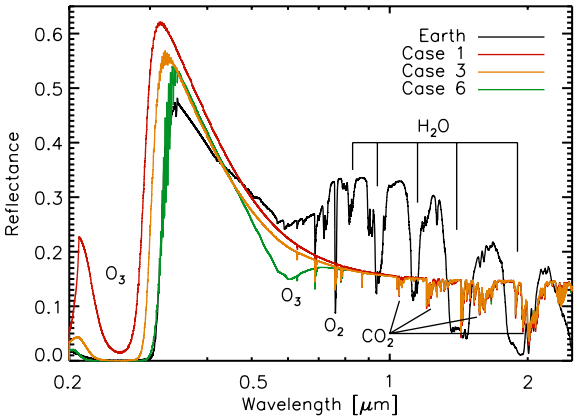

Figure 1: Reflectance of an Earth-sized "Mars analogue" around an M dwarf with different levels of hydrogen depletion, compared to that of Earth, showing increased abundance of CO_2 photolysis products O_2, and O_3 with decreasing H (water) abundance. Lower case numbers refer to less H depletion. From [9].

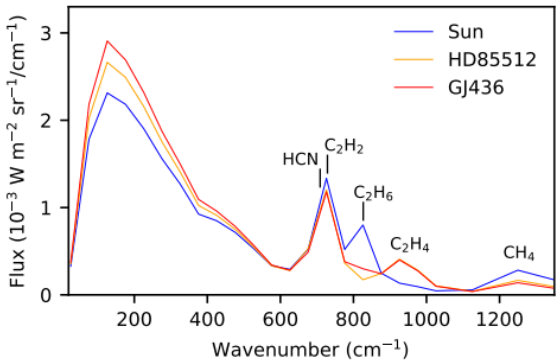

Figure 2. Emission from a Titan analogue orbiting the Sun (blue), an K dwarf (yellow), and an M dwarf (red) with major spectral features labeled. From [10].

Titan: Titan's atmosphere is composed of mostly N_2 and CH_4 with significant trace species and aerosols stemming from their photolysis. C_2 hydrocarbons and HCN, in particular, are thought to be haze precursors, and parameterizations of their production and loss rates have given satisfactory rates of haze production [11]. The haze is vital to Titan's atmosphere's thermal balance and chemistry, and affects the flux of organics reaching its surface. [10] showed that altering the spectrum of incoming stellar radiation changes the abundance of different trace species differently, reflecting the complex chemical cycles in play. Emission from such a world can be used to probe photochemical processes at work, as shown in Figure 2. [10] also showed that the haze abundance does not change significantly, which may complicate future efforts to probe deep into the atmospheres of Titan-like exoplanets.

Venus: Like Mars, Venus's atmosphere is composed of mostly CO_2 and is thus vulnerable to photolytic conversion to CO and O_2. However, due to the low H_2O abundance in the mesosphere where photolysis occurs, most of the work in keeping CO_2 abundances high is done via reactions with chlorine radicals [12]. In addition, sulfur chemistry plays a major role in generating the opaque cloud decks and is potentially responsible for significant UV absorption [13]. There are several interesting avenues of investigation for probing photochemistry of Venus analogues orbiting M dwarfs: (1) how do the chlorine, sulfur, and HO_x cycles change around an M dwarf? (2) how would the atmospheric composition respond to changes in abundance in important trace species and photolysis parent molecules like HCl and SO_2? (3) what are the observational consequences of (1) and (2) and are they detectable with JWST and future large telescopes? We will investigate these questions using the latest validated Venus version of KINETICS [14].

References: [1] Dressing C. D. and Charbonneau D. (2015) *ApJ*, 807, 45. [2] Shields A. L. et al. (2016) *Phys. Rep.*, 663, 1. [3] Joshi M. (2003) *Astrobiology*, 3, 415. [4] Luger R. and Barnes R. (2015) *Astrobiology*, 15, 119. [5] Barclay T. et al. (2018) Submitted to AAS journals, arXiv:1804.05050. [6] Nair H. et al. (1994) *Icarus*, 111, 124. [7] Li C. et al. (2015) *ApJL*, 803, L19. [8] France K. et al. (2016) *ApJ*, 820, 89. [9] Gao P. et al. (2015) *ApJ*, 806, 249. [10] Lora J. M. et al. (2018) *ApJ*, 853, 58 [11] Lavvas P. P. et al. (2008) *PSS*, 56, 27 [12] Yung. Y. L. and DeMore W. B. (1982) *Icarus*, 51, 199. [13] Frandsen B. N. et al. (2016) *GRL*, 43, 11146. [14] Zhang X. et al. (2012) *Icarus*, 217, 714.

SIMPLE MODELS OF TERRESTRIAL PLANET ENERGY BALANCE: UNDERSTANDING MOIST AND RUNAWAY GREENHOUSE STATES C. Goldblatt[1], [1]School of Earth and Ocean Sciences, University of Victoria, Victoria, BC, Canada. czg@uvic.ca.

Introduction: To quote the inimitable John Green*: "It has always worried me that simple models of climate do not seem to work very well" [1]. This irks me in particular as regards the tutorial models of Earth's energy balance which are given to every undergraduate climatology class: these introduce the concept that an absorbing atmosphere that is colder than the surface are responsible for greenhouse warming, but obscure the physics beyond that. In the case of Earth and other damp planets, where warming evaporates ocean and so adds absorber to the atmosphere, the rich physics of runaway and super-greenhouses is missed. These are physics are quite important to understanding Earth-like planets. Herein, I will develop simple models which do represent the relevant physics and thus contribute to a qualitatively different understanding of terrestrial planet climatology.

The problem with standard models: No doubt that everyone at this meeting has solved a model for a surface and one-layer atmosphere in radiative equilibrium. The atmosphere is transparent to solar (shortwave) radiation, and absorbs fraction ε, between 0 and 1, of the terrestrial (longwave) radiation. The surface reflects fraction α of the incident solar radiation, and is a black body with respect to thermal radiation. Thus energy balance equations are written:

$(S/4)(1 - \alpha) = \sigma T_s^4 - \varepsilon\sigma T_a^4$

$\varepsilon\sigma T_s^4 = 2\varepsilon\sigma T_a^4$

where S is the solar constant, Ts and Ta are the surface and atmospheric temperatures, and σ is the Stefan-Boltzman constant. These are solved:

$T_s = [\, S(1 - \alpha) / (4\sigma(1 - \varepsilon/2)) \,]^{0.25}$

$T_a^4 = 0.5 T_s^4$

The total OLR is

$F_{TOA} = \varepsilon\sigma T_a^4 + (1 - \varepsilon)\sigma T_s^4$

Inspection of these indicates that an increase in surface temperature will always lead to an increase in outgoing longwave radiation (OLR). This is a profound, and in some cases dangerous, misunderstanding of the behavior of moist atmospheres.

Physics: Two physical phenomenon are key to the energy balance of moist atmospheres, the super-greenhouse and runaway greenhouse.

The super-greenhouse. The so-called super-greenhouse, which describes the decrease in OLR with warming of a moist tropical column [2]. This arises as a threshold behavior, as a very moist boundary layer means that the surface can no longer be at or near radiative equilibrium and surface energy balance requires convection. Rapid moistening of the free troposphere increases the optical depth of the atmosphere and causes the effective emission level to raise to a higher temperature level [3]. Less energy is then emitted. This is rather important to understanding the behavior of Earth's tropics, and to how the transition to a uniformly moist climate (i.e. expansion of the tropics) would operate.

The runaway greenhouse. The transition from a moist greenhouse to Venus is mediated first by the runaway greenhouse. As water becomes a major component of the atmosphere, the temperature of effective emission tends space tends to a constant. Thus the emission to space is constant; see development of the physics in [4], review in [5] and new model calculations in [6]. The existence of a limiting OLR flux means that absorption of sunlight in excess of that will lead to unchecked warming and the total evaporation of the ocean. This physics is not at all represented in typical simple models, which is very problematic.

A new model with a runaway greenhouse: A new model is developed by altering the specification of OLR. An initial set of equation is described here, which no doubt will be improved by the time the meeting comes about. Emissivity is set as

$\varepsilon = 1 - e^{-\tau}$,

where optical depth comprises contributions from water vapour and other greenhouse gases

$\tau = \tau_{H2O} + \tau_{dry}$.

I take $\tau_{dry} = 0.5$, somewhat similar to Earth's atmosphere. Optical depth from water is directly proportional to a representative saturation vapor pressure;

$\tau_{H2O} = k p_{sat}$

with absorption coefficient k = 0.001. Specification of atmospheric radiative temperature, T_r, is key to representing the runaway greenhouse. When the atmosphere is not optically thick from water, the radiative temperature will be the bulk atmospheric temperature T_a. When the atmosphere is optically thick with water, radiation is emitted only from the level where $\tau_{H2O} \sim 1$. Thus I set

$T_r = (1 - \varepsilon_{H2O})Ta + \varepsilon_{H2O} T_{limit}$, for $T_a < T_x$

$T_r = (1 - \varepsilon_{H2O})Ta + \varepsilon_{H2O} T_{limit} + 0.01(T_a - T_x)^2$,

for $T_a \geq T_x$

where T_{limit} = 265K. is the blackbody temperature corresponding to a limiting flux of 282Wm^{-2}. This parameterization, with parameters tuned as above, well represents modern radiative transfer model out-

put. The modification for high $T > T_x$, where T_x = 600K, is a cludge to represent thermal exit from the runaway greenhouse via 4μm thermal emission from a hot upper atmosphere. A version of the model was developed in [7].

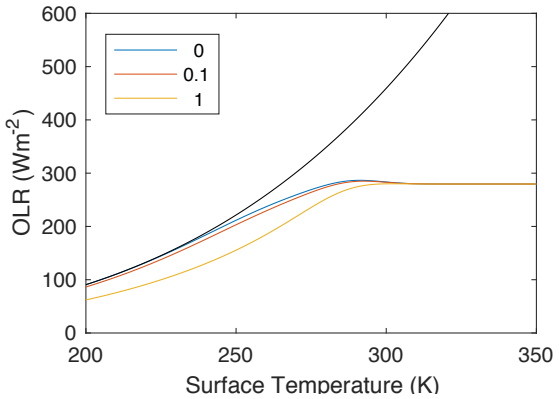

Figure 1: Outgoing longwave radiation (OLR) described by the heuristic model for a few different τ_{dry}.

Example model output is in Figure 1. This illustrates that the major features of the dependence on thermal radiation on temperature are represented.

Applications: Like many good abstracts, work which is not finished when the abstract is written is promised for the time of the meeting. The existing model is sufficient for heuristic explanation of the runaway greenhouse. An intermediate complexity model (a set of ODEs similar to [4]) has also been developed, which will allow a more formal description of T_{limit} and will address why this asymptotes as early as it does (the oft-quoted statement that the T-p curve has reached the saturation vapour pressure curve is manifestly not correct). That model can also be modified to account for the driving of the super-greenhouse. These can be further expanded with a meridional dimension, to describe the propagation of warm moist climates from the equator outward. My suspicion is that a bistability between damp and moist climates will be found, and described in time to make my presentation at the meeting more fun.

* John Green, 1931-2012, made important contributions to general circulation theory in terms of baroclinic instability [8]; known to the author as a the somewhat curmudgeonly retired faculty who sat in the front of seminars and either slept or heckled.

[1] Green, J. S. A. (2002) *Weather*, 57, 431–439, doi:10.1256/wea.223.01. [2] Stephens, G. et al. (2016). *J. Climate*. 29, 5469-5482 [3] Dewey M. and Goldblatt C. (2018) *Geophys. Res. Lett*., in review. [4] Nakajima S. et al. (1992) *J. Atmos. Sci.*, 49, 2256-2266. [5] Goldblatt C. and Watson A. J. (2012) *Phil. Trans. Roy. Soc.*, 370, 4197-4216. doi: 10.1098/rsta.2012.0004 [6] Goldblatt C. et al. (2013) *Nature Geosci*. 6, 661-667. doi:10.1038/ngeo1892 [7] Goldblatt, C. arXiv:1608.07263 [8] Gadian A. et al. (2002) *Weather*, 67, 193, doi:10.1002/wea.1957.

PHYSICAL FEEDBACKS ON STRATUS CLOUD AMOUNT RESOLVE THE FAINT YOUNG SUN PARADOX. C. Goldblatt[1], V. McDonald[1], and K. McCusker[2], [1]University of Victoria, czg@uvic.ca, vmcd@uvic.ca, [2]Rhodium Group, kmccusker@rhg.com

Introduction: Geological evidence suggests that Earth was mostly warm and not glaciated during the Archean, despite Earth receiving only around 80% of the present day amount of sunlight. 1-D models require higher abundances of greenhouse gases than geochemical proxies permit, whereas some 3-D models permit lower greenhouse gas inventories, but for reasons which are somewhat opaque.

Here, we show that physically motivated changes to low cloud (stratus) amount likely played a large role in resolving the FYSP. The amount of stratus cloud is strongly linked to lower tropospheric stability [1] [2], with a stronger inversion at the planetary boundary layer trapping moisture and giving a higher stratus cloud fraction. By hypothesis, an Archean situation where the surface is heated less by sunlight and the atmosphere is heated more by absorption of thermal radiation with a stronger greenhouse, should feature a weaker inversion and less stable lower troposphere. Hence, with a weaker sun but stronger greenhouse, we expect less stratus clouds.

Experiment: To test this hypothesis, we run a set of carefully controlled General Circulation Model experiments using the Community Atmosphere Model. We change only the solar constant and CO2 mixing ratio, increasing CO2 and decreasing the solar constant so that the global mean surface temperature remains the same. We do not change anything else, so as to focus directly on a single hypothesis, and to keep the model as near to known conditions as possible.

Results: We find that at 80% of modern solar constant: (1) only 30,000 ppmv CO2 is required to maintain modern surface temperatures, versus the expectation of 80,000 ppmv from radiative forcing calculations. (2) The dominant change is to low cloud fraction, decreasing from 34% to 25% (Figure 1), with an associated reduction in short-wave cloud forcing of 20W/m/m (Figure 2). This can be set in the context of a 50W/m/m radiative deficit due to the weaker sun, so the cloud feedback contributes two-fifths of the required warming. (3) There is a reduced meridional temperature gradient such that the poles are 4 to 8 K warmer than present, which will further contributes to the avoidance of glaciation (Figure 3).

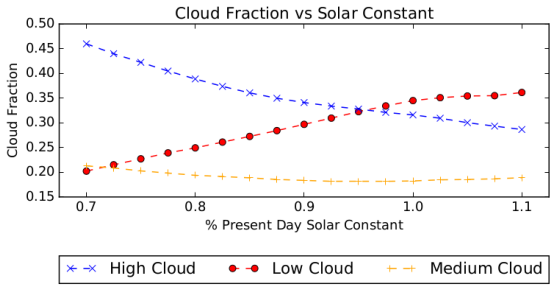

Figure 1. Global average cloud fraction for decreasing solar constant.

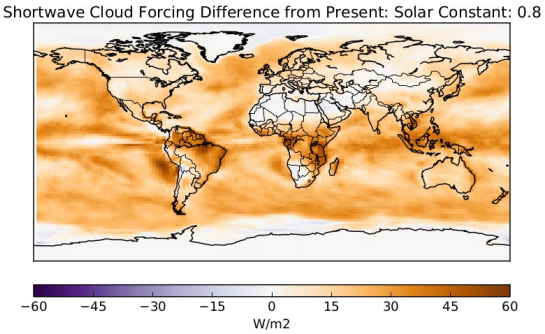

Figure 2. Shortwave cloud forcing difference between 80% present day solar constant and present day solar constant.

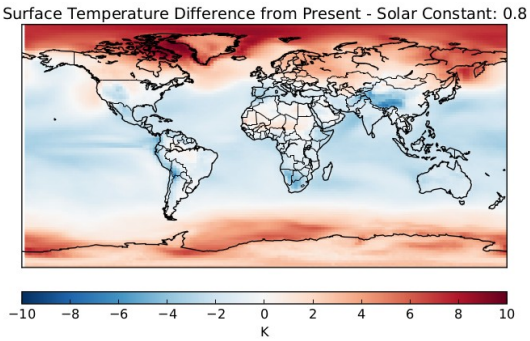

Figure 3. Meridional temperature gradient difference between 80% present day solar constant and present day solar constant for same global mean surface temperature.

References:

[1] Slingo J. (1987) *Quart J Royal Meteor Soc, 113*, 899–927. [2] Wood R. and Bretherton C.S. (2006) *J. Climate*, *19*, 6425-6432.

PLANETARY CLIMATE DYNAMICS OVER A WIDE RANGE OF ORBITAL AND ATMOSPHERIC CHARACTERISTICS

. I. Guendelman[1] and Y. Kaspi[1], [1]Weizmann Institute of Science, Rehovot, Israel, 76100, Email: ilai.guendelman@weizmann.ac.il

More than 3500 planets have been detected outside of our Solar System, and with future missions planned this tally will increase together with our ability to characterize the different planets and their atmospheres. It is expected that the different planets will vary in their planetary parameters and atmospheric characteristics [1]. Thus, understanding how the climate depend on different planetary parameters is important for studying the habitability potential of the different planets, and will also improve our basic understanding of atmospheric physics.

Using an idealized aquaplanet general circulation model [2], modified to include seasonal forcing, we study the surface temperature and the Hadley circulation response to changes in the obliquity, rotation rate, orbital period and atmospheric mass of terrestrial planets.

We find that increasing the obliquity and orbital period the seasonality increases, and the resulting climate is composed mainly out of two extreme season, winter and summer, where the transition seasons, are very week and even absent. We show that increasing the atmospheric mass, reduces the temperature gradient and warms the surface temperature, and by slowing down the planet's rotation rate the meridional temperature gradient becomes weaker.

Based on our model results we suggest an empirical power law for the ascending and descending branches of the Hadley circulation and for its strength. This power law shows that the Hadley cell becomes wider and stronger as we increase the obliquity and orbital period or lower the atmospheric mass and rotation rate. We explain physically these results and compare the results to number of theoretical predictors for the position of the Hadley cell ascending branch [3,4,5]. From this study, we suggest to consider the regions of ascending and descending branches of the Hadley circulation as a possible future observable of exoplanets atmosphere, as they are strongly correlated to the latitudinal cloud population. We also discuss the habitability potential dependence on the different parameters.

References:

[1] Kaspi Y. and Showman A.P (2015). *Astrophys. J.*, 804, 60. [2] Frierson D. M., Held I.M, and Zurita-Gotor P. (2006), *J. Atmos. Sci.*, 63, 2548-2566. [3] Lindzen R.S and Hou A.V. (1988), *J. Atmos. Sci.*, 45, 2416-2427. [4] Neelin J.D and Held I.M (1987), *Mon. Weath. Rev.*, 115, 3-12. [5] Kang S.M, Held I.M, Frierson D.M and Zaho M. (2008), *J. Climate*, 21, 3521-3532.

THE IMPACT OF PLANETARY ROTATION RATE ON THE REFLECTANCE SPECTRUM OF TERRESTRIAL EXOPLANETS. S. D. Guzewich[1], J. Lustig-Yaeger[2], R. Kopparapu[1], and M. J. Way[3], [1]NASA Goddard Space Flight Center, Greenbelt, MD 20771 (scott.d.guzewich@nasa.gov), [2]University of Washington, Seattle, WA 98195, [3]NASA Goddard Institute for Space Studies, New York, NY 10025.

Introduction: Future large space telescopes observing terrestrial exoplanets in visible and near-infrared wavelengths, such as the Large Ultraviolet, Optical, and Infrared Surveyor (LUVOIR) or the Habitable Exoplanet Imaging Mission (HabEx), will see a complex spectrum with possibly numerous characteristics of the planet creating degenerate spectral signatures. In addition to well-known factors such as gas abundances, aerosols and clouds, and surface ocean and land patterns, the planetary rotation rate will provide an additional complication. Terrestrial planets in our own star system have sidereal day lengths that vary from ~24 hours (Earth and Mars), to ~16 Earth days for Titan, and ~-243 Earth days for Venus. For planets such as Titan and Venus, the surface is obscured in these wavelength ranges. However, for planets such as Earth, the rotation rate directly impacts patterns of clouds and surface ice that effect the reflected spectrum of the planet.

We evaluate the impact of planetary rotation rate on the observed reflected light spectrum of an Earth-like exoplanet using simulations with the Resolving Orbital and Climate Keys of Earth and Extraterrestrial Environments with Dynamics (ROCKE3D) global climate model (GCM) [1] and then feed the GCM output into the Planetary Spectrum Generator (PSG) [2] and Spectral Mapping Atmospheric Radiative Transfer (SMART) [3] radiative transfer models to generate reflected light spectra of our simulated planets.

GCM Simulations: We conducted 11 simulations using the ROCKE3D GCM with varied rotation rates: 1x, 4x, 8x, 16x, 32x, 64x, 128x, 243x (corresponding to a 3:2 spin-orbit resonance), 256x, 365x, and 365x with 0° obliquity (all relative to Earth's 24 hour day length). All simulations utilize a fully-coupled dynamic ocean, solar insolation, terrestrial obliquity (i.e., 23°, except one of the 365x simulations where it is set to 0°), and Earth atmospheric composition (400 ppm CO_2, prescribed O_3, CH_4, and N_2O). The topography used in the model is Earth-like, but with a "bathtub" ocean bathymetry to eliminate the chance that the ocean freezes to the bottom in shallow water. Surface vegetation is eliminated, a 50/50 sand-clay soil is used, and we employ a uniform land surface albedo of 0.3.

All simulations are run until they reach radiative equilibrium, which is defined as the net radiative balance of the planet being ±0.2 W/m^2 and then for a further 100 years. This results in each simulation being run for 500-1000 simulated years.

Radiative Transfer Codes: We employ two sophisticated radiative transfer (RT) codes to model the reflected light spectrum from our GCM simulations: the Planetary Spectrum Generator and SMART. These radiative transfer models resolve the structure of molecular bands, surface reflectivity, and cloud scattering in much more detail than native GCM radiative transfer, which enables the study of observables relevant to future space-based, coronagraph-equipped telescopes (e.g. HabEx/LUVOIR). The utilization of two independent RT codes provides confidence in the robustness of the observables. Both codes perform radiative transfer calculations to compute high-resolution spectra via line-by-line. PSG is also publicly available through NASA Goddard, providing a means to develop a GCM-to-PSG pipeline in future that can be shared with the community. SMART has been validated against solar system objects and has been used to study a wide variety of types of atmospheres.

Discussion: The planetary climate undergoes a significant shift as the rotation rate of the planet slows. Rather than having distinct mid-latitude and polar climate zones, the planet moves into an "all tropics" climatic regime where the Hadley cells reach to the poles and the equator-to-pole temperature gradient is markedly reduced (Figure 1). As rotation rate is slowed, equatorial superrotation develops in the upper troposphere and stratosphere at rotation rates of ~16-32x (Figure 2), before dissipating as the rotation rate continues to slow (beyond 32x) and atmospheric motion weakens.

The ocean circulation also undergoes substantial alterations with at first a broadening of the main north-south currents (i.e., the Gulf Stream and Kuroshio currents) and eventually a full reversal of the Antarctic circumpolar current (Figure 3).

References:

[1] Way, M.J. et al. (2017) *Astrophys. J. Supp. Series*, 231. [2] Villaneuva, G.L. et al. (2018) *J. of Quant. Spec. and Rad. Transfer*, submitted. [3] Meadows V.S. and D. Crisp (1996), *J. of Geophys. Res*., 101, E2.

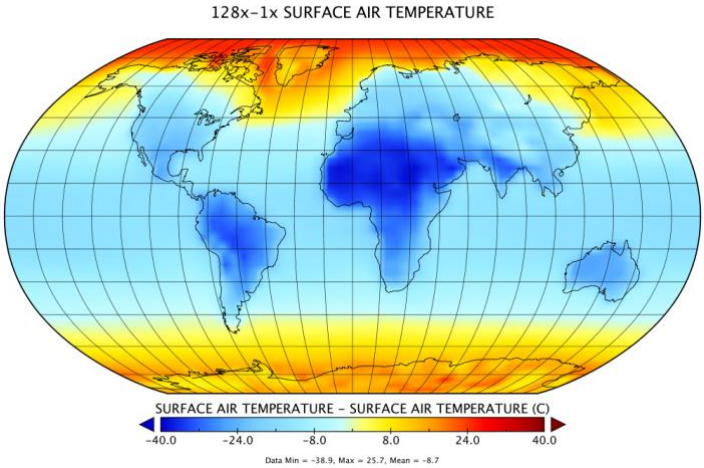

Figure 1. Surface air temperature change between a 128x and 1x Earth day rotation rate simulation. The low-and mid-latitudes are substantially cooled while the poles are warmed.

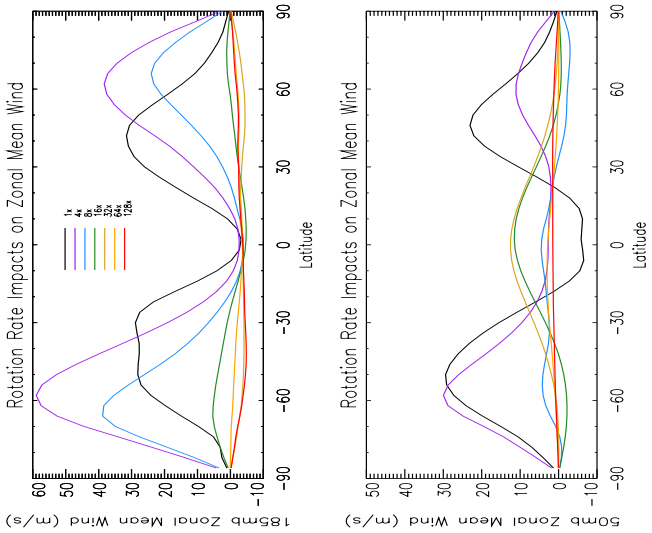

Figure 2. Zonal mean zonal wind at 185mb (top) and 50mb (bottom) for simulations ranging between 1x and 128x Earth day rotate rate. The 16x and 32x simulations exhibit equatorial superrotation at 50mb.

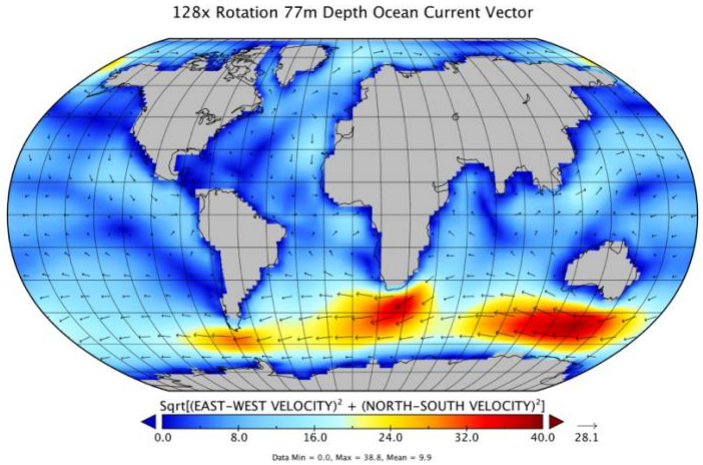

Figure 3. Ocean current vectors and velocity for the 128x Earth day rotation rate simulation. The Antarctic circumpolar current is reversed (i.e, flowing east-to-west) relative to Earth.

WHAT DOES IT TAKE TO GLACIATE? EXPLORING THE CLIMATIC LINK BETWEEN ATMOSPHERIC METHANE AND THE RISE OF OXYGEN.
C. E. Harman[1,2,*], L. E. Sohl[2,3], E. T. Wolf[4], M. J. Way[2], K. Tsigaridis[2,3], A. D. Del Genio[2], [1]Department of Applied Physics and Applied Mathematics, Columbia University, New York, NY 10025, [2]NASA Goddard Institute for Space Studies, New York, NY 10025; *chester.e.harman@nasa.gov; [3]Center for Climate Systems Research, Columbia University, New York, NY 10025; [4]Laboratory for Atmospheric and Space Physics, Department of Atmospheric and Oceanic Sciences, University of Colorado, Boulder, CO 80303

Introduction: One of the longstanding questions related to the climate evolution of the Earth links the atmospheric composition (and more specifically, the inventory of greenhouse gases) and the climate of the Archean and Paleoproterozoic Earth, centered around the Great Oxidation Event (GOE) [1-3]. An increasingly nuanced view of the complexities involved in keeping the early Earth warm has evolved, and general circulation models (GCMs) predict temperate climates with even modest greenhouse gas inventories [4]. Further constraints on the Archean, ranging from variations in total atmospheric pressure [5], the partial pressure of N_2 [6], an essentially equatorial supercontinent [7] which more closely resembles that of the Neoproterozoic (Fig. 1), and decreased solar luminosity [5], all play roles in determining the required additional forcing and thus the absolute quantities of greenhouse gases such as CO_2, CH_4, and H_2. In turn, the evidence for glacial events following the GOE can be seen as a further constraint on the both the preceding and resulting atmospheric composition – that is, given the assumed rapidity of the loss of CH_4 [2], the bulk atmosphere would remain approximately constant across two distinct climatic regimes. The question is then, what does it take to glaciate from an otherwise ice-free CO_2 and CH_4 climate?

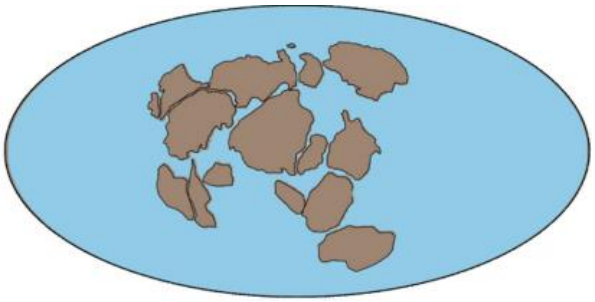

Figure 1: Continental configuration for the Neoproterozoic Earth (~715 Mya) in the ROCKE-3D GCM [8]; this bears a striking resemblance to the proposed Kenorland supercontinent [7].

The ROCKE-3D GCM [8] leverages our understanding of the modern Earth's atmospheric chemistry and climate to simulate an increasingly diverse pool of planet types. ROCKE-3D has been used to simulate the climatology of modern and paleo-Earths [8], early Venus [9], and temperate terrestrial planets orbiting M dwarf host stars [10,11]. Here, we describe bookending simulations using best estimates for the full suite of surface and atmospheric variables [5-7,12] appropriate to the end of the Archean and start of the Paleoproterozoic (~2.4 Gya). These are meant to explore the climatic ramifications of the loss of atmospheric CH_4 and the concomitant rise of free O_2: one simulation representing the CH_4-rich Archean (~3,000 ppm), and the second with diminished CH_4 (~100 ppm) and modest O_2 (0.1%). The loss of methane results in a much cooler climate.

References: [1] Kasting 2005 *Pre. Res.* **137(3-4)** 119. [2] Kopp *et al.* 2005 *PNAS* **102(32)** 11131. [3] Haqq-Misra *et al.* 2008 *Astrobio.* **8(6)** 1127. [4] Wolf & Toon 2013 *Astrobio.* ***13*(7)** 656. [5] Som, S. M., et al. 2016 *Nat. Geo.*, ***9*(6)** 448. [6] Marty *et al.* 2013 *Science*, **342(6154)** 101. [7] Pesonen *et al.* 2003 *Tectonophysics* **375(1-4)** 289. [8] Way *et al* 2017 *ApJS* **231** 12. [9] Way *et al* 2016 *GRL* **43** 12. [10] Fujii *et al* 2017 *ApJ* **848** 100. [11] Del Genio *et al* 2017 *arXiv:*1709.02051. [12] Olson, S.L., *et al.* 2018 *arXiv:*1803.05967.

IMPLEMENTING A NEW EARTH DUST LIFTING SCHEME IN MARS GLOBAL CIRCULATION MODELS. V. L. Hartwick[1] and O. B. Toon[2], [1]University of Colorado-Boulder, Boulder, CO (viha1825@colorado.edu), [2]Department of Atmospheric and Oceanic Sciences, University of Colorado-Boulder

Introduction: Dust activity on Mars fundamentally impacts its present day climate through radiative feedback and by acting as sites for ice cloud nucleation. However, the process by which dust is lifted from surface reservoirs into the atmosphere is poorly understood. The most advanced general circulation models for Mars introduce physically based lifting schemes whereby dust flux is dependent on local wind speeds (usually to the third power) and an arbitrarily defined threshold wind stress that must be exceeded for lifting to begin [1,2]. In general, the threshold wind stress and a mass scaling constant are chosen to reproduce the observed pattern and timing of dust activity on Mars. While more realistic than simulations that prescribe a constant or temporally variable background dust distribution, the physically based lifting scheme is still simple and assumptions have potentially large-scale repercussions. Specifically, the best dust lifting parameterizations for Mars do not currently account for changes in soil erodibility (the ease with which dust is lofted from different soil types) or soil moisture. In particular, highly erodible soils require a lower threshold wind stress or less energetic surface winds to induce lifting and the mass flux at each wind speed is proportionally increased. Mars is assumed to be globally highly erodible. However, there may be spatial variation that corresponds with sand dunes, dry lake beds, etc that will impact the distribution of the most active dust lifting regions. Moreover, if "sand grains" that drive dust lifting are actually cemented dust, then the dust particles may need high winds to break them loose.

Kok et al. 2012, 2014 develop a suite of dust lifting parameterizations for Earth that more realistically address the impact of soil properties (including size distribution of particles, interparticle cohesion, soil moisture, and erodibility) on vertical dust flux as well on the disruption brittle aggregates that are more easily lofted and broken apart in the process of saltation-sandblasting. In studies of the modern Earth climate, these improvements more realistically simulate the distribution of dust activity globally without prescribing preferred lifting or source regions [5]. Simulations indicate that dust lifting is extremely sensitive to soil properties and the specifically the soil threshold friction velocity. Of note, the wind speed dependence of lifting can involve a power law higher than the third power because higher energies are required to fragment "sand" grains. This higher power law makes dust lifting more dependent on rare high wind speeds. Kok's parameterization is easy to implement in global circulation models since lifting depends on commonly defined variables in general circulation models

Here, we present results from the NCAR Community Atmosphere Model for Mars (MarsCAM) coupled with a physically based, state of the art cloud and dust physics developed for Earth: the Community Aerosol and Radiation Model for Atmospheres (CARMA). We implement a new dust lifting scheme based on advanced parameterizations for Earth [3,4]. We investigate its impact on the distribution and timing of dust activity throughout the Mars year and its role in generating observed interannual variability.

Dust Lifting Scheme:

Dust is lifted in regions where the wind stress exceeds a threshold of 22.5mN/m2 [2] following Eq. 1 (4).

$$F_d = C_d \frac{\rho_a (u_*^2 - u_{*t}^2)}{u_{*st}} \left(\frac{u_*}{u_{*t}}\right)^{\frac{C_\alpha (u_{*st} - u_{*st0})}{u_{*st0}}} \quad \text{(Eq. 1)}$$

F_d is the instantaneous mass flux in kg/m^2/s for a given surface wind speed, u_*. Dust lifting is initiated if wind speeds exceed the threshold, u_{*t}. Erodible soils will have higher mass fluxes at lower wind speeds (the most highly erodible soils have a threshold wind stress = u_{*st0}) and initiate dust lifting at smaller threshold wind stresses (C_d).

Results are compared with simulations of dust lifting based on standard lifting schemes used on Mars[2].

As a preliminary study, we investigate the influence of the final exponent (how much mass is injected at a particular wind speed) on the generation of interannually varying, sporadic dust storms. Additional work is needed to study the spatial distribution of erodibility across the martian surface.

Acknowledgements: This work is funded by NASA's Planetary Habitability Program NX16AO80G

References:

[1] C. Newman et al. (2002) J. Geophys. Res. Planets. 103, E12 [2] M.A. Kahre et al. (2006) J. Geophys Res. 111, E06008 [3] J. F. Kok et al. (2011) PNAS, 103(3), 1016-1021 [4] J. F. Kok et al. (2014) Atmos. Chem. Phys. 14, 13023-13041 [5] J. F. Kok et al. (2014b) Atmos. Chem. Phys. 14, 13043-13061

SOLAR FORCING OF THE ABRUPT LAST GLACIAL INCEPTION. F. He[1,2], P. U. Clark[2] and A. E. Carlson[2], [1]Center for Climatic Research, Nelson Institute for Environmental Studies, University of Wisconsin-Madison, Madison, WI 53706, USA, fenghe@wisc.edu, [2]College of Earth, Ocean, and Atmospheric Sciences, Oregon State University, Corvallis, Oregon 97331, USA, Peter.Clark@oregonstate.edu, acarlson@coas.oregonstate.edu.

Introduction: Over the past one million years, the Earth has experienced rather regular ice-age cycles with a dominant 100-kyr periodicity, with every ~90,000 years of a cold glacial period followed by ~10,000 years of a warm interglacial period. According to the Milankovitch theory, changes in summer insolation in the Northern Hemisphere high latitude are responsible for glacial cycles through their impacts on ice-sheet mass balance. The last interglacial peaked around 128,000 years ago when Northern Hemisphere summer insolation was at its maximum. The global climate probably reached its optimum as the Antarctica was almost ~5 ºC warmer than present [1]. Global sea level was substantially higher than now, reaching 5 to 10 meters higher than current sea level, with contributions from both the Greenland and Antarctic ice sheets [2]. Because atmospheric CO_2 concentrations were similar to the pre-industrial level of 280 ppm [3], the warmer last interglaciation and higher sea level suggest that the climate system was very sensitive to the insolation forcing.

Abrupt Last Glacial Inception: Global climate cooled substantially and rapidly between 125,000 and 116,000 years ago, when Northern Hemisphere summer insolation decreased as a result of the precession and obliquity cycles of the Milankovitch forcing. Both Greenland and Antarctic temperatures decreased by almost half of the amplitudes of their glacial/interglacial changes [1, 4], and North Atlantic SSTs also decreased abruptly by ~4 ºC around 116,000 years ago [5]. In contrast, atmospheric CO_2 and global sea level did not change substantially during this early stage of the interglacial/glacial transition [2, 3]. The decoupling between global sea level, atmospheric CO_2 and the global surface temperature change during the last glacial inception is puzzling, with vital implications for projecting future changes arising from anthropogenic forcing.

Solar Forcing of the Last Glacial Inception: In this presentation, we will show the results from TraCE-LIG, the first Transient synchronously coupled global ClimatE simulation of Last InterGlaciation (LIG) in Community Climate System Model Version 3 (CCSM3) [6], which spans the periods between 140,000 and 107,000 years ago. TraCE-LIG is able to produce a climate optimum around 124,000 years ago and a rapid last glacial inception around 119,000 years ago due to the gradual changes of orbital forcing. In TraCE-LIG, the gradual reduction of the Northern Hemisphere summer insolation associated with precessional and obliquity forcing produces gradual cooling of ~2.5 ºC in the Northern Hemisphere annual extratropical surface temperature between 124,000 and 119,000 years ago. However, the simulated Northern Hemisphere annual extratropical surface temperature dropped abruptly by over 4 ºC in less than 100 years at ~119,000 year ago to initiate the rapid glacial inception in TraCE-LIG. The analyses of the coupled atmosphere-ocean-sea ice system in TraCE-LIG suggests that the rapid glacial inception results from the positive feedbacks between the northward oceanic heat transport associated with the Atlantic Meridional Overturning Circulation (AMOC) and the sea-ice expansion in the Labrador Sea associated with the solar forcing. The lead-lag analysis shows the expansion of sea ice is faster and leads the AMOC during the rapid glacial inception, suggesting that the solar forcing is the ultimate cause of the rapid last glacial inception.

References: [1] Jouzel J. et al. (2007), *Science, 317*, 793-796. [2] Dutton A. et al. (2015) *Science, 349,* aaa4019. [3] Bereiter B. et al. (2015) *Geophysical Research Letters, 42*, 542-549. [4] Andersen K. K. et al. (2004) *Nature, 431,* 147-151. [5] Oppo, D. W. et al. (2006), *Quaternary Science Reviews, 25*, 3268-3277 (2006). [6] Collins W. D. et al. (2006). *Journal of Climate, 19*, 2122-2143.

EVRYSCOPE DETECTION OF THE FIRST PROXIMA SUPERFLARE: IMPACTS ON THE ATMOSPHERE AND HABITABILITY OF PROXIMA B. W. S. Howard[1] and M. A. Tilley[2], and H. T. Corbett[1], and A. A. Youngblood[3], and R. O. Parke Loyd[4], and J. K. Ratzloff[1], and N. M. Law[1], and O. Fors[1,5],and D. del Ser[1,5], and E. L. Shkolnik[4], and C. A. Ziegler[1], and E. E. Goeke[1], and A. D. Pietraallo[1], and J. Haislip[1], [1]Department of Physics and Astronomy, University of North Carolina at Chapel Hill, Chapel Hill, NC 27599-3255, USA, wshoward@unc.edu, [2]Dept. of Earth & Space Sciences, University of Washington, Seattle, WA, USA, [3]NASA Goddard Space Flight Center, Greenbelt, MD, 20771, [4]School of Earth and Space Exploration, Arizona State University, Tempe, AZ, 85282, USA, [5]Institut de Ciències del Cosmos (ICCUB), Universitat de Barcelona, IEEC-UB, Martí i Franquès 1, E08028 Barcelona, Spain.

Introduction: Proxima b is a terrestrial-mass planet in the habitable zone of Proxima Centauri [1]. Proxima Centauri's high stellar activity however casts doubt on the habitability of Proxima b. Superflares (extreme stellar events with an estimated energy release of at least 10^{33} erg) and any associated energetic particles may permanently prevent the formation of a protective atmospheric ozone layer, leading to UV radiation levels on the surface which are beyond what some of the hardiest-known organisms can survive, e.g. [2, 3].

The Proxima superflare: In March 2016, the Evryscope array of small optical telescopes [4] recorded the first superflare seen from Proxima Centauri. Proxima increased in optical flux by a factor of ~68 during the superflare and released a bolometric energy of $10^{33.5}$ erg, ~10X larger than any previously-detected flare from Proxima. Over the last two years the Evryscope has recorded 23 other large Proxima flares ranging in energy from $10^{30.6}$ erg to $10^{32.4}$ erg; coupling those rates with the single superflare detection, we predict at least 5 superflares occur each year [5].

Impacts on the climate of Proxima b: We employ a coupled photochemical and radiative-convective planetary climate model to determine the effects of the observed flare activity on the potential habitability of Proxima b [2].

Atmospheric impacts and ozone loss. We use the Evryscope flare rates to model the photochemical effects of NO_x atmospheric species generated by particle events from this extreme stellar activity, and show that the repeated flaring may be sufficient to reduce the ozone of an Earth-like atmosphere by 90% within five years; complete depletion may occur within several hundred kyr [5].

Surface UV Environment. Without ozone, the UV light produced by the Evryscope superflare would have reached the surface with ~100X the intensity required to kill simple UV-hardy microorganisms [6], suggesting that life would have to undergo extreme adaptations to survive in the surface areas of Proxima b exposed to these flares.

We compare the UV surface environment of Proxima b to that of the early Earth, which may have undergone significantly higher UV fluxes during the early evolution of life. Archean Earth climate models give UV surface fluxes on Earth during the pre-biotic (3.9 Ga ago) and early Proterozoic (2.0 Ga ago) epochs [7]. Assuming full ozone-loss, the surface UV-B flux during the Proxima superflare was an average of 2X higher than that 3.9 Ga ago and 3X higher 2.0 Ga ago, although between flares the UV flux was much lower than Earth's, because late M-dwarfs are far fainter in the UV than solar-type stars. The UV-C superflare flux was 7X higher than that 3.9 Ga ago and 1750X higher than 2.0 Ga ago; again, the UV-C flux potentially reaching Proxima's surface is the critical difference compared to Earth's environment [5].

Implications for nearby terrestrial planets: Two-thirds of M-dwarfs are active [8], and superflares will significantly impact the habitability of the planets orbiting many of these stars, which make up the majority of the Galaxy's stellar population. Measuring the impact of superflares on these worlds will thus be a necessary component in the search for extraterrestrial life on planets discovered by the NASA TESS mission [9] and other surveys. Beyond Proxima, Evryscope has already performed similar long-term high-cadence monitoring of every other bright Southern TESS planet-search target, and will therefore be able to measure the habitability impact of stellar activity for these stars.

References: [1] Anglada-Escudé G. et al. (2016) *Nature, 536,* 437. [2] Tilley M. A. et al. (2017) *ArXiv e-prints*, arXiv:1711.08484. [3] Grießmeier J. M. et al. (2016) *A&A*, 587, A159. [4] Law N. M. et al. (2015) *PASP*, 127, 234. [5] Howard W. S. et al. (2018) *ApJL*, in press. ArXiv e-prints, arXiv:1804.02001. [6] Gascón J. et al. (1995) *Curr Microbiol*, 30, 177. [7] Rugheimer S. et al. (2015) *ApJ*, 806, 137. [8] West A. A. et al. (2015) *ApJ*, 812, 3. [9] Ricker G. R. et al. (2014) *Proc. SPIE, Space Telescopes and Instr.*, 9143, Abstract # 914320.

Spectral Content Variations through a Solar Cycle and Abetting Decrease in Spectral Albedo of Glacial Ice.

G. B. Hughes[1], J. Adams[1], and J. M. H. Cockburn[2]
[1]California Polytechnic State University, 1 Grand Avenue, San Luis Obispo, CA; 93407, gbhughes@calpoly.edu
[2]University of Guelph, 50 Stone Rd East, Guelph ON, N1G 2W1, jaclyn.cockburn@uoguelph.ca

Introduction: Satellite measurements indicate that peak amplitude variation in (broadband) total solar irradiance (TSI) through solar cycles 21 and 22 was ~1 W m^{-2} [1-3]. However, the broadband TSI increase was not evenly distributed across all wavelengths. Appreciable increases in ultraviolet (UV) irradiance (200–400 nm) with corresponding decreases at optical wavelengths were observed during solar maxima [1,4].

Spectral albedo of snow-covered ice decreases markedly from visible (0.95 near 600 nm) into UV wavelengths (0.80 near 380 nm, and falling rapidly toward shorter wavelengths) [5,6]. The abetting tandem of increased UV irradiance during solar maxima and decreased spectral albedo of glacial ice in UV wavelengths infers that differential meltwater volume could be produced over a surface ice field through a solar cycle. If the effect is real, solar activity may represent a significant variable factor in energy budgets for some glaciers. Evidence from models and observations is presented to explore the dual, abetting UV processes.

Physical Model: A model is developed to estimate changes in meltwater volume over a glacial ice field that could be produced by the two UV phenomena. Daylight-hour energy flux over a glacial surface area is calculated from potential clear-sky insolation. A specified effective broadband albedo determines absorbed energy, which supplies latent heat of fusion to the ice, creating meltwater. Summing daily meltwater totals during a specified melt season produces an estimate of total seasonal meltwater volume, $\hat{V}_{MS}$:

$$\hat{V}_{MS} = \sum_{d \in MS} \left[V_C(d) + \frac{[\,1 - \alpha_e(\varphi_\odot)\,]A_W}{\rho \Delta H_f} \int_{t \in d} \hat{I}(\varphi_\odot, d, t)\, dt \right]$$

The effective albedo $\alpha_e(\varphi_\odot)$ at Schwabe cycle phase $\varphi_\odot$ is implemented as a free parameter, with estimated values based on observations of spectral albedo in optical and some UV wavelengths, based on previous work [5]. Potential clear-sky insolation $\hat{I}(\varphi_\odot, d, t)$ is estimated for melt-season day *d* at time *t* using a function of solar irradiance at the top of the atmosphere, baseline atmospheric transmission, solar geometry and topography of the ice field [7]. The meltwater production model is used to estimate total meltwater volume in a melt season at a specified Schwabe cycle phase and corresponding estimate of effective albedo. Under an assumption that the convectional component $V_C(d)$ of total meltwater is statistically stationary on time scales of a solar cycle, a solar activity component of total meltwater can be isolated. Total solar-effect meltwater volume is calculated for values of the solar parameters over a range of values representing variability through a solar cycle. A differential seasonal meltwater volume attributable solely to the presumed abetting UV forcing mechanism is produced.

Simulations: The meltwater volume model is implemented in Matlab, for a specified geographic setting. Simulations confirm that the observed variation in broadband TSI over a solar cycle (with constant albedo) does not have an appreciable effect on total seasonal meltwater volume. Simulation results also confirm the evident deduction that changes in albedo (with constant spectral irradiance) have a linear effect on meltwater volume; 5% reduction in effective albedo doubles meltwater production. Simulations that combine a decrease in UV albedo and an increase in UV irradiance indicate that significant changes in meltwater volume are expected throughout a solar cycle.

Case Study: The dual UV phenomena are modeled in the specific context of erstwhile Iceberg Lake, AK (60° 46' N, 142° 57' W) [8,9]. For at least 1500 years, Iceberg Lake was bounded between the Tana glacier and an ice dam; in 1999, the lake suddenly emptied completely, likely due to drainage as the ice dam receded. Watershed area of 74 km^2 feeding the lake was predominantly covered by three small alpine glaciers [9]. Several sediment cores were recovered from the dry lakebed; the cores displayed a typical glacio-lacustrine 'varve' pattern.

Glaciolacustrine Varves. The term varve is used to describe a particular pattern of alternating layers exhibited in some sediments and sedimentary rocks. Layers are distinguished by contrasting color and texture that result from annual cycles of deposition. Seasonal temperature and/or rainfall cycles can drive large variations in water volume supplied to a lake or other catchment; variations in water supply affect the quantity and texture of waterborne sediment delivered to the catchment. Seasonal temperatures that result in intervals of ice-covered and open water can further affect sediment delivery and preservation, e.g., via effects on water column turbulence.

Varve-Sunspot Comparison. Annual layers in Iceberg Lake sediments provide a unique opportunity for investigating potential effects of solar activity on seasonal meltwater input, since annual sediment accumulation serves as an accurate proxy for seasonal meltwater volume. A varve thickness sequence from Iceberg

Lake [8] is compared to the sunspot record, 1610-1995 C.E. [10]. Statistical measures of correlation and causation all support the same conclusion: that patterns observed in the Iceberg Lake varve thickness sequence are not likely to be the result of a random response to the solar activity signal ($\alpha \leq 0.05$).

At least some spectral power present in the varve signal within the Schwabe frequency band is significantly greater than the pink-noise floor ($\alpha \leq 0.05$) (Fig. 1). Thus, some periodic components in the varve signal are not likely to result solely from the pink-noise component of the varve process. Spectrograms display visually intriguing co-evolution patterns of prominent spectral features. Maunder (1645-1715 CE) and Dalton (1796-1820 CE) minima are clearly discernible as pan-spectral lulls in both spectrograms. Spectral content in the varve signal strengthens as the solar cycle intensifies. Potential effects of climate on varve-thickness at Iceberg Lake within the Schwabe periodicity are discounted due to low temporal and spectral correlation with measured regional climate variables.

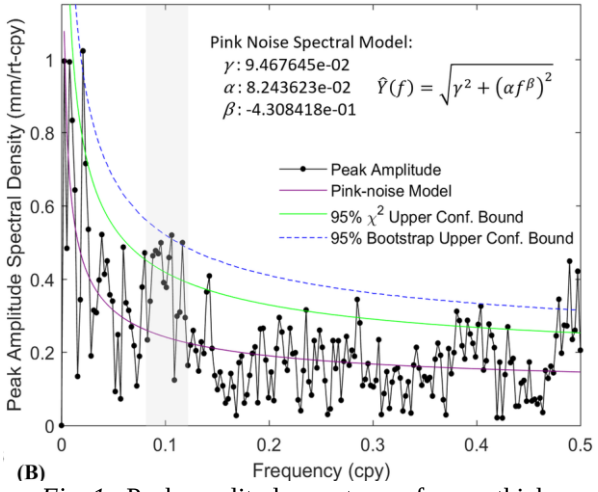

Fig. 1. Peak amplitude spectrum of varve thickness from Iceberg Lake, 1610-1995 C.E.

Etiology. Statistical and spectral correlation cannot form a basis for concluding a causal link. An etiology can be advanced by formulating and applying generally discriminating criteria for causal relationships among correlated time-series records. The Henle-Koch-Evans (HKE) postulates [11] were developed to establish causation of disease by microorganisms. Analogs of HKE postulates adapted for the specific context of two observational records are formulated, e.g., effect cannot precede a putative cause; effect must not be observed in the absence of the putative cause; etc. A suite of discriminating tests applied to the Iceberg Lake varve thickness and sunspot records are all consistent with a solar influence on varve thickness at the Schwabe periodicity, and do not present any clear contradiction of the hypothesized causal relationship.

Putative Solar Activity Effect. Sediment density and estimated basin area [8] are used to determine total sediment volume for a selected annual accumulation at Iceberg Lake. Suspended sediment concentration (SSC) is calculated for the modeled differential meltwater volume and the observed difference in varve thickness amplitude between solar maximum and minimum. A <5% reduction in effective albedo can produce a peak amplitude variation of 5-7 mm, as is observed in the Iceberg Lake varve thickness sequence. Derived SSC values are comparable to observations from similar glacial outflows.

Conclusions: It is probable that solar activity contributed to variations in varve thickness at Iceberg Lake near the Schwabe periodicity through direct modulation of meltwater volume [12]. Direct solar forcing may partially account for persistently observed glacial mass-balance deficits. The putative forcing mechanism would be pronounced at high latitudes and high elevations, where Earth's atmosphere absorbs less of the ultraviolet energy emitted by the Sun due to relatively thin and dry atmosphere. Processes that reduce polar ozone concentration would exacerbate a solar activity UV effect on glacial ice melting, suggesting a potential link between human activities that reduce atmospheric ozone concentration and recently described acceleration of polar ice cap melting.

References:

[1] C. Fröhlich and J. Lean (2004) *Astron. Astrophys. Rev.*, **12**(4), 273-320.
[2] R.C. Willson (1997) *Science* **77**(5334), 1963-1965.
[3] R.C. Willson and H.S. Hudson (1991) *Nature*, **351**(6321), 42-44.
[4] J.L. Lean, G.J. Rottman, H.L. Kyle, et al. (1997) *J. Geophys. Res.*, **102**(D25), 29939-29956.
[5] A. Malinka, E. Zege, G. Heygster and L. Istomina (2016) *The Cryosphere*, **10**(6), 2541-2557.
[6] T.C. Grenfell and D.K. Perovich (1984) *J. Geophys. Res.*, **89**(C3), 3573-3580.
[7] Z. Yong, L. Shiyin and D. Yongjian (2007) *J. Glaciol.*, **53**(180), 91-98.
[8] M.G. Loso (2009) *J. Paleolimnol.*, **41**(1), 117-128.
[9] K.E. Diedrich and M.G. Loso (2012) *J. Paleolimnol.*, **48**(1), 115-132.
[10] D.V. Hoyt and K.H. Schatten (1998) *Sol. Phys.*, **179**, 189-219.
[11] A.S. Evans (1976) *Yale J. Biol. Med.*, **49**(2), 175-195.
[12] G. Hughes, J. Adams and J.M.H. Cockburn (2018) *Can. J. Earth Sci.*, **in press**.

GCM experiments on occurrence condition of the runaway greenhouse state: aquaplanets and landplanets. M. Ishiwatari[1], S. Noda[2], K. Nakajima[3], Y. O. Takahashi[4], S. Takehiro[5], Y.-Y. Hayashi[4], [1]Faculty of Science, Hokkaido University, momoko@gfd-dennou.org, [2]Graduate School of Science, Kyoto University, [3]Department of Earth and Planetary Sciences, Faculty of Sciences, Kyushu University, [4]Graduate School of Science, Kobe University, [5]Research Institute for Mathematical Sciences, Kyoto University

Introduction: Aiming for assessing the potential habitability of extrasolar terrestrial planets, the existence condition of liquid water on planetary surfaces has been discussed (e.g., [1]). One of the main issues is the examination on the occurrence condition of the runaway greenhouse state. The runaway greenhouse state is defined as a state in which incident flux given to the atmosphere exceeds the radiation limit: the upper limit of outgoing longwave radiation (OLR) emitted from the top of the moist atmosphere on a planet with ocean[2]. In the runaway greenhouse state, thermal equilibrium cannot be realized. Numerical experiments on the runaway greenhouse state for various conditions has been performed by the use of atmospheric general circulation models (AGCMs). For aquaplanets which are covered with ocean all over the surface, it has been discussed that atmospheric circulation affects the occurrence condition of the runaway greenhouse state under Earth-like condition (e.g., [3]) and that cloud albedo significantly affects the occurrence condition under synchronously rotating planet condition[4]. GCM experiments for landplanets has been also performed. A land planet is a planet which possesses water on its surface much less than Earth. It was shown that the runaway greenhouse state does not emerge for the value of solar constant of 1.7 times of present Earth's value[5]. Above described previous studies did not examine the dependence of the occurrence condition of the runaway greenhouse state on parameters such as planetary rotation rate, obliquity, and so on. One may think that the occurrence condition of the runaway greenhouse state changes with planetary rotation rate since large scale atmospheric circulation structure, and hence water vapor distribution in the atmosphere, changes according to the values of planetary rotation rate[6]. However, our speculation is that, regardless of planet configurations, the runaway greenhouse state emerges when global mean absorbed solar radiation flux exceeds the maximum values of OLR. In order to confirm our speculation, we perform a numerical experiments with an AGCM for various experimental setups.

Model: We use the AGCM developed by our research group, DCPAM (http://www.gfd-dennou.org/library/dcpam). The basic equations of DCPAM are primitive equations in spherical geometry. Subgrid physical processes are parameterized with standard methods used in terrestrial Meteorology. The amount of cloud water is calculated with integrating a time dependent equation including generation, advection, turbulent diffusion, and extinction of cloud water. Extinction rate of cloud water is assumed to be proportional to the amount of cloud water, and extinction time is given as an external parameter. Solar constant is varied from 1.0 times to 2.3 times of present Earth's value. Two kinds of spatial and temporal distribution of solar flux are used: one for synchronously rotating planets with fixed dayside and nightside, and the other for an Earth-like, non-synchronously rotating planets with diurnal and seasonal changes. For the horizontal discretization, we use the spherical spectral transform method with triangular truncation at total wavenumber 21 (T21). As the vertical coordinate, $\sigma = p/p_s$ is adopted, where p_s is surface pressure. The number of vertical levels is set to 26.Following two series of experiment are performed: (1) Aquaplanet series. The entire surface is assumed to be a ``swamp ocean" with zero heat capacity. (2) Landplanet series. A bucket model[7] is applied to all of the surface. Three initial conditions for ground water are used: uniform distributions with 20, 40, and 60 cm depth of water.

Results: In aquaplanet series experiments, the upper limit of OLR emerges with increasing the value of solar constant regardless the existence of clouds and solar flux distribution. It seems that runaway greenhouse state appears when global mean absorbed solar radiation flux exceeds the maximum values of OLR. This results suggest that the occurrence condition of the runaway greenhouse state is determined by a common mechanism. In presentation, we will also show the results of landplanet series experiment.

References: [1] Kasting J. F. et al. (1993) Icarus, 101, 108-128. [2] Nakajima S. et al. (1992) J. Atmos. Sci., 49, 2256-2266. [3] Leconte J. et al. (2013) Nature, 504, 268-271. [4] Yang J. et al. (2013) Astro. Phys. Lett., 771, L45. [5] Abe Y. et al. (2011) Astrobiology, 11, 443-460. [6] Kaspi Y. and Showman A. P. (2015) Astro. Phys. J., 804:60. [7] Manabe S. (1969) Mon. Weather Rev., 97, 739-774.

MARS CLIMATE AND VOLATILE EVOLUTION. B.M. Jakosky, Laboratory for Atmospheric and Space Physics, University of Colorado, Boulder, CO USA, bruce.jakosky@lasp.colorado.edu.

Introduction: Fundamental questions exist on the nature of the Mars climate at the present epoch, its evolution through time over the four-billion-year history reflected on the surface and in the atmosphere, and in the processes responsible for climate change. These processes and the evolution of the system connect up through the behavior of Martian volatiles on the one-year timescale and how these add up year by year to produce the long-term behavior. I'll examine the behavior of Mars climate and volatiles, starting from the annual behavior and building up to long-term evolution.

Annual and interannual behavior: At the annual level, there are three interconnected aspects of the climate and volatile behavior:

- The seasonal cycles of atmospheric water, dust, and CO_2, which are connected to the solar forcing and the response largely of the polar caps.
- Photochemical processes in the atmosphere that can lead to loss of CO_2 and H_2O to space.
- Interactions with the solar EUV and the solar wind that can strip gas from the top of the atmosphere to space.

The seasonal cycles are observed to vary from one year to another, and to show behavior that can vary on the decades-long or century-long timescale. As a result, it is not clear what type of behavior is representative of the present epoch, if there is such a thing. In addition, the eleven-year solar cycle varies the forces leading to and driving escape to space.

Obliquity timescales: Solar forcing varies due to the changing orbital elements, largely but not entirely focused on the axial obliquity. On 10^5- and 10^6- year timescales, the evolution of obliquity is well determined, but it becomes chaotic and unpredictable on 10^7-year and longer timescales. As a result, the guiding center of the obliquity can wander between essentially 0 and ~60°. At values larger than today's 25°, solar forcing of the poles is stronger, and the atmospheric behavior (water and dust cycles in particular) may be very different. One possibility is that the north polar cap may have formed in its current incarnation in only the last 5 million years when the obliquity appears to have dropped to its current value.

Amazonian and Hesperian behavior: The Hesperian lasted from around 3.7 b.y.a. to about 3.0 b.y.a., and the Amazonian since then. The Hesperian was dominated by the catastrophic flooding, with the associated uncertainty of where the water went. Did the water pond up in the northern lowlands and percolate into the crust or freeze in place? Or was it subsequently lost to space through an as-yet-undefined process that would have allowed for greater loss than at present?

In the Amazonian, ice appears to have been emplaced into thick deposits in the mid-latitudes. Was this a one-time emplacement, or does the water come and go with the orbital forcing? That is, do these processes represent one-time sinks for water? What is the total inventory of water locked up in these deposits?

Noachian: The Noachian was dominated by more-abundant water and an enhanced loss of water and CO_2 to space. Loss of volatiles to space appears to be a primary mechanism that drove changes in the climate during this period, resulting from increased stripping by solar EUV and the solar wind. We can use the observations of the loss to space at the present (as observed by the MAVEN spacecraft) to extrapolate to earlier periods and to determine the early loss when the solar behavior was different.

Volatile inventory and outstanding questions: We can construct an inventory for Martian CO_2 that includes supply from both early outgassing and volcanic release of juvenile gas and loss to various sinks. Sinks for CO_2 include loss to space by solar-wind and EUV stripping, impact ejection to space, the polar ice caps, polar and non-polar water/CO_2 clathrate hydrate, formation of carbonates, and carbonate deposition in the deep regolith. Each of these can be quantified and, together, can account for the loss of an early thick CO_2 atmosphere.

In order to fully understand these issues and to quantify the history of Martian volatiles, the following questions must be addressed:

- What role does exposed H_2O ice in the summertime south-polar region play in the seasonal water cycle? What is the net annual exchange of H_2O between the poles today?
- Is the source of H_2O from the north summertime residual cap the white ice cap or the dark lanes, or some combination?
- What atmospheric dust and H_2O behavior is representative of the present epoch?
- Do we understand the seasonal cycles well enough to extrapolate to other epochs with confidence? How do we extrapolate dust behavior (and its effects on the H_2O cycle) to other obliquities?
- What is the effect of obliquity on loss of H to space, either by changing the O content of the atmosphere or through the H_2O?

- What fraction of the water contained in intrusive and extrusive volcanics actually is released to the atmosphere?
- Has the water released from catastrophic flooding been sequestered in the northern lowlands or crust or lost to space? If the former, has it been removed from the system without fractionation of D/H?
    - Has the water ice that has been identified below the surface today been removed from the surface system permanently, or can it diffuse back? Has it been removed from the system without fractionation of D/H?
    - Does the control of H loss by O loss (as described by McElroy) extend to other epochs (high obliquity, early periods when the atmosphere was different and loss was greater)?
    - Does the O lost to space come from CO_2 or H_2O or some combination? How much H_2O and CO_2 have been lost to space?
    - How much CO_2 was in the early atmosphere, and what process removed C to space to give the observed isotopic fractionation?

USING DEEP SPACE CLIMATE OBSERVATORY (DSCOVR) MEASUREMENTS TO STUDY THE EARTH AS AN EXOPLANET. Jonathan H. Jiang, Jet Propulsion Laboratory, California Institute of Technology, Pasadena, California (Jonathan.H.Jiang@jpl.nasa.gov)

Motivation: In the famous photograph of planet Earth taken by the Voyager 1 spacecraft from 6 billion kilometers away on February 14, 1990, the Earth appears as a single-point light, a Pale-Blue Dot. However, the use of Earth images for exoplanet studies has been limited in scope. Theoretical models have suggested that information about Earth's rotational period and surface properties may be obtained from variations of its reflected light. Empirically testing this idea requires observations of a long temporal baseline.

Data and Results: More than two years of Earth images taken from L1 point by DSCOVR spacecraft are used to produce time series of multi-wavelength, single-point light sources, in order to extract information on planetary rotation, weather and cloud patterns, surface type (ocean, land, vegetation), and orbit around the Sun. In what follows, we assume that these properties of the Earth are unknown, and instead attempt to derive them from first principles. These conclusions are then compared with known data about our planet. We further simulated phase angle changes, as well as the minimum data collection rate needed to determine the rotation period of an exoplanet.

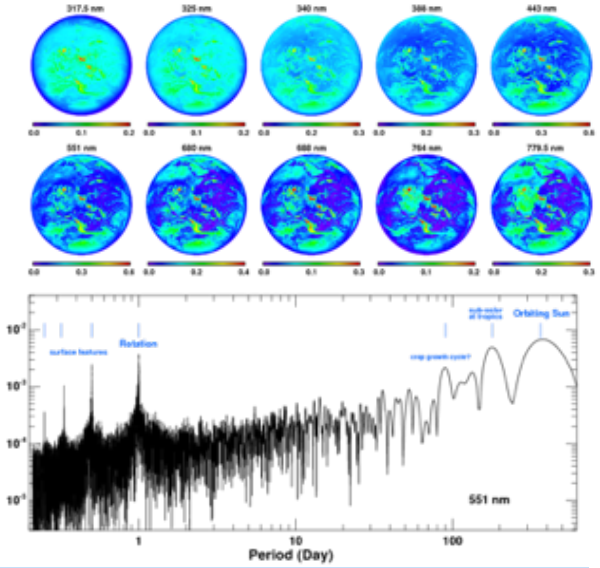

Top: DSCOVR 10 wavelength imagery of the Earth taken at 9:22 UTC, February 8, 2017; **Bottom**: Fourier series power spectra of the Earth's 551 nm single-point reflected lights reveal information about the Earth rotation and orbital periods, as well as surface features.

Significance: This method of using the time evolution of a multi-wavelength, reflected single-point light source, can be deployed for retrieving a range of intrinsic properties of an exoplanet around a distant star. Pontential applications include using measurements from the soon-to-be launched JWST and future WFrist experiments and thus contribute to exoplanet research.

References: Jiang, J.H. et al. Using Deep Space Climate Observatory Measurements to Study the Earth as An Exoplanet, Astronomical Journal, in press, 2018..

Acknowledgement: This work was partly supported by a Exoplanet Study Initiative at the Jet Propulsion Laboratory, California Institute of Technology

THE LAND BIOSPHERE AND PLANETARY CLIMATE: FEEDBACKS TO HABITABILITY. N. Y. Kiang[1], [1]NASA Goddard Institute for Space Studies, 2880 Broadway, New York, NY 10025, Nancy.Y.Kiang@nasa.gov.

Plants first colonized the land starting 460 Mya, gradually transforming climate through impacts on the water, energy, and carbon cycles. Does life on land lead to homeostatisis or unstable feedbacks to climate, and at what temporal and spatial scales? This talk reviews our understanding of how life on land (including humans) alters climate and the global carbon budget, at the catchment scale to global circulation patterns, and at the diurnal to geologic time scales. I review how land biosphere effects on climate have been investigated in various modeling studies, from toy Daisy Worlds to weather models to Earth System Models that simulate paleoclimates to climate change in the next few centuries. I finally review how the land surface has been treated in various idealized planetary climate modeling experiments, and how these choices or parameterizations affect the bounds of simulated climatologies, the habitable zone, and choices of metrics of habitability. Utlimately, feedbacks between life and the atmosphere lead to a co-evolution of both and the continued diversification of life. Such diversity may demonstrate distinct epochs as useful benchmarks for exoplanets, according to certain metrics, but for which the future is unknown.

CYCLONIC ACTIVITIES ON JUPITER AND EARTH; CATASTROPHIC ATMOSPHERIC PHENOMENA OF THE WAVE NATURE: EL-NINO, CYCLONS, TORNADO.

G.G. Kochemasov; IGEM of the Russian Academy of Sciences, 35 Staromonetny, 119017 Moscow, RF, kochem.36@mail.ru

Atmosphere is one of the outer geographical envelops occurring under influence of the tectonics of the solid Earth [2]. In its structure is the first order feature – global tectonic dichotomy made by the fundamental wave long 2πR. The uplifted continental hemisphere opposes to the subsided Pacific one. This global structure is complicated by superimposed sectors due to the first overtone wave2 (long πR). Corresponding to the Earth's orbit tectonic granulation has size πR/4 due to the wave πR/2. Characteristic tectonic formation of this size (~5000 km in diameter) is a Precambrian platform or a craton with its folded frame. Eight such granules are placed in the great planetary ring – equator.

To the tectonic dichotomy in the atmosphere correspond two global cells: one with the lower pressure with a centre of constant measurements in Darwin (Australia) on the continental hemisphere and the second with the higher pressure with a centre in the Easter Island in the Pacific hemisphere (Fig. 1) . From the point of view keeping the angular momentum such opposition of atmospheric pressures is understandable: to the uplifting eastern hemisphere with increased radius corresponds the lower pressure, to the subsided oceanic western hemisphere with diminished radius corresponds the higher pressure. Periodic changes of this stable configuration of pressures- increasing pressure in Darwin and lowering over Easter Island – leads to a change of oceanic current in the Pacific, increasing water temperature and origin of unfavorable often catastrophic conditions in the environment (Fig. 2).

Cyclones or typhoons with diameters up to several thousands km – cells of the lower pressure – arise normally in the tropics (Fig. 3). Their sizes are typically rather smaller than calculated for tectonic granules (5000 km). One might explain this by a tendency of diminishing sizes of objects in the tropical and equatorial belts for the purpose of diminishing their angular momentum. This process of diminishing is characteristic also for other geospheres. For example, in the lithosphere (crust) there is subsidence of platform bases, in the anthroposphere there is a global phenomenon of pygmeoidness. According to the Le to Chatelier principle, diminishing sizes of atmospheric cells (granules) are compensated by increasing speed of their rotation for keeping their angular momentum. Such rapidly rotating objects, and also taking in moisture for increasing their mass, come down to coasts and inlands with downpours and hurricanes.

Tornado – smaller rotating objects possess huge destructive force. Their sizes are connected with atmospheric cells made by rotating atmosphere. Under rotating frequency 1/1 day their theoretical size is πR/1460 or ~14 km in diameter. In fact their size is smaller, reaches about 8 km. This decrease also can be connected with their occurrence in the tropical zones with increased radius demanding decrease of sizes and masses of objects for decreasing the angular momentum. A consequence of this is increase of rotating speed with catastrophic results (Fig. 5).

Recently discovered with help of infrared device (Yuno project, 2018,[1]) cyclonic chains around both poles of Jupiter might be compared with famous catastrophic terrestrial cyclones. Jovian cyclones make chains of 8 around the North Pole and 5 around the South Pole. In case of Earth 8 tectonic granules of the wave nature and πR/4 size encircle the planet along the equator (grand planet's ring). At the western Pacific hemisphere four of these granules are presented by a chain of cyclones in the atmosphere (Fig.3). An essential difference of the jovian and terrestrial chains is in their positions: on Earth it belongs to the longest equatorial ring, on Jupiter to a much shorter ring in high latitudes near to the North Pole (Fig.4). Another important difference is in relative sizes of the storms. On Earth they are smaller (as if, squeezed), on Jupiter they are larger, more massive. The positions of both chains should explain this taking into account difference of their angular momentum. The equatorial belt with the larger angular momentum requires squeezing objects to diminish momentum, the high latitude zones with smaller radius and momentum require more massive objects. All this for equilibration of momenta in various zones of a rotating body. Significantly squeezed terrestrial equatorial cyclones are catastrophically rapidly rotating.

References: 1. Adriani A., Muru A., Orton G., Hansen C., Altieri F et al Clusters of cyclones encircling Jupiter's poles // Nature, 2018, v. 555, # 7695, 216-219. doi:10.1038/nature25491. **2**. Kochemasov G.G. Reflection of the Earth's tectonic dichotomy in the atmosphere, dendrosphere, and anthroposphere (the geospheres coupling of the two-faced Earth)// 'Planet Earth" system, Moscow, LENAND, 2016, 496 pp.(p. 179-181)(In Russian). **3**. Trenberth K.E., P.D.Jones, P.

Ambenje, R. Bojariu et al., 2007: Observations: Surface and Atmospheric Climate Change. In: Climate Change 2007: The Physic al Science Basis. Contribution of Working Group I to the Fourth Assessment Report of the Inter-governmental Panel on Climate Change [Solomon S., D. Qin, M. Manning, Z. Chen, M. Marquis, K.B. Averyt, M. Tignor and M.L. Miller (eds.)] 2007, Cambridge University Press, Cambridge, United Kingdom and New York, NY. USA.

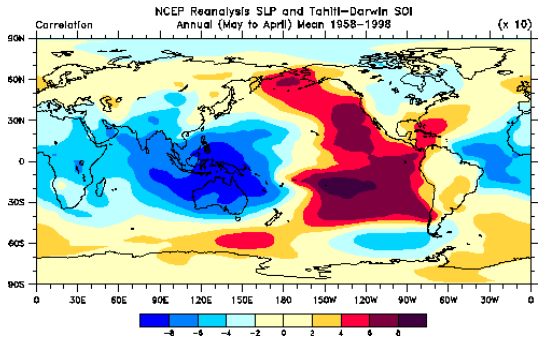

Fig. 1. High and low atmospheric pressures (many years observations) [3].

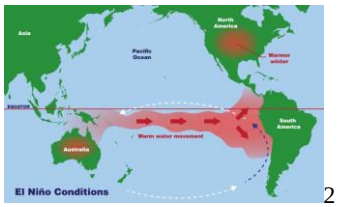

2 Fig. 2. .Origin of El-Nino.

5 Fig. 5. Tornado in USA.

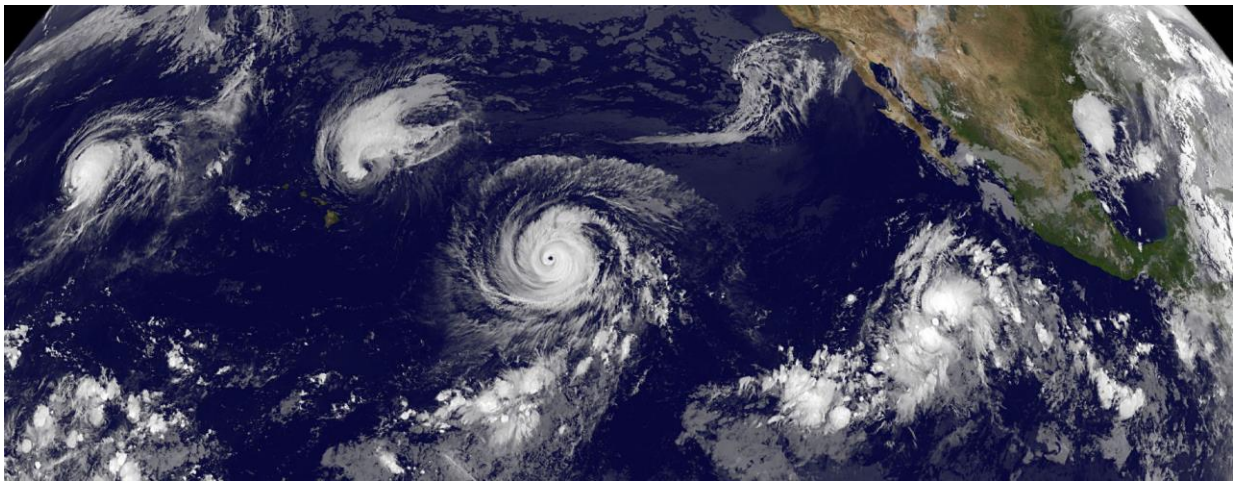

3

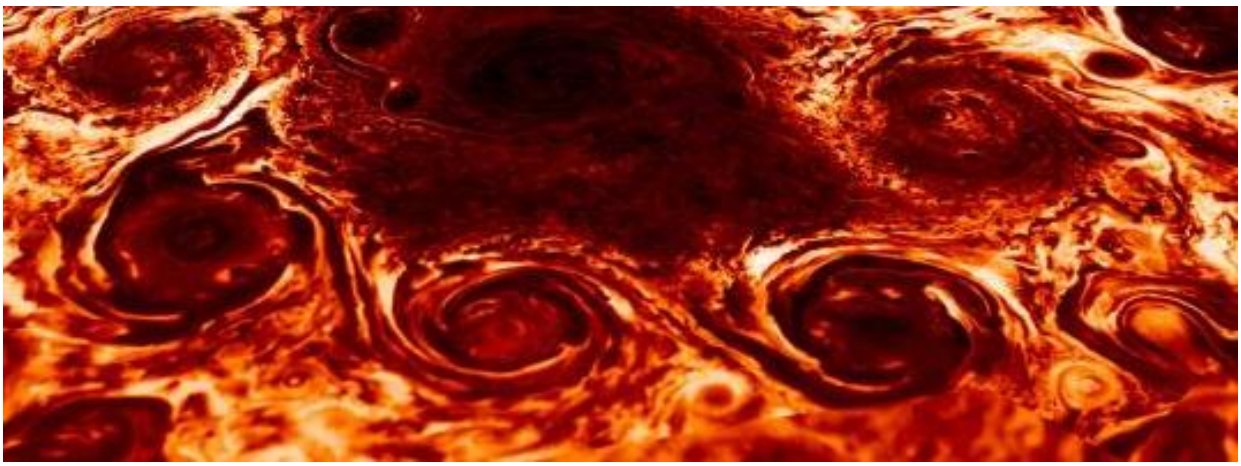

4

Fig. 3. Cyclones on Earth. (over the Pacific). Fig. 4. Cyclones on Jupiter (North Pole) [1]

.

The Emergent Linearity of Outgoing Longwave Radiation in a Moist Atmosphere: Implications for the climates of Earth and Extrasolar Planets. Daniel D.B. Koll[1] and Timothy W. Cronin[1], [1]Department of Earth, Atmospheric and Planetary Science, Massachusetts Institute of Technology; dkoll@mit.edu.

Satellite observations and radiative calculations show that Earth's outgoing longwave radiation (OLR) is an essentially linear function of surface temperature over a wide range of temperatures (>60 K; see Figure 1). Although the evidence for a linear relation was first pointed out more than 50 years ago, it is still unclear why this relation is valid.

Linearity implies that Earth's OLR does not follow the non-linearity suggested by the Stefan-Boltzmann law, σT_s^4. Moreover, linearity also has profound consequences for past and future climate change: if OLR is approximately linear, then Earth's longwave climate feedback, $dOLR/dT_s$, is approximately constant, such that radiative forcing has the same impact in warm as in cold climates.

Here we present a simple semi-analytical model that explains Earth's linear OLR as an emergent property of an atmosphere whose greenhouse effect is dominated by a condensible gas. We show that linearity arises from a competition between the surface's increasing thermal emission and the narrowing of spectral window regions with warming, and breaks down at high temperatures once continuum absorption cuts off spectral windows. Our model provides a new way of understanding the longwave contribution to changes in Earth's climate sensitivity. Moreover, our model predicts that atmospheres dominated by exotic condensible greenhouse gases also develop a near-linear OLR, such as hot rocky exoplanets covered with lava oceans and with silicate-oxide vapor atmospheres or cold super-Earths beyond the outer edge of the habitable zone with thick CO_2 oceans and atmospheres. Future space telescopes could thus study these exotic worlds as analogs of our own H_2O-dominated climate.

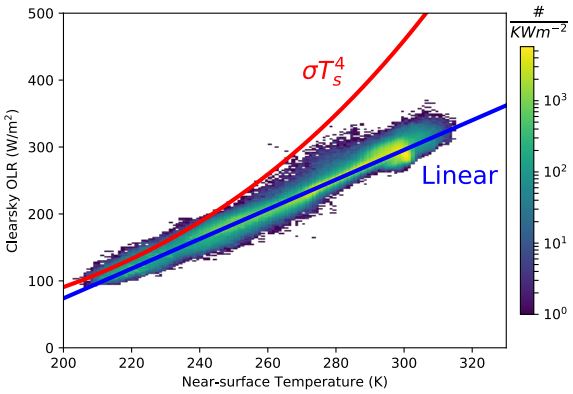

Figure 1: Earth's outgoing longwave radiation (OLR) strongly deviates from the thermal emission of a blackbody, σT_s^4. Instead, the dependence of OLR on surface temperature can be fitted well using a simple linear regression ($r^2 = 0.97$). Shown are monthly-mean clear-sky OLR and near-surface temperatures from satellite and reanalysis datasets.

The Atmospheric Circulation and Cloud Behavior in a Large Suite of Terrestrial Planet GCMs. T.D. Komacek[1] and D.S. Abbot[1], [1]Department of the Geophysical Sciences, University of Chicago, Chicago, IL 60637, USA (tkomacek@uchicago.edu).

Introduction: The recent detections of nearby systems with terrestrial exoplanets in or near the habitable zone (e.g., TRAPPIST-1, Proxima Centauri, GJ 1132, LHS 1140) and the upcoming launch of the *James Webb Space Telescope* motivate a broad investigation into the properties that control the habitability of terrestrial exoplanets. This requires a detailed understanding of how the atmospheres of terrestrial planets vary throughout the potential parameter space we might explore with future observations. Notably, water clouds are expected to play a key role in determining planetary habitability [1,2]. However, more work is needed to understand how cloud behavior and the atmospheric circulation that controls it varies over the possible parameter space of terrestrial exoplanets.

To date, there has been a variety of work done to explore the effect of changing incident stellar flux, incident stellar spectrum, rotation period, surface pressure, planetary radius, and surface gravity on the atmospheric climate dynamics of terrestrial exoplanets [3-8]. However, no unified approach that includes non-grey radiative transfer and cloud effects has been used to study the atmospheric circulation and cloud behavior of terrestrial exoplanets over this parameter space. In this work, we explore how the climates of terrestrial exoplanets around both G and M dwarf stars vary as a function of incident stellar flux, rotation period, surface pressure, planetary radius, surface gravity, and liquid cloud particle size.

Simulations: We use the ExoCAM model [9] with updated water vapor absorption coefficients. This is the same version of the model that was used in [7,8] to study the effects of incident stellar flux and host star spectrum on the climate of tidally-locked terrestrial exoplanets. We consider aquaplanets with atmospheres composed only of nitrogen and water vapor. As in [7], we run one set of models using M-dwarf spectra with effective temperatures of 2600 and 4000 K which assumes that the planets are spin-synchronized. In this set of models, we set the rotation period of the planet equal to its orbital period that the planet should have for a given incident stellar flux. We additionally run a suite of models with the same M-dwarf spectra where we assume spin synchronization but do not vary the rotation period in a physically consistent way. Instead, in this suite of models we individually adjust the rotation period, incident stellar flux, planetary radius, surface pressure, gravity, and cloud particle size. We do so in order to isolate the effects of each parameter on the resulting climate. Lastly, we run a suite of simulations for planets around a Sun-like star, varying the same suite of parameters as for the M-dwarf models above.

Parameter space exploration. For the simulations around M-dwarfs with a rotation period set by assuming spin synchronization, we vary the incident stellar flux from 0.544 - 1 F_{Earth} as shown in Table 1, with 4 simulations each around M-dwarfs with T_{eff} = 2600 and 4000 K. For simulations of planets orbiting M-dwarfs with T_{eff} = 2600, 4000 K and orbiting a Sun-like star, we vary planetary parameters as shown in Table 1. Hence, we run 24 simulations for each incident spectrum spanning this parameter space, for a total of 80 simulations in our full suite of models.

Results: We analyze these simulations in order to understand how the atmospheric dynamics and cloud distribution of terrestrial exoplanets are affected by their planetary properties. We explore how the atmospheric dynamics of our ExoCAM simulations that include non-grey radiative transfer and cloud effects differ from the models of [4] that do not consider these effects. Additionally, we expand upon the work of [8] to include the effects of varying planetary radius, surface pressure and surface gravity. We also isolate the effects of varying rotation period and incident stellar flux on the day-night temperature contrasts of tidally-locked terrestrial exoplanets. Finally, explore how varying this wide range of planetary parameters affects the dynamical regimes of the atmospheres and the transition between atmospheric circulations dominated by day-night flow to those with zonal jets.

We explore the basic-state climate from these simulations in order to determine how varying planetary parameters affects habitability. We study the cloud distribution of these models in order to determine how the cloud radiative effects change with varying planetary parameters. Additionally, we isolate the individual dependence of the cloud fraction on both rotation period and incident stellar flux in our suite of tidally-locked M dwarf simulations in order to understand the properties that control cloud formation near the substellar point. Lastly, we calculate model phase curves, transmission spectra, and emission spectra to ascertain the effects of clouds on future observations of terrestrial exoplanets.

Planetary Parameter	Value (Earth units)
Incident Stellar Flux	0.544, 0.667, 0.816, 1
Rotation Period	0.25, 0.5, 1, 2, 4, 8, 16
Planetary Radius	0.5, 0.707, 1, 1.414, 2
Surface Gravity	0.5, 0.707, 1, 1.414, 2
Surface Pressure	0.25, 0.5, 1, 2, 4
Liquid Cloud Particle Size (micron)	7, 14, 21

Table 1: Parameter space explored in our suite of models. Each parameter is varied individually, with all other parameters fixed to the value for Earth.

References:

[1] J. Leconte et al. *Nature*, 529:59, 2016. [2] J. Yang et al. *ApJL*, 771:L45, 2013. [3] J. Yang et al. *ApJL*, 787:L2, 2014. [4] Y. Kaspi and A.P. Showman. *ApJ*, 804:60, 2015. [5] R.K. Kopparapu et al. *ApJ*, 819:84, 2016. [6] E.T. Wolf et al. *ApJ*, 837:107, 2017. [7] R.K. Kopparapu et al. *ApJ*, 845:5, 2017. [8] J. Haqq-Misra et al., *ApJ*, 852:67, 2017. [9] E.T. Wolf and O.B. Toon. *JGR: Atmospheres*, 120:5775, 2015.

Comparison of climate sensitivity and feedbacks calculated by a traditional and a new equation

C. Kurt[1] and A.E. Dessler [2],
[1,2] Dept. of Atmospheric Sciences, Texas A&M University, College Station, TX 77843

Introduction: We analyzed the climate feedbacks splitting into the components using the ensemble of 28 different models from the Coupled Model Intercomparison Project Phase 5 (CMIP5). Two different feedback schemes were calculated and compared for two sets of model experiments (abrupt quadruple CO2 increase and control simulations in which the forcing is fixed to pre-industrial period values). In the first scheme, feedbacks are calculated from a traditional energy balance equation which relates the top of the atmosphere radiative flux anomalies to surface temperature anomalies. In the second framework, energy balance equation is related to 500hpa tropical atmospheric temperature anomalies. The details of this new framework is explained in a recent paper [1]. They showed that the new framework produces a tighter correlation with the top of the atmosphere energy imbalance. One of the advantages of using the second parameterization method for the energy balance equation is to calculate the equivalent climate sensitivity more accurately. Furthermore, the effect of obtaining a tighter correlation when 500hpa tropical atmospheric temperature anomalies are used as regressor instead of surface temperature anomalies is more pronounced in the satellite observations such as CERES data. Hence, the second scheme is more suitable when studying climate sensitivity and feedbacks for the observational data.

Top of the atmosphere fluxes associated with each feedback component are calculated using radiative kernels. In general, feedbacks derived from the control ensemble or from the satellite observations produce larger spread when the traditional energy balance equation is used relative to the feedbacks computed using the second scheme. This effect is also seen in the abrupt 4xCO2 simulations, however, to a lesser degree. In this presentation, I will review our analyzes for each feedback components both in terms of the surface and the tropical atmospheric temperature including their spatial features and evolution in time. Using the same energy balance equations, I will compare the equivalent climate sensitivity (ECS) analyses made by using both schemes and discuss the contribution of the individual feedback component to uncertainties in ECS.

References:

[1] Dessler, A., & Forster, P. (2018, February 6). An estimate of equilibrium climate sensitivity from interannual variability. https://doi.org/10.17605/OSF.IO/4ET67.

SOLAR-DRIVEN CLIMATOLOGY OF EARTH'S EXTENDED ENVIRONMENT. J. L. Lean,
Space Science Division, Naval Research Laboratory, Washington, DC 20375, Judith.lean@nrl.navy.mil

Introduction: Solar radiation is the primary energy source for the Earth and other terrestrial planets in the solar system. This energy establishes the thermal structure of Earth's extended environment and initiates chemical and dynamical processes that couple adjacent domains in space and time (Figure 1).

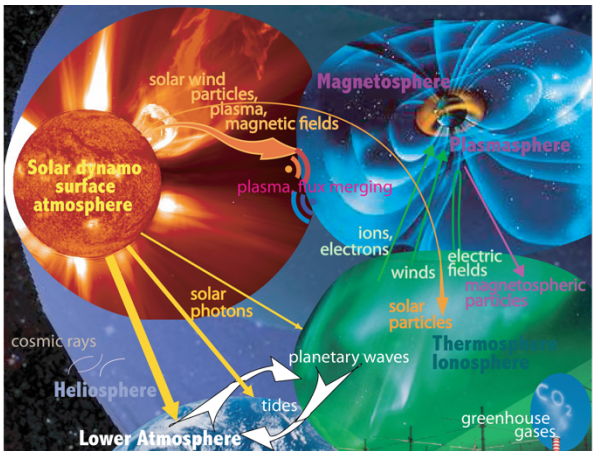

Figure 1. The coupled Sun-Earth System.

The Sun's spectrum at visible and near infrared wavelengths is typical of a black body at 5770 K, with peak emission near 500 nm [1]. This radiation heats Earth's surface, which then radiates thermally to space; the balance between incoming and outgoing energy establishes the planet's surface temperature. Solar radiation at ultraviolet and extreme ultraviolet wavelengths exceeds that of a black body by orders of magnitude; this energy heats the Earth's middle and upper atmosphere, which absorb it completely. Solar UV dissociation of molecular oxygen produces the protective ozone layer and EUV photoionization of oxygen and nitrogen produces the ionosphere.

Earth's elliptical orbit around the Sun, tilted at 23.4° to the ecliptic plane, modulates solar radiation reaching Earth; this modulation drives the dominant variability modes observed in the Earth's environment from surface to space [2]. There is an annual cycle in solar radiation received at Earth (of magnitude ±3.4%) because the Earth is closer to the Sun in January than in July. As well, the distribution of (daily averaged) received solar radiation is hemispherically symmetric at the equinoxes but asymmetrical at the solstices, producing additional annual and semiannual oscillations throughout Earth's extended environment (Figure 2).

Solar radiant energy also varies intrinsically as a result of fluctuations in the Sun's magnetic activity which has dominant cycles at 11, 80-90, 200-210 and 2,500 years. Bright faculae and dark sunspots occur more frequently and with larger areas during times of higher solar activity. These features alter the background (quiet) radiation from the Sun's surface and throughout its atmosphere, thereby altering solar radiant energy at all wavelengths of the electromagnetic spectrum. Variations in solar irradiance at ultraviolet wavelengths (a few percent) and extreme ultraviolet wavelengths (tens of percent) are larger than at visible and near infrared wavelengths (tenths of percent). Solar irradiance variability drives changes in the Earth's environment at 11 years and also 27-days, which is the period of the Sun's rotation on its axis. The 11-year cycle determines the amount and area of facular and sunspot features on the Sun and solar rotation alters their distributions on the hemisphere of the solar disk projected to the Earth. At the Earth's surface the magnitude of the solar activity-related cycles is orders of magnitude smaller than the orbital-driven seasonal variability, but in the upper atmosphere it is more than twice as large. This reflects, in part, the much smaller solar cycle variation in visible solar radiation (~0.1%) that heats the Earth's surface than in EUV radiation absorbed in the upper atmosphere (>50%), relative to the 7% orbital change.

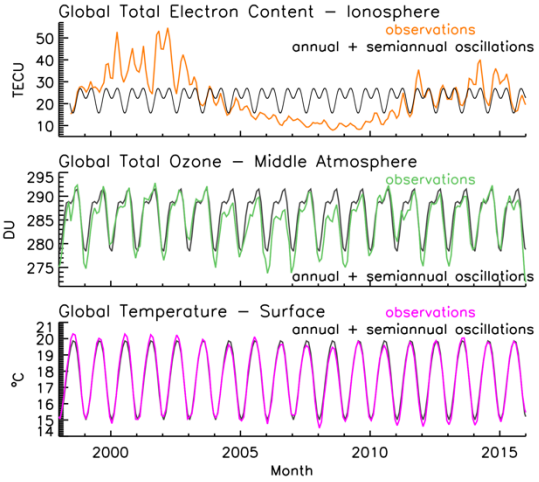

Figure 2. Annual and semiannual oscillations driven by changing Sun-Earth geometry pervade the Earth's environment. Seasonal fluctuations manifest in the global surface temperature (bottom), the total ozone concentration of the middle atmosphere (~30 km, middle) and the total number of electrons in the ionosphere (~250 km, upper). Solar activity further modulates the solar radiation at earth. imposing an additional 11-year cycle on terrestrial temperature and composition. This is most evident in the ionosphere and upper atmosphere, where the magnitudes of the annual and semiannual cycles are larger during times of high solar activity (e.g., 2000-2002) than during solar minima (e.g., 2008-2010).

The solar-driven climatology of Earth's environment thus manifests as a combination of orbitally-driven fluctuations in received solar radiation and solar-activity-driven fluctuations in solar irradiance. The typical approach for determining climatological variations at the Earth's surface, in the lower and middle atmosphere and for the ozone layer, is to first deseasonalize the observations by removing the (orbital-driven) seasonal cycle, taken to be constant and determined as the average of monthly variations observed over many years. This approach assumes the absence of variability in seasonality, i.e, that drivers of Earth's climatology, whether from natural or anthropogenic influences, do not modulate seasonality itself. This assumption is not valid for observations in the upper atmosphere where the solar activity cycle significantly modulates seasonality [3]. For example, the amplitude of the annual oscillation in total electron content is 3× larger, and the SAO amplitude 5× larger, at solar activity maxima than minima.

Following deseasonalization, time series of terrestrial variables such as global surface temperature and total ozone (Figure 3) are analyzed to detect and identify the multiple causes of their climatology. At the surface and in the middle atmosphere, solar and anthropogenic forcings are the primary influences on decadal time scales, with the strength of the solar component increasing relative to the anthropogenic component at higher altitudes. Volcanic activity and internal variability, such as that associated with the El Niño Southern Oscillation (ENSO) and the quasi biennial oscillation (QBO), produce variability on times scales of months to years, and must be properly quantified in order to extract the longer-term solar and anthropogenic components [4].

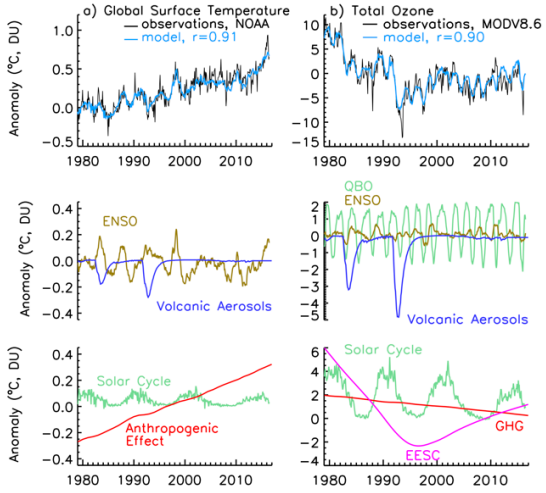

Figure 3 Shown in the upper panel are the deseasonalized observations of (a) global surface temperature and (b) total ozone in the atmosphere. Also shown are statistical models of the variability of the deseasonalized observations in terms of known forcing influences, including ENSO and volcanic aerosols (second panel) and solar activity and anthropogenic gases (bottom row). Adapted from [1].

The increase in solar radiative energy during high solar activity drives dynamical response in the terrestrial atmosphere. More of the increased energy is deposited at low latitudes. This alters the tropospheric circulation that transports excess energy at low latitudes to higher latitudes (Figure 4, from [1]). It further alters the meridional flow in the stratosphere from the summer to winter hemisphere, which overlies, and interacts with, the tropospheric circulation. Zonal inhomogeneities in the meridional flow manifest primarily at the interfaces of the tropospheric circulation cells and alter the longitudinal character of, for example, the circumpolar vortex (polar jet) and intertropical convergence zone. Consequently the terrestrial response pattern to solar irradiance variability has significant regional inhomogeneities that differ notably from the distribution of the forcing itself.

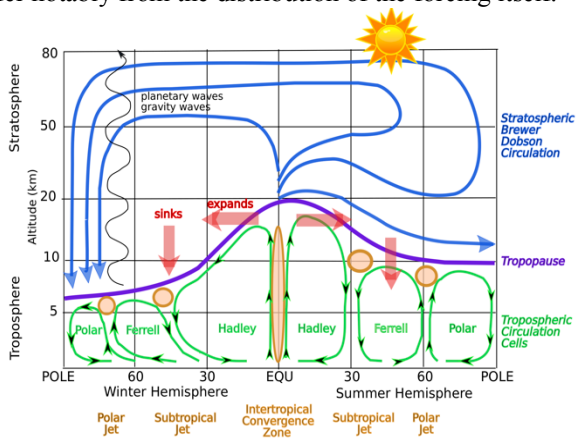

Figure 4 Schematic of meridional flows in Earth's lower atmosphere (troposphere) and middle atmosphere (stratosphere). Increased solar energy alters the thermal gradient from the equator to the poles that drives the meridional flows in the troposphere and from the summer to winter hemisphere in the stratosphere.

References:

[1] Lean, Judith (2017), Sun climate connections, *Oxford Research Encyclopedias, Climate Science*, DOI: 10.1093/acrefore/9780190228620.013.9.

[2] Picone, J. M., J. Lean, M. Jones, Jr., and R. R. Meier (2018), Sun−Earth geometry and the seasonal variation of received solar radiation, *Earth & Space Science,* manuscript in preparation.

[3] Lean, J. L., R. R. Meier, J. M. Picone, F. Sassi, J. T. Emmert, and P. G. Richards (2016), Ionospheric total electron content: Spatial patterns of variability, *J. Geophys. Res. Space Physics*, 121, 10,367–10,402, doi:10.1002/2016JA023210.

[4] Lean, Judith (2018), Observation-based detection and attribution of twenty-first century climate change, *WIREs Climate Change*, 9, doi: 10.1002/wcc.511

Additional Information: The Chief of Naval Research and NASA funded this work.

EXPLORATION OF PLANETARY ATMOSPHERES AND CLIMATES FROM AN ENERGY PERSPECTIVE. L. Li[1] and X. Jiang[2], [1]*Department of Physics, University of Houston, Houston, TX, 77204 (lli7@central.uh.edu)*, [2]*Department of Earth and Atmospheric Sciences, University of Houston, Houston, TX, 77204.*

Introduction: From the energy perspective, there are some important processes in the planetary atmospheric systems, which include radiant energy budget, radiative transfer, and energy conversion. The radiant energy budget and its temporal variation influence the thermal structure of these atmospheric systems. Furthermore, the transfer and distribution of radiant energy within these atmospheric systems can generate mechanical energy to drive atmospheric circulation, weather, and climate. For giant planets, the radiant energy budget and the related internal heat can help understand the evolutionary history of planets.

Here we present some recent progresses in exploring the radiant energy budgets and mechanical energy cycles in the atmospheric systems of the gas giant planets (Jupiter and Saturn) and terrestrial bodies (e.g., Earth and Titan) in our solar system.

Planetary Energies: There are different types of energies on planets and moons [1]. We mainly focus on two energies: the radiant energy and the mechanical energy. For planets and moons, the radiant energy includes two components: the absorbed solar energy and the emitted thermal energy. The radiant energy budget sets critical constraints for the total energies of planets and moons. Furthermore, the transfer and distribution of the radiant energy can generate mechanical energy for the atmospheric systems on planets and moons. The mechanical energy is generally described by the Lorenz energy cycle [2] in which the incoming solar radiation generates potential energy that is transferred to kinetic energy and is finally lost to dissipation.

The studies of radiant and mechanical energies have wide interests in the fields of astronomy, planetary sciences, and atmospheric sciences. In this study, we discuss the radiant energy budget and the Lorenz energy cycle, which are the two important processes related to the radiant and mechanical energies.

Previous Studies And Limitations: The radiant energy budgets of planets and moons in our solar system have been explored for a long time. For our home planet-Earth, the absorbed solar energy basically balances the emitted thermal energy at a global scale, even though small energy imbalance exists [3]. Regarding to the giant planets, the emitted thermal energy is generally larger than the absorbed solar energy, and an internal heat is inferred (e.g., [4-5]). The previous studies of the radiant energy budgets of giant planets are based on observations with significant limitations (e.g.,[6-7]). Therefore, the radiant energy budgets of giant planets should be re-examined with more complete observations.

The Lorenz energy cycle [2] is widely used in the studies of the atmospheres of Earth (e.g., [1]) and other planets (e.g., [8-9]). However, studies of the long-term characteristics of the global atmospheric energy cycle are lacking. The satellite-based global data sets in the modern satellite era make it possible to examine the long-term variations of the Lorenz energy cycle of the global atmosphere on our home planet.

Recent Progresses: We have made some progresses in understanding the radiant energy budgets and the Lorenz energy cycles on some planets and moons in our solar system, which are introduced as below.

Jupiter's radiant energy budget and internal heat. Based on the observations from the Cassini spacecraft, we first measure Jupiter's emitted thermal power [10]. Then we measure Jupiter's albedo in the domain of wavelength and phase angle, which is shown in Fig. 1. Jupiter's albedo is further used to determine Jupiter's radiant energy budget and internal heat [11]. Our study suggests that Jupiter's internal heat is 7.485±0.160 W/m^2, which is significantly larger than 5.444±0.425 W/m^2 from the previous estimate [12].

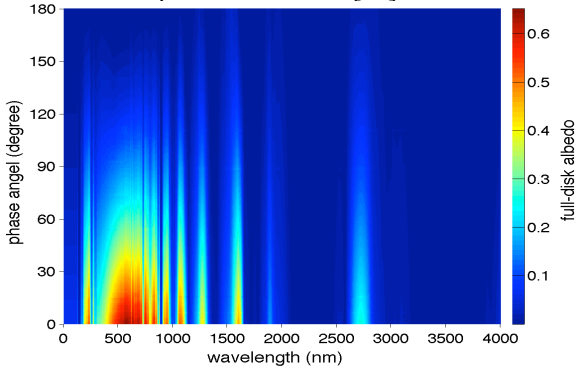

Figure 1. Jupiter's albedo in the domain of phase angle and wavelength (from [11]).

Saturn's varying emitted power. The Cassini observations are also used to examine the radiant energy budget of Saturn. We first find that Saturn's emitted power significantly changed from the Voyager epoch to the Cassini epoch [13]. Our study based on the long-term Cassini observations [14] also suggests that the seasonal cycle plays important roles in the temporal variations of Saturn's emitted power (Fig. 2). Figure 2 also show that the 2010 giant storm significantly modified Saturn's emitted power especially in the storm latitudes.

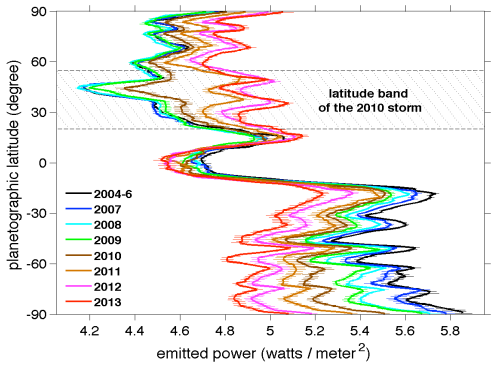

Figure 2. Saturn's emitted power (from [15]).

Titan's radiant energy budget. We conduct the measurements of Titan's emitted power for the first time [14], which indicate that Titan's global energy budget is in equilibrium within measurement error. We also examine the temporal variation of Titan's emitted power [15], which suggests that the global emitted power decreased by 2.5±0.6% from 2007 to 2013.

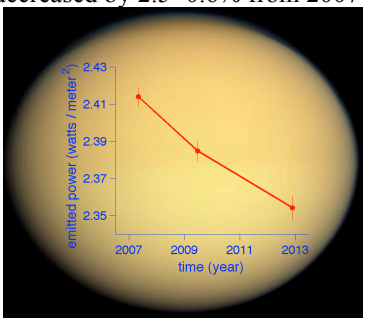

Figure 3. Titan's emitted power (refer [15]).

Earth's Lorenz energy cycle. Based on the two best meteorological data sets (NCEP and ECMWF) during the modern satellite era (1979-2013), we update the mean state of the Lorenz energy cycle of the global atmosphere [16], which corrects some components in the classical picture [17]. Then we explore the temporal variations of the Lorenz energy cycle (Fig. 4), which suggests that the efficiency of the global atmosphere as a heat engine increased during the modern satellite era [18].

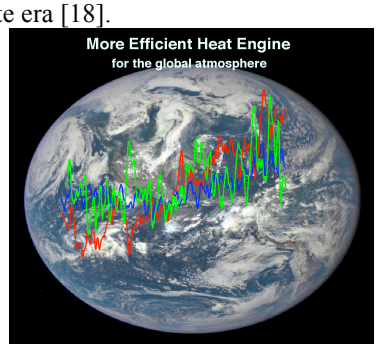

Figure 4. Earth's energy cycle (refer Pan et al., 2017).

Future Work: There are still plenty of studies that need to be accomplished for a better understanding of the radiant energy budgets and Lorenz energy cycles of planets and moons. For example, the energy budgets of Saturn and Titan and their temporal variations can be examined with the Cassini long-term observations. In addition, we plan to examine the radian energy budgets of other astronomical bodies in our solar system (e.g., Uranus, Neptune, Mercury, Venus, Mars, Enceladus, and Europe) and conduct the corresponding comparative studies (Fig. 5).

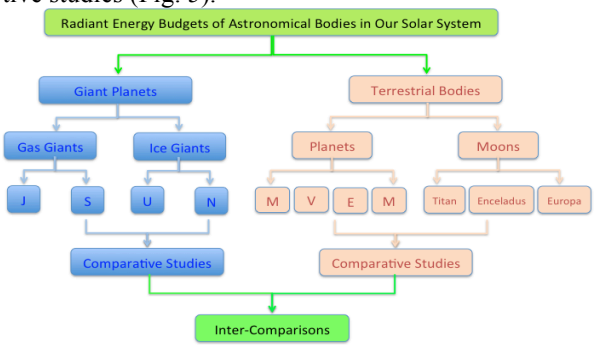

Figure 5. Comparative studies of planetary energy.

The Lorenz energy cycles of the global atmospheres of Earth and Mars have been studied (e.g., [5] [9]), but the studies of the Loren energy cycles of other planets and moons with significant atmospheric systems (e.g., giant planets, Venus, and Titan) are lacking. It will be interesting to examine the Lorenz energy cycles on these planets and moons with new observations and numerical simulations.

References: [1] Peixoto J. P. and Oort A. H. (1992) *Physics of Climate*. [2] Lorenz E. N. (1955) T*ellus* 7, 157–167. [3] Hansen J. et al. (2005) *Science* 308, 1431-1435. [4] Smoluchowski R. (1967) *Nature* 215, 691-695. [5] Hubbard W. B. (1968) *APJ* 152, 745-754. [6] Conrath B. J. et al. (1989) in *Origin and Evolution of Planetary and Satellite Atmospheres.* [7] Ingersoll A. P. (1990) *Science* 248, 308-315. [8] Schubert G. and Mitchell J. (2013) in *Comparative Climatology of Terrestrial Planets*,181–191. [9] Tabataba-Vakili F. et al. (2015) *GRL* 42, 8320-8327. [10] Li L. et al. (2012) *JGR*. doi:10.1029/2012JE004191. [11] Li L. et al. (2018) *Nature Communications,* accepted with minor revision. [12] Hanel R. A. (1981) *JGR* 86, 8705-8712. [13] Li L. et al. (2010) *JGR* 115, E11002. [14] Li L. et al. (2011) *GRL* 38, Art. No. L23201. [15] Li L. (2015) *Scientific Reports*, doi:10.1038/srep08239. [16] Li L. et al. (2007) *GRL* 34, L16813. [17] Oort A. H. (1983) *NOAA Professional Paper* 14, 180-226. [18] Pan Y. et al. (2017) *Nature Communications* 8, 14367.

Acknowledgements: We gratefully acknowledge the Cassini CIRS, ISS, and VIMS teams for recording the data sets of Jupiter, Saturn, and Titan. We also thank the NCEP and ECMWF for Earth's data sets. Finally, we acknowledge the support from the NASA ROSES CDAP, NEWS, and PDART programs.

EVOLVED CLIMATES FOR THE TRAPPIST-1 PLANETARY SYSTEM. A. P. Lincowski[1,2], V. S. Meadows[1,2], D. Crisp[2,3], T. D. Robinson[2,4], R. Luger[1,2], J. Lustig-Yaeger[1,2], and G. N. Arney[2,5], [1]Department of Astronomy and Astrobiology Program, University of Washington, Box 351580, Seattle, WA 98185, USA (alinc@uw.edu), [2]NAI Virtual Planetary Laboratory, Seattle, WA, USA, [3]Jet Propulsion Laboratory, California Institute of Technology, M/S 183-501, 4800 Oak Grove Drive, Pasadena, CA 91109, USA, [4]Department of Physics and Astronomy, Northern Arizona University, Flagstaff, AZ 86011, USA, [5]NASA/Goddard Space Flight Center, Greenbelt, MD 20771, USA.

Introduction: The launch of the *James Webb Space Telescope* (JWST) within the next few years will provide an unprecedented opportunity to characterize the atmospheres and climates of small, nearby planets around small, cool, red M dwarf stars, which are very different from the Sun. M dwarfs are the most common stars in the Galaxy [1], and their small planets are likely common [2], so understanding the environments of these planets is key to understanding the broader origins and evolution of terrestrial planets. A number of small planets have already been discovered around nearby M dwarfs, both inward of and around their star's habitable zone (HZ) [3–10]. These planets generally have lower densities, indicating they may be that are generally more volatile-rich than Earth and Venus, although most of them may also have higher densities [11]. These planets also experience a very different evolutionary history than our Solar System, as their stars undergo an extended super-luminous pre-main-sequence phase, which can result in a runaway greenhouse phase for up to a billion years [12]. To inform terrestrial exoplanet characterization attempts with upcoming instruments, we couple our new 1D VPL Climate model [13] with a photochemical model, both of which have Solar System heritage and validation, to determine possible climates for evolved O_2 and CO_2-dominated atmospheres that could be possible around planets in the seven-planet TRAPPIST-1 system [5–7]. These atmospheres produce different spectral features that may be used to distinguish evolutionary histories and determine current habitable or environmental states for planets in or near the habitable zones of M dwarfs.

Methods: To model the evolved atmospheres of M dwarf planets, we used the VPL Climate model [13], a generalized, terrestrial-based 1D radiative-convective-equilibrium climate model incorporating a rigorous line-by-line, multi-stream, multi-scattering radiative transfer code SMART [14], as its core. This climate model has been tested and validated against observations and atmospheric measurements of Mars, Earth, and Venus [13]. The VPL Climate model employs linear flux Jacobians to efficiently timestep the radiative fluxes, and mixing length theory for convective heat transport. Condensation and evaporation, with the associated latent heat, are included and generalized for any relevant gases for which appropriate thermodynamic data is available. The VPL Climate code is now coupled to a terrestrial photochemical model that has been applied to a variety of worlds [15], and which here we have extended to include Venus.

We apply this coupled model to potential climates and atmospheric compositions for the TRAPPIST-1 planets, which span both ends of the habitable zone [5–7]. We model a diversity of potential environments for comparison, including: a range of O_2-, and CO_2-dominated climates, from severely desiccated, to outgassing and Venus-like; and moist Earth-like environments. These environments may result from outgassing during and after the super-luminous pre-main-sequence phase. We model the climates and chemical abundances of these different environments, including the radiative effects of water or sulfuric acid clouds, as appropriate. We compare these environments with Earth and Venus.

Results: The atmospheres modeled are very different from those in our Solar System due to both the possible starting compositions resulting from a more intense early evolutionary phase, and due to the different spectral energy distribution of a late M dwarf like TRAPPIST-1 compared to the Sun. These diverse possible environments for each modeled planet demonstrate that a planet's position in the habitable zone does not guarantee habitability, though HZ planets are the most likely to have temperate conditions. Temperate (potentially habitable) conditions are a strong function of atmospheric composition. Under a sufficiently strong greenhouse, we find that hot, uninhabitable conditions are possible in a terrestrial environment even beyond the outer edge of the habitable zone for planets that undergo an early runaway greenhouse.

The temperature profiles of these planets differ considerably from Solar System terrestrials. Completely desiccated O_2-dominated atmospheres around late-type M dwarf stars can exhibit strong near-surface temperature inversions and an anti-greenhouse effect due to O_2-O_2 collisional induced absorption of near-IR radiation from the star, along with ozone absorption of outgoing radiation. However, even a small amount of

outgassed water and SO_2 can significantly heat the lower atmosphere of these planets within the HZ, and eliminate the inversion layer. Alternatively, CO_2-rich (Venus-like) atmospheres formed early on via strong stellar and atmospheric evolution, and maintained by the lack of a surface ocean, can provide sufficient warming to elevate surface temperatures in the HZ well above 373 K. These alien Venus-like environments have temperature structures and sulfuric acid formation remarkably similar to Venus, though planets significantly hotter than Venus cannot condense sulfuric acid. The aqua planets were modeled with oxygen similar to Earth, but ozone generation and absorption for such planets is less robust, resulting in very weak stratospheres compared to Earth.

Aerosols have a substantial effect on planetary climate. If fed by outgassing, sulfuric acid clouds can form in the atmospheres of non-ocean bearing planets of different bulk atmospheric compositions around M dwarfs, and aerosol layers cause large decreases in surface temperature. Conversely, Earth-like water-ice clouds have little effect on surface temperature, but do affect the temperature profile (and hence, the observable spectrum).

The figure provides a sample of the modeled climates for TRAPPIST-1 e, including those for O_2-dominated cases that are either completely desiccated or include continual outgassing, as well as Venus-like cases, with and without sulfuric acid aerosols, and habitable aqua planet atmospheres, with and without clouds. These climates are very different, with surface temperatures spanning a difference of ~350 K, even though all environments shown receive the same stellar irradiation (~2/3 of Earth's).

Conclusions: We have used a new terrestrial 1D climate-photochemistry model suite to simulate a variety of possible terrestrial atmospheric compositions around M dwarfs. These planetary environments may exhibit climates and chemical abundances very different from those found in our Solar System, demonstrating the importance of a generalized terrestrial planet climate modeling suite and the importance of photochemistry in shaping planetary climates. In the next 5 years, the TRAPPIST-1 system in particular may provide the opportunity to study planetary evolution within and exterior to the habitable zone within a single system.

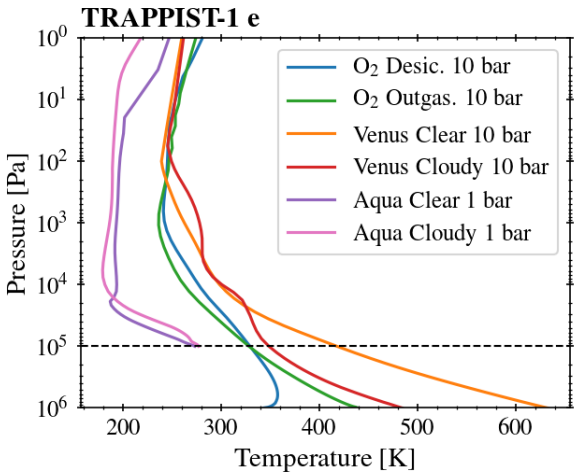

Figure: Converged temperature profiles (pressure vs temperature) modeled for TRAPPIST-1 e. The atmospheric composition, including trace species due to outgassing and photochemistry, substantially affects planetary climate.

References: [1] Henry, J. T. et al. (2006) *AJ*, 132, 2360. [2] Ballard, S. & Johnson, J. A. (2016) *ApJ*, 816, 66. [3] Berta-Thompson, Z. K. et al. (2015) *Nature*, 527, 204. [4] Anglada-Escudé, G. et al. (2016) *Nature*, 536, 437. [5] Gillon, M., et al. (2016) *Nature*, 533(7602), 221–224. [6] Gillon, M., et al. (2017) *Nature*, 542(7642), 456–460. [7] Luger, R. et al. (2017) *Nature Astronomy*, 1(May), 129. [8] Dittmann, J. A. et al. (2017) Nature, 544, 333. [9] Shvartzvald, Y. et al. (2017) *ApJL*, 840, L3. [10] Bonfils, X. et al. (2018) A&A, 613, A25. [11] Grimm, S. L. et al. (2018), A&A, 613, A68. [12] Luger. R. & Barnes, R. (2015) *Astrobiology*, 15(2), 119–143. [13] Robinson, T. D. & Crisp, D. (2018) *JSQRT*, 211, 78. [14] Meadows, V. S. & Crisp, D. (1996) *JGR*, 101(E2), 4595–4622. [15] Meadows, V. S. et al. (2018) *Astrobiology*, 18(2), 133–

Climates of High Obliquity Terrestrial Planets in Idealized Simulations with a Seasonal Cycle. A. H. Lobo[1] and S. Bordoni[2], [1]California Institute of Technology (1200 E. California Blvd. MC 150-21, Pasadena, CA, 91125. lobo@caltech.edu), [2]California Institute of Technology (1200 E. California Blvd. MC 131-24, Pasadena, CA, 91125. bordoni@gps.caltech.edu)

Ongoing discoveries of terrestrial exoplanets suggest that these planets might span a wide range of climatic regimes and atmospheric circulations, which will strongly impact their habitability. In this study, we perform a systematic exploration of the influence of obliquity on the climate of a terrestrial exoplanet with an idealized general circulation model with a completely uniform lower boundary of small thermal inertia. We consider a wide range of possible obliquities, from earth-like values of 23.5 degrees up to 90 degrees.

We compare simulations with annual mean forcing with simulations with a seasonally varying insolation forcing. Consideration of seasonal cycles yields climates and atmospheric circulations that are vastly different from those without, in terms of wind patterns, Hadley circulations strength and extent, and hydrological cycle. Most importantly, high obliquity climates are dominated by seasonally-reversing strong and broad cross-equatorial Hadley circulations that reverse with seasons and which accomplish most of the moisture, energy and momentum transports from the summer into the winter hemisphere.

Seasonal precipitation patterns also feature interesting peculiarities that are not evident in simulations without a seasonal cycle of insolation. In Earth-like low obliquity cases net precipitation (the difference between precipitation and evaporation) is primarily balanced by mean moisture flux convergence in the tropics and eddy moisture flux convergence in the extratropics. In high obliquity cases, however, storage effects become increasingly important in the polar regions because of rapid temperature changes. More specifically, as polar temperatures drop quickly from their maximum values around the summer solstice, the water vapor in the atmospheric column rapidly condenses out, producing large amount of precipitation there. At lower latitudes, peak precipitation is primarily associated with seasonally migrating convergence zones within the Hadley circulation. As the solstice-season cross-equatorial Hadley cells become broader with increasing obliquity, peak precipitation becomes progressively more separated from their poleward boundary and widely used diagnostics are no longer applicable. The lower-level moist static energy maximum, for instance, does not provide a good predictor of maximum precipitation and of the Hadley cell edge. The energy flux equator performs reasonably well, though it is outperformed by predictions made by simpler angular momentum-conserving arguments. This emphasizes the need for more robust theories that are broadly applicable to climates more exotic than Earth's.

THE CIRCULATION AND VOLATILE CYCLES OF SOLAR SYSTEM ATMOSPHERES. J. M. Lora[1], [1]UCLA (595 Charles Young Drive, Los Angeles, CA 90095; jlora@ucla.edu)

Introduction: Terrestrial worlds in the Solar System have a wide range of atmospheres and climates, whose diversity presents interesting opportunities (and challenges) for comparative studies. Atmospheric masses vary wildly, for instance—from Pluto's microbar (and highly variable) surface pressure to Venus' 90 bar—even between planets that are otherwise similar. Similarly, planetary rotation rates vary significantly, and therefore put their atmospheres in distinct circulation regimes. Volatile cycles play critical roles in many of these atmospheres, but are also extremely different since the volatiles in question range from minor constituents to the principal atmospheric gas.

In this review I will describe and compare the climate systems of terrestrial worlds in our Solar System with a focus on atmospheric circulations, and the connection to hydrologic or volatile cycles.

Circulation Regimes: I will discuss some salient features of the general circulation of planetary atmospheres, like Hadley circulations, baroclinic storm tracks, and the transition between these. Venus and Titan are slowly rotating bodies, whose atmospheric flows are therefore less influenced by the Coriolis force than those of Earth and Mars. Nevertheless, the transition between an "all-tropics" circulation and the more familiar case is not sharp, and permits a range of combinations, like nearly global Hadley cells with shallow high-latitude baroclinic systems, in the case of Titan.

Hydrologic and volatile cycles: I will also discuss energy transport by the atmospheric circulation, and the key roles played by volatile species, as well as the surface distribution of their condensed phase. On Earth and Titan, secondary constituents of the atmosphere partake in active hydrologic cycles that strongly respond to and interact with the general circulation, as well as couple with the surface, and are principal features of the climate. On Mars and Pluto, the primary atmospheric constituents condense, so their cycling affects atmospheric mass and the seasonal behavior of the circulation.

In all four cases, the climates of these worlds have likely changed over geologic time, and changes in the behavior of these cycles have left imprints on the surface that might be used to reconstruct past states to better understand planetary climate dynamics.

TITAN'S TROPICAL HYDROLOGICAL CYCLE : CONSTRAINTS FROM HUYGENS, CASSINI AND FUTURE MISSIONS

Ralph D. Lorenz[1] [1]Space Exploration Sector, JHU Applied Physics Laboratory, Laurel, MD 20723, USA. (Ralph.lorenz@jhuapl.edu)

Introduction: Only two worlds in the solar system, Earth and Titan, feature rain falling onto a solid surface in the present epoch. By presenting familiar cloud convection, precipitation and hydrological processes [1] in an exotic environment with a different working fluid, Titan serves as a planet-scale laboratory in which to understand these important phenomena at a more fundamental level. Additionally, these processes significantly modify Titan's landscape, transporting organic material via fluvial sediment transport and via solution erosion and evaporite formation. Thus to decode Titan's geological record and to understand the provenance of surface organics, the rates and character of meteorological and hydrological processes need to be assessed.

Huygens Measurements: The Huygens probe made a single sounding of Titan's atmosphere at 10^{o}S around 9am local solar time, in 2005 (L_s~300^{o}, late southern summer). This revealed multiple features in the potential temperature profile, indicating a nascent planetary boundary layer at ~300m, and inflections at 1,2 and 3km which may be vestigial and/or seasonal boundary layers [2]; the 3km layer likely is the control on the spacing of dunes that circle Titan's low latitudes.

The near-surface methane humidity was about 50%, an amount too small to provide Convective Available Potential Energy (CAPE) for strong cumulus convection. However, parts of the tropospheric profile were saturated, and could permit stratiform rain or drizzle; some turbulence characteristics in the atmosphere are consistent with those measured in clouds on Earth. However, no direct evidence for such hydrometeors was seen, beyond a thin layer of cloud opacity at 21km.

In a comparative climatology sense, the methane profile is an interesting allegory for the likely water vapor profile in the early Venus atmosphere (and that of the Earth in the future when the solar luminosity evolves to high levels), in that the tropopause 'cold trap' is a rather leaky one on Titan – from a value of ~5% at the surface, the methane mixing ratio falls to only ~1.5% in the stratosphere, in contrast to the much smaller abundance of water in the Earth's stratosphere.

An important observation was made at the surface, which was the apparent release of methane and other organics from the heated inlet of the mass spectrometer instrument, the surface science lamp, and perhaps the body of the probe itself. Images of the probe environs suggest it landed in a stream bed, littered with cobbles on a sandy substrate.

The question naturally arose of 'when was this area last rained on?' (although in principle it could have rained elsewhere in a catchment area and the moisture conveyed by the ephemeral river generated as a 'flash flood'.) This is difficult to constrain: one could apply models of vapor transport in a regolith to see how deep the surface should dry out (like many models applied to Mars water vapor exchange) but many parameters are poorly constrained. More importantly, the moisture in the pore space evidently contained less volatile compounds than methane, such as ethane and perhaps benzene. The equilibrium vapor pressure of methane above such an organic mixture could easily be as low as 50% of the saturation value for the pure liquid, in which case this moisture would never dry out, being in equilibrium with the humidity in the air.

Cassini Geomorphology and Circulation Models: The large-scale circulation on Titan is of course different due to the different atmospheric pressure, planetary rotation rate and annual timescale, such that the mean meridional ('Hadley') circulation is usually interhemispheric, with only a transient symmetry phase around equinox. The effect – indicated in Global Circulation Model (GCM) results for over a decade – is to dessicate the low latitudes. Indeed, Cassini mapping shows that Titan's equatorial regions are dominated by large sand seas, whose dunes indicate dry conditions for much of the time. Similarly, the polar regions (and the north in particular) have lakes and seas of methane, which models suggest accumulate during the summer rains (the configuration of Titan's solar eccentricity and pole orientation giving a longer cooler summer in the North). Further geomorphological indicators being used to compare with GCMs are detailed dune morphologies and orientation, and the presence at intermediate latitudes of alluvial fans [3] which are associated with particularly intense rainfall and fluvial transport.

Cassini Cloud Observations: Compared to the Earth, where average cloud cover is of the order of 50-65%, Titan is relatively cloud-free, with pre-Cassini observations indicating cover of ~0.2-1% cloud cover.

A recent paper [4] summarizes Cassini observations of cloud activity throughout the 13 year mission: Clouds were generally more prevalent in the summer hemisphere, but there were surprises in locations and timing of activity: southern clouds were common at mid-latitudes, northern clouds initially appeared much sooner than model predictions, and north-polar summer convective systems did not appear before the mission

ended. Differences from expectations constrain atmospheric circulation models, revealing factors that best match observations, including the roles of surface and subsurface reservoirs. The preference for clouds at mid-northern latitudes rather than near the pole is consistent with models that include widespread polar near-surface methane reservoirs in addition to the lakes and seas, suggesting a broader subsurface methane table is accessible to the atmosphere.

Rain Observations: Cassini has observed two events of surface darkening associated with cloud activity; these are best interpreted as rain events. In 2004 Arrakis Planitia (34,000km^2, 80^{o}S) and in 2010 Concordia Regio (510,000km^2, 20^{o}S [5]). Together, these represent ~0.7% of Titan's surface, in 6 years. Crudely, 100% of the surface would then be rained on in 6*100/0.7~860 years. In reality of course, the Cassini record is unlikely to be complete ('missing' events might be estimated by assuming that rain cells, as on Earth, follow some distribution like a power law) and thus the recurrence interval will be somewhat shorter. However, the order of magnitude is remarkably consistent with the other considerations herein.

Future Missions : While there is an important contribution to be made from groundbased observations in tracking the seasonal distribution of large-scale cloud systems, significant progress will require both orbital and landed/aerial measurements. A Titan orbiter using cameras, spectrometers, and ideally a cloud-profiling radar could observe the evolution of individual storms and constrain the precipitation process. Extended in-situ measurements of winds, temperatures and humidity would be important to understand variability in these properties and to constrain GCMs. Additionally, measurements of soil moisture and hydrological parameters of the surface are important to understand The Dragonfly relocatable lander [ ] proposed to NASA's New Frontiers program could contribute in these areas via long-term landed weather and surface property measurements, imaging and repeated flights that profile the meteorological parameters of the lower atmosphere.

Conclusions and perspective : Considered as a 'relaxation oscillator' the current (heat flux) going through the Titan climate system is small, but the capacitor (moisture content of the atmosphere) is much higher, leading to violent but rare precipitation events. Thus Titan may serve as an example of the evolution of the terrestrial climate (with a warming atmosphere, able to hold moisture) to a destructive extreme. It therefore begs further study by observation and modeling.

References: [1] Haynes, A., R. D. Lorenz, and J. I. Lunine, 2018. A post-Cassini view of Titan's methane cycle, Nature Geoscience, 11, 306-313 [2] Lorenz, R. D., P. Claudin, J. Radebaugh, T. Tokano and B. Andreotti, A 3km boundary layer on Titan indicated by Dune Spacing and Huygens Data, Icarus , 205, 719–721, 2010 [3] Faulk, S.P., Mitchell, J.L., Moon, S. and Lora, J.M., 2017. Regional patterns of extreme precipitation on Titan consistent with observed alluvial fan distribution. Nature Geoscience, 10(11), p.827. [4] Turtle, E. P. et al., 2018. Titan's meteorology over the Cassini mission: Evidence for extensive subsurface methane reservoirs, Geophysical Research Letters, in press doi:10.1029/2018GL078170 [5] Turtle, E.P., et al., 2011. Rapid and extensive surface changes near Titan's equator: Evidence of April showers. science, 331(6023), pp.1414-1417. [6] Lorenz R.D. et al. (2018) APL Tech Digest, in press.see also http://dragonfly.jhuapl.edu

CURRENT STATUS AND FUTURE DIRECTIONS OF CLIMATE MODELING. D. R. Marsh, Atmospheric Chemistry Observations and Modeling, National Center for Atmospheric Research, P.O. Box 3000, Boulder, CO 80307 (marsh@ucar.edu).

Introduction: Our current capability to simulate the past, present and future climate of the Earth depends on the fidelity of what have become known as Earth System Models (ESMs). These models have their developmental roots in the General Circulation Models (GCMs) first used to simulate the global dynamics of only the atmosphere in the 1960s. ESMs extend GCMs by coupling the atmosphere to interactive ocean, sea ice and land ice (i.e., ice sheet) models. In addition, these models include representations of the ecosystems of the land and ocean, and vegetation that dynamically adjusts to changing climate and changing land use; processes that determine the fluxes of trace gases, aerosols and water between the land, ocean and atmosphere. Such fluxes affect the modelled climate by, for example, modifying the radiative heating and cooling rates of the atmosphere and changing the surface albedo of snow and ice via the deposition of black carbon and dust. Also critical to determining the distribution of radiatively active gases and aerosols is the inclusion of interactive chemistry. It is not unusual for an ESM to calculate the concentrations of a hundred or more atmospheric constituents and aerosol types.

Current status: Examples of state-of-the-art ESMs include NCAR's Community Earth System Model [1], the Met Office Global Coupled model 2.0 [2], GFDL's ESM2 [3] and Max-Planck-Institute's MPI-ESM [4]. Development of models such as these is driven on part by a desire to participate in the coupled model intercomparison projects (CMIPs) of which Phase 6 is underway [5]. The purpose of these projects is to understand how the Earth responds to both anthropogenic and natural forcing, and to estimate how the climate will change in the future. It also provides a framework for model evaluation. Extended numerical experiments are conducted under a variety of emission and forcing scenarios to identify critical feedbacks in the climate system, quantify uncertainty and bias in model predictions, and aid in the detection and attribution of global and regional climate change. CMIPs have become a critical part of the international assessments of climate change, e.g., those by the Intergovernmental Panel on Climate Change. However, contributing to CMIPs is not the only use of ESMs. These same models are being integrated into data assimilation systems to provide weather and air quality forecasts. They are also being extended to higher altitudes and including ionospheres and electrodynamics to study space weather. The adaptation of climate models to model the atmospheres of other planets typically lags the Earth version by a model generation or two. This is due to the difficulty in modifying the dynamical core and physics packages that are often 'hard-wired' for the Earth. Versions of the NCAR atmospheric model have been used to model Mars [6], Venus [7], Titan [8] and Saturn [9]. The ocean-coupled version has been used to look at ice-albedo feedbacks in exoplanets [10]. The Met Office GCM is used as the core of the OPUS-Vr model of Venus [11]. Almost invariably, adaptation of these models has necessitated implementing a new radiative transfer (RT) code. Interestingly, the RT code in use in the Met Office ESM supports other planetary atmospheres and has been integrated into the ROCKE-3D GCM [12], a flexible GCM for rocky planets. Similar flexibility built into the latest generation of ESM should make migration of these codes to other planets easier than it has been in the past.

Future development: It is very likely that the spatial resolution of ESMs will continue to increase, with the limiting factor being computational resources. Higher resolution models can better resolve terrain and rely less on parameterizations of sub-grid scale processes, such as gravity waves. Improving cloud microphysics and cloud-aerosol interactions will also likely be a major focus. The line between climate and weather models will blur as the demand for seasonal and decadal predictions increases. New dynamical cores will be adopted that allow for regionally refined resolution to improve regional climate and weather predictions.

It is not clear whether planetary climate modeling will continue to track ESM development. Certainly many of the new capabilities in atmospheric chemistry will be valuable in modeling the composition of early Earth, Titan, exoplanets. The Earth climate modeling community would also benefit from adopting more flexible "planetary' physical parameterization that would better handle possible future extreme climate scenarios.

References: [1] Hurrell, J.W. et al. (2013) *BAMS, 94,* 1339–1360. [2] Williams, K.D., et al. (2015) *Geosci. Model Dev.,* 8, 1509-1524. [3] Dunne, J.P. et al., (2012) *J. Climate*, 25, 6646–6665. [4] Giorgetta, M. A., et al. (2013), *J. Adv. Model. Earth Syst.*, 5, 572–597. [5] Eyring, V. et al. (2016), *Geosci. Model Dev.* 9, 1937-1958. [6] Urata, R.A. and Toon, O.B. (2013) *Icarus*, 226, 229-250. [7] Parish et al. (2011), *Icarus,* 212, 42-65. [8] Larsen, E.J.L et al. (2015) *Icarus,* 254, 122-134. [9] Friedson, A.J. and Moses, J.I. (2012) *Icarus*, 218, 861-875. [10] Shields, A.L. et al. (2013) Astrobio. 8, 715-739. [11] Mendonça, J.M. and Read, P.L., *Planet. Space. Sci.*, 134, 1-18. [12] Way, M.J. et al. (2017) *ApJ.*, 231, 1-22.

Lessons from Akatsuki: Comparative Meteorology. K. McGouldrick[1], [1]University of Colorado Boulder – Laboratory for Atmospheric and Space Physics (3665 Discovery Dr, Boulder, CO 80303, kevin.mcgouldrick@lasp.colorado.edu).

Introduction: The Comparative Climatology of the Terrestrial Planets series of workshops exemplifies the recognition of the necessity to comprehend the planets of our Solar System in a comparative way. In the last twenty years, planetary science has experienced a transition from having been restricted to the study of only the nearest handful of planets in our stellar system, to the scientifically liberating confirmation of thousands (and inference of billions) of planets existing beyond this Solar System. In the upcoming twenty years, the next generation of space telescopes, including TESS, JWST, and others under concept development, will collect data that will provide the capacity to begin to reveal the defining characteristics of these exoplanets, including those characteristics that will be able to help us to determine how habitable those planets might be. In order to make sense of this data, it will be necessary to leverage our existing knowledge of planetary atmospheres in our own solar system in order to leverage the very data-limited information we will obtain from exoplanets. JAXA's Akatsuki spacecraft [1] has been orbiting Venus since December 2015, building a four-dimensional picture (temporal, vertical, and two-dimension horizontal) of the Venus atmosphere by means of multi-wavelength imagery and radio occultation profiling. The Akatsuki mission has demonstrated how it is possible to explore the comparative meteorology of extra-terrestrial planets. In short, Akatsuki has shown that it is both possible and necessary to investigate a planetary atmosphere as a highly coupled and dynamically evolving planetary system.

Characterizing Exoplanets: For most exoplanets, we are now capable of characterizing only the mass and/or radius of an exoplanet, and the distance from its star. The former can provide only a crude estimate of the planetary composition, and the latter an estimate of the nominal radiative energy input to the planet. However, what the planet "does" with that energy input depends strongly upon characteristics we still are incapable of measuring: planetary albedo and atmospheric composition. Fortunately, it is anticipated with the onset of next generation space telescopes that transit spectroscopy will provide us with a glimpse into the composition of exoplanetary atmospheres, and allow us to better refine our estimates of predicted surface properties.

Extraterrestrial and Exoplanetary Comparisons: If we hope to understand exoplanets through the context of our Solar System planets, we need to have sufficient confidence that we understand our Solar System planets in the context of Earth. And, because of the nature of transit spectroscopy, this understanding that will map from Earth to the Solar System to Exoplanets relies heavily upon atmospheric studies – at least for the near future – as that is where most of our exoplanetary data will be focused. However, over a half-century of planetary exploration, the sum total of atmospheric data describing atmosphere-bearing terrestrial planets in our Solar System boils down to many tens of fly-bys, a few multi-year orbiters, and a handful of in situ stations. And that is considering all of the terrestrial atmosphere-bearing planets: Venus, Mars, and Titan! Venus is already the most heavily studied atmosphere in the Solar System (in terms of time and data), after Earth, but imagine trying to understand the climate of the Earth from about ten radiosondes spread over fifty years, a handful of orbiters with irregular and partial views of the atmosphere, and two in-situ stations returning data for about two days.

The Future: In order to understand a planetary atmosphere, we need to study it like a planetary atmosphere. That is, as opposed to a typical planetary surface, a typical planetary atmosphere is a highly coupled, rapidly evolving, four-dimensional beast with seemingly innumerable degrees of freedom. Characterization of such a machine requires a gargantuan amount of data. In order to characterize Earth's atmosphere requires thousands of meteorological ground stations reporting about ten times per day, with two vertical sounding atmospheric profiles obtained twice daily from several hundred of these. This is in addition to thirty or so satellites in Low Earth Orbit collecting high spatial resolution measurements of key meteorological parameters, and a handful of Geostationary satellites providing global context and dynamics. Perhaps it is not necessary to replicate the multiple Terabytes of data collected from the Earth's atmosphere over the course of a day, but a step in that direction is necessary if we ever hope to truly embark in an adventure of Comparative Climatology of Terrestrial Planets.

References:

[1] Nakamura M. et al. (2016) *Earth, Planets, Space, 68*, 75. [2] McGouldrick, K. (2018) *Nature Geosciences, 11*, 4-5.

APPLYING SCIENCE TO FICTION: A LOOK AT THE FICTIONAL PLANET *MESKLIN*. M. M. McKinney, University of California, Los Angeles (mmckinney@atmos.ucla.edu).

Introduction: In the modern field of planetary science, there exists a wide array of known and posited exoplanets to analyze and model. But going back even just a few decades, the majority of exoplanets were fictional. One of these fictional planets is particularly interesting, in part because it was based on a contemporary finding of a potential exoplanet in the 61 Cygni system [1].

While this finding is now known to be false, the planet spawned from it remains an interesting attempt at a truly alien world. This planet is *Mesklin*, developed by Hal Clement for his 1953 novel *Mission of Gravity*.

Mesklin: The planet described in [1] was 16-times Jupiter's mass. Clement wanted to use this as a setting, and thus needed it to be habitable to both native lifeforms and (at least to a degree) humans. Mesklin was given a solid surface, with most of its mass crushed into degenerate matter near at its core [2]. The native lifeforms could traverse this surface, and its high gravity, just fine, but humans would be crushed even with futuristic support.

The solution to this gave Mesklin its most distinctive feature: high rotation, to the point that the planet flattens into an oblate spheroid. With a rotation rate of just 17.75 minutes, the effective gravity at the equator was reduced to 3g, within human tolerance provided the right support suit.

Climate: What would the climate be on this unusual world? The orbit described in [1] would place it well out of the habitable zone for liquid water, but partially within that of liquid methane. The orbit however is also highly elliptical, meaning its closest approach could boil away any liquid methane it might have.

In this presentation, I will explore the creation and design of Mesklin. Focus will be placed on planetary climate, including radiative temperature and basic moisture processes. Did Clement get his calculations correct back in 1953? And what sort of climate could such a planet have?

References: [1] Strand K. A. (1943) *Publications of the Astronomical Society of the Pacific,* 55(322), 29. [2] Clement H. (2002) *Heavy Planet.*

THE ROLE OF ATMOSPHERIC PRESSURE ON MARS SURFACE PROPERTIES AND EARLY MARS CLIMATE MODELING. Michael A. Mischna[1] and Sylvain Piqueux[1], [1]Jet Propulsion Laboratory, California Institute of Technology, 4800 Oak Grove Dr., Pasadena, CA, 91109, USA, michael.a.mischna@jpl.nasa.gov

Introduction: The thermal conductivity of the martian regolith is controlled by atmospheric pressure, via interstitial pore space gas conductivity within the soil. This dependence has an overall effect of raising thermal inertia (TI) values with increased atmospheric pressure, a configuration analogous to having indurated surface material instead of fines. Greater TI will affect the size and timing of areas for which transient liquid water may form. We propose an obliquity-driven cycle of surface evolution that accounts for this behavior.

Background: The atmosphere of early Mars was thicker than the present atmosphere of ~610 Pa, perhaps by as much as 100-fold [1]. This is necessary to explain many of the fluvial features recorded in the geologic record which require both surface temperatures and pressures to be higher than their present-day values.

In order to better understand the martian environment, modelers use general circulation models (GCMs) to simulate Mars' climate, e.g. [2-4]. These models, typically based on terrestrial climate models, but modified to incorporate martian physics, require knowledge of surface conditions—parameters like surface albedo, TI and topography. Traditionally, early Mars climate modelers have adopted present-day surface conditions to use during early Mars simulations, largely because of lack of any better knowledge of the actual conditions.

Of the surface parameters noted above, TI stands out as having a component that can be readily modified for early Mars conditions, even in the absence of any direct knowledge of surface composition or material properties. Thermal inertia is a compound function of the near-surface regolith thermal conductivity, density and specific heat, with the regolith thermal conductivity being strongly controlled by the atmospheric pressure [X]; hence, we should expect the TI of the surface on early Mars to be somewhat greater than today because of the increased thermal conductivity caused by more atmospheric gas in interstitial pore spaces within the soil.

We have explored this gas-pressure effect on surface TI by running the MarsWRF GCM [4] for both present-day (610 Pa) and early Mars (61,000 Pa) surface pressures, using two global maps of surface TI: 1) a present-day map as calculated by [5], and 2) a modified map calculated for an atmospheric pressure of 61,000 Pa.

Results: To determine the impact of using the proper TI on Mars climate simulations, we use annual average surface temperature as our metric, and compare the difference in this value across the planet using both the present-day and 'early Mars' TI maps. Results are shown in Figure 1, which reveals only a marginal difference between the two. In essence, it appears 'OK' to use present-day TI for Mars paleoclimate studies.

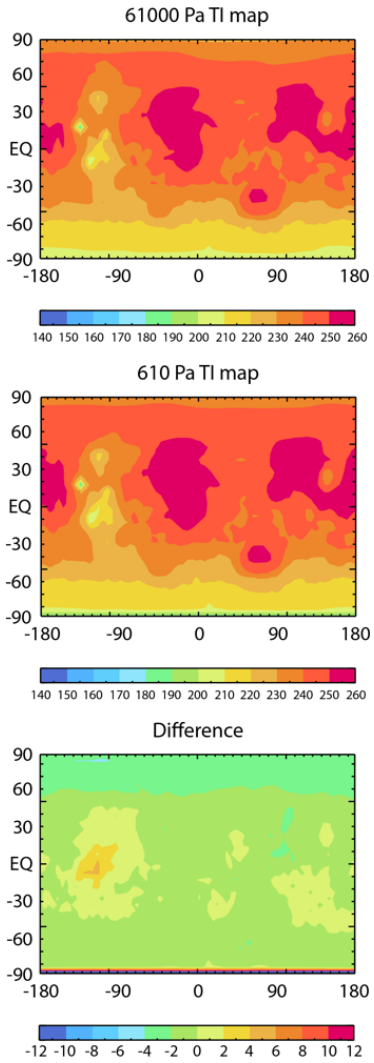

Figure 1: Annual average surface temperature, assuming 100x present-day surface pressure (61,000 Pa), with **(top)** TI map for a thick atmosphere or **(middle)** TI map for the present day thin atmsophere. **(bottom)** Difference showing a negligible effect of using the 'wrong' thermal inertia in paleoclimate studies.

The reverse, though, we have found not to be true, and using larger (i.e. 'early Mars') TI values for the present day will yield annual average surface temperatures as much as 10-12 K colder than using the 'correct' values. Of course, we have direct measurements of thermal inertia, so this is not generally a modeling concern, but when put into the context of shorter-term, orbitally

driven climate variability on Mars (i.e., on 10^6-10^7 year cycles), it presents some interesting questions.

Apart from being a result of higher surface pressure, greater TI is also consistent with having a more indurated surface material (i.e., duricrust). Duricrust can be formed from having both surface salts and more water-rich conditions. The former is widely observed on Mars [6], and the latter may be found during, for example, higher obliquity periods in martian history [7-8]. The combination of moisture and salt will cause loosely bound surface material (dust) to bind together. This will decrease the peak-to-peak range in both diurnal and annual temperatures, and may be expected to occur episodically, any time conditions are right, as during high obliquity periods in martian history.

Presently, on Mars, we observe regions with indurated material, and other regions covered with dust. This suggests an ongoing process of disaggregation and erosion of the bound material back into its constituent dust particles through what is likely an aeolian process [9]. In the absence of adequate moisture in the local environment, such as when obliquity is low, this is irreversible (until, perhaps, the next rise in obliquity). This dusty material has a lower thermal inertia, and a greater peak-to-peak diurnal temperature range than its indurated predecessor, and is the condition we presently observe on Mars. Helping to maintain this state may be the presence of nighttime CO_2 frost, as observed by [10]. Turbidization of the near-surface material from deposition and sublimation of CO_2 frost maintains a disaggregated surface, and helps prevent reformation of indurated surface material.

Conclusions: Together, this is consistent with a pattern of behavior on 10^6-10^7 year timescales—at least in recent Mars history—when surface properties, particularly TI, are regulated by the obliquity cycle (Figure 2). During periods of higher overall TI, peak surface temperatures do not reach values as high as the present day, with its lower TI. This makes it more difficult to reach the frost point temperature, and to support liquid water at the martian surface (Figure 3).

When modeling the martian climate, then, care must be taken to consider the anticipated conditions of the surface during these 'higher TI' periods—it is likely that simulations of recent Mars, using present-day TI values, are overestimating surface temperatures, and the likelihood of surface liquid water.

References: [1] Hu, R. *et al.*, (2015), *Nat. Commun.*, 6:10003. [2] Forget, F. *et al.*, (1999), *JGR*, 104, 24155-24175. [3] Haberle, R. *et al.*, (2003), *Icarus*, 161, 66-89. [4] Toigo, A. *et al.* (2012), *Icarus*, 221, 276-288. [5] Putzig, N. and Mellon, M. (2007), *Icarus*, 191, 68-94. [6] Davila, A. *et al.* (2013), *Int. J. Astrob.*, 12, 321-325. [7] Jakosky, B. and Carr, M. (1985), *Nature*, 315, 559-561. [8] Mischna, M. *et al.* (2003), *JGR,* 108, 5062. [9] Mustard, J. *et al.* (2001), *Nature*, 412, 411-414. [10] Piqueux, S. *et al.* (2016), *JGR*, 121, 1174-1189.

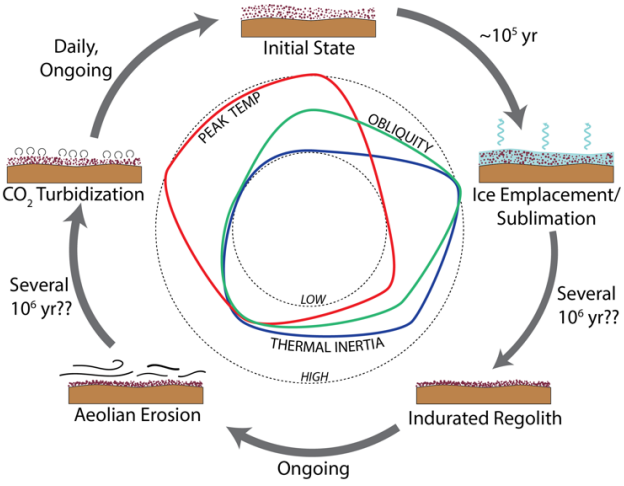

Figure 2: Notional timeline for evolution of martian surface over obliquity cycles, showing the processes modifying surface properties. Red/green/blue curves show relative values (low to high) of peak temperature, obliquity and TI over the obliquity cycle.

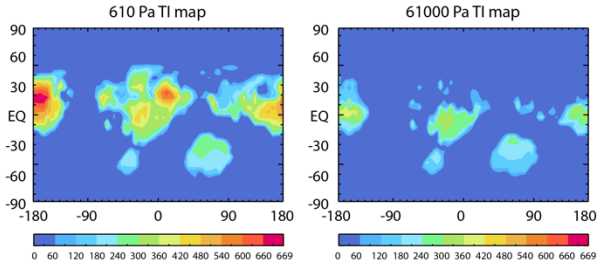

Figure 3: Map view of Mars from MarsWRF simulations showing number of days per year for which peak daytime temperature >273 K and surface pressure >610 Pa for **(left)** present-day TI map and **(right)** higher pressure/greater TI map. The right panel is consistent with more indurated surface material. Differences represent those areas where liquid water can no longer transiently form, or can form over fewer days, during higher obliquity periods due to this TI effect.

COMPARATIVE CLIMATOLOGY OF PLANETS WITH AND WITHOUT GLOBAL OCEAN SYSTEM. Y. Miura, Yamaguchi University, Yamaguchi, 753-0074, Japan. moonyas50@gmail.com.

Introduction: Climatology of terrestrial planets has been discussed from material differences of Earth Science. Climate of planet Earth has been defined in atmosphere originally among three systems of atmosphere (gas state), ocean (liquid state) and rock-minerals (solid state) [1-3]. The main purpose of comparative climates of planets in this study is discussed of global systems of three materials states of rock solid, ocean liquid and atmosphere vapor-gas.

Formation of three systems on planet Earth: The main separation of light and heavy parts of fragments and ion-molecules has been caused by extreme condition of collision process (with dynamic high temperature and pressure conditions) on primordial rocky planets (without any air or liquid systems) originally [4]. From comparative stability of material states, *solids of mineral rocks* are used to be remained as developed rocks at lower temperature and pressure. However, global and/or continuous collisions on planets are produced and remained as vapor-gas state as *atmosphere* at the highest temperature and pressure conditions. In this formation processes, intermediate state of fluid-liquid system (*ocean*) is seriously difficult to be produced and remained between gas and solid states. This is mainly because there are no stoppers in vapor-gas system (except any rocky solids as bubble texture globally). This is another reason to be formed ocean system only water planet Earth of the Solar System finally [4-6].

Climate of Earth type planet: Present climates of Earth-type planets have been produced without global ocean system. This means that there are no material circulation processes among three systems except air and solid states, which are formed wind-induced atmosphere mainly as in Mars and Venus. If there are no circulation process (by material compositions and lower temperature), fluid liquid on any planetary and satellite celestial bodies show regional process (without global activity) as in Titan and Pluto on the System. This is the same situation on exosolar systems because of fundamental material processes.

Summary: The present study summarized as follows:

1) Planets are formed air-solid system at collisions of planetary formation.

2) Ocean liquid system can be formed only Earth planet because of it complicated formation process.

3) Main climates of air-solid planets are found as wind-induced circulation climate (as in Mars and Venus).

4) Main climates of air-fluid-solid celestial bodies are found as less circulated climate (as in Pluto and Titan), which are the similar situation on exosolar systems..

Acknowledgements: Author thanks many scientists discussed for the present study.

References: [1] Climate Prediction Center (NWS). *Climate Glossary* (2006). http://www.cpc.noaa.gov/. [2] Bowden A.J.; Cynthia V. Burek C.V. and Wilding R. (2005). *History of palaeobotany:* Geological Society. 293. ISBN 978-1-86239-174-1. [3] French B. M. (1990) EOS Trans. AGU, 71, 411-414. [4] Miura Y. (1995): *Shock-Wave Handbook* (Ed. by Takayama K, Springer-Verlag Tokyo), 1073-1176. [5] Miura Y. (2007): LPS XXXVIII (LPI,USA), abstract# 1277. [6] Miura Y. (2006): Proc.ICEM06 (Ube, Yamaguchi), 112-113.

EMPLOYING RAY_TRACING TO PROBE MARS ATMOSPHERE.

T. Nikolaidou[1],
[1] University of New Brunswick, Canada (Thalia.Nikolaidou@unb.ca)

Introduction:

Applying principles of electromagnetic wave propagation one is able to trace the transmission of a radio wave through a medium.

On Earth, a such ray-tracing technique is primarily employed to quantify the atmospheric delay experienced by the Global Positioning System (GPS) and other Global Navigation Satellite System (GNSS) signals.

On Mars, although studies have explored the requirements for a GPS system around the planet, existing limitations prevent its realization in the near future.

However, a similar ray-tracing technique could be utilized to study the Martian atmosphere. Examining the delay caused by the neutral atmosphere and ionosphere would provide knowledge on the characteristics of the layers.

This study uses the ray-tracing technique as an exploratory tool to aid Mars meteorology. The initial experiments focus on its neutral atmosphere and aim to contribute to the understanding of its structure, circulation and dynamics. A comparative to Earth analysis will be presented.

Upon successful implementation of the novel experiment, the study will extend to the ionosphere layer. Validation with the Mars Express Radio Science Experiment (MaRS) [1] data, where possible, will also take place.

Mars atmosphere is simulated using the Mars Climate Database (MCD) [2].

References:

[1] Pätzold et al. (2009). Mars: Mars express radio science experiment. European Space Agency, (Special Publication) ESA SP. 217-245

[2] Weblink:http://www-mars.lmd.jussieu.fr/mars/-info_web/-user_manual_5.2.pdf

ONLINE STEM EDUCATION AND AEROSPACE MICRO-LESSON IN NIGERIA
(A panacea to African Development)

A. O. Ogunbiyi[1], [1]Aerospace Palace International, Nigeria (P. O. Box 6929, Sapon, Abeokuta, Ogun State, Nigeria. E-mail address: ceo@aviationpalace.space, aviationpalace@gmail.com)

Around the globe, particularly in developing countries, women and youths lack opportunities to obtain the education that they so desperately need and deserve. Cultural stigmas, religious restrictions, and oppressive laws keep women trapped in desperate poverty and ignorance, unable to obtain the education that might give them hope. History has shown time and again that educating girls provides benefits to the economies of nations. In many cases, changes in cultural attitudes and the legal status of women have resulted in economic benefits that break the cycle of centuries of poverty in just a single generation. The fields of Science, Technology, Engineering, and Mathematics (STEM) are critical to any nation seeking to grow in the 21st century global economy. A robust economy will require citizens thoroughly equipped to compete in the science and technology fields. STEM-focused education responds to the reality that a nation's future will be built its capacity for innovation and invention

To grow the industrial and technological sectors of an economy, you need skilled, trained workers. UNESCO, the United Nations Educational, Scientific, and Cultural Organization, has stated that "Capacity in science and technology is a key element in economic and social development. Promoting science education at all educational levels, and scientific literacy in society in general, is a fundamental building block to building a country's capacity in science and technology."

Our online STEM Education and Aerospace Micro-Lesson in Nigeria is an idea of Aerospace Palace Academy Nigeria and designed to inspire, influence, and mould the next generation of aerospace scientists and engineers by providing a series of resources and programming to teachers, students, parents, and aerospace professionals. The programs enlighten and engage our global community of future aerospace professionals by helping them learn more about science, technology, engineering, and mathematics. Nigeria has suffered a series of decadence in Aerospace and STEM Education, therefore our mission is to stimulate a lasting interest in the STEM disciplines, with the goal of encouraging students to pursue careers in these fields. This is accomplished by actively involving students in the support of authentic research currently being conducted on the International Space Station (ISS) or in a NASA ground-based laboratory. Through collaboration with NASA, AIAA, Space Foundation and NASA researchers, we create educational mini-curriculum for the university, college, high school or middle school classroom that engages students as research assistants, providing data for the Principal Investigator.

To addressed this problem, we created Aerospace Palace Academy, Nigeria which is an innovative organization dedicated to promote increased participation in post-secondary Science, Technology, Engineering and Mathematics (STEM) education in developing nations and underserved group in developed nations around the world. Our education programs are a direct response to the reality that our future will be built on innovation and invention and creative problem-solving. To meet this need, we collaborate with schools, governments, organizations, and philanthropists to accomplish its mission. We are committed to nurturing world-class student STEM projects that can contribute to and support technological innovation in developing nations. The STEM fields are critical to any national economy seeking to grow in a 21st century global economy. As UNESCO stated, a robust economy will require citizens to be thoroughly equipped to compete in the science and technology fields. STEM-focused education responds to the reality that a nation's future will be built its capacity for innovation and invention.

Our mission is to stimulate a lasting interest in the STEM disciplines, with the goal of encouraging students to pursue careers in these fields. This is accomplished by actively involving students in the support of authentic research currently being conducted on the International Space Station (ISS) or in a NASA ground-based laboratory. This will inspire young generation in developing nations and underserved group in developed nations around the world to pursue careers in science, technolo-

gy, engineering, and mathematics (STEM); for the future will be built on people's capacity to innovate, invent, and solve problems creatively.

Through collaboration with NASA and NASA sponsored researchers, we create an educational mini-curriculum for the high school or middle school classroom that engages students as research assistants, providing data for the Principal Investigator, (PI). Currently, we have a collaborative relationship with several NASA or NASA supported researchers. The program is delivered and managed via our Website (www.aviationpalace.space); each teacher being assigned a password protected page for management and program delivery.

During our mission students briefly learn about the scientist and their research, participate in classroom experiments or activity that mirrors the research experiment on the ISS, and then do some type of an analysis and data gathering activity. These hands-on inquiry-based activities are supported by near-real time digital and video images downlinked from orbit and provided to the classroom via our website. Also provided are real time images of a control ground experiment being conducted by BioServe Space Technologies, a NASA Research Partnership at the University of Colorado or elsewhere.

Student research supports the work of the PI, while meeting the educational goals of the classroom and final student data is provided to the PI for review and, if appropriate, inclusion into research databanks.

Our missions typically require between three and seven classroom periods and could involve:

1. Introduction of NASA and its mission
2. Introduction of PI and research focus
3. Instruction on download and use of any required software
4. Conducting the research (the heart of the mission) which may include:
   - (i) Hypothesis development
   - (ii) Classroom lab activity mirroring the actual research
   - (iii) Observation and photo/video analysis
   - (iv) Data recording and submission
   - (v) Formulate conclusions
   - (vi) Evaluation

Our programme is an internet based, education program for upper elementary, middle and high school students and higher institutions. We employ current NASA research to reach and inspire "the next generation of explorers." To challenge Nigerian students and their counterparts in developing countries to excel in math and science through their active participation in space–based research.

Our missions allow students to participate in ongoing space-based research. Students participate in NASA research through analysis of photo or video data from current experiments being conducted by a NASA scientist. Student data will be reviewed and, if appropriate, included in the research databases.

Through our projects and in conjunction with our partners, we have developed an AIAA approved curriculum covering over 42 lessons including the following: The Earth's Hemisphere, Trash in Space, Living in Space, Large Numbers, Observing the Moon, Up, up, and Away in my Beautiful Balloon, How Long is a Day?, Orbital Dynamics, Transit of Mercury, Jackie Cochran, Gemini VIII, Air Speed, Asteroids and Dinosaurs, Spinning Ball of Water in Space, Metric Units of Measurement, How Do Airplanes Fly?, Parallax and the Size of the Solar System, NASA's Hedgehog Robot, The Mariner Project, How Long is a Year?, Images from Space, The Magnus Effect, The Rosetta Mission, Measuring the Size of the Universe, Antoine de Saint-Exupéry, Spot the Space Station, How High is it?, Everyday Drones, Divisibility Rules, Earth's Temporary Moons, Ride a Sounding Rocket, Earth's Weather, Navigating the Skies, Pi Day, Hanny's Voorwerp, International Day of Human Space Flight, Aerial Refueling, Sensing Weather from a Distance, Crossing the Atlantic by Air, Solar Eclipse, Errors, Hoaxes, and Just Plain Bad Science, The International Geophysical Year. This programme will take several class periods of between 1-5 hours per day and we are also adopting online lectures format to be able to reach out to those who might not have time to attend the classroom lectures.

The Need for Our App for Android, Iphone and Window Users: Our feasibility study showed that majority of our target audience spend most of their time on their mobile phones and laptops using various applications on the go than they do inside a conventional classroom, hence we decided to take our virtual classroom to every home where a phone, laptop and internet facilities exist. We need grants to support our innovation in the area of development of our e-learning innovation center and our official education mobile App compatible with android, iPhone, blackberry and windows for the online STEM Education; so that students can access the online courses on the go and further inspire, influence, and mould the next generation of aerospace scientists and engineers to reach for greater heights. This will also provide a series of resources and programming to teachers, students, parents, and aerospace professionals wherever they are. We want to develop a world-class education app and e-learning innovation center which will be culturally & technologically acceptable and use-friendly all over the world.

References:

[1] American Institute of Aeronautics and Astronautics, (2018) Micro-Lesson and K-12 STEM Education materials (www.aiaa.org) [2] Space Foundation, (2018) Space Liaison Teacher Reference Materials (www.spacefoundation.org) [3] Orion's Quest (2017).

COEVOLUTION OF OCEANIC AND ATMOSPHERIC CHEMISTRY. S. L. Olson[1,2], [1]NASA Astrobiology Institute Alternative Earths Team, Department of Earth Sciences, University of California, Riverside (solso002@ucr.edu), [2]Department of Geophysical Sciences, University of Chicago

Earth's ocean and atmosphere are in constant communication through sea-air gas exchange, and they have thus co-evolved as a coupled system over our planet's geologic history. The ocean and atmosphere have not, however, evolved in chemical equilibrium with each other. There are three key reasons:

1. gas exchange involves only the uppermost layer of the ocean. The majority (>90%) of the ocean volume is not in direct contact with the atmosphere.
2. although gas exchange is geologically rapid, it is slow compared to the biological and photochemical processes that control the production and destruction of gases within the ocean and atmosphere, respectively.
3. non-volatile phases (e.g., Fe^{2+}, SO_4^{2-}) play an important role in shaping the chemical landscape of the ocean but do not participate in atmospheric chemistry.

The result is that the bulk ocean and the atmosphere may develop, and maintain, very different chemistries—with important consequences for Earth's biological and climatic evolution.

This talk will probe the complex relationships between oceanic and atmospheric chemistry, including several case studies from Earth's history. These examples will highlight the difficulties faced by geochemists seeking to reconstruct Earth's atmospheric evolution using proxies hosted by marine sediments—and by exoplanet observers hoping to constrain the surface environment of an alien world using spectral signatures of its atmosphere. Of additional emphasis will be the importance of the marine biosphere and oceanographic processes for modulating the atmospheric abundance of greenhouse gases such as CH_4 and N_2O.

Generalizing the Habitable Zone: Temperate Continental Regions on Some Snowball Planets. A. Y. Paradise[1,2,a], K. Menou[1,2,b], D. Valencia[1,2,c], and C. Lee[3,d]. [1]Department of Astronomy & Astrophysics, University of Toronto, 50 St George St, Toronto, ON M5S 3H4, Canada, [2]Centre for Planetary Sciences, Department of Physical and Environmental Sciences, University of Toronto, 1265 Military Trail, Toronto, ON M1C 1A4, Canada, [3]Department of Physics, University of Toronto, 60 St George St, Toronto, ON M5S 1A7, Canada. [a]paradise@astro.utoronto.ca. [b]menou@astro.utoronto.ca. [c]valencia@astro.utoronto.ca. [d]clee@atmosp.physics.utoronto.ca.

Introduction: Classically, the "Habitable Zone" is defined in terms of insolation or distance from the parent star, using the transition to hot runaway greenhouse as the inner edge and the breakdown of CO_2 greenhouse warming as the cold, outer edge [1,2]. These limits can be generalized to parameter spaces other than insolation by simply describing a 'hot edge' and a 'cold edge'. The 'cold edge' is commonly described as the transition to Snowball climates, in which sea ice extends from the poles to the equator [e.g. 3,4,5]. Under these assumptions, the 'habitable zone' is better described as the 'temperate zone', as the use of the Snowball limit to delineate the cold edge carries the implicit assumption that only temperate planets have habitable surfaces. We argue that 'habitable' could be better-construed as any terrestrial planet which features any temperate surface conditions.

The motivation for this argument is that sub-freezing average global temperatures do not necessarily imply local sub-freezing temperatures everywhere on the planet. However, if temperate areas are confined to certain regions, they may not be captured by the zonal and global averages used in most lower-dimensional models. Previous studies have introduced the idea that planets could be only partially or transiently habitable [6], through mechanisms such as high obliquity or high eccentricity [7]. We use PlaSim, an intermediate-complexity GCM, to argue that Earth-like Snowball planets can develop seasonal or even permanent inland temperate, ice-free regions without triggering a retreat of sea ice. These results further imply that, contrary to previous assumptions [e.g. 3, 5, 8], continental carbon-silicate weathering may continue during Snowball episodes. This would serve to limit the likelihood that planets with low CO_2 out-gassing rates undergo limit cycling between Snowball and temperate climates.

Summary of Methods: We use an intermediate GCM called PlaSim. PlaSim uses a spectral core to solve prognostic equations for humidity, vorticity, divergence, temperature, and pressure, and evaluates a set of physical parameterizations on a rectangular latitude-longitude grid. PlaSim includes a mixed-layer slab ocean, thermodynamic sea ice, a land model using a bucket model for soil hydrology, and a complete hydrological cycle including clouds, large-scale and convective precitation, surface snow and ice, and surface runoff. PlaSim uses a shortwave and a longwave band to compute radiative transfer, including CO_2, water, and ozone as absorbers. A full description of the model is found in [9].

We run PlaSim at T21 resolution (5.61 degree resolution at the equator) with 10 vertical layers, using globally-cold initial conditions, for a range of insolations and CO_2 partial pressures to identify climates near the Snowball deglaciation point. We measure the continental weathering rate for these models using a simple non-dimensional parameterization that depends on CO_2 partial pressure, precipitation, and surface temperature [8, 10, 11]. This is a parameterization for net global weathering, so we evaluate it at each grid cell and then compute an area-weighted average over the land surface.

Summary of Results: We find that for planets with Earth-like continents and obliquity, approximately 35% of the land surface has temperate daily-average temperatures during Northern Hemisphere summer, primarily at mid-latitudes. Near the Snowball deglaciation limit and at 1300 W/m^2, these models weather CO_2 at approximately 9% of modern Earth's weathering rate. In these models, temperate areas are present seasonally, but not permanently. Our near-deglaciation model at this insolation has 24 millibars of CO_2, which accounts for the moderate weathering rate. When the planet's obliquity and eccentricity are set to 0, and the continents replaced by a flat equivalent-area rectangular super-continent centered on the equator, temperate conditions are preferentially found in the inland tropics and persist year-round (Fig. 1). Some terrestrial planets experiencing Snowball episodes could therefore maintain habitable surface conditions throughout much of the Snowball episode.

We compare the weathering rates observed near the deglaciation limit to the limit for temperate stability to identify stable regions of the out-gassing parameter space (Fig. 2). We find that at higher out-gassing rates, only temperate climates are likely to be stable, but at lower out-gassing rates, there may no geochemical equilibria, only snowball climates may be stable, or either climate state may be stable for a given insolation and out-gassing rate.

Our finding of temperate land surface depends most strongly on glacial dynamics, as any ice sheets

covering inland regions must collapse in order for the lower soil albedo to raise the surface temperature. The global hydrological cycle during Snowball episodes is greatly reduced, suggesting that continental ice sheets should collapse in some regions. However if the ice sheet is thick enough, then losses at the surface of the ice sheet may be insufficient for the glacier to collapse. Our weathering results are modulated by the strength of any erosion-based supply limits. If erosion rates during Snowball episodes are low, then weathering will be significantly reduced. We do not make any assumptions about what supply limit might be appropriate for Snowball climates, as this should depend strongly on topography.

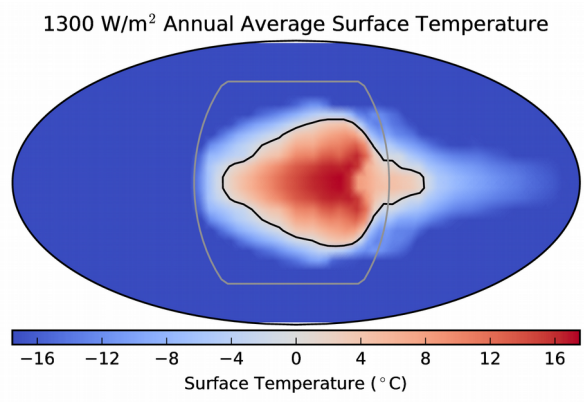

Fig. 1: Annual average surface temperature presented in a Mollweide projection for a model with zero obliquity or eccentricity, 1300 W/m^2 insolation, and a super-continent rectangular in latitude and longitude and centered on the equator (grey contour). Topography is ignored. The cold end of the temperature scale is truncated at -16 Celsius, and the 0 Celsius isotherm is the black contour. This planet is in a Snowball state, with sea ice at the equator, but exhibits persistently temperate conditions in continental regions.

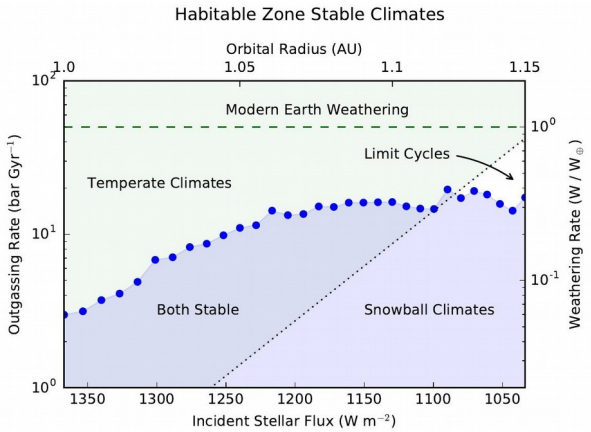

Fig. 2: Different weathering equilibrium states at different insolations and CO_2 out-gassing rates, for a model with Modern Earth continents, obliquity, and eccentricity. The diagonal dotted line is the limit for temperate weathering stability, and the blue dots indicate the continental weathering we observe near Snowball deglaciation in our models. The green dashed line indicates our assumed Modern Earth out-gassing and weathering rate (which we assume to be in equilibrium). We therefore suggest 4 regions of parameter space, where the stable weathering equilibrium may either be temperate climates, Snowball climates, both, or where no climate represents weathering equilibrium, at which point the climate would oscillate between temperate and Snowball states [3,5,8].

Conclusion: We find that for a range of Earth-like planetary parameters, inland areas may remain temperate during Snowball episodes, either seasonally or persistently. These warm temperatures permit moderate carbon-silicate weathering at higher CO_2 partial pressures, which decreases the likelihood of unstable climate cycling at low out-gassing rates.

References: [1] Hart M. H. (1979) *Icarus*, *37*, 351–357. [2] Kasting J. F. et al. (1993) *Icarus*, *101*, 108–128. [3] Haqq-Misra J. et al. (2016) *ApJ*, *827*, 120. [4] Abbot D. S. (2016) *ApJ*, *827*, 117. [5] Paradise A. Y. and Menou K. (2017) *ApJ*, *848*, 33. [6] Spiegel D. et al. (2008) *ApJ*, *681*, 1609–1623. [7] Linsenmeier M. et al. (2015) *Planetary and Space Science*, *105*, 43–59. [8] Menou K. (2015) *Earth and Planetary Science Letters*, *429*, 20–24. [9] Fraedrich K. (2005) *Meteorologische Zeitschrift*, *14*, 299–304. [10] Berner R. A. (1994) *American Journal of Science*, *294*, 56–91. [11] Abbot D. S. (2012) *ApJ*, *756*, 178.

REVERSE WEATHERING AND EARTH'S CLIMATE. N. J. Planavsky[1], T.T. Isson[1], and B. Kalderon-Asael[1], [1]Department of Geology and Geophysics, Yale University, 06511.

Introduction and Findings: Despite a Sun with lower luminosity, Earth's early climate was marked by apparent stability with rare catastrophic glaciations. We will make a case that elevated rates of reverse weathering—the consumption of alkalinity and the generation of acidity accompanying clay authigenesis—dramatically enhanced the retention of carbon within the ocean-atmosphere system, and led to the sustenance of a significantly elevated atmospheric carbon dioxide concentrations. Although dampened by sluggish kinetics today, more prolific rates of reverse weathering would have persisted under the pervasively silica-rich conditions that dominated Earth's early oceans. Further, with extensive reverse weathering, the establishment of a potent negative feedback between marine pH and authigenic clay formation would have greatly enhanced climate stability by mitigating large swings in atmospheric carbon dioxide concentrations. The ecological rise of siliceous organisms would have dampened the reverse weathering buffer, destabilizing Earth's climate system.

In addition we will present a new carbonate Lithium isotope record spanning the last three billon years of Earth's history, that reconstructs the evolution of seawater lithium isotope values and provides a new perspective on the evolution of the coupled carbon and silica cycles. The global lithium isotope mass balance is controlled foremost by fractionations that occur during incongruent weathering of silicate minerals in terrestrial environments, and by the formation of authigenic clay minerals in the marine realm (reverse weathering). We generated Li isotope data from over 700 marine carbonates samples. Our sampling focused on micritic carbonates but included belemnites, brachiopods, and marine cements. In total, we sampled from 83 stratigraphic units that range in age from 3.0 Ga to the modern. We found a predominance of low Li isotope values in the Precambrian, which indicates weathering intensities and the extent of reverse weathering in the sediment pile were significantly elevated relative to modern.

Evidence from the geochemical record suggests that organisms have played a critical role in shaping the composition of Earth's oceans and atmosphere, which in turn also structures the biosphere. Perhaps most notably, methanogens and oxygenic phototrophs have transformed Earth's surface environments since the Archean. The most recent chapter of Earth's history, the Phanerozoic, was one shaped foremost by eukaryotic life. If our estimates are correct, then the switch to a biologically controlled silicon cycle with the rise of silica biomineralizing eukaryotes would have initiated a significant waning of reverse weathering rates. This transition would have led to a drop in baseline atmospheric carbon dioxide concentrations and the establishment of a more volatile (responsive) climate system, directly linked to a decrease in the buffering strength of oceans. Notably, we find this paradigm to be consistent with geologic evidence for a decline in authigenic marine clays and the weakening of Earth's thermostat as indicated by the onset of more frequent greenhouse-icehouse oscillations since the latest Precambrian. Had siliceous organisms never evolved, Earth's surface environment would be significantly warmer and oceans far more acidic than they are today, with potential implications for the evolution of Phanerozoic life and their associated metabolisms. More detailed Phanerozoic atmospheric carbon dioxide concentrations trends could reflect, at least in part, variations to the ecological success of siliceous organisms through reverse weathering. Future models seeking to explore climatic evolution on terrestrial bodies ought to consider both forward (weathering) and backward (reverse weathering) processes governing global alkalinity budgets and the buffering strength of oceans.

DYNAMICS, STRUCTURE AND IMPORTANCE OF DEEP ATMOSPHERIC CONVECTION ON EARTH, MARS, AND TITAN. S. C. R. Rafkin, Southwest Research Institute, 1050 Walnut Street, Suite 300, Boulder, CO, rafkinw.swri@gmail.com.

Introduction: Earth, Mars, and Titan (EMT) all exhibit deep convection driven by diabatic heating. On Earth and Titan the heating is a result of latent heat release associated with the phase change of water and methane, respectively. On Mars, radiative heating of dust provides buoyancy. From a dynamical standpoint, the response of an atmosphere to diabatic heating is independent of the source of that heating—condensation, dust, aliens, or magic—it doesn't matter. Consequently, the dynamics in the atmospheres of EMT respond in similar ways and, likewise, the dynamics feedback and modulate deep convection in similar ways. Deep convection is also known to play a critical role in the water vapor and momentum budget of Earth. Within the last decade, deep convection has been shown to be important for the Mars dust cycle. The methane cycle of Titan is also likely to be sensitive to the infrequent but intense deep convection, but this is largely hypothetical based on limited modeling results and even more sparse observational evidence.

Deep Atmospheric Convection: Deep convection results when the combination of diabatic heating and adiabatic cooling results in air that is warmer than its environment, e.g., [1]. Dynamics are agnostic about the source of the diabatic heating; the governing equations for this process contains a generic source term (often represented by the symbol $\dot{Q}$. All that matters is the structure and temporal evolution of that heating. All other things being equal, an atmosphere will respond identically to identical heating regardless of the origin of that heating. Consequently, to the extent that atmospheres of EMT are similar in structure, they respond similarly to heating and the behavior of Mars dust storms, Titan methane storms, and Earth thunderstorms should be similar.

The evolution of a convective storm on EMT can be different, because of the way the storms themselves feedback or affect their environment. For example, the cold outflow from an Earth or Titan storm can separate the convective cell from the unstable air that it relies upon for maintenance or growth, e.g., [2][3]. Dust does not evaporate, so dust storms cannot produce cold outflow through microphysical processes. However, shadowing by the storm could produce cooler air due the strong interaction of radiation and dust. Further, winds generated from a Mars storm can directly enhance the dust lifting which leads to a direct diabatic effect, whereas increased winds on Earth or Titan have muted and secondary indirect impacts on diabatic heating, if at all.

Convective Organization: The storm environment can result in convective organization. For Earth, the necessary environment for the development of squall lines, mesoscale convective complexes, and tropical cyclones are well known, e.g., [4]. Model simulations show that Titan could develop squall lines similar to Earth under similar environmental wind shear onditions [5]. On Mars, dust storms may behave more closely to tropical systems on Earth, requiring weak wind shear and deep adiabatic layers in order to grow and mature [6].

Deep Convective Transport: The importance of deep convection on Earth has been known for well over half a century, e.g., [7][8]. Rafkin [9] hypothesized that deep transport on Mars driven by topographic circulations might play a similar role. Later modeling studies, e.g., [6][10], indicated that radiative heating of dust could also produce deep convective dust plumes and larger-scale convective structures. Vertical dust profiles from the Mars Climate Sounder (MCS) revealed elevated maxima of dust mixing consistent with what would be expected by rapid, deep transport e.g., [11]. This observational evidence confirmed that the dust cycle, and therefore the thermal structure and dynamics of Mars, was sensitive to deep convection.

Methane convection on Titan is strongly analogous to Earth, but there are key differences. First, the frequency and coverage of Titan's convection is far less compared to Earth. This might be expected to limit the relative importance of Titan's convection on global scale cycles. Second, Titan's convection is far deeper and contains relatively greater abundances of vapor and condensate compared to Earth. Thus, even though more sparse and less frequent than on Earth, the vigor and transport of Titan's convection may compensate in the Titan climate system. Titan general circulation model simulations [12] found that latent heating from deep convection had important effects on the Hadley Cell. Observations of Titan, largely from Cassini, are generally too infrequent to unambiguously or definitively identify the role or importance of deep convection, but based on experience with Earth and Mars, it should be expected that the deep convection will produce noticeable impacts on the abundance and structure of methane and its photochemical byproducts in the upper troposphere and lower stratosphere. Rapid and deep injection of high methane abundance air into the stratosphere is

generally not considered in photochemical models of Titan; diffusion is the primary transport term.

Conclusions: The similarities and differences between deep convection on Earth, are compared and contrasted. While the basic physics of deep convection is driven by diabatic heating, the storms can alter their evolution and feedback to the environment in different ways. The organization of convective systems on Titan and Mars appear to have close analogs to system on Earth. The importance of convection in any atmosphere, not just EMT, is *likely* to have an important effect. Neglect of deep convective processes and transport is, therefore, likely to leave a gap in the understanding of atmospheric climate systems.

References: [1] Rennó, N. O., and Ingersoll, A. P. (1996). *JAS*, 53(4), 572-585. [2] Weisman, M. L., and Klemp, J. B. (1986), *In Mesoscale meteorology and forecasting*, 331-358. [3] Hueso, R., and Sánchez-Lavega, A. (2006), *Nature*, 442(7101), 428. [4] Weisman, M. L., and Klemp, J. B. (1982). *MWR*, 110(6), 504-520. [5] Rafkin, S. C., and Barth, E. L. (2015), *JGR*, 120(4), 739-759. [6] Rafkin, S. C. (2009). *JGR*, 114(E1). [7] Riehl, H., and Malkus, J. (1961). *Tellus*, 13(2), 181-213. [8] Zipser, E. J. (2003). *In Cloud Systems, Hurricanes, and the Tropical Rainfall Measuring Mission (TRMM)*, 49-58. [9] Rafkin, S. C. (2003), *Mars Atmosphere Observation and Modeling Workshop.* [10] Spiga, A., et al., (2013). *JGR Planets*, 118(4), 746-767. [11] Heavens, N. G., et al., (2011). *JGR Planets* 116(E1). [12] Mitchell et al. (2009), *Icarus*, 203, 250-264.

Additional Information: If you have any questions or need additional information regarding the preparation of your abstract, call the LPI at 281-486-2142 or -2188 (or send an e-mail message to publish@hou.usra.edu).

Please DO NOT Submit Duplicates of Your Abstract; should you find it necessary to replace or repair your abstract PRIOR TO the submission deadline, return to the abstract submission portion of the meeting portal and click on the "Update" link that appears next to the title of the abstract you submitted.

THE ROLE OF METHANE ON AN ICY EARLY MARS AND IN EXOPLANETARY ATMOSPHERES

R. M. Ramirez[1], R.A. Craddock[2] and L. Kaltenegger[3], [1]Earth-Life Science Institute, email: rramirez@elsi.jp, [2]The Smithsonian Institution, email: craddockb@si.edu, [3]Carl Sagan Institute, email: lkaltenegger@astro.cornell.edu

Introduction: The early martian climate has been debated for decades and will continue to be a controversial topic for some time to come. The valley networks, which are fluvial features that are large enough to rival the largest erosional features on the Earth [1] (Figure 1), are the best evidence for an abundance of surface liquid water early in Mars' history. Although some investigators believe that early Mars had an icy and cold climate, others argue that the geological and climatological evidence supports a warm and semi-arid climate instead.

Recently, it has been shown that invoking icy climates for early Mars faces additional challenges: 1) icy planetary surfaces require higher greenhouse gas concentrations to achieve warm (> ~ 273 K) surface temperatures, plus 2) very icy climates are prone to atmospheric collapse. In spite of this, methane, in hypothetical CO_2-rich atmospheres, was proposed to have possibly warmed such an icy early Mars [2]. Moreover, methane has been shown to have a warming effect on planets orbiting the Sun, like early Mars [2, 3]. We first show recent simulations that illustrate this *ice problem* for early Mars atmospheres that contain and do not contain methane. We also assess the plausibility of such solutions using climatic, photochemical, and geologic arguments, concluding with our preferred interpretation. We then assess the effects of methane for exoplanets located near the outer edge of the habitable zone around different star types and speculate about the implications for life throughout the cosmos.

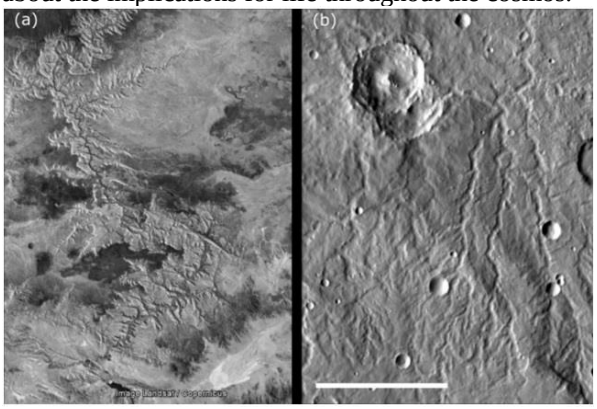

Figure 1: The Grand Canyon (**a**) versus a Martian dendritic river system (**b**) (Arabia quadrangle; 12° N, 43° E). Scale bar is 60 km long. Image adapted from ref: 1 (*Nature Geoscience*).

Methods: We used a single-column radiative-convective climate model first developed by Kasting et al. [4] and updated in recent studies [5-6]. We assumed that the Sun (and other stars) remains fixed at a solar zenith angle of 60° as in previous works [5-6]. An average martian solar flux value of 439 W/m^2 was assumed for early Mars conditions ~3.8 Ga. Atmospheres are mostly composed of CO_2 (80 – 99%) with varying amounts of (1-20%) CH_4 or H_2. Simulations are cloud-free unless otherwise specified.

Results: We show that warming a relatively non-glaciated early Mars above 273 K requires considerably lower greenhouse gas pressures than does an icy planet [6] (Figure 2). In contrast, the surface pressure threshold required to achieve warm conditions increases ~10 – 60% for transient warming models, depending on ice cover fraction. No warm solution (analogous to atmospheric collapse in 3-D models) is possible for ice cover fractions exceeding 40%, 70%, and 85% for mixed snow/ice and 25%, 35%, and 49% for fresher snow/ice at H_2 concentrations of 3%, 10%, and 20% respectively.

In addition, we perform a second set of calculations, replacing H_2 with CH_4, finding that absorption by methane at solar wavelengths competes with that in the thermal infrared. This behavior produces significant upper atmospheric absorption that inhibits CO_2 cloud formation [6] (Figure 3; implications discussed below). This effect also tends to cancel out some of the greenhouse effect, cooling the surface while simultaneously trying to warm it.

Discussion: The high albedo of surface ice reflects a proportion of stellar energy back out to space, which makes it harder to transiently warm an icy surface than a less icy one. Compounding this albedo effect, the high thermal inertia of ice could exacerbate the difficulties in warming icy surfaces beyond the results shown here [6,7]. This is because CO_2 clouds may partially mute the ice albedo effect according to 3-D simulations of pure CO_2 atmospheres [7]. However, in CO_2-rich atmospheres that also contain CH_4, perhaps as a result of serpentinization [2], CO_2 cloud formation would be drastically reduced, maximizing the severity of the ice albedo problem and making transiently warm solutions harder to achieve [1][6]. Alternatively, in CO_2 atmospheres rich in H_2, high amounts of CH_4 are also expected [8]. Thus, the ice albedo problem remains a major issue in atmospheres that contain significant amounts of either CH_4 and H_2, making it challenging to transiently warm an icy early Mars using those

gases [1]. We then show why a warm and semi-arid climate for early Mars is the best solution given the available evidence [1][9]

So, what does all of this mean for exoplanets? We perform similar calculations showing that the greenhouse efficacy of methane is a strong function of the spectral class, and although it is a decent greenhouse gas for hot stars like our Sun [2][6], CH_4 actually *cools* planets orbiting mid-K- to M-stars [3]. Thus, although ice albedo is significantly lower for planets orbiting M-stars than it is for the Sun [10], M-star planets in the HZ may still exhibit planetary surfaces that are too cold to support life. If life akin to that on Earth ever evolved on Mars (or on other exoplanets), microbes undergoing methanogenesis would produce CH_4 via conversion of free H_2 and CO_2 [3]. On planets orbiting hotter stars, this stabilizing feedback leads to habitable surface conditions. In contrast, on planets orbiting cooler stars, methanogenesis would trigger cooling until conditions become too cold for life to exist (assuming life had arisen at all). Thus, planets with dense CO_2-CH_4 atmospheres around hotter stars may suggest inhabitance whereas those same atmospheres around colder stars may just stay frozen [3]. The trends and conclusions of this study are unaffected by any potential revisions to CO_2-CH_4 or CO_2-H_2 collision-induced absorption [11].

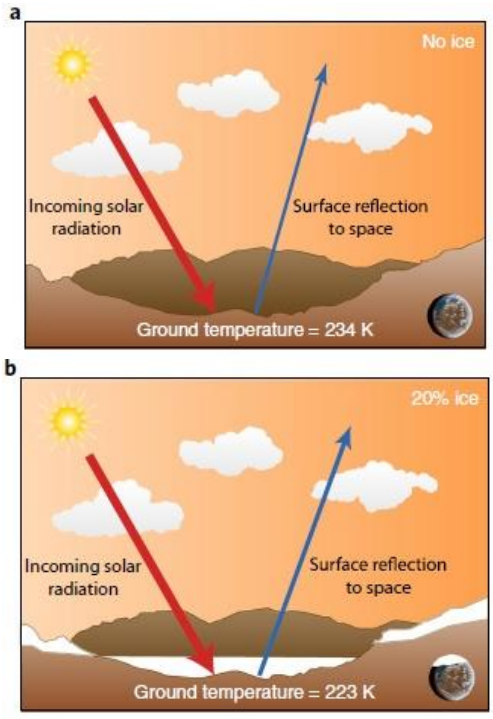

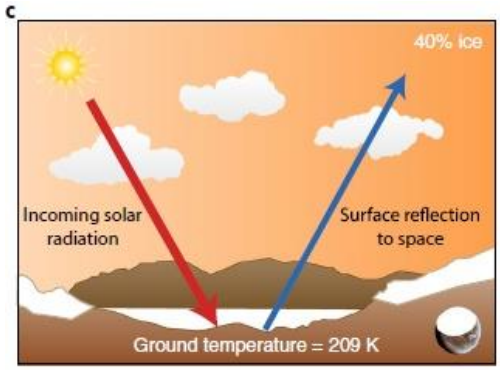

Figure 2: Simplified surface energy balance for early Mars (a – c), showing the decrease in surface temperature with increasing amounts of surface ice. The resultant increase in surface reflectivity is represented by a widening blue arrow. Images adapted from ref: 1 (*Nature Geoscience*).

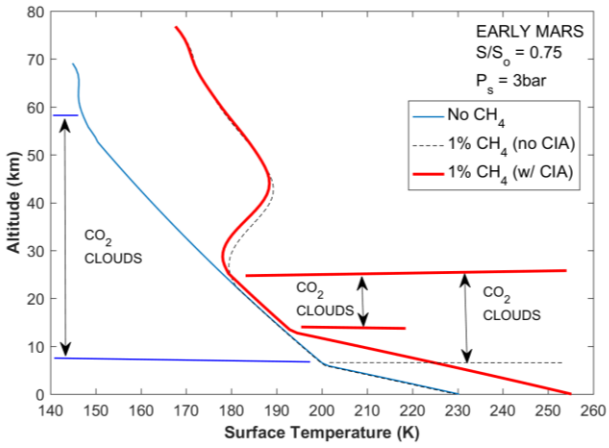

Figure 3: Vertical temperature profiles for fully-saturated 3 bar CO_2 early Mars (S/S_o = 0.75) atmospheres with 1% CH_4 and no collision-induced absorption (white dashed line), 1% CH_4 with CO_2-CH_4 collision-induced absorption (solid blue line) and no CH_4 (red line) [6].

References:

[1] Ramirez, R.M. and R.A. Craddock, (2018) *NatGeo* 11, 230 – 237 [2] Wordsworth, R.D. et al. (2017) GRL 44, 2, 665-671 [3] Ramirez, R.M. and L. Kaltenegger (2018) ApJ 858, 2 [4] Kasting J.F. et al., (1993), Icarus, 101, 108-128. [5] Ramirez, R.M. et al. (2014) *NatGeo*., 7,59- 63 [6] Ramirez, R.M. , (2017), Icarus, 297, 71-82 [7]Forget et al., 2013), Icarus 222, 1, 81 – 99.[8] Batalha N. et al. (2015) Icarus 258, 337-349. [9] Craddock, R.A. and Howard, A.D. (2002). JGR, 107, E11 [10] Shields, A.L. et al. (2013) AsBio 13. 8, 715 – 739. [11] Martin, T. et al. (2018) Icarus (in review).

THE IMPORTANCE OF ANOXYGENIC PHOTOSYNTHESIS FOR CLIMATE AND ATMOSPHERIC BIOSIGNATURES ON REDUCING WORLDS. C. T. Reinhard[1,2] and K. Ozaki[2,3], [1]School of Earth & Atmospheric Sciences, Georgia Institute of Technology, 311 Ferst Dr., Atlanta, GA 30332 (chris.reinhard@eas.gatech.edu), [2]NASA Astrobiology Institute, Mountain View, CA, [3]Department of Environmental Science, Toho University, 2-2-1 Miyama, Funabashi, Chiba 273-8510, Japan (kazumi.ozaki@sci.toho-u.ac.jp)

Introduction: The evolution of different forms of photosynthetic life has profoundly altered the activity level of the biosphere, modulating the flow of energy through surface environments and radically reshaping the composition of Earth's oceans and atmosphere over time. Here, we explore the role of microorganisms that use reduced iron (Fe) as an electron donor for photosynthesis ('photoferrotrophs') in controlling Earth's early climate. Using a coupled model of atmospheric photochemistry and the ocean biosphere we show that interaction between photoferrotrophy and H_2-based photosynthesis gives rise to a non-linear amplification of surface methane cycling, widening the range of geochemical boundary conditions that allow for stable, warm climate states. We then propose and discuss a novel set of regulatory feedbacks linking primitive photosynthesis, global H-Fe-C cycling, and the stability of planetary climate on the early Earth and possibly other Earth-like planets.

Methods: We employ a suite of models and offline climate calculations. First, we utilize a coupled photochemical-ecosystem model (Fig. 1) in which a 1-box ocean biosphere is regulated stoichiometrically by geophysical and gas exchange fluxes and is coupled to a 1-D model of atmospheric photochemistry [see also 1]. The photochemical model includes 73 chemical species (39 long-lived species, 31 short-lived species, and 3 aerosol species) participating in 359 chemical reactions, with transport via eddy and molecular diffusion to an altitude of 100 km within a 1-km grid. We then perform a Monte Carlo analysis of a simplified global redox balance model, which employs a numerical solution to our ocean biosphere model and a parameterized atmospheric photochemistry linking surface fluxes of CH_4 to steady-state atmospheric pCH_4.

Global surface temperature is evaluated offline based on the radiative-convective climate model of [2], assuming a solar luminosity equivalent to the Sun at 2.8 billion years ago (Ga). In our Monte Carlo analysis of the climate system, we retrieve a subset of models with the sampling criteria that global average surface temperature exceeds 288 K [3] and the atmospheric CH_4/CO_2 ratio is below 0.2 [e.g., a largely haze-free atmosphere; 4]. For our analysis of anoxygenic photosynthetic biosignatures, we roughly follow the 'abiotic' case presented by [5] and add to this results from our simplified numerical model with parameterized photochemistry.

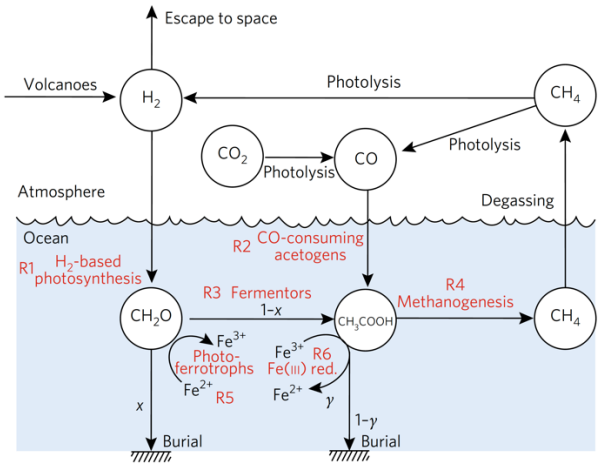

Figure 1. Schematic depiction of our default primitive biosphere model. The primary source of reducing power (given in terms of H_2) is outgassing from the solid Earth. A fraction of organic matter produced by H-based (R1) and Fe-based (R5) anoxygenic photosynthesis, x, is buried in sediments and the remaining fraction is converted to CH_4 (and CO_2) by fermenters (R3), Fe-reducers (R6) and methanogens (R4). A certain fraction of iron oxides produced by photoferrotrophs, γ, is reduced to Fe^{2+} via Fe reduction before burial. CH_4 generated by methanogenesis is liberated to the atmosphere and is converted to H_2 via photolysis.

Results: We find a marked increase in atmospheric pCH_4 and surface temperature with the inclusion of both H- and Fe-based photosynthesis relative to either metabolism acting in isolation (Fig. 2). In particular, coupling of both forms of photosynthesis dramatically widens the range of geophysical boundary conditions consistent with warm, haze-free conditions. Importantly, this result is not necerssarily reliant on an early evolutionary emergence of acetoclastic methanogenesis [6, 7]. Similarly, biospheres containing both H- and Fe-based photosynthesis sustain significantly higher atmospheric pCH_4 levels than comparable abiotic planets, though in many cases even entirely H-based photosynthetic biospheres should be distinguishable from abiotic scenarios.

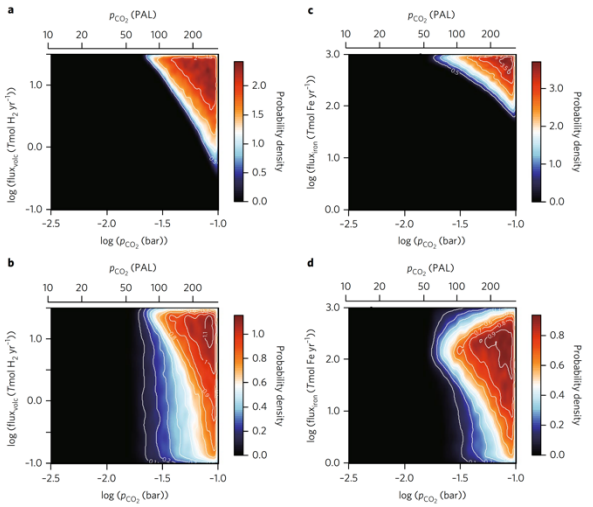

Figure 2. Monte Carlo simulations showing the probability density of model solutions with warm (≥ 288 K) and largely haze-free ($CH_4/CO_2 \leq 0.2$) conditions. Shown in (a) and (b) are probability distributions in a phase space of total H_2 outgassing flux and atmospheric pCO_2 for our Case 1 (H-based photosynthesis only) and Case 2 (both forms of photosynthesis) biospheres. Shown in (c) and (d) are probability distributions in a phase space of ferrous iron upwelling flux and atmospheric pCO_2 assuming exclusively Fe-based photosynthesis and our Case 2 biosphere. Note the log scales for *x* and *y* axes in all panels.

Discussion and Conclusions: Our results suggest that the combined effects of H-based and Fe-based anoxygenic photosynthesis would have been important for regulating atmospheric pCH_4 and surface temperature on the early Earth given plausible geophysical reductant fluxes [7]. Combined with potential changes to surface albedo, cloud properties, and possibly atmospheric pressure [e.g., 8-11], our results suggest that clement or even warm surface temperatures would have been achievable on the Archean Earth with a biosphere powered entirely by anoxygenic photosynthesis, potentially representing an entirely distinct climate state from those of the prebiotic [12] and post-oxygenic Earth. More broadly, we suggest that the synergistic effects of H- and Fe-based photosynthesis and may represent a critical component of the climate system of primitive Earth-like planets around dim stars, and in many cases should be remotely detectable through their impact on atmospheric pCH_4.

In the simulations presented here we impose atmospheric pCO_2 as a boundary condition, when in reality our model implies a series of feedbacks linking the carbonate-silicate cycle, geophysical Fe^{2+} fluxes, and the atmospheric CH_4/CO_2 ratio that have not been previously explored. We are currently developing an open-system H-C-Fe model to test this hypothesis, with the aim of ultimately broadening the scope of these impacts to encompass a range of star types and geophysical boundary conditions.

References:

[1] Kharecha P. et al. (2005) *Geobiology, 3,* 53–76. [2] Haqq-Misra J. D. et al. (2008) *Astrobiology, 8,* 1127–1137. [3] Blake R. E. et al. (2010) *Nature, 464*, 1029–1032. [4] Arney G. (2016) *Astrobiology, 16,* doi:10.1089/ast.2015.1422. [5] Krissansen-Totton J. et al. (2018) *Science Advances, 4*, doi:10.1126/sciadv.aao5747. [6] Fournier G. P. and Gogarten J.P. (2008) *J. Bacteriol., 190*, 1124–1127. [7] Ozaki K. et al. (2018) *Nature Geosci., 11*, 55–59. [8] Goldblatt C. et al. (2009) *Nature Geosci., 2*, 891–896. [9] Goldblatt C. and Zahnle, K. (2011) *Clim. Past, 7*, 203–220. [10] Charnay, B. et al. (2016) *JGR: Atmospheres, 118*, 10414–10431. [11] Wolf E. T. and Toon O. B. (2016) *Astrobiology, 14*, 241–253. [12] Wordsworth R. and Pierrehumber R. (2013) *Science, 339*, 64–67.

REVISITING THE EARLY EARTH'S METHANOGEN BIOSPHERE A. Rushby[1], S.Domagal-Goldman[2], S. Som[1,3], A. Wofford[2], G. Arney[2] and T. Hoehler[1],
[1]NASA Ames Research Center (andrew.j.rushby@nasa.gov), [2]NASA Goddard Space Flight Center, [3]Blue Marble Space Institute of Science

Introduction: Atmospheric methane (CH_4) acts as a potent greenhouse gas and regulator of planetary climate, as well as a potential biosignature. Methane concentrations were considerably higher in the anoxic Archean atmosphere of the early Earth (c.2.5 Gyr), with significant effects on climate and atmospheric photochemistry. The potential for methane to warm the Earth during the Archean, which received 25-30% less solar radiation from the young Sun, has been considered by earlier work [1]. Geochemical evidence of organic-rich haze during the Neoarchean has been well established by [2], while their photochemical modelling reveals a potential bistable regime between hazy and haze-free states likely mediated by variations in biological methane production. However, while many of the 'sink' terms of the Archean global methane cycle are relatively well constrained, the 'source' terms (i.e. biological methanogenesis) are less so. A variety of studies have sought to model this early methane cycle and quantify the resulting atmospheric and climatic impacts (e.g. [3]) to reveal a complex suite of interactions between the biosphere, geosphere, and atmosphere. Here, we present results from a study that seeks to investigate the operation of a hypothetical Archean methanogenic biosphere inhabiting the anoxic sediments overlying the ocean crust, particularly focusing on the uptake of hydrogen from volcanic sources (both subaqueous and subaerial), as well as the production and efflux of methane from the ocean into the atmosphere and the associated climatological impacts thereof.

Methods: In order to investigate the operation of a putative methanogen biosphere during the Archean eon, particularly in terms of the ability of a microbial community to alter this early, secondary atmosphere and climate, we leveraged a 1-dimensional coupled photochemical/climate code. The model uses *k*-coefficients for climate, and a series of coupled differential equations for photochemistry. See [4] for details of the photochemical code, whereas the climate model was originally developed by [5] and has since been modernized by several workers; see [6] for details of the climate code used in this project. Significant additions to this model include the addition of an ocean sediments layer with thermodynamically constrained methanogen biosphere and coupled biogeochemical cycling to a multi-layer ocean. We track volcanically produced hydrogen as it is bound with CO_2 to produce energy through methanogenesis, also producing CH_4 as a byproduct of this metabolic reaction which is then released into the water column, and eventually the atmosphere, at rates and at maintenance energies determined by the updated cell-scale diffusion reaction model presented in [7].

Results: Preliminary results from this ongoing project demonstrate that high hydrogen fluxes are required for methanogenesis to proceed efficiently in the Archean. This suggests that any putative methanogenic community would be spatially localized and restricted to areas in which this hydrogen flux is highest, for example around deep sea hydrothermal vent systems.

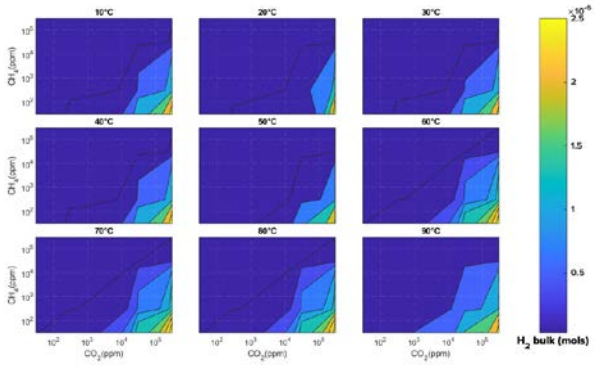

Figure 1: Preliminary results from a microbial ecosystem model demonstrating the amount of H_2 required for methanogenesis to proceed (hypothetically at 100% efficiency) as a function of CO_2/CH_4 ratio and surface temperature.

We note (figure 1) that the threshold for methanogenesis in our microbial sediment communities has relatively little dependence on the atmospheric CO_2/CH_4 ratio (as the H_2 gradient needed to provide the necessary flux of H_2 in the cell to sustain methanogenesis at maintenance (no growth) is much greater minimum hydrogen concentration inside the cell needed to enable methanogenesis to begin), and that temperature provides the strongest control the efficiency of this process (except under conditions where $pCO_2 < pH_2$). Therefore, we also explore the effect of varying levels of differentiated subaqueous and subaerial volcanism on microbial localization and efficiency, and note that the very high levels of subaerial volcanism required to maintain a sufficient hydrogen flux into the

ocean points to a possible decoupling of the ocean/atmosphere system in terms of hydrogen cycling. This also suggests a potential negative feedback between atmospheric methane, temperature, and the growth of the methanogenic microbes, in which the rate of methane produced and expelled from the ocean into the atmosphere is both a function of and control on the surface temperature.

Conclusions: This work has bearing on both paleoclimatology (in terms of a potential climate feedback during the Archean) and the study of the earliest microbial communities on the Earth, but also on our understanding of the processes that control the formation of hazes in anoxic atmospheres. This topic is of particular interest in terms of exoplanet biosignatures, as detecting atmospheric signals of sediment-dwelling methanogenic microbes in anoxic environments will be challenging. Therefore, developing a greater understanding of any potential (bio)geochemical control on the CO_2/CH_4 ratio and the cycling and processing of these species will be invaluable for future studies.

References: [1]Haqq-Misra, J.D., Domagal-Goldman-S.D., Kast-ing, P.J, & Kasting, J.F. (2008). *Astrobiology* **8**(6). [2]Zerkle, A.L., Claire, M.W., Domagal-Goldman, S.D., Farguhar, J., & Poulton, S.W. (2012). *Nat.Geoscience* **5**. [3]Kharecha, P., Kasting, J., & Siefert, J. (2005). *Geobiology* **3**(2). [4]Arney, G., Domagal-Goldman, S.D., Meadows, V.S. (2018). *Astrobiology* **18**(3).[5]Kasting, J.F., Ackerman, T.P. (1986). *Science* **234**.[6]Kopparapu, R.K., Ramirez, R., Kasting, J.F., Eymet, V., Robinson, T.D., Mahadevan, S., Terrien, R.C., Domagal-Goldman, S.D., Meadows, V.S., Deshpande, R. (2013). *ApJ* **765**(2). [7] Hoehler, T. (2004). *Geobio* **2**(4).

Atmosphere-mantle volatile exchange throughout planetary evolution. Laura Schaefer, Arizona State University, School of Earth and Space Exploration, PO Box 876004, Tempe, AZ 85287-6004, lschaefer@asu.edu

Introduction: Atmosphere-mantle volatile exchange is important throughout the lifetime of a rocky planet, from magma oceans during planet formation to deep volatile cycles throughout the planet's geologic lifetime. Fluxes of volatiles into and out of the mantle play a key role in the stability of habitable conditions at the surface on geological timescales. In this talk, I will review atmosphere-mantle volatile exchange on Earth, Venus, and Mars and applications to exoplanets.

Magma ocean-atmosphere exchange: Common volatiles such as water, CO_2 and N_2, as well as more minor species such as CH_4, H_2, and NH_3, are soluble in silicate melts [1-5], and therefore exchange with the atmosphere throughout the solidification process will determine both the amount of volatiles that become trapped in the solidified interior, as well as the composition and abundance of volatiles present in the atmosphere after the magma ocean has solidified [6-7]. Early oceans may result from the collapse of a steam-dominated magma ocean atmosphere. Escape of steam from early magma oceans may be an explanation for the divergent evolution of Venus and Earth [8], and could be a particular problem for rocky exoplanets around small M dwarf stars, potentially leading to the build-up of massive O_2 atmospheres [9,10] or alteration of the planet's oxidation [11,12].

Surface weathering reactions: Reactions of the atmosphere with the surface of a planet will be a major sink of atmospheric gases and can therefore strongly impact the climate of the planet. The present day crusts of Mars and Venus are dominantly basaltic in composition with small regions (<10%) of possible felsic material on both planets [13,14]. Present day Earth has a bimodal crustal distribution with felsic continents of variable age and very young basaltic oceanic crust. The growth rate of the felsic continental crust remains a highly debated topic [15-18]. Surface weathering rates depend on surface temperature [14], as well as the composition of the surface; typically mafic minerals weather more quickly than felsic minerals [15]. Therefore surface-atmosphere reactions will vary with planet age based on the evolution of the crustal composition as well as climate.

The most important weathering reactions involve CO_2 and water (both gaseous and liquid), which can produce carbonates, as well as hydrous and oxidized minerals. The reaction of CO_2 with silicates to produce carbonate minerals creates a negative climate feedback due to the temperature dependence of the reaction and the warming greenhouse behavior of CO_2 in the atmosphere [19-21]. The formation of hydrated silicates will sequester water out of the atmosphere and will have a likely very minor influence on climate by reduce the abundance of water vapor in the atmosphere. However, hydration reactions may also produce H_2 gas as a by-product which can potentially escape and allow progressive oxidation of the planet.

Deep volatile cycles: Volatile fluxes out of the mantle are dictated by the rate of volcanism, whereas fluxes into the mantle will depend strongly on the tectonic style of the planet as well as the weathering reactions that are responsible for removal of atmospheric gases. Mobile lid planets such as the Earth may actively transport these trapped volatiles into the mantle through subduction [21, 22], whereas stagnant lid or episodic lid planets may have more sporadic or limited transport of volatiles into the mantle [23, 24]. A schematic diagram showing the deep volatile cycles for the present-day Earth is shown in Figure 1.

For the exoplanet population, it still remains unclear if larger rocky planets will be able to undergo plate tectonics and Earth-like volatile cycles. For planets that do, higher planetary masses will lead to higher mantle pressures that may influence mantle viscosity and therefore the rates of deep volatile cycles. This may lead to slower outgassing and therefore delayed ocean formation on larger planets (Figure 2) [25].

References:

[1] Holloway, J.R. & Blank, J.G. 1994. Rev. Mineral. 30, 185-230. [2] Papale, P. 1997. Contrib. Mineral. Petrol. 126, 237-251. [3] Mysen, B.O. et al. 2008. Am. Mineral. 93, 1760-1770. [4] Hirschmann, M.M. et al. 2012. Earth Planet. Sci. Lett. 345-348, 38-48. [5] Ardia, P. et al. 2013. Geochim. Cosmochim. Acta, 114, 52-71. [6] Abe, Y. & Matsui, T. 1985 J. Geophys. Res. 90, C545-C559. [7] Elkins-Tanton, L.T. 2008. Earth Planet. Sci. Lett. 271, 181-191. [8] Hamano, K. et al. 2013. Nature, 487, 607-610. [9] Luger & Barnes 2015, [10] Schaefer, L. et al. 2016. Astrophys. J., 829, 63. [11] Wordsworth, R.D. et al. 2018 Astronom. J., 155, 195. [12] Sharp, Z.D. et al. 2013. Earth Planet. Sci. Lett., 380, 88-97. [13] Gilmore et al. 2017, [14] Ehlmann & Edwards 2014, [15] Armstrong, R.L. 1981. Phil. Trans. Roy. Soc. Lond. A, 301, 443-472. [16] Belousova, E.A. et al. 2008. Lithos, 119, 457-466. [17] Dhuime, B. et al. 2012. Science, 335, 1334-1336. [18] Korenaga, J. 2018. Earth Planet. Sci. Lett. 482, 388-395. [19] Walker et al. 1981, [20] Kump et al. 2000, [21] Sleep, N.H. & Zahnle, K. 2001. J. Geophys. Res.

106, 1373-1399. [22] McGovern, P.J. & Schubert, G. 1989. Earth Planet. Sci. Lett. 96, 27-37. [23] Morchhauser, A. et al. 2011. Icarus, 212, 541-558. [24] Dorn, C. et al. 2018. arXiv:1802.09264. [25] Schaefer, L. & Sasselov, D. 2015. Astrophys. J., 801, 40. [26] Karato, S. 2014. Treatise on Geophys.

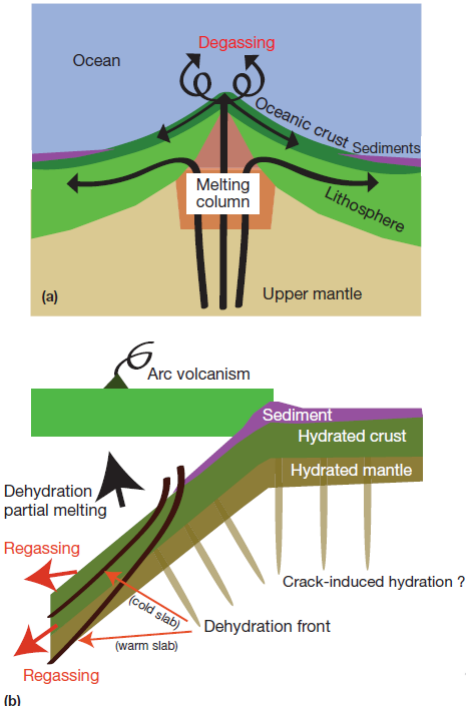

Figure 1 Schematic diagram of deep volatile cycle operating on the present-day Earth. Water is outgassed from the mantle predominantly at mid-ocean ridges (a), where it partitions preferentially into the melt phase. Water is partially returned to the mantle in subducting slabs in hydrated crustal minerals and in fluids in sediments (b). From [26].

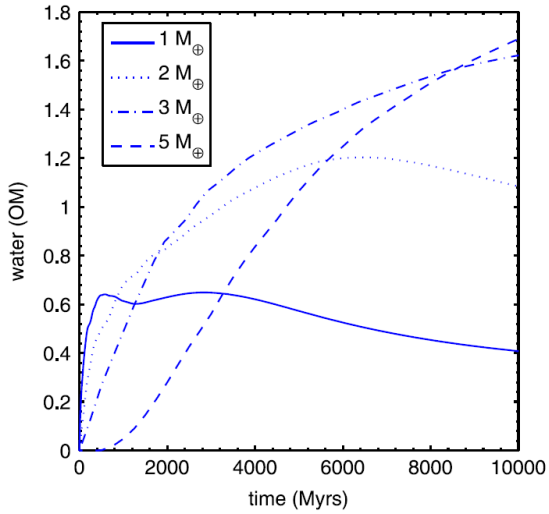

Figure 2 Water reservoir at the surface of rocky planets undergoing plate tectonics, using pressure- and water-dependent mantle viscosity. Water fluxes into and out of mantle depend on rate of subduction, mantle viscosity, and mantle thermal evolution. From [25].

ADVANCING THE STATE OF THE ART OF MARTIAN WEATHER AND CLIMATE MODELING WITH ORBIT-SPIN COUPLING. J. H. Shirley, Jet Propulsion Laboratory, California Institute of Technology, Pasadena, CA. (James.H.Shirley@jpl.nasa.gov).

Summary: Extending the forward time resolution of atmospheric forecasts remains a central goal for atmospheric modeling. On Earth, the existence of coherent oscillations of the atmospheric system with cycle times > 1 yr, such as ENSO and the NAO (i.e., the 'El Nino-Southern Oscillation' and the 'North Atlantic Oscillation'), has raised hopes for developing improved longer-term weather and climate forecasting. However, these terrestrial atmospheric oscillations typically exhibit significant interannual variability in amplitude and phasing, which presently limits their utility for developing seasonal and longer-term advance forecasts.

Spectacular global-scale dust storms (GDS) represent the preeminent form of atmospheric interannual variability on Mars. These storms occur during the southern summer season on Mars, in some Mars years, but not in others [1,2]. The intermittent occurrence of GDS on Mars has long been recognized as an important unsolved problem in the physics of planetary atmospheres [3].

An important step forward in numerical modeling of the Mars atmosphere is reported in [4] and [5]. Multi-year simulations obtained using the MarsWRF atmospheric global circulation model (GCM) with radiatively active dust and orbit-spin coupling are now able to replicate the historic record of Mars years with and without global dust storms with a success rate of 77%. Atmospheric conditions diagnostic to the occurrence or non-occurrence of GDS were successfully simulated in 17 of the 22 Mars years of the available record. Statistical significance at the 99% level was obtained in a comparison of success rates between an occurrence model with stochastic forcing and those of the GCM forced by orbit-spin coupling [4]. We are unaware of any other study that can claim similar success in reproducing the known first-order variability of a planetary atmosphere on time scales ranging from years to decades.

The GCM employed in [4] and [5] differs from the prior state of the art by the inclusion within the dynamical core of the model of *orbit-spin coupling accelerations*. A derivation leading to the identification and description of these accelerations is found in [6]. Mischna & Shirley [7] initially evaluated the response of the Mars atmosphere to the predicted dynamical "coupling term accelerations" (CTA) using a GCM in which 'interactive dust' effects were deliberately excluded. Important predictions of the orbit–spin coupling hypothesis were comprehensively evaluated in [7]. On the basis of these results, [4] and [7] were able to conclude that proof of concept for the orbit-spin coupling hypothesis had been achieved.

The physical hypothesis of [6] as tested in [4, 5, 7, and 8] is directly applicable to other planets with atmospheres. In this presentation we will describe key features of the predicted dynamical forcing and the modeled atmospheric response to the forcing. Despite the many significant differences between the atmospheres of Mars and the Earth, we will point out a number of opportunities for hypothesis testing (in future investigations) that could potentially lead to marked improvements in our understanding of the fundamental causes of atmospheric interannual variability of the terrestrial planets, and thereby to improved forecasting capabilities, on seasonal and longer time scales.

References: [1] Zurek, R. W., and L. J. Martin (1993), *JGR* 98, 3247-3259. [2] Shirley, J. H. (2015), *Icarus* 252, 128-144. [3] Haberle, R. M. (1982), Science 234, 459-461. [4] Shirley, J. H. et al. (2018), *Icarus* (in revision). [5] Newman, C. E., et al. (2018), *Icarus* (in revision). [6] Shirley, J. H., *Plan Space Sci*. 141, 1-16. [7] Mischna, M. A., and J. H. Shirley (2017), *Plan. Space Sci*. 141, 45-72. [8] Shirley, J. H., and M. A. Mischna (2017), *Plan Space Sci*. 139, 137-150.

Atmospheric circulations of lakes and seas on Earth and Titan. Alejandro Soto[1] and Scot Rafkin[1], [1]Southwest Research Institute, Boulder, CO, USA (asoto@boulder.swri.edu).

Introduction: With the discovery of lakes and seas on Titan, a moon of Saturn, we now have a second planet where the atmosphere interacts with the regional scale bodies of surface liquid. Whereas on Earth the lakes and seas are made of liquid water, the seas and lakes on Titan are filled with methane, and possibly ethane. We have been studying the atmospheric dynamics over the lakes and seas of Titan, using recently developed mesoscale models to simulate the Titan atmosphere. Here we discuss some examples of how the atmospheric circulations of the lakes and seas of Titan differ from the circulations seen on Earth.

Earth vs Titan: There are a number of ways that lake/sea circulations differ between Earth and Titan. At the regional and global scale, Titan has a pole to pole large scale circulation (i.e., Hadley circulation) that results in a seasonal cycle where the polar regions act as the tropic. Because methane is the condensable species on Titan, analogous to water on Earth, the properties of methane vapor generate a sequence of atmospheric circulations different from that seen on Earth.

Surface heating driven circulation over lakes on Earth. Typically on Earth, when the sun rises over a lake, the surrounding land warms faster than the lake surface. This results in positive buoyancy over the land, and hydrostatic low pressure over the land relative to the air pressure over the surface of the lake. A direct thermal circulation forms in which the near surface air over the lake is divergent with a wind that blows from the lake onto the land. This is traditionally known as a lake breeze or sea breeze.

Evaporation-driven circulation over lakes on Titan. On Titan, the circulation develops differently due to the increased buoyancy of methane. Although the land on Titan will warm faster than the lake or sea similar to the Earth, the evaporation of methane over the lakes will initially create a plume of buoyant, methane filled air. Methane vapor is more buoyant than water vapor, particularly on Titan where the atmospheric mixing ratio of methane can be several times greater than water on Earth . Therefore, there is a tendency for the evaporated methane to rise before a sea breeze circulation can form, forcing a plume-driven land breeze circulation (see top panel in Figure 1).

The Titan lake/sea surface cools due to evaporation as the land breeze intensifies. Eventually, the atmosphere above the lake begins to cool through sensible heat fluxes, increasing the atmospheric density that drives a sea breeze circulation acting in opposition to the land breeze (see the bottom panel of Figure 1). Destructive interference between the two circulations results in a decrease of near-surface winds. The atmospheric stability also increases, which tends to decrease latent and sensible heat fluxes.

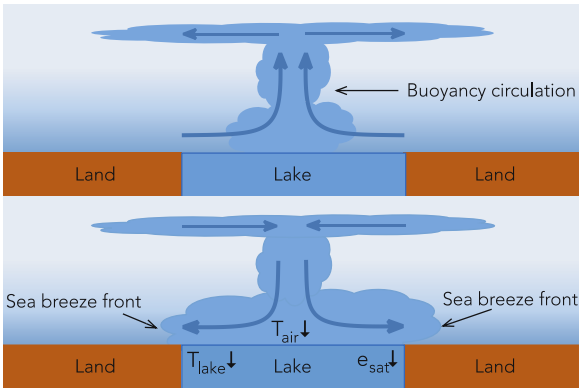

Figure 1. Idealized stages in the development of an atmospheric circulation over a Titan lake or sea. The top stage shows a plume-driven land breeze circulation; the bottom stage shows a sea breeze circulation.

The land breeze and sea breeze circulations compete over the lakes and seas of Titan. The outcome of this competition depends on the details, including the lake/sea size, shape, and initial thermal conditions. Regardless, the dynamics of these Titan lakes and seas evolve differently than the dynamics that we see on Earth.

Conclusion: We will discuss the similarities and differences of the atmospheric circulations over Titan and Earth, and show how different parameters determine the relative importance of the lake breeze and plume circulations on Titan. This comparison allows us to understand how these atmospheric dynamics are a universal phenomena that can manifest in a surprising number of ways.

THE EXOPLANET YIELD LANDSCAPE FOR FUTURE SPACE TELESCOPE MISSIONS. C. C. Stark[1], M. Bolcar[2], K. Fogarty[1], L. Pueyo[1], A. J. Eldorado Riggs[3], G. Ruane[3], R. Soummer[1], K. St. Laurent[1], and N. T. Zimmerman[2], [1]Space Telescope Science Institute (3700 San Martin Dr. Baltimore, MD 21218; cstark@stsci.edu), [2]NASA Goddard Space Flight Center, [3]California Institute of Technology.

Introduction: Several future space telescope concepts, including LUVOIR and HabEx, propose to directly image and characterize Earth-like extrasolar planets. The expected number of potentially Earth-like planets that could be characterized, or the yield, is a crucial metric that informs us of the scientific productivity of these missions. By performing realistic simulations of such missions we can calculate this critical yield metric, investigate efficient observation methods, and better understand the data quantity, quality, and scientific return.

Detection Technologies: To directly image exo-Earths, these missions must use coronagraphs and/or starshades to suppress starlight by a factor of 10^{10} to reveal the faint planet next to the star. These instruments differ significantly in implementation and as a result, have widely different observational strengths and weaknesses. I will review these technologies, their limitations, how to use them efficiently, and their scientific return.

Telescope Design: The starlight suppression technology and the telescope work together as a system; telescope design choices can positively or negatively impact the exoEarth candidate yield. I will review the major telescope design decisions at a high level, present why these choices matter, and how these choices impact the resulting exoplanet science.

Exoplanet Yield Landscape: Putting the above together, I will show exoEarth-optimized yields for a broad range of future mission concepts, including coronagraph- and starshade-based missions, as well as hybrid missions, as a function of telescope aperture. I will illustrate important break-points and regions for future improvement. I will show where the HabEx and LUVOIR mission concepts fit into this range and present expected yields for a broad range of exoplanets.

Did outburst of Supermassive Black Hole Sagittarius A cause an extreme glaciation on earth?

Thomas Tao, StannTron, Inc., thomastao@verizon.net, thomastao@stanntron.com

Introduction:

A disruptive theory [1] is emerging that suggests our planet earth went through a radical climate change during the late Miocene right before Pliocene from 5.9 to 5.33 million years ago (MYA), with an initial cooling starting 5.9 MYA, then an extreme cooling at 5.6 MYA and its abrupt ending at 5.33 MYA, resulting in a most extensive glaciation event "Miocene Glacier" since the dinosaur's era. This previously unidentified late Miocene Glacier has been suggested to cause an unprecedented ocean receding with the ocean depth dropping by 2 miles (3500 to 4000 meters) and all continental lands covered with 4 miles thick ice sheets on average, except for around the equator.

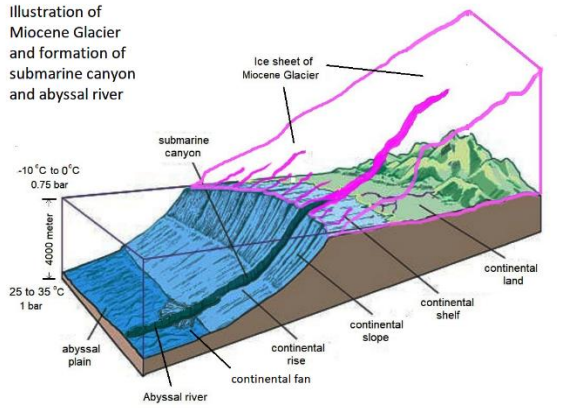

The theory of "Miocene Glacier" was first hypothesized by Thomas Tao, the author, as the origin of vast submarine canyons and abyssal rivers found miles deep at ocean bottoms, nevertheless it has been suggested to be the cause of many significant geological phenomenon such as the Grand Canyon in USA and biological extinctions and emergences of new species during 5.9 to 5.33 MYA such as the split of Chimpanzees leading to the rise of human race [1].

This theory has been supported by compelling evidences such as dating of rocks of ocean bottom abyssal rivers, extensive salt formations at ocean bottoms, vast land formations such as Ogallala formation in the United States of America, worldwide canyons in semi-arid regions, and significant evolutional events [1], etc. However it challenges inevitably existing, some widely popular views.

Yet what had caused this extreme climate change of the "Miocene Glacier" during 5.9 to 5.33 MYA remains to be resolved. Among many possibilities the cosmic ray outburst from the supermassive black hole in the center of our own milky way, Sagittarius A [2] [3] [4], ca 6 MYA, emerges as the leading candidate.

The timing of Sagittarius A outburst coincides with the newly identified late Miocene Glacier. The outburst is known to be extremely powerful and our solar system as expected should have been impacted by the blast of cosmic rays forcefully, for example its X-ray was projected to outshine our own sun [4] in our solar system. And researchers from University of Kansas and NASA concluded that ionizing cosmic rays induced cooling or glaciation on earth, as suggested to be the potential cause of glaciation in Ordovician 440 MYA [5] that resulted in mass extinctions.

What is missing or puzzling was that no apparent geological or climate change event on earth had been identified to link to the outburst so far. Coincidently the theorized late Miocene Glacier 6 – 5 MYA could be the exact product of the Sagittarius A Outburst, so do we find the missing link that have been implied to [4] [5]?

Yet many urge questions must be answered before we draw a conclusion linking the cosmic event with the extreme climate changes on earth at 6-5 MYA, and these important questions include but not limit to:

(1) The precise time and the duration or the length of the Sagittarius A outburst;
(2) The energy profiles and the ionizing particle distributions (including photons such as gamma rays) of the outburst;
(3) When these energetic particles (including gamma rays, alpha, beta and gamma particles, muons, etc.) reached earth and what were their flux intensities, did they reach earth as waves at different times as implied by the cooling events in the Miocene Glacier?
(4) Comprehensive mechanism of ionizing particles induced cooling or snow precipitation on earth;
(5) Verification of the late Miocene Glacier.

The key question is can we match the glaciation event "Miocene Glacier" with the outburst?

Nevertheless if proven to be true the theorized event of the late Miocene Glacier [1] and the outburst of Sagittarius A [2] [3] [4] may emerge to be the most important breakthrough of connecting cosmic rays with climate changes found on earth [5]. Author strongly encourages researchers to scrutinize these new findings and more importantly to participate in resolving these unresolved yet pressing issues.

References:

[1] Tao, Thomas. (2018). *The Origin of Abyssal Rivers, the Grand Canyon and Man.* Amazon, ISBN-13: 978-1-7320150-1-2.

[2] J. Bland-Hawthorn, Philip R. Maloney, Ralph S. Sutherland, and G. J. Madsen (2013). Fossil Imprint of a Powerful Flare at the Galactic Center along the Magellanic Stream. *The Astrophysical Journal, 778:58*.

[3] Rongmon Bordoloi, Andrew J. Fox, Felix J. Lockman, Bart P. Wakker, Edward B. Jenkins, Blair D. Savage, Svea Hernandez, Jason Tumlinson, Joss Bland-Hawthorn, Tae-Sun Kim (2017). Nuclear Outflow of the Milky Way: Studying the Kinematics and Spatial Extent of the Northern Fermi Bubble. *The Astrophysical Journal, Vol 834 No 2*.

[4] Pau Amaro-Seoane, Xian Chen. (2018). Our Supermassive Black Hole Rivaled the Sun in the Ancient X-ray sky. *Astronomy & Astrophysics*.

[5] A.L.Melott, B.S.Lieberman, C.M.Laird, L.D.Martin, M.V.Medvedev, B.C.Thomas, J.K.Cannizzo, N.Gehrels, C.H.Jackman (2004). Did a gamma-ray burst initiate the late Ordocivian mass extinction? *International Journel of Astrobiology 3(1)*, 55-61.

Computing Models of M-type Host Stars and their Panchromatic Spectral Output. D. Tilipman[1], J. L. Linsky[1], M. Vieytes[2] and K. France[3]. [1]JILA, University of Colorado and NIST, Boulder, CO 80309-0440 (contact: dennis.tilipman@colorado.edu); [2]Instituto de Astronoma y Fsica del Espacio (CONICET-UBA), C.C. 67, Sucursal 28, C1428EHA, Buenos Aires, Argentina; [3]LASP, University of Colorado Boulder, CO 80309-0600.

Introduction: We have begun a program of computing state-of-the-art model atmospheres from the photospheres to the coronae of M stars that are the host stars of known exoplanets. For each model we are computing the emergent radiation at all wavelengths that are critical for assessing photochemistry and mass-loss from exoplanet atmospheres. In particular, we are computing the stellar extreme ultraviolet radiation that drives hydrodynamic mass loss from exoplanet atmospheres and is essential for determing whether an exoplanet is habitable. The model atmospheres are computed with the SSRPM radiative transfer/statistical equilibrium code developed by Dr. Juan Fontenla. The code solves for the non-LTE statistical equilibrium populations of 18,538 levels of 52 atomic and ion species and computes the radiation from all species (435,986 spectral lines) and about 20,000,000 spectral lines of 20 diatomic species.

The first model computed in this program was for the modestly active M1.5 V star GJ 832 by Fontenla et al. [1]. We will report on a preliminary model for the more active M5 V star GJ 876 and compare this model and its emergent spectrum with GJ 832. In the future, we will compute and intercompare semi-empirical models and spectra for all of the stars observed with the HST MUSCLES Treasury Survey, the Mega-MUSCLES Treasury Survey, and additional stars including Proxima Cen and Trappist-1.

References:

[1]Fontenla, J. M., Linsky, J. L., Witbrod, J., et al. 2016, ApJ, 830, 154.

A MINIMUM COMPLEXITY MODEL FOR INVESTIGATING LONG-TERM PLANETARY HABITABILITY. Toby Tyrrell[1], [1]Ocean and Earth Science, National Oceanography Centre Southampton, University of Southampton, SO14 3ZH, UK. Toby.Tyrrell@soton.ac.uk.

Introduction: In order to understand how it was possible for life to develop all the way to intelligence on Earth, it is necessary to understand how Earth's climate stayed habitable. Geological data and the continuity of life suggest that Earth's climate remained continuously habitable throughout the last 3 or 4 billion years. It is not obvious, however, how this thermal habitability was maintained. The 25% increase in solar luminosity ('Faint Young Sun paradox') might have been expected to lead to intolerable conditions [1]. In addition, the short residence time of carbon at Earth's surface (<1 million years) suggests a susceptibility to rapid climate swings and therefore a predisposition to long-term instability [2]. Silicate weathering is often proposed as a thermostat [3] but there are doubts about whether it actually acted this way.

Investigating the phenomenon of long-term habitability is challenging. Because of the timescales involved, observing the phenomenon is out of the question. Experiments are likewise not feasible. Complex climate models cannot be run for billions of years. Simpler models can, however, be used.

Model: A new, fast, minimum-complexity model will be described. It aims to represent climate feedbacks rather than the whole climate system because the feedbacks are deemed to be most critical for long-term climate evolution. Parsimony is prioritized: fundamentals necessary for simulating climate regulation (tendencies to lose or maintain thermal habitability) are included but other aspects that are not essential for this question are purposefully excluded, even where it is possible to incorporate them accurately.

The model is intended to be general rather than a model of Earth specifically. Insights into Earth's habitability are thus sought through trying to understand the behavior of a large population of potentially habitable planets.

Initial Results: Results will be presented from a first application of the model. 100,000 planets were given randomly generated climate feedbacks. They were then tested to see if they stayed habitable for 3 billion years when exposed to random perturbations (for instance asteroid impacts, supervolcano eruptions) and long term forcings (for instance stellar evolution, supercontinent cycle).

It was found that most never stayed habitable, only a small number always stayed habitable (all 100 reruns) and ~9% sometimes stayed habitable (in many cases very infrequently, e.g. on only 1 or a few out of 100 reruns). Most planets that remained habitable on a single run did not usually remain habitable. By implication, therefore, Earth's 3 to 4 billion years of habitability was most likely a contingent outcome rather than having been certain at the outset.

This modelling approach has the potential to yield insights into how Earth happened to remain habitable for so long.

References:

[1] Sagan C. and Mullen G. (1972) *Science, 177*, 52-56. [2] Berner R.A. and Caldeira K. (1997) *Geology, 25*, 955-956. [3] Walker J.C., Hays P.B. and Kasting J.F. (1981) *JGR(O), 86*, 9776-9782.

THE PLANETARY SPECTRUM GENERATOR (PSG): AN ONLINE SIMULATOR OF EXOPLANETS.

G. L. Villanueva[1], M. D. Smith[1], S. Protopapa[2], S. Faggi[1,3], A. M. Mandell[1], C. D. Author[2], [1]NASA-Goddard Space Flight Center (geronimo.villanueva@nasa.gov), [2]South West Research Institute (SWRI), [3]NASA Postdoctoral fellow (USRA).

Abstract: We have developed an online radiative-transfer suite (https://psg.gsfc.nasa.gov) applicable to a broad range of exoplanets (e.g., terrestrial, super-Earths, Neptune-like and gas-giants). The Planetary Spectrum Generator (PSG) can synthesize planetary spectra (atmospheres and surfaces) for a broad range of wavelengths (0.1 μm to 100 mm, UV/Vis/near-IR/IR/far-IR/THz/sub-mm/Radio) from any observatory (e.g., JWST, HST, Keck, SOFIA, ARIEL, LUVOIR, OST). This is achieved by combining several state-of-the-art radiative transfer models, spectroscopic databases and planetary climatological models (e.g., Parmentier equilibrium P/T models and Kempton EOS chemistry).

Planetary generator: PSG has a 3D orbital calculator for all confirmed exoplanets, while the radiative-transfer models can ingest billions of spectral lines from hundreds of species from several spectroscopic repositories. It integrates the latest radiative-transfer and scattering methods and includes a realistic noise calculator that integrates several telescope / instrument configurations (e.g., interferometry, coronagraphs) and detector technologies (e.g., CCD, heterodyne detectors, bolometers). Such an integration of advanced spectroscopic methods into an online tool can greatly serve the planetary community, ultimately enabling to retrieve planetary parameters from remote sensing data, to efficiently plan mission strategies, to interpret current and future planetary data, to calibrate spectroscopic data and to develop new instrument/spacecraft concepts.

PSG capabilities – psg.gsfc.nasa.gov
A 3D (three-dimensional) **orbital calculator** for all solar system bodies and confirmed exoplanets, for Nadir, limb and occultation geometries.
The tool ingests **billions** of spectral **lines** and spectral **constants** from almost 1,000 chemical species from several spectroscopic repositories (e.g., HITRAN, CDMS, USGS, GSFC-Fluor).
Accurate **atmospheric profiles and surface** templates are available for the main bodies (e.g., Venus, Earth, Mars, Titan, Uranus, Pluto).
Radiative transfer performed with several modules: **PUMAS**, **correlated-K**, **non-LTE** fluorescence, and **surface models**
The code synthesizes **fluxes** in any desired unit.
The tool allows applying **terrestrial transmittances** for a broad range of conditions (altitude and water, also from SOFIA and balloons).
For exoplanets, it includes the possibility to integrate **realistic stellar templates** (0.15-300 μm), and the high-resolution ACE Solar spectrum (2-14 μm) for G-type stars.
It includes a **noise and signal-to-noise calculator** for quantum and thermal detectors, at any observatory (e.g., Keck, ALMA, JWST).

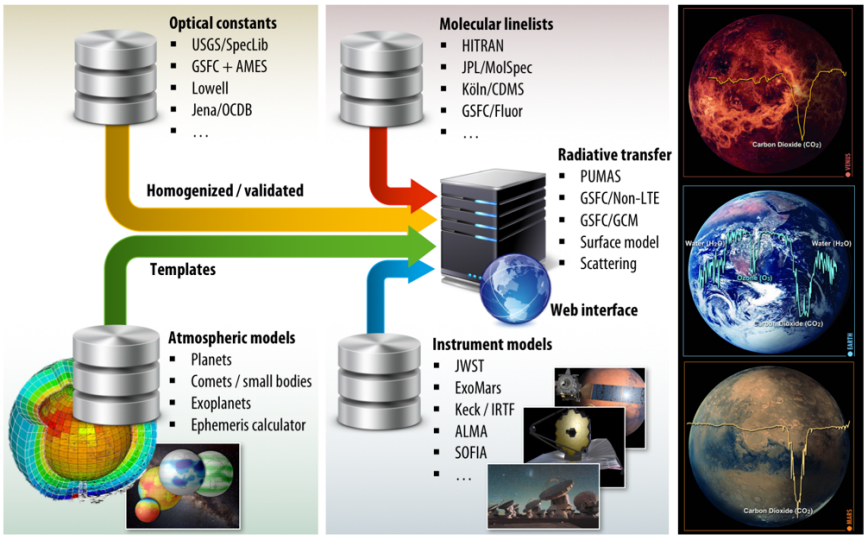

The tool can synthesize a broad range of planetary spectra by combining a modern and versatile online radiative transfer suite that uses state-of-the-art spectroscopic databases. The modules are computationally optimized, with a typical runtime of one second.

TITLE:

Effects of dipolar magnetic fields in Space Weather at outer magnetospheres

AUTHORS:

Liang Wang[1,2], Chuanfei Dong[1,2], Ammar Hakim[2], Amitava Bhattacharjee[1,2], Kai Germaschewski[3]

[1] Princeton University

[2] Princeton Plasma Physics Laboratory

[3] University of New Hampshire

ABSTRACT:

Some terrestrial bodies within our solar system have strong, intrinsic magnetic fields, in a few cases, Earth-like, dipolar fields. These magnetic fields play critical roles in Space Weather within the bodies' magnetospheres, through highly dynamic interaction with the magnetic field and plasmas carried by impinging solar wind, etc. In this presentation, we report self-consistent computational modeling of magnetospheric dynamics near the Mercury, as well Ganymede, a moon of Jupiter. Mercury has an inductive layer that can significantly modify the magnetospheric responses to the solar wind, and thus the magnetic field strength, plasma distribution, etc., very near the planet's surface. The other interesting case, Ganymede, does not interact with solar wind directly, but resides in the massive magnetosphere of Jupiter. The orientation of Ganymede's dipole field is very similar to that of the Earth's in the situation of southern interstellar magnetic field, but is much weaker in magnitude, thus weaker "shielding". Also, the Jupiter plasmas impact the moon's surface at a low Mach number, thus no bow shock can form; instead, a pair of tube-like structures, called Alfvén wings, are formed. In this presentation, we will compare the similarities and discrepancies of magnetosphere dynamics at Mercury and Ganymede, due to their vast different parameters and configurations. We will also discuss connections to the Earth's Space Weather and implications for improving our prediction technologies.

HOW STUDIES OF ANCIENT EARTH INFORM STUDIES OF ANCIENT VENUS: VENUS' EVOLUTIONARY HISTORY AND ITS IMPLICATIOS FOR VENUS-LIKE EXOPLANETARY WORLDS.

M. J. Way[1] and A. D. Del Genio[1,2], [1]NASA Goddard Institute for Space Studies, New York, New York, 10025, USA (michael.way@nasa.gov) [2](anthony.d.delgenio@nasa.gov).

Introduction: The planetary community has spent decades trying to better understand the climatic history of early Earth. This has been a challenge because of the well-known Faint Young Sun Paradox [1]. This challenge has driven innovative research in constraining early Earth's atmospheric density/pressure [2,3,4], constraining the longevity of Earth's primordial magma ocean with probable outgassing of volatiles [5], volatile delivery via the LHB and Late Veneer [6,7], and the composition of the early Earth's atmosphere [8]. Given that it is likely that Venus formed with similar elemental abundances as Earth we would like to leverage what we know about early Earth to better inform what we might about early Venus. For example, it is remarkable that the Earth has managed to maintain the same atmospheric pressure to within a factor of 2 for most of its history while also maintaining relatively clement conditions with a few short-term exceptions. This clearly points to its ability to balance the amount of CO_2 and N_2 in its atmosphere to allow for liquid surface water for most of the past 4Gy. Exactly how Earth managed this is still up for debate, but we know that Venus has not managed this trick today and in the recent past. The question is why has Venus failed to do so? Did it outgas and lose most of its volatiles very early in its history because of a long-lived magma ocean [9]? Even if it did was there no second chance for Venus via volatile delivery from the LHB or Late Veneer? For example, recent work by [10] demonstrates that Earth could have received 5-30% of its water in the late Veneer. Venus could have received similar amounts and this fits within the bounds of the Pioneer Venus D/H measurements indicating a water equivalent layer (WEL) of 4-525m [11], possibly enough for a shallow ocean. We have explored some of these later scenarios in the hope to not only better understand the early history of Venus and its subsequent evolution, but also the implications for Venus-like exoplanetary worlds being discovered today.

Simulations:
ROCKE-3D [12], a 3-D General Circulation Model, was used for all of the simulations described herein. We assume that Venus' present day orbital parameters were unchanged in the past 4Gy; if it rotated much faster it would have most likely lost its water early [13]. We assume that early Venus would had a similar type of atmosphere to early Earth or early Mars, meaning something between a 1 bar CO_2 dominated atmosphere and a 1 bar N_2 dominated atmosphere with 400ppmv CO_2. A solar spectrum from 2.9Gya was utilized for most experiments, although a present day solar spectrum and insolation was also simulated along with a single simulation at 4.2Gya. Topography was taken from the Magellan mission & two types of worlds were created: 1. A "land-planet" world with a 10m WEL spread as lakes in the lowest lying regions (see Figure 1) 2. A "shallow ocean planet" with 310m WEL [13]. We also simulated an aquaplanet of 900m depth with a flat bathymetry & a modern Earth topography since there are so many uncertainties about the relationship of present day Venus topography to what it may have been over the previous 4Gyrs. Earth's own topographic changes have been substantial.

Discussion:
Figure 2 shows the maximum grid point surface temperature for each simulation. The key thing to notice that that the surface temperature does not increase markedly for the N_2 dominated atmospheres with insolation from 2.9Gya to present day: 2001W/m^2 (S0X=1.47) to 2600W/m^2 (S0X=1.91), S0X=1.0 is modern Earth's incident flux of 1361W/m^2. Only the Earth topography case (Earth/Venus) shows substantial warming. The CO_2 dominated atmospheres are warmer in the early history of the two simulations presented. Here the heating from the greenhouse effect of CO_2 wins over the lower/cooler insolations in those periods: 4.2Gya (1914W/m^2) and 2.9Gya compared to the modern. The dotted lines demonstrate one evolutionary possibility where the world goes from a CO2 dominated atmosphere to an N2 dominated one, as may have happened in early Earth's history.

Figure 3 contains the mean surface temperatures over 1/6th of a diurnal cycle. The differences are again marginal with increasing insolation for the N_2 dominated atmospheres, except again the Earth topography case (Earth/Venus) shows greater variation.

Figure 4 shows the highest grid point value of stratospheric water vapor for each simulation averaged over 1/6th of a diurnal cycle. The pure CO_2 runs at 2.9Gya & 4.2Gya approach what we term the "Kasting-limit" after the work of [14] who showed that if stratospheric water concentrations reach f(H_2O)~3x10^{-3} an entire Earth's ocean may be lost over the lifetime of the Earth (~4.5Gy). At present day insolations the aquaplanet

and Earth topography (Earth/Venus) also reach this limit, but only for a single grid cell.

In conclusion, we believe our studies demonstrate that the reason for Venus' evolution to its present climatic state may be more interesting than a simple response to the gradual warming of our sun over the past 4Gyr. The key to understanding Venus' evolutionary history will only be found by revisiting our sister world to obtain better constraints on its water loss history and its geomorphology through time. In the meantime we can hope that Venus' exoplanetary twins will also help inform our understanding of our closest planetary neighbor, and vice-versa.

References: [1] Ringwood (1961) Geoch et Cosmoch Acta, 21, 295 [2] Som et al. (2016) Nat GeoSci DOI:10.1038/NGEO2713, [3] Som et al. (2012) Nature 484, 359 [4] Marty et al. (2013), Science 342, 101 [5] Lebrun et al. (2013) JGRP 118, 1155 [6] Morbidelli & Wood (2015) in The Early Earth: Accretion and Differentiation, Eds Baldro & Walter. [7] Morbidelli et al. (2018) Icarus 305, 262. [8] Olson et al. (2018) arXiv:1803.05967 [9] Hamano et al. 2013 Nature 497, 607 [10] Greenwood et al. 2018, Sci Adv 4, eaao5928 [11] Donahue & Russell (1997) in Venus II pp3-13 [12] Way, M.J. et al. (2017) Astroph Journ Suppl, 231, 1 [13] Way, M. J., et al. (2016) Geophy Res Lett, 43, 8376-838 [14] Kasting et al. (1993) Icarus 101, 108.

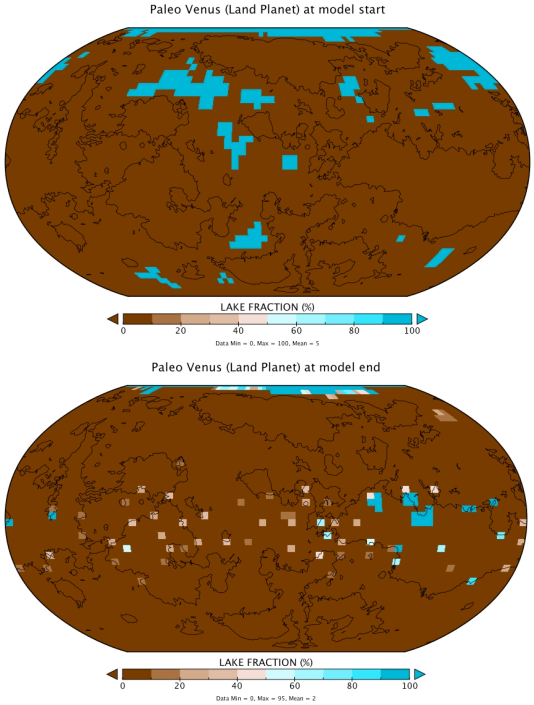

Figure 1. Land planet with 10m water equivalent layer. 1a shows initial distribution of water in low lying topographic regions. 1b shows where the model moves the water (due to evaporation & precipitation) after 4000 model years.

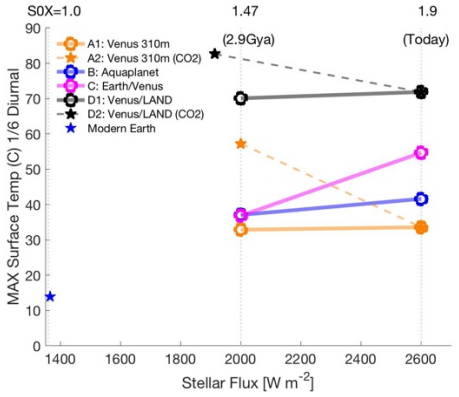

Figure 2. Black star is a 1 bar 97% CO_2, 3% N2 atmosphere at 4.2Gya. Yellow star is a 1 bar 100% CO_2 atmosphere at 2.9Gya. All other points are 1 bar N_2 dominated atmospheres + 400ppmv CO_2 + 1ppmv CH_4. Blue star is modern day Earth. Points represent maximum (MAX) grid point surface temperature in each run. Points are averaged over 1/6th of a diurnal cycle.

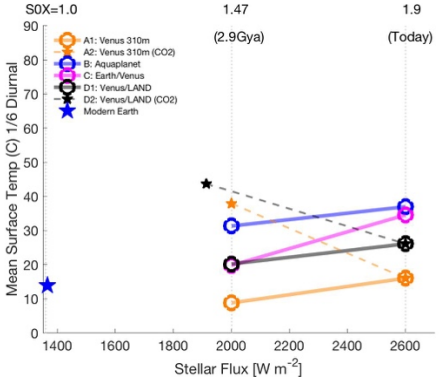

Figure 3. As in Figure 2, except the points here represent the global mean surface temperature in each run.

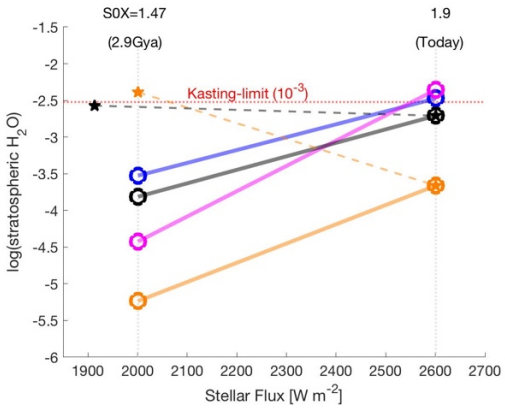

Figure 4. Maximum stratospheric water vapor for a given grid cell averaged over 1/6th of a diurnal cycle.

Venus' Early Potential for Habitability: Connecting Climate and Geologic Histories. M. B. Weller[1], A. Lenardic[2], M. Jellinek[3], J. Seales[2], and M. Way[4] [1]Institute for Geophysics, Jackson School of Geosciences The University of Texas at Austin, Austin, TX (mbweller@ig.utexas.edu), [2]Department of Earth Science, Rice University, Houston, TX, USA, [3] Department of Earth, Ocean, and Atmosphere, University of British Columbia, Vancouver, BC, Ca. [4]NASA Goddard Institute for Space Studies, New York, NY, USA

Introduction A key observation and open question in the Earth and Planetary Sciences is that the Earth is seemingly unique in that it exhibits plate tectonics and a buffered climate allowing liquid water to exist at the surface over its geologic lifetime. While we know plate tectonics is currently in operation on the Earth, the timing of its onset, the length of its activity, and its prevalence outside the Earth are far from certain. Recent work suggests that the Earth has not always been within a plate-tectonic regime, and that it has evolved over time. Multiple lines of geochemical and geologic evidence, as well as geophysical models of planetary evolution, suggest the Earth initiated in a stagnant-lid (one plate-planet), followed by an "adolescent" episodic-lid (alternating between stagnant and mobile-lids), before settling into a "mature" modern style of plate-tectonics (mobile-lid) [*e.g.*, 1 – 6]. This implies that life and habitable conditions have existed on the Earth during episodic behavior, and models of an episodic early Earth further show habitability to be viable [7].

Currently, Venus shows no clear evidence of Earth-like plate tectonic activity or surface conditions. Observations reveal a world that has both a thick 92 bar atmosphere, comprised of 96.5% CO2 and surface temperatures of ~740 K, and been resurfaced by vast volcanic plains that cover ~ 80% of the surface, which are thought to have been emplaced in the last 300 – 1000 Myr [8 – 10], perhaps 'catastrophically' [9, 10]. These observations, along with inferences of limited large scale shortening [11], are consistent with suggestions of an episodic-lid regime [12 – 14].

Here we ask a simple question, if an early episodic Earth could support a life (a habitable climate), through climatic excursions (snowball Earth) [e.g., 15 – 17], a faint young sun [*e.g.*, 18, 19], and variable tectonic states [*e.g.*, 1 – 6], what of Earth's "twin", Venus? Could an episodic Venus have been habitable? We examine this possibility, and show links between atmospheric evolution, habitability, and the deep interior.

Evolution of the Surface/Atmosphere System: Episodic-lids serve as a transitory state between stagnant-lid and mobile-lid regimes. As a consequence, the episodic-lid behavior is often an amalgam of the two end-member states: low mobility (no surface/interior cycling), low melt, and high internal temperature stagnant-lid; and high mobility (surface interaction and cycling), moderate to high melt, and lower internal temperature mobile-lid. Figure 1 shows pCO_2 (normalized), released from melt production, and mantle scale weathering rates (normalized) for a type example episodic-lid. Spikes in values are associated with overturn events (high surface activity and interior cycling). Each overturn increases the atmospheric pCO_2 by 10 – 30x, despite feedback effects from weathering processes. Once outgased, weathering associated with mantle scale processes (*e.g.* orogenic-linked weathering at convergent margins) are insufficient to remove excess CO_2 - associated with an overturn spike- from the atmosphere. Each overturn event creates a new, higher value baseline (increasing atmospheric CO_2 in a ratcheting-type effect). However, overturns (spacing, magnitude) themselves are stochastic and as a result the baseline values are specific history dependent.

The effects of an increase in pCO_2 from a melt source on a proxy climate system are shown in Figure 2. In this case the proxy is Earth-like in land/water distribution and initial surface temperatures, assuming early Earth and Venus are otherwise identical (*e.g.*, not a runaway greenhouse), consistent with inferences from models of planetary evolution [*e.g.*, 3], and the suggestion that Venus could have supported liquid water in the past [*e.g.*, 25]. Age acts as a proxy for distance. Therefore, Venus' response at 0.72 AU acts as a older (higher insolation) Earth. Initially, an early Earth-like planet (1AU) has a strong potential for an early snowball state, however, increasing pCO_2 results in a greater potential for climates that allow for liquid water as the solar luminosity increases (bottom to top branch as the Sun ages, Figure 2). In comparison, Venus type solutions at the same time, have greater insolation, and a decreased likelihood for temperatures that allow for global glaciations, and instead favor temperatures in the past that allow for liquid water (*e.g.*, top branches of Figure 2), suggesting early Venus may have had an advantage over the early Earth for surface temperatures, and the potential for liquid water. As the Suns luminosity increases, the potential surface temperature is pushed to the higher extremes of the warmer surface temperature branches (upper left corner Figure 2).

This work suggests that an episodic Venus has the potential to allow for liquid water, and consequently habitability. If Venus could support life, it suggests a fundamental rethinking of plate-tectonics links to habitability, and how habitable zones are defined, that is Venus is at the edge of the current habitable zone because it currently does not have liquid water, not be-

cause it is inherently incapable of having liquid water at present [*e.g.*, 6].

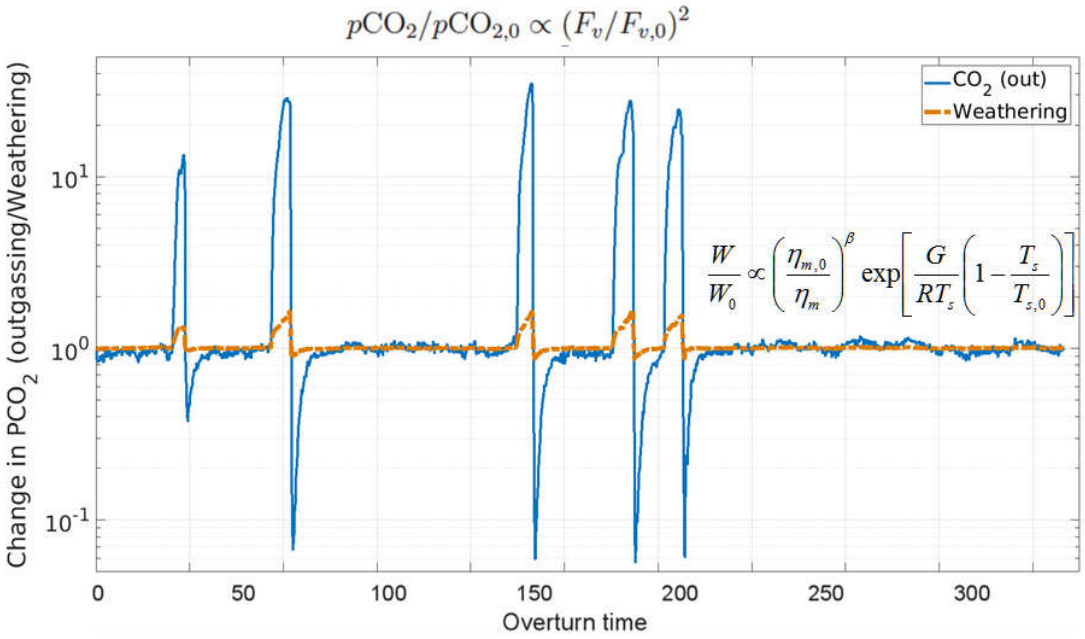

Figure 1: Selected results from the finite element code CitcomS [20 – 22] showing change in pCO_2 calculated from an episodic-lid (F is volcanic flux). pCO_2 is normalized at overturn time 0, and is calculated from melt production using established solidus formulations for peridotite melt [23]. Weathering rate is normalized, and calculated using a mantle scale formulation [7, 24]. η_m is mantle viscosity, T_s is surface temperature, G, β, and R are constants [e.g. 7, 24]. The overturn time (x-axis, all panels) corresponds to the time a parcel takes (on average) to traverse the mantle. The Rayleigh number (definition for basally heated systems using the viscosity at the system base) is $6 \cdot 10^5$, with a temperature-dependant viscosity contrast of $6 \cdot 10^4$, an input internal heating rate of 45 (decreased from higher values), and a yield strength of $1 \cdot 10^5$.

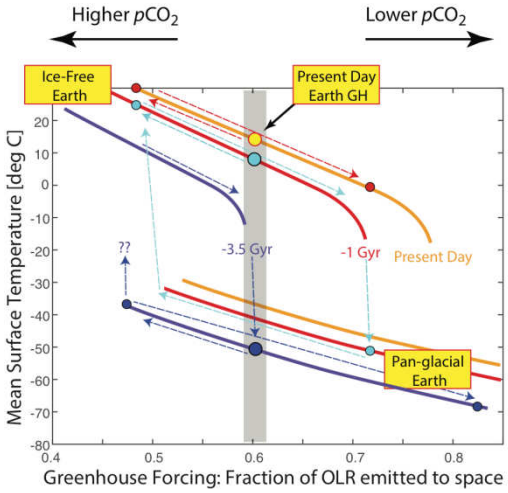

Figure 2: (Reproduced from [7]) Earth's potential surface temperature response to an O(100) increase in pCO2 from melting sources [7, 24], assuming that the unperturbed greenhouse forcing is fixed at a present-day Earth values (large-filled circles). The signal for current day insolation, does not alter the climate of the planet to a pan-glacial or an ice-free state (small red-filled circles and dashed arrows). 1 billion years ago, the signal does drive the model climate to vary between variably warm solutions and a pan-glacial state (light blue-filled circles and dashed arrows). Further back in time, 3.5 billion years ago, the pCO2 signal carries the globally glaciated model planet into a snowball state and also potentially out of this solution (dashed arrow with a question mark). Note: Age is a proxy for distance. Venus-type solutions will be shifted to younger ages do to its closer stellar proximity.

References: [1] Debaille et al (2013), EPSL, 373, 83–92; [2] O'Neill & Debaille (2014), EPSL, 406, 49-58; [3] Weller et al., (2015), Earth Planet. Sci. Lett. 420, 85–94; [4] O'Neill, et al. (2016), Physics of the Earth and Planetary Interiors, 255, 80-92; [5] Lenardic et al., (2016), Astrobiology 16(7), 9 pp.; [6] Weller, M.B., and Lenardic, A., (2017). Geoscience Frontiers 9, 91e102 ; [7] Lenardic, et al., JGR 25th anniversary issue, E005089. [8] McKinnon et al. (1997) , Venus II, Arizona Univ. Press, pp. 969–1014; [9] Schaber, et al. (1992), JGR, 97, 13257–13301; [10] Strom et al. (1994) , 99, JGR 10899–10926; [11] Kiefer, LPSC 44, # 2541; [12] Schubert et al. (1997), Venus II, Arizona Univ. Press, pp. 1245–12888; [13] Nimmo and McKenzie (1998), Annu. Rev. Earth Planet. Sci. 26, 23–51; [14] Moresi and Solomatov, (1998), JGR, 133, 669-682; [15] Hoffman et. al., Science 281, 1998; [16] Hoffman et al., Terra Nova, 14-3, 2002; [17] G^3 3-6, Schrag et al., 2002. [18] Sagan and Mullen, Science 177, 1972; [19] Feulner, Review of Geophysics, 50-2 2012; [20] Moresi and Solomatov (1995), Physics of Fluids,7 (9), 2154-2162. [21] Zhong, et al. (2000), JGR, 105, 11063–11082, [22] Tan, E., et al. (2006), G3, 7, Q06001. [23] Hirschmann, M., Geo-chem. Geophys. Geosyst., (2000), 2000GC000070; [24] Jellinek and Jackson (2015), Nature Geoscience. [25] Way et al., (2016), GRL, 10.1002/2016GL069790

ABIOTIC OXIDATION OF PLANETARY ATMOSPHERES: PHYSICAL MECHANISMS AND CONSEQUENCES FOR CLIMATE, HABITABILITY AND BIOSIGNATURES

R. D. Wordsworth[1,2], [1]School of Engineering and Applied Sciences, Harvard University, Cambridge, MA 02138, USA. [2]Department of Earth and Planetary Sciences, Harvard University, Cambridge, MA 02138, USA. *rwordsworth@seas.harvard.edu*.

Terrestrial planets segregate iron in their cores and lose hydrogen to space, which tends to cause a buildup in the oxidizing power of their surfaces and atmospheres over time. The rate at which the process proceeds is fundamental to determining the eventual composition of the planet's atmosphere and to whether or not the planet can develop and sustain a biosphere. It is also essential to understanding when we can treat O_2 as a biosignature in the atmospheres of potentially habitable exoplanets.

In this review, I begin by discussing the early atmospheric evolution of Venus, Earth and Mars in the solar system. I summarize the evidence for and models of early water loss and oxidation on Venus and discuss possible drivers of oxidation on Earth, including mantle disproportionation [1], atmospheric water and methane photolysis [2-3], biological sequestration of N_2 [4,5] and impact degassing [6]. I then discuss redox on Mars, focusing in particular on whether episodic emission of reducing gases such as methane and hydrogen may hold the key to solving the faint young Sun problem [7-9].

Next, I discuss water loss and irreversible oxidation in the context of exoplanets. I begin by reviewing the key atmospheric observations of rocky exoplanets that we expect to be possible in the 5-10 year time frame. Then, I review recent modeling work showing the ways in which some exoplanets, particularly those around M-dwarf stars, could build up long-lived abiotic oxygen atmospheres [5,10-11], leading in some cases to false positives for life. Recent work indicates that a planet's orbital distance and initial water inventory are two key determinants for buildup of an abiotic O_2 atmosphere, which suggests we may be able to use oxygen to hunt for biospheres on some exoplanets within the next decade [12,13]. I finish by describing the key theoretical, observational and experimental steps that need to be taken to advance our understanding of planetary oxidation in future.

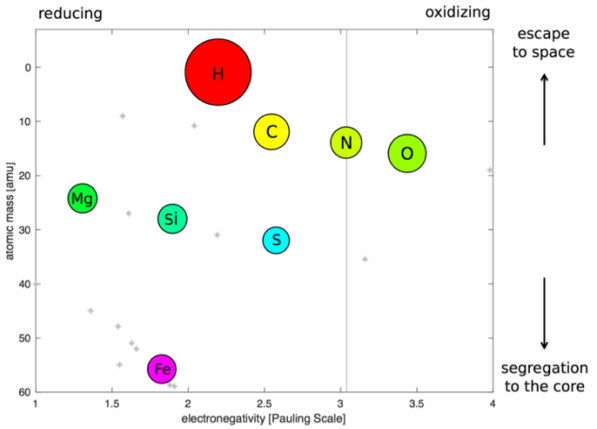

Figure 1: Plot of atomic mass vs. electronegativity for major elements in the solar system (from [12]). The abundance, high electronegativity and intermediate atomic mass of oxygen (O) means there is always a tendency for rocky planet atmospheres and surfaces to oxidize in situations where gravitational differentiation is effective.

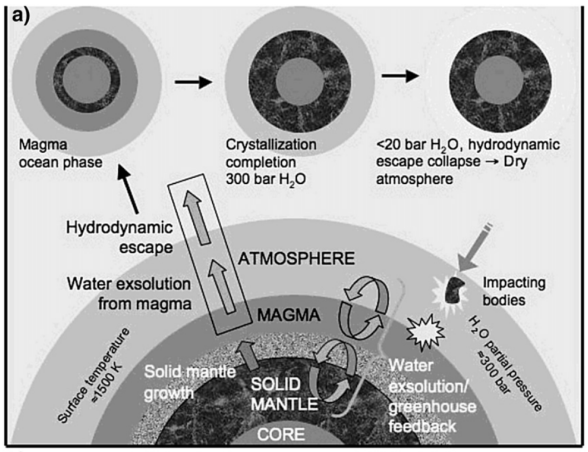

Fig. 2. Sequence of events occurring in an early magma ocean water loss phase for Venus (from Gillmann et al., 2009 [14]). Due to its higher received solar flux, Venus may have undergone a much longer magma ocean phase than Earth or Mars, leading to far more extensive oxidation via H_2O photolysis and hydrogen loss [14-16].

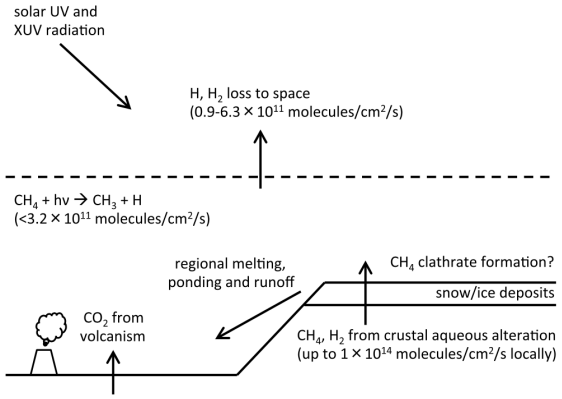

Fig. 3 Mars today is hyperoxidized at the surface, but episodic release of reducing gases in the Noachian period 3-4 Ga could have caused sufficient warming to resolve the faint young Sun problem [7-9]. Figure from [9].

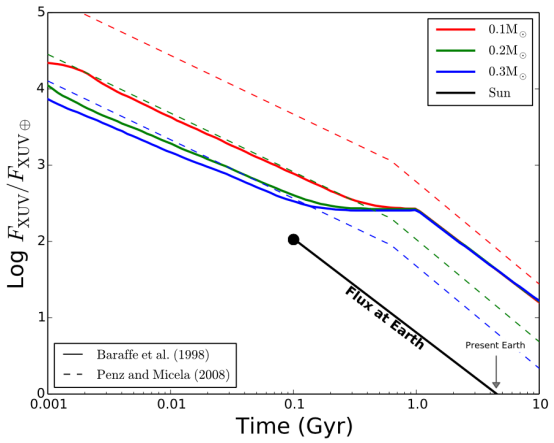

Figure 4: The extended pre-main sequence phase and enhanced XUV flux of M-dwarf stars can cause very significant water loss in the planets that orbit them [10,17]. To understand whether this will lead to abiotic buildup of O_2 in the planets' atmospheres, coupled interior-atmosphere evolution modeling is required [11-12]. Figure from [10].

References:

[1] Frost, D. J. and McCammon, C. A. (2008) *AREPS*, 36, 389–420.
[2] Kasting, J. F. and Pollack J. B. (1983), *Icarus*, 53, 479–508.
[3] Catling, C. J., et al. (2001), *Science*, 293, 839–843.
[4] Tomkins, A. G., et al. (2016). *Nature*, 533, 235.
[5] Wordsworth, R. and Pierrehumbert, R. (2014) *ApJL*, 785, L20.
[6] Zahnle, K., Schaefer, L., and Fegley, B. (2010). *Cold Spring Harb Perspect Biol*, *2*(10).
[7] Wordsworth, R., and Pierrehumbert, R. (2013). *Science*, *339*(6115), 64-67.
[8] Ramirez, R. M., et al. (2014). *Nature Geoscience*, *7*(1), 59.
[9] Wordsworth, R., et al. *GRL* 44.2 (2017): 665-671.
[10] Luger, R., and Barnes, R. (2015) *Astrobiology*, 15, 119-143.
[11] Schaefer, L., et al. (2016), *ApJ*, 829, 63.
[12] Wordsworth, R., et al. (2018) *AJ*, 155-195.
[13] Snellen, I., et al. (2013). *ApJ*, *764*(2), 182.
[14] Gillmann, C. et al. (2009), *EPSL*, 286, 503–513.
[15] Hamano, K., et al. (2013). *Nature*, *497*(7451), 607.
[16] Wordsworth, R. (2016), *EPSL*, 447, 103-111.
[17] Tian, F., and Ida, S. (2015). *Nature Geoscience*, *8*(3), 177.

INCREASED ICE COVERAGES on TRAPPIST-1e, LHS 1140b and Proxima b by SEA ICE DYNAMICS

Jun Yang[1] and Weiwen Ji[1], [1]Dept. of Atmospheric and Oceanic Sciences, Peking University, Beijing, China (Yi He Yuan Road No. 5, Hai Dian, Beijing, 100871, China; junyang@pku.edu,cn and jacksd@pku.edu.cn).

Abstract: TRAPPIST-1e, LHS1140b and Proxima b are the nearest Earth-size exoplanets in the surface liquid-water habitable zones of M dwarf stars. Current and future telescope missions are able to characterize their atmospheres and climates because of the fact that they are within 40 light years away. Previous studies with 3D global climate models [1-3] suggested that these three planets may be in "Eyeball" [4] or "Lobster" [5-6] climate state which is ice-free around the substellar region but ice-covered elsewhere. Sea ice dynamics, however, have not been considered seriously in the previous studies. Using a fully coupled atmosphere--ocean--sea-ice--land model with active sea ice dynamics, Here we show that sea ice flows driven by surface winds are able to significantly shrink the ice-free area or even push the planets into globally ice-covered snowball states, similar to Super-Europa but with thin ice at the substellar point [7]. Photosynthetic life can develop under the thin ice although they will not be detected by distant observers. These results suggest that sea ice dynamics is a critical factor in examining the possible climates of exoplanets near the outer edge of the habitable zone.

References: [1] E. T. Wolf (2017) *ApJ Letters*, 839, L1. [2] A. D. Del Genio, *et al.* (2017) *Astrobiology* (*submitted*), arxiv.org/abs/1709.02051. [3] M. Turbet, E. Bolmont, J. Leconte, *et al.* (2018) A&A, A86, 1-22. [4] R. T. Pierrehumbert (2011) *ApJ Letters*, 726, L8. [5] Y. Hu and J. Yang (2014) PNAS, 111, 629-634. [6] J. Yang, *et al.* (2014) *ApJ Letters*, 796, L22. [7] J. Yang and W. Ji (2018), *in preparation*.

CLIMATIC EFFECT OF IMPACTS ON THE OCEAN. K. J. Zahnle[1], [1]NASA Ames Research Center (Mail Stop 245-3, Moffett Field CA, Kevin.J.Zahnle@NASA.gov).

Introduction: Impact-generated spherule layers provide information pertinent to the environmental consequences of very large impacts on Earth. The spherules are condensed from high velocity impact ejecta ballistically distributed worldwide. These ejecta comprise material from both the impacting body and the target. Much of this material was vaporized or atomized (in the sense of small droplets of fluid, although doubtless some of the vapor species were atomic) in the impact event, cooled and condensed, and then was re-melted or partially evaporated again on re-entry into the atmosphere far from the crater. The energy deposited in the atmosphere by the re-entering ejecta heat the stratosphere where the particles stop to the temperature of hot lava, and thermal radiation from the superheated stratosphere heats the lower atmosphere, any land surfaces, and the evaporate the surface of the ocean; how hot the atmosphere gets and how much water gets evaporated depends on the scale of the impact. The molten or solid raindrops and hailstones eventually fell out of the atmosphere and onto land or into the ocean over the course of hours and days to pile up as spherule beds, and later the finer dust falls out over months and years.

The most famous example of a spherule layer is in the global boundary clay deposited by the K/T impact 66 Ma. In Europe, far from the Chicxulub crater in the Yucatan, the layer is about 3 mm thick comprising 0.25 mm spherules. The iridium in the boundary clay was the first-discovered signature of a cosmic impact. The chromium isotopes in the spherules imply that the impactor was kin to carbonaceous chondrites [1].

It is still somewhat astounding to learn that there are of order ten spherule layers as thick or thicker than the K/T layer known from the Archean [2-5]. There are four or five layers in the Late Archean ca 2.5-2.7 Ga. The Paraburdoo layer, perhaps the most interesting because it was deposited in quiet waters that must have been very far from the crater, is 2 cm thick and very Ir-rich, so much so that the spherules are of order 50% exogenic by mass [4]. Here the Cr isotopes indicate and affinity with ordinary chondrites. There are another 4-8 layers in the Barberton Greenstone Belt with thicknesses ranging from 10 cm to more than 100 cm [5]. To the extent examined, the Cr isotopes suggests carbonaceous chondritic material. The S3 layer ca 3.24 Ga is 25 cm thick, distal, and iridium-rich; and the S5 layer ca 3.25 Ga may record an impact ten times bigger. If these local estimates of spherule bed thickness are extrapolated globally, they suggest that these to impact events were comparable in energy release to those that formed the lunar Orientale and Imbrium impact basins 500 million years earlier.

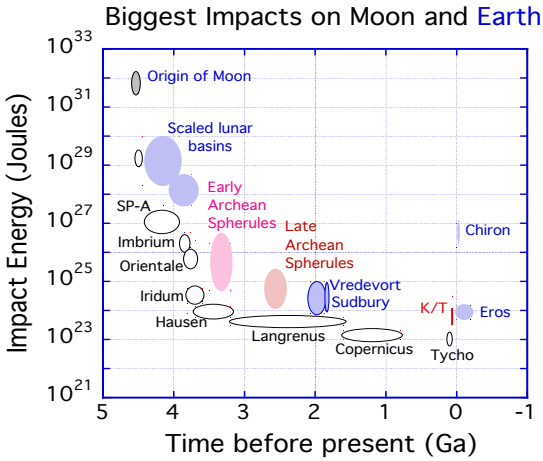

Figure 1. Looking backward: the history of the biggest impacts on the Moon and Earth. The Archean spherules are usually taken to imply that at least ten impacts as big or bigger than the K/T (Chixculub) took place between 2.5-3.5 Ga. Looking forward: the chance that Eros strikes Earth is of the order of 10%, the chance that Chiron strikes Earth is on the order of 0.0001%. Adapted from [6].

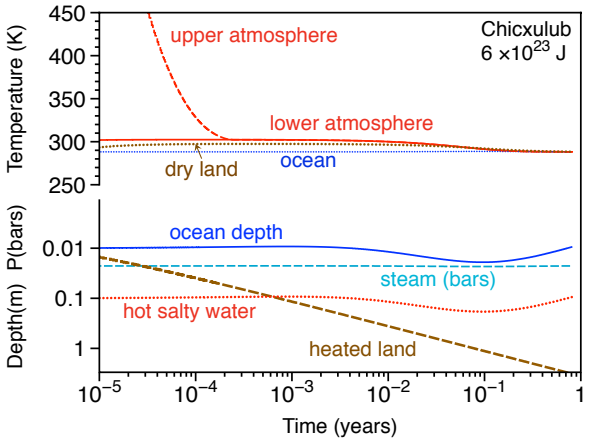

Figure 2. Short-term heating by a high-energy Chicxulub (K/T) impact. The modeled impact is of a 20 km asteroid at 15 km/s striking a 300-m deep shallow sea. The energy released by the impact falls just short of causing major direct thermal perturbations. Most of the environmental consequences came later from the

impact winter induced by the blocking of sunlight by dust, smoke, and sulfate.

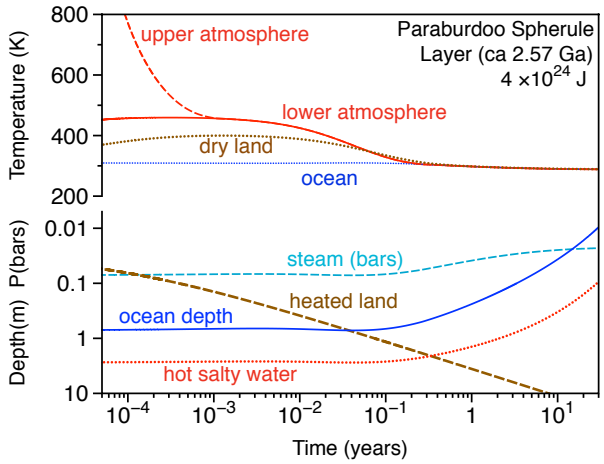

Figure 3. Global environmental evolution after the impact that created the Paraburdoo spherule layer. The upper meter of the ocean is evaporated, which leaves a 2 meter residuum of salty water that floats because it is hot. Thermal radiation from impact ejecta stopped in the atmosphere raise the surface temperature of dry land to 400 K and the troposphere may reach 450 K. The thermal wave from the hot surface penetrates a meter or two into the ground.

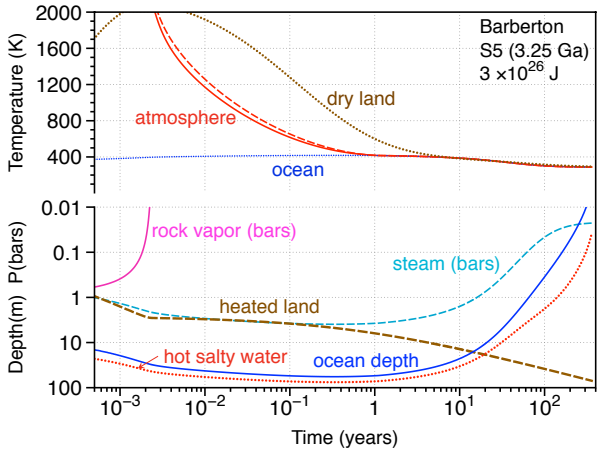

Figure 4. The Barberton S5 spherule layer is the thickest spherule bed and, if globally representative, is by inference the largest impact reported by [5]. In this simulation dry land surfaces melt and flow. The sterilizing thermal wave penetrates 10 meters into the ground. Fifty meters of water evaporates from the seas leaving 70 meters of hot salty water on top of the ocean (which stays cool at depth). The surface temperature even over the oceans is hot (400 K), a temperature that adds 3 bars of steam to the atmosphere.

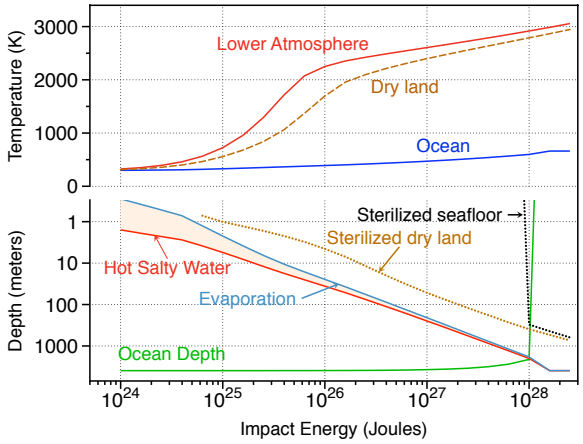

Figure 5. Impacts on Earth, from Chicxulub to the remote possibility of Ceres. The top panel shows the highest temperatures reached in the troposphere, at the ocean's surface, and on land. The bottom panel shows the depth of ocean water evaporated; the depth to which the ocean is sterilized by hot salty water; the depth to which dry land is sterilized; and the depth to which exposed oceanic crust is sterilized. Sterilization is defined as temperature exceeding 400 K. A more nuanced model would show that adverse environmental effects are patchy and thus the planet more habitable after enormous impacts than evident here.

Summary. In the Late Archean 2.5-2.7 Ga, impact events such as the one that deposited the Paraburdoo Spherule Layer, heated land surfaces to 400 K. Conditions were not conducive to mesophilic photosynthesizers on land. The bigger Barberton Greenstone Belt spherule layers (S3, S5), when fully extrapolated, correspond to the lands being sterilized and surface waters heated to 330K (S3) or even to 400 K (S5). Lowe & Byerly [5] describe more extreme environmental consequences that would be commensurate with an Imbrium scale impact (>3x10^{26} J, >100 km diameter impactor), whcih would correspond to a global ejecta layer on the order of 10 m, although the evidence seems more consistent with ~ 1 m.

References:

[1] Kyte F. et al. (2003) *Geology 31,* 283–286. [2] Lowe D. et al. (1986) *Geology 14,* 83-86. [3] Simonson B.M. and Glass B. (2004) *Ann. Rev. Earth Planet. Sci. 32*, 329–61. [4] Lowe D. and Byerly G. (2015) *Geology, 90,* 1151–1154. [5] Simonson M. M. et al. (2010) *LPSC 41,* 2386. [6] Sleep N.H. et al. (1989) *Nature 342,* 139–142.